TECHNISCHE UNIVERSITÄT DARMSTADT
INSTITUT FÜR MASSIVBAU

24

Eric Brehm

Reliability of Unreinforced Masonry Bracing Walls

Probabilistic Approach and Optimized Target Values

DISSERTATION

Heft 24 Darmstadt 2011

Reliability of Unreinforced Masonry Bracing Walls

Probabilistic Approach and Optimized Target Values

Dem Fachbereich Bauingenieurwesen und Geodäsie
der Technischen Universität Darmstadt
zur Erlangung des akademischen Grades eines
Doktor-Ingenieurs (Dr.-Ing.)
vorgelegte

DISSERTATION

von

Dipl.-Ing. Eric Brehm

aus
Seeheim-Jugenheim / Hessen

D 17

Darmstadt 2011

Referent:	Prof. Dr.-Ing. Carl-Alexander Graubner
Korreferent:	Prof. Marc A. Maes, PhD

Herausgeber:

Prof. Dr.-Ing. Carl-Alexander Graubner

Anschrift:

Institut für Massivbau – Fachgebiet Massivbau
Petersenstrasse 12
64287 Darmstadt

http://www.massivbau.to

Brehm, Eric:

Reliability of Unreinforced Masonry Bracing Walls
Probabilistic Approach and Optimized Target Values

1. Auflage Darmstadt

Dissertation // Institut für Massivbau, Technische Universität Darmstadt; Heft 24

ISBN 978-3-942886-02-4

Dr.-Ing. Eric Brehm

Curriculum vitae not included in digital version.

VORWORT

Die vorliegende Arbeit entstand während meiner Tätigkeit als wissenschaftlicher Mitarbeiter am Institut für Massivbau der Technischen Universität Darmstadt.

Meinem Doktorvater Herrn Prof. Dr.-Ing. Carl-Alexander Graubner danke ich aufrichtig für seine Unterstützung, das mir entgegengebrachte Vertrauen und die mir eröffneten Möglichkeiten. Sie haben mir viel beigebracht.

Herrn Prof. Marc A. Maes, PhD, möchte ich sehr herzlich für das Interesse an meiner Arbeit und für die Übernahme des Korreferates danken.

Meinen aktuellen und ehemaligen Kolleginnen und Kollegen danke ich ganz besonders für die in beruflicher und privater Hinsicht ausgesprochen herzliche und angenehme Zeit am Institut, an die ich mich gerne erinnern werde. Meinen Zimmerkollegen Herrn Dr.-Ing. Frank Ritter, Herrn Dipl.-Wirtsch.-Ing. Torsten Mielecke und Herrn Dr.-Ing. Tilo Proske danke ich für das stets vorhandene Interesse und die Diskussionsbereitschaft bezüglich meiner Forschungsarbeit. Frau Renate Mohr danke ich für die vielfache Unterstützung im Rahmen meiner Tätigkeit am Institut. Diesen Personen danke ich außerdem besonders für die aus unserer gemeinsamen Zeit am Institut erwachsene Freundschaft.

Ein ganz besonderer Dank geht an Herrn Dr.-Ing. Simon Glowienka, der mich bei der Anfertigung der Arbeit in besonderem Maße unterstützt hat und bereits als Betreuer meiner Diplomarbeit Begeisterung für die Zuverlässigkeitstheorie in mir geweckt hat.

Ein weiterer, ganz besonderer Dank geht an Prof. Shelley Lissel, PhD, für die Beratung bei der Erstellung und Durchsicht meiner Arbeit.

Der größte Dank gilt meiner lieben Frau Elisabeth und meinen Eltern, Dipl.-Ing. Wolfgang und Uta Brehm. Ohne Euch wäre dies alles nicht möglich gewesen.

Darmstadt, September 2011 Eric Brehm

Zusammenfassung

Aussteifungsscheiben sind integrale Bauteile in Mauerwerksgebäuden, werden in der Bemessungspraxis jedoch selten nachgewiesen. Dies liegt an einer in DIN 1053-1 enthaltenen Regelung, die es erlaubt den Aussteifungsnachweis auszulassen. Diese Regelung basiert jedoch auf gänzlich anderen Bauweisen als sie aktuell im Stand der Technik sind. Des Weiteren sind die Tragfähigkeiten auf Basis aktuellen Bemessungsnormen an den Vorgängernormen und Erfahrungswerten kalibriert worden. Daher stellt sich die Frage nach dem tatsächlich vorhandenen Zuverlässigkeitsniveau dieser Wandscheiben.
Diese Arbeit enthält eine systematische Analyse der vorhandenen Zuverlässigkeit von Aussteifungsscheiben in üblichen Mauerwerksgebäuden. Dabei werden verschiedene analytische Modelle zur Bestimmung der Querkrafttragfähigkeit von Aussteifungsscheiben untersucht und deren Modellunsicherheit bestimmt über einen Auswertung von Versuchsdaten. Ziel ist die Identifikation des realistischsten Modells.
Ein vollständiges stochastisches Modell wird anschließend aufgestellt und die vorhandene Zuverlässigkeit einer Vielzahl von Wandscheiben bestimmt. Dabei wird zwischen rechnerischer und „eigentlicher“ Zuverlässigkeit unter Berücksichtigung des Ausnutzungsgrades der Wandscheiben unterschieden.
Abschließend wird ein volkswirtschaftlich optimaler Wert der Zuverlässigkeit mit der Methode der voll-probabilistischen Optimierung bestimmt, um so einen Vergleichswert für die vorhandene Zuverlässigkeit zu erhalten. Eine wirtschaftliche Ausnutzung des Mauerwerks bei Bemessung nach DIN 1053-1 kann dabei nachgewiesen werden.

Abstract

Bracing walls are essential members in typical masonry structures. However, design checks are only performed rarely in Germany. The reason for this is a paragraph in the German design code DIN 1053-1 which allows for neglection of this design check. This paragraph is based on different construction methods than they are the current state of the art. Additionally, the capacities according to current design codes have been calibrated on basis of previous design codes and experience. Consequently, the provided level of reliability remains unknown.
In this thesis, a systematic analysis of the provided level of reliability is conducted. Analytical models for the prediction of the shear capacity of the walls are analyzed and assessed with test data to identify the most realistic model. A complete stochastic model is set up and the reliability of typical bracing walls is determined. It is differed between the theoretical level of reliability and the “actual” level of reliability taking into account the realistic utilization of the walls.
Finally, an optimal target value for the reliability is derived by full-probabilistic optimization to be able to assess the previously determined provided reliabilities. An efficient use of masonry in the design according to DIN 1053-1 can be verified.

Table of Contents

NOTATION AND ABBREVIATIONS

ψ	combination factor according to DIN EN 1990/NA
ψ	factor to regard the moment distribution over the wall; load combination factor according to DIN 1055-100
$\lambda(p)$	intensity of Poisson process depending on parameter p
λ_I	Likelihood estimators
λ_v	shear slenderness ($\lambda_v = \psi \cdot h_s/l_w$)
σ_X	standard deviation of X
$\rho_{X,Y}$	coefficient of correlation of X and Y
A_w	factor that accounts for times of reconstruction
b	constant benefit derived from a structure (monetary)
$B(p)$	benefit derived from a structure depending on parameter p (monetary)
$C(p)$	structural cost depending on parameter p (monetary)
C_0	structural cost (constant)
CoV_X	coefficient of variation of X, also referred to as V_X
$D(p)$	term affiliated with risk depending on parameter p (monetary)
e	eccentricity, [m]
$f(p)$	risk indicator, [-]
$f(x,y)$	function of x and y
F^*	regression parameter, [-]
f_b	compressive strength of unit, [N/mm²]
f_{bt}	tensile strength of unit, [N/mm²]
f_m	compressive strength of masonry, [N/mm²]
f_{mo}	compressive strength of mortar [N/mm²]
f_v	shear strength, [N/mm²]
f_{v0}	cohesion, [N/mm²]
$g(x)$, $G(x)$	function of x
H	failure consequences (monetary)
H	failure consequences (monetary)
h	height of wall, [m]
L	Likelihood density
l_w	length of wall, [m]
m_X	mean of X
n	number of tests, samples etc.

t	thickness, [m]
$Z(p)$	target function for parameter p
α	factor accounting for long-term effects (α = 0.85 according to DIN 1053)
α_i	sensitivity values
α_u	level of utilization
α_w	factor that accounts for roughness of terrain
β_R	compressive strength of masonry according to DIN 1053-1, [N/mm²]
β_{RHS}	cohesion according to DIN 1053-1, [N/mm²]
β_{RZ}	tensile strength of unit according to DIN 1053-1, [N/mm²]
λ	buckling slenderness ($\lambda = h_k/t$)

Definition of non-dimensional quantities:

$n_i = \frac{N_i}{t \cdot l_w \cdot f_k}$	axial load
$v_i = \frac{V_i}{t \cdot l_w \cdot f_k}$	horizontal shear load

Abbreviations and acronyms

AAC	autoclave aerated concrete (here, mostly refers to the unit-mortar-combination 4 / TLM)
C	concrete
CB	clay brick (here, mostly refers to the unit-mortar-combination 12 / GPM IIa)
CS	calcium silicate (here, mostly refers to the unit-mortar-combination 20 / TLM)
GPM	general purpose mortar
LDC	light-density concrete
LM	lightweight mortar
MCS	Monte Carlo-Simulation
PDF	probability distribution function
RC	reinforced concrete
TLM	thin layer mortar
URM	unreinforced masonry

1 INTRODUCTION

1.1 Motivation and Goal

Everything is uncertain. Nothing can be predicted with absolute certainty. This basic fact leads to the idea of probabilistic and stochastic treatment of problems in every possible field of interest. In structural engineering, most problems are solved by deterministic approaches to avoid difficult and complex stochastic solutions. Simplified methods, trying to combine deterministic and stochastic approaches, such as the semi-probabilistic safety concept, have been developed and represent the state of the art in structural design. Nevertheless, fully-probabilistic approaches guarantee the most efficient solutions and provide a thoroughly assessed reliability. The latter is especially important, since every structure is unique. As the basis for semi-probabilistic approaches, fully-probabilistic analyses should be performed.

Reliability and risk are key issues in a quickly developing world. Considering the substantial consequences that potentially arise in case of failure of structures, structural reliability gains special importance. Structural failure causes many consequences, not only direct consequences such as the cost of rebuilding, but many indirect consequences such as contamination of the environment, collapse of infrastructure and – most important – fatalities. In general, the socio-economic impact is significant.

Masonry is the most widely used material for walls in construction of residential and office buildings, as shown in Table 1.1-1. As one of the oldest and most traditional building materials, masonry is thought to be reliable and safe.

Table 1.1-1 Contributions of the different wall materials to the construction of residential buildings in Germany in 2007 (DGfM (2008))

Wall material	Contribution to the building volume in %	Contribution to the structural cost in %
Masonry	77.9	77.2
RC and structural steel	11.1	11.2
Timber	10.2	10.8
Other	0.8	0.8

While the experience in the application of masonry is vast, occurrences of structural failure of masonry structures are seldom reported. This, actually positive, fact leads to two major questions: Is the use of masonry efficient? If so, is the lack of reported failures a result of the large reliability of masonry or is it based on other reasons? The evaluation of the reliability of masonry members has been done empirically in the past. In more recent years, the first scientific studies on the reliability of masonry members have been published (*Schueremans (2001)*; *Glowienka (2007)*). However, these studies focussed on the reliability of masonry members subjected to flexure. Perhaps more important to structural integrity are the masonry walls subjected to in-plane shear as part of the bracing system of

the building. For modern unreinforced masonry, reliability of shear walls has not been assessed yet.

One possible reason is the complex load-carrying behaviour of masonry walls subjected to in-plane shear. Many models exist in the literature, following different approaches. Finite element modelling is difficult and not favourable to reliability analysis due to the considerable computational capacity required and the lack of specific material data for each masonry type and unit-mortar-combination. Analytical models need to be assessed and verified with test data to enable the identification of an appropriate model that can be used in a reliability analysis to obtain realistic results. Structural reliability can only be assessed when corresponding target values and benchmarks are available, and only a few recommendations are available (see *JCSS (2001)* and EN 1990). Although the target reliability has to depend on the consequences in case of failure of the structure; it is surprising that the individual risk of a structure is usually not taken into account. The safety concept provided by the current design codes is independent of the individual risk. Recently, DIN EN 1990 introduced "consequence classes" for different kinds of structures and therefore for different severity of failure consequences. This more detailed view on the relationship between failure consequences and target reliability has not yet found its way into masonry design. Thus, the classification of the individual risk and accounting for it in the design is not yet possible. Consequently, the risk (failure consequences times failure probability) of typical masonry buildings requires investigation and definition. Another indication of the need for probabilistic assessment, especially for masonry structures, is the large difference in safety factors that are applied internationally (see Table 1.1-2) assuming that the target reliabilities are similar all over the world. In this thesis, a rational reliability analysis of unreinforced masonry shear walls will be performed and a reliable value of the target reliability will be derived.

The goal of this thesis is the evaluation of the currently provided level of reliability of masonry houses in Germany and the comparison to the current target values provided in the design codes. Additionally, a new recommendation for a target value especially for typical residential masonry structures is supposed to be derived.

Table 1.1-2 Comparison of international safety factors in masonry design (Glowienka (2007))

Country	Masonry	Load	
	γ_M [a]	γ_G [b]	γ_Q [c]
Germany	1.50	1.35	1.50
Switzerland	2.00	1.30	1.50
England	2.50 - 3.50	1.20 - 1.40	1.40 - 1.60
Australia	1.67 - 2.22	1.20 - 1.35	1.50
USA	1.25 - 2.50	1.20	1.30 - 1.60
Canada	1.67	1.25 - 1.40	1.50

[a] safety factor on the material
[b] safety factor on the dead load
[c] safety factor on the live load

1.2 Thesis Organization

To study the reliability of masonry shear walls requires several steps. The required knowledge about reliability analysis and safety concepts in structural design are presented, followed by an explanation of the load-carrying behaviour of masonry with a focus on the determination of the shear capacity. This is necessary since, without an in-depth understanding of the load-carrying behaviour, accurate prediction of the load-carrying capacity is impossible.

From the load-carrying behaviour, the relevant material properties can be identified. These will be discussed and stochastic models, necessary for the formulation of the reliability problem, will be derived. This is very important; only if the stochastic models are realistic can useful results be obtained. Some recommendations for stochastic models can be derived from the literature; others are not yet available and have to be generated from test data. Subsequently, several models for the prediction of the shear capacity will be analysed and evaluated using test data to assess the accuracy of these models. The preceding steps will include the application of Bayesian methods to update available data and to obtain more realistic results since the database is incomplete for the different masonry products and unit-mortar-combinations of modern masonry.

Since reliability of a structural member is always a result of the member's capacity as well as of the loads acting on the member, the loads also have to be analysed. The vertical loads, divided into dead and live loads, will be discussed and the required stochastic models will be provided. The relevant horizontal load that causes the occurring shear is the wind load since typical masonry structures are built upon stiff reinforced concrete basements. Therefore earth pressure is not taken into account. Additionally, this thesis focuses on the reliability of masonry structures in Germany where seismic loads almost never govern the design.

The reliability analysis is executed for a large number of masonry members. These members will be designed according to the current design codes for masonry in Germany, DIN 1053-1 (1996) and DIN 1053-100 (2007), and the current draft of the National Annex to Eurocode 6, DIN EN 1996-1-1/NA (2010), to represent common members in Germany. Thus, the reliability provided by the respective code will be obtained. The members differ mainly in unit material and slenderness ratio h_w/l_w. The parameters will be studied and analysed. As a result, the distributions of reliability for typical masonry members are derived. The results for the different codes will be compared and an average value of reliability within the practically relevant range of parameters will be defined. The values obtained for the reliability are believed to represent the status quo as societally accepted reliability and will be seen as the status quo for the reliability of masonry shear walls in Germany.

Finally, an economically optimal value of the target reliability will be determined by probabilistic optimization. In this optimization, the benefit derived from a typical masonry structure, the structural cost and the failure consequences linked to the structure are considered. Typical masonry scenarios are modelled and the failure consequences will be classified.

To conclude, the obtained reliability values are assessed and evaluated. A recommendation for the target reliability of typical masonry structures will be determined aiming at sufficiently safe and efficient design of masonry shear walls subjected to in-plane shear.

2 BASICS OF RELIABILITY ANALYSIS

2.1 General

The following chapter introduces reliability analysis as it is used in the field of structural engineering. The relevant terms will be defined and the methods of analysis which are used in this thesis will be explained. However, the field is wide; a detailed presentation of the current state of knowledge would go beyond the scope of this thesis. So, the basics will only be explained briefly. Basic understanding of mathematical, stochastic and probabilistic methods is assumed. For further information the reader is referred to *Benjamin & Cornell (1970), Spaethe (1992), Melchers (1999)* and *Rackwitz (2004)*.

2.2 Introduction

Every system, be it a structure or software, has certain constraints. These constraints are linked to the purpose of the system; in case of structural members, constraints represent the design criteria such as load-carrying capacity or thermal-insulating properties. Any shortcoming in one of the constraints will lead to poor performance of the system. In case of structural elements, this means e. g. that a member which does not provide the required load-carrying-capacity will likely fail. Since every parameter is random, a model can never be certain, and the probability of falling short in one of the constraints has to be determined. This leads to the concept of reliability analysis.

The main difference between traditional engineering approaches and methods of reliability analysis lies within the stochastic treatment of the design variables. Traditional approaches treat variables as deterministic values. By considering the variables as random, the probability of exceeding a certain limit state can be calculated. The required stochastic distributions and methods will be provided and explained in this chapter. The two most important limit states in structural engineering are serviceability limit state (SLS) and ultimate limit state (ULS). A typical formulation of a limit state is given by

$$Z = g(X) = G(X_1, ..., X_n) = 0 \qquad \text{Eq. 2-1}$$

The limit state is a function of the basic variables X_1 to X_n. These represent any considered parameter and may be typical parameters as in the deterministic models, such as e. g. dimensions or loads, but also parameters like model uncertainties or environmental conditions. It should be noted that limit states are commonly defined for a member, which is usually a component of a structural system. The reliability of the structural system will likely be different from the reliability of the member. If the structural system can be analysed well, it might be described by a set of limit state functions.

The limit state functions, however, consist of a number of basic variables, such as compressive strength or dead load. These basic variables have to be described by means of

stochastic analysis using stochastic distributions. The corresponding methods will be explained in the following section.

2.3 Stochastic Modelling of Random Variables

2.3.1 Mutual Distributions in Typical Engineering Problems

In structural engineering, most problems include more than one random variable. A very typical example is the measurement of climate data. At the same point in time, different data is obtained such as wind speed, air temperature or relative humidity of the air.

The mutual distribution in general form for the two-dimensional case (two random variables) can be calculated from the following equation.

$$F_{X,Y}(x,y) = \int_{-\infty}^{x}\int_{-\infty}^{y} f_{X,Y}(u,v)\,dudv \qquad \text{Eq. 2-2}$$

Of course, the probability density function (PDF) is the derivative of $F_{X,Y}$.

Often, the probability density function for an event under certain conditions is required, i.e. the PDF for event X under the condition that event Y occurs at the same time. The PDF for this case can be calculated from

$$f_{X|Y}(x,y) = \frac{f_{X,Y}(x,y)}{f_Y(y)} \qquad \text{Eq. 2-3}$$

The corresponding probability distribution is again the integral of the density.

A special and important case is given when the variables are stochastically independent, e.g. compressive strength and cross-sectional area of a masonry member. In this case, the conditioned PDF equals the PDF for the single variable.

$$f_{X|Y}(x,y) = f_X(x) \text{ and } f_{Y|X}(x,y) = f_Y(y) \qquad \text{Eq. 2-4}$$

The mutual PDF is then

$$f_{X,Y}(x,y) = f_X(x)\cdot f_Y(y) \qquad \text{Eq. 2-5}$$

In almost all engineering problems, the number of random variables is large and the random variables are often linked by mathematical operations. Consider the load-carrying capacity of an unreinforced concrete member subjected to centric compression. The capacity is a product of the compressive strength of the concrete X and the cross-sectional area Y. Both are random variables; thus the load-carrying capacity Z is also random. Since the load-carrying capacity is the variable of interest, its distribution has to be determined

from the distributions of compressive strength and cross-sectional area. In general formulation, the probability distribution of $Z = X \cdot Y$ becomes

$$f_Z(z) = \frac{1}{|y|} \cdot \int_{-\infty}^{\infty} f_{X,Y}\left(\frac{z}{y}, y\right) dy \qquad \text{Eq. 2-6}$$

For the complementary case of $Z = X/Y$, the PDF is

$$f_Z(z) = |y| \cdot \int_{-\infty}^{\infty} f_{X,Y}(zy, y)\, dy \qquad \text{Eq. 2-7}$$

For variables that contribute to a sum, the PDF of $Z = a \cdot X + b \cdot Y$ is

$$f_Z(z) = \frac{1}{|a|} \cdot \int_{-\infty}^{\infty} f_{X,Y}\left(\frac{z - b \cdot y}{a}, y\right) dy \qquad \text{Eq. 2-8}$$

However, functional operations of random variables normally lead to complex mathematical problems which often can only be solved by application of numerical methods. Monte Carlo simulation (MCS) has proven to be an especially valuable tool (see section 2.5.3.2).

2.3.2 Stochastic Moments

To define a probability distribution, basic information is required such as the type of distribution and the stochastic parameters. The most common parameters are the so-called stochastic moments which can be derived for several orders. The first order and second order moments, mean and standard deviation respectively, are important while higher-order moments are normally not required for the definition of a distribution. The mean represents the expected value. In case of a set of test data, the mean m_X can be calculated simply as the arithmetic mean of the sample with size n.

$$m_X = \frac{1}{n} \cdot \sum_{i=1}^{n} x_i \qquad \text{Eq. 2-9}$$

In case of a continuous distribution, the mean is determined from

$$m_X = \int_{-\infty}^{\infty} x \cdot f_X(x)\, dx \qquad \text{Eq. 2-10}$$

The mean represents the general tendency of a distribution. The scatter, however, is represented by the standard deviation, as shown in Figure 2-1. The standard deviation σ_X for a sample with size n can be calculated from Eq. 2-11.

$$\sigma_X^2 = \frac{1}{n} \cdot \sum_{i=1}^{n} (x_i - m_X)^2 \qquad \text{Eq. 2-11}$$

The square of the standard deviation is referred to as variance. Note, that the standard deviation is always positive. For continuous distributions, the variance becomes

$$\sigma_X^2 = \int_{-\infty}^{\infty} \left(x_i - m_X\right)^2 \cdot f_X\left(x\right) dx \qquad \text{Eq. 2-12}$$

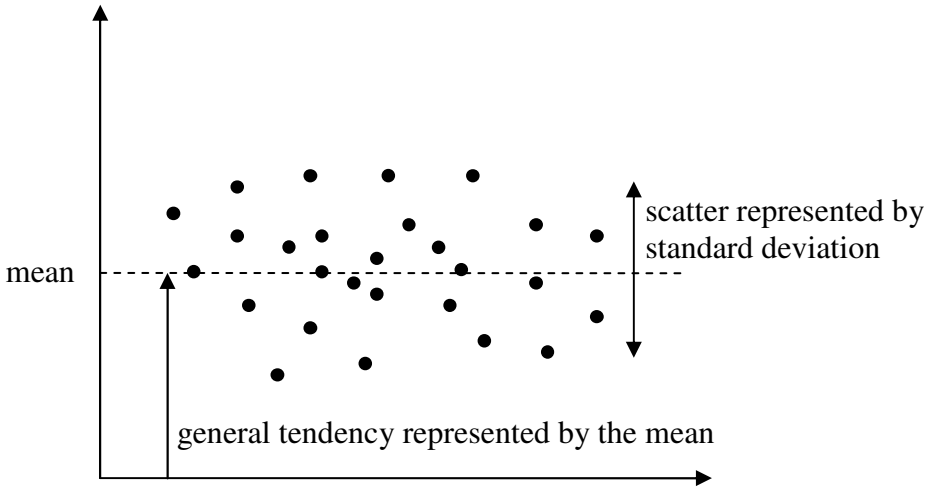

Figure 2-1 Schematic representation of mean and standard deviation

Mean and standard deviation are dimension quantities and have to be seen as a pair to compare distributions and rate the scatter. Therefore, the ratio of standard deviation-to-mean is often used for easier assessment. This ratio is referred to as coefficient of variation CoV_i or V_i and is often given in percent.

$$V_X = CoV_X = \frac{\sigma_X}{m_X} \qquad \text{Eq. 2-13}$$

In case of distributions that have a functional relation, the moments can be computed dependant on the moments of the contributing distributions. For a multiplicative relation between the uncorrelated distributions $Z = X \cdot Y$, the moments can be derived from the following equations.

$$m_Z = m_X \cdot m_Y \qquad \text{Eq. 2-14}$$

$$\sigma_Z^2 = m_X^2 \cdot \sigma_Y^2 + m_Y^2 \cdot \sigma_X^2 + \sigma_X^2 \cdot \sigma_Y^2 \qquad \text{Eq. 2-15}$$

$$CoV_Y = \sqrt{CoV_X^2 + CoV_Y^2 + CoV_X^2 \cdot CoV_Y^2} \qquad \text{Eq. 2-16}$$

For a linear relationship between the distributions with $Z = a \cdot X + b \cdot Y$, the stochastic moments for the mutual distribution are

$$m_Z = a \cdot m_X + b \cdot m_Y \qquad \text{Eq. 2-17}$$

$$\sigma_Z^2 = a^2 \cdot \sigma_X^2 + b^2 \cdot \sigma_Y^2 + 2 \cdot a \cdot b \cdot COV\left(X,Y\right) \qquad \text{Eq. 2-18}$$

where *COV(X,Y)* is the covariance. This covariance is a measure for the dependence of the variables *X* and *Y*. In the simple two-dimensional case, COV(*X*,*Y*) can be calculated from

$$COV\left(X,Y\right) = \int_{-\infty}^{\infty}\int_{-\infty}^{\infty}\left(x - m_X\right)\cdot\left(y - m_Y\right)\cdot f_{X,Y}\left(x,y\right)dxdy = m_{XY} - m_X \cdot m_Y \qquad \text{Eq. 2-19}$$

In case of independent variables, *COV(X,Y)* equals zero. The covariance is often simplified to a non-dimensional quantity for easier handling. It is then referred to as correlation coefficient $\rho_{X,Y}$ as defined in Eq. 2-20.

$$\rho_{X,Y} = \frac{COV\left(X,Y\right)}{\sigma_X \cdot \sigma_Y} \qquad \text{Eq. 2-20}$$

where $-1 \leq \rho_{X,Y} \leq 1$. A coefficient of variation of $\rho_{X,Y} = 1$ describes a full, uni-directional correlation while $\rho_{X,Y} = -1$ is a full correlation in the other direction.

2.4 Parameter Estimation

2.4.1 General

In the previous section, stochastic distributions and operations as well as stochastic moments were explained. However, the required stochastic parameters normally remain unknown and have to be estimated from test data. Since the estimates depend on the sample significantly, the obtained moments can only be considered estimates and are actually random. To obtain the true stochastic moments to describe the actual distribution of all values, an infinitely large sample size would be required. However, to derive estimates of the stochastic moments, a variety of mathematical methods is available which will be explained in the following sections.

2.4.2 Method of Moments

This method represents the easiest and most commonly used method for estimating the stochastic moments because the estimates $\overline{x}$ for mean and *s* for standard deviation are independent of the distribution type.

This yields

$$x = \frac{1}{n} \cdot \sum_{i=1}^{n} x_i \qquad \text{Eq. 2-21}$$

$$s^2 = \frac{1}{n-1} \cdot \sum_{i=1}^{n} \left(x_i - \bar{x} \right)^2 \qquad \text{Eq. 2-22}$$

Due to the dependence of the estimates on the sample size n, the question of accuracy arises. Consequently, so-called confidence intervals have been derived that give the probability that the real stochastic moments are within a given range. Assuming normal distribution, for the mean the confidence interval is

$$P\left[\bar{x} - \frac{\sigma_X \cdot k_{\alpha/2}}{\sqrt{n}} < m_X < \bar{x} + \frac{\sigma_X \cdot k_{\alpha/2}}{\sqrt{n}} \right] = 1 - \alpha \qquad \text{Eq. 2-23}$$

$$k_{\alpha/2} = \Phi^{-1}\left(1 - \alpha/2\right) \qquad \text{Eq. 2-24}$$

where $1\text{-}\alpha$ is the probability that the statement is true. In structural engineering, α is commonly chosen as $\alpha = 0.05$ (see DIN EN 1990). However, application of Eq. 2-23 requires the standard deviation σ_X. In cases of unknown standard deviation, the confidence interval becomes:

$$P\left[\bar{x} - \frac{s \cdot t_{\alpha/2;n-1}}{\sqrt{n}} < m_X < \bar{x} + \frac{s \cdot t_{\alpha/2;n-1}}{\sqrt{n}} \right] = 1 - \alpha \qquad \text{Eq. 2-25}$$

where $t_{\alpha/2;n-1}$ is the corresponding value of the t-distribution with $n\text{-}1$ degrees of freedom.

Normally, it is not clear whether the standard deviation is known or unknown. By assessing Eq. 2-23 and Eq. 2-25, *Benjamin & Cornell (1970)* found that the differences between σ_X and s become negligible for $n \geq 25$. For further information and tables, see *Kühlmeyer (2001)*.

2.4.3 Maximum Likelihood

A popular method of estimating the stochastic parameters is the so-called Maximum Likelihood principle. This method allows for direct estimation of the stochastic parameters for any differentiable distribution. The idea behind it is to calibrate the parameters in such a way that the sample provides maximum probability of occurrence (Likelihood) of the desired parameters; hence the name of the method. The mutual density of a sample with n independent random variables can be determined from the following equation.

$$L = \delta\left(x_1 \middle| \lambda_1, ..., \lambda_i \right) \cdot ... \cdot \delta\left(x_n \middle| \lambda_1, ..., \lambda_i \right) \qquad \text{Eq. 2-26}$$

where λ_i are unknown parameters of the density δ. To achieve the target, the maximum (or minimum, respectively) of this function, referred to as the Likelihood function, has to be determined. For matters of simplicity, this is often carried out by use of the logarithm of the Likelihood function. By partial differentiation and setting the equation equal to zero, a system of equations can be derived which allows for the determination of the un-

known parameters λ_i ("Maximum Likelihood estimators") which can then be used to calculate the stochastic moments of the mutual distributions. For more information, see e.g. *Papula (2001)*.

This method appears to be more difficult than the method of moments in the previous section. However, there is a significant advantage: The variance of the parameters can be calculated directly depending on the sample size. This is especially important in case of small sample sizes which are often the case in structural engineering. To determine the variance, the inverse of the Fisher matrix D has to be determined to yield the so-called variance-covariance matrix C_λ. The matrix for the two-dimensional case is

$$D(\lambda) = \begin{bmatrix} -\frac{\partial^2 \ln L}{\partial \lambda_i^2} & -\frac{\partial^2 \ln L}{\partial \lambda_i \partial \lambda_k} \\ -\frac{\partial^2 \ln L}{\partial \lambda_i \partial \lambda_k} & -\frac{\partial^2 \ln L}{\partial \lambda_k^2} \end{bmatrix} \qquad \text{Eq. 2-27}$$

$$C_\lambda = D(\lambda)^{-1} \qquad \text{Eq. 2-28}$$

Evaluation of the matrix yields the desired variances and covariances. A very important case is that of normally distributed random variables. For this case, the Likelihood function can be written as

$$L = \left(\frac{1}{\sqrt{2\pi} \cdot s} \right)^n \cdot \exp\left(-\frac{1}{2 \cdot s^2} \cdot \sum_{i=1}^{n} (x_i - m)^2 \right) \qquad \text{Eq. 2-29}$$

The corresponding logarithm is

$$\ln L = -\frac{n}{2} \cdot \ln(2\pi) - n \cdot \ln s - \frac{1}{2 \cdot s^2} \cdot \sum_{i=1}^{n} (x_i - m)^2 \qquad \text{Eq. 2-30}$$

Differentiation in terms of m and s provides the desired Likelihood estimators.

$$\frac{\partial \ln L}{\partial s} = -\frac{n}{s} + \frac{1}{s^3} \cdot \sum_{i=1}^{n} (x_i - m)^2 \qquad \text{Eq. 2-31}$$

$$\frac{\partial \ln L}{\partial m} = \frac{1}{s^2} \cdot \left(-n \cdot m + \sum_{i=1}^{n} x_i \right) \qquad \text{Eq. 2-32}$$

The corresponding elements of the Fisher matrix are

$$\frac{\partial^2 \ln L}{\partial s^2} = \frac{n}{s^2} - \frac{3}{s^4} \cdot \sum_{i=1}^{n} (x_i - m)^2 \qquad \text{Eq. 2-33}$$

$$\frac{\partial^2 \ln L}{\partial m^2} = -\frac{n}{s^2} \qquad \text{Eq. 2-34}$$

$$\frac{\partial^2 \ln L}{\partial s \partial m} = \frac{2}{s^3} \cdot \left(n \cdot m - \sum_{i=1}^{n} x_i \right) \qquad \text{Eq. 2-35}$$

2.4.4 Bayes' Theorem

As shown above, parameter estimates strongly depend on the sample size. One of the most common problems in assessing engineering problems is a lack of data. Thus, methods have to be found to make up for this shortcoming. In many cases, prior information is available in the form of data from other sources or expert's opinions. These can be used to practically enlarge the sample size and consequently lead to better estimates for the desired stochastic parameters. This method is referred to as "*Data Updating*" and is based on the theorem developed by *Thomas Bayes* (1702-1761) and published in *Bayes (1763)*.

The difference to classical statistics is the idea of introducing the stochastic parameters as random variables θ_i instead of treating them as deterministic. The parameters are considered to be correct with a certain probability. Thus, the estimators are correct with a certain, conditioned probability $P(\theta/x)$. For a very large amount of data, uncertainty in the estimation becomes negligible and thus, the parameters Θ_i would become constant.

The estimated prior parameters follow a stochastic distribution which can be updated with the new data (e.g. further test data), as shown in Figure 2-2. *Glowienka (2007)* illustrated the compressive strength of a masonry unit before and after the update as well as the corresponding Likelihood distribution. It can be seen that not only the mean but also the deviation of this posterior density could be improved significantly. It has to be mentioned that the prior and posterior distributions are often chosen to be the same type of distribution since this allows for the formulation of closed-form solutions ("conjugated priors"). A detailed description of the theory can be found in *Rüger (1999)* or *Raiffa & Schlaifer (1961)*. In the following, the method will be presented briefly.

Consider $f_X(x|\theta)$ to be the distribution of a random variable dependant on θ and $f_\theta(\theta)$ is the prior PDF of the corresponding vector of parameters, while $f_\theta(\theta|x)$ is the posterior PDF of the vector of parameters. Bayes' theorem leads to the following relationship:

$$f_\theta(\theta|x) = \frac{f_X(x|\theta) \cdot f_\theta(\theta)}{f_X(x)} = \frac{f_X(x|\theta) \cdot f_\theta(\theta)}{\int f_X(x|\theta) \cdot f_\theta(\theta) d\theta} \qquad \text{Eq. 2-36}$$

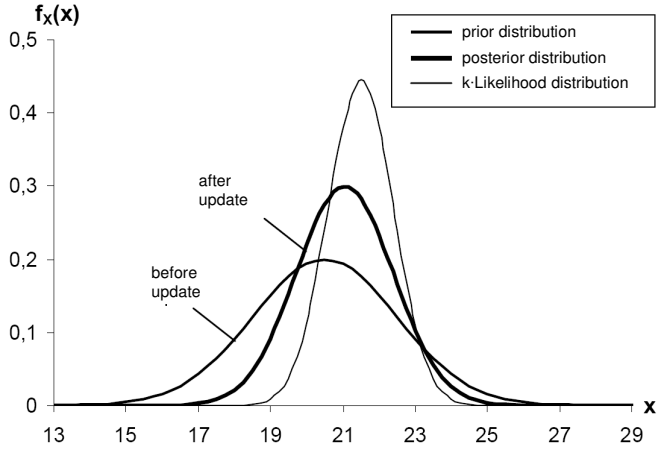

Figure 2-2 *Method of Data Updating shown by the example of normally distributed mean compressive strength of a masonry unit (Glowienka (2007))*

The integral in the denominator in Eq. 2-36 is taken over the range of θ. The PDF $f_X(x)$, which is unknown, refers to the PDF of $f_X(x|\theta)$ without the influence of the deviation of the parameter θ. This PDF can be derived from the Likelihood distribution of the measured data. For uncorrelated data, the following equation holds.

$$f_X\left(x|\theta\right) = f_X\left(x_1|\theta\right)\cdot\ldots\cdot f_X\left(x_n|\theta\right) = \prod_{i=1}^{n} f_X\left(x_i|\theta\right) = L\left(\theta|x\right) \qquad \text{Eq. 2-37}$$

The most common formulation of the posterior PDF (one stage Bayes) is

$$f_\theta\left(\theta|x\right) = k\cdot L\left(\theta|x\right)\cdot f_\theta\left(\theta\right) \qquad \text{Eq. 2-38}$$

This formulation is possible since the integral in Eq. 2-36 can be treated as a constant factor that only converts $f_\theta(\theta|x)$ into a true PDF by setting the area under the PDF equal to one.

A very important aspect of updating is its possibility of continuous application. The update can happen as often as required with the obtained posterior distribution serving as the prior distribution for the next updating cycle.

As mentioned before, larger sample sizes will make the Likelihood distribution and the Bayes' distribution approximate the real distribution of *X*. However, this leads to the fact that with growing sample size updating will become less effective. Updating is the most effective when only little prior information is available that is strongly scattered. Thus, it should be evaluated beforehand if an update can be effective.

If the PDF of *X* is provided, the prior PDF of the parameters is often chosen in such a way that the posterior PDF has the same kind of distribution ("conjugated prior distributions"). An overview of this special kind of distribution is presented in *JCSS (2001)*.

For the important case of normally distributed parameters, a closed-form solution is available. In this solution, a Gamma-distribution is chosen as the prior PDF for a normally

distributed random variable X with unknown mean and standard deviation since in this case the prior PDF equals the posterior PDF.

$$f_{M,\Sigma}(\mu,\sigma) = \frac{\sqrt{n}}{\sigma\cdot\sqrt{2\pi}}\cdot\exp\left[-\frac{n}{2}\left(\frac{\mu-m}{\sigma}\right)^2\right]\cdot\frac{\left(\frac{\nu}{2}\right)^{\nu/2}\cdot\frac{2}{s}\cdot\left(\frac{s^2}{\sigma^2}\right)^{\frac{\nu+1}{2}}}{\Gamma\left(\frac{\nu}{2}\right)}\cdot\exp\left(-\frac{\nu\cdot s^2}{2\cdot\sigma^2}\right) \quad \text{Eq. 2-39}$$

where the posterior parameters are

$$n'' = n + n' \quad \text{Eq. 2-40}$$

$$m'' = \frac{n\cdot m + n'\cdot m'}{n''} \quad \text{Eq. 2-41}$$

$$\nu'' = \nu' + \delta(n') + \nu + \delta(n) - \delta(n'') \quad \text{Eq. 2-42}$$

$$s''^2 = \frac{\nu'\cdot s'^2 + n'\cdot m'^2 + \nu\cdot s^2 + n\cdot m^2 - n''\cdot m''^2}{\nu''} \quad \text{Eq. 2-43}$$

$$\nu = n - 1 \quad \text{Eq. 2-44}$$

where $\delta(n') = 0$ for $n' = 0$ and $\delta(n') = 1$ for $n' > 0$; same for n and n''.

In many cases, prior information is available in the form of expert's opinions. This information can also be included in the updating process by transformation of this data into "equivalent" samples of data. *Rackwitz (1982)* derived this method from testing procedures for material strength. The prior parameters are

$$m' = \frac{\hat{h}}{\overline{h}} \quad \text{Eq. 2-45}$$

$$s' = \overline{h}^{-1/2} \quad \text{Eq. 2-46}$$

$$n' = \left(\breve{h} - \frac{\hat{h}^2}{\overline{h}}\right)^{-1} \quad \text{Eq. 2-47}$$

$$\nu' \approx \left(\ln\overline{h} - \tilde{h}\right)^{-1} \quad \text{Eq. 2-48}$$

$$\overline{h} = \frac{1}{k}\cdot\sum_1^k h_i;\ \tilde{h} = \frac{1}{k}\cdot\sum_1^k \ln h_i;\ \hat{h} = \frac{1}{k}\sum_1^k h_i\cdot m_i;\ \breve{h} = \frac{1}{k}\cdot\sum_1^k h_i\cdot m_i^2 \quad \text{Eq. 2-49}$$

where $m_i = \overline{x}_i$ and $h_i = 1/s^2$. Note that in this case the condition according to Eq. 2-44 does not hold anymore.
The PDF of the corresponding random variable *X* is given by Eq. 2-50. The type of the posterior PDF is a modified t-distribution; note that *X* was previously normally distributed.

$$f_Y(t) = \frac{1}{\sqrt{\pi \cdot \nu''}} \cdot \frac{\Gamma\left(\frac{\nu''+1}{2}\right)}{s'' \cdot \sqrt{\frac{n''+1}{n''}} \cdot \Gamma\left(\frac{\nu''}{2}\right)} \cdot \left[1 + \frac{t^2}{\nu''}\right]^{-\frac{\nu''+1}{2}} \qquad \text{Eq. 2-50}$$

$$t = \frac{y - m''}{s''} \cdot \sqrt{\frac{n''}{n''+1}} \qquad \text{Eq. 2-51}$$

For sufficiently large *n*, the t-distribution converges to the normal distribution and can often be approximated by a normal distribution. However, lognormally distributed random variables can also be treated similarly by transformation into the normal space. This can be done according to the following equations.

$$m_u = \ln(m_X) - \frac{1}{2} \cdot \ln\left(1 + V_x^2\right) \qquad \text{Eq. 2-52}$$

$$s_u = \sqrt{\ln\left(1 + V_x^2\right)} \qquad \text{Eq. 2-53}$$

where m_x is the mean and V_x is the coefficient of variation for the lognormally distributed random variable and m_u and s_u are the normally distributed parameters. Note that the corresponding Bayes distribution then changes from a *t*-distribution to a *log t*-distribution so that the random variable *y* has to be substituted with *ln(y)*. According to *JCSS (2003)*, this distribution can be approximated for n'', ν''> 10 with the parameters according to the following equations.

$$m_u = m_u'' \qquad \text{Eq. 2-54}$$

$$s_u = s_u'' \cdot \sqrt{\frac{n''}{n''-1} \cdot \frac{\nu''}{\nu''-2}} \qquad \text{Eq. 2-55}$$

The mean m_x and coefficient of variation V_x of the lognormal distribution can then be determined by retransformation according to Eq. 2-50 and Eq. 2-51.

$$m_x = \exp\left(m_u - \frac{1}{2} \cdot s_u^2\right) \qquad \text{Eq. 2-56}$$

$$V_x = \sqrt{\exp\left(s_u^2\right) - 1} \qquad \text{Eq. 2-57}$$

2.5 Structural Reliability

2.5.1 General Idea and History of Reliability Analysis

Structures have to be safe, reliable and serviceable over their service life. While most people have an idea about the terms “safety” and “serviceability”, the term “reliability” remains abstract. In contrast to the two former terms, reliability can be clearly quantified and calculated. Thus, it is useful for engineering practice since it can be considered a property of the respective structure. Safety and serviceability cannot be quantified in terms of figures. The only thing the user should be aware of is the fact that no structure can ever be totally safe. This is impossible due to the random nature of every property. Therefore reliability is required as a measure of the probability that a structure will stay safe and serviceable.

To ensure design of reliable structures different concepts have been developed. The currently used concepts have several things in common; they are deterministic and define safety factors that are applied to so-called characteristic values of resistance and load to either increase or reduce a certain property. These safety factors need to be calibrated and a possible method is probabilistic analysis. More information on the safety concepts is provided in section 2.7.

Structural reliability is a function of the probability of failure which can be calculated by stochastic treatment of engineering design problems. In the following, typical methods for the calculation of the probability of failure will be explained. A certain focus will be set on the definition of the target reliability, a value that includes economic and cultural aspects. This value is important since it can change design from efficient to inefficient and is responsible for safe or unsafe structures. In the past, mainly empirical methods have been used for the calibration of this value. Figure 2-3 shows the traditional, empirical determination (“trial and error”) of optimal design using a wall as an example.

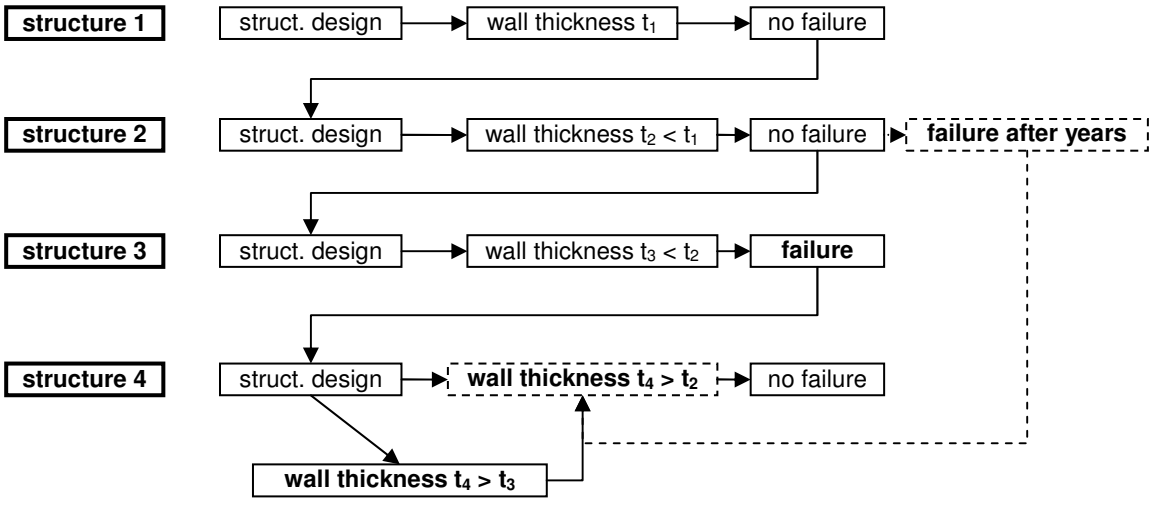

Figure 2-3 Empirical derivation of optimal design

Mayer (1926) suggested consideration of deviations in design by stochastic methods to achieve better design in terms of safety and reliability. The advantages of a stochastic approach are obvious; the reliability of new kinds of structures, construction methods or materials can be assessed without many years of application history. Due to the fact that reliability is a property of a structure that can be calculated, it can be introduced into codes and thus foster a consistent design of structures. However, due to the complex mathematical solutions and lack of computational capacity, it took years until this approach became a research focus. *Freudenthal (1947, 1956)* provided especially valuable ideas and progress to the theory of structural reliability.

The safety concepts that are used in current design codes were essentially developed in the 1960s and 1970s. However, the development of the safety concepts was hampered by the lack of data for the calibration of the safety factors, together with the complex mathematical treatment. Thus, it was attempted to derive simplified solutions. In 1976, the *CEB (Comité Euro-International du Beton)* developed the *First Order Reliability Method* (FORM), see *CEB (1976)*. In the same year, the *Joint Committee on Structural Safety (JCSS)* was founded. Ever since, this committee has supported the evolution of reliability methods and stochastic techniques as well as the enlargement of the available database. The findings led to the publication of the "Probabilistic Model Code" (*JCSS (2003)*) which provides stochastic models for various basic variables in civil engineering. However, a section on masonry is still missing. Additionally, the *Second Order Reliability Method* (SORM) was developed which provided engineers with a simplified method for the determination of a good estimate of the reliability. Today, *FORM* and *SORM* are still standard methods of reliability engineers. In the following years, *Rackwitz* at the TU München made especially significant contributions to the progress in reliability analysis (a comprehensive summary is provided in *Rackwitz (2004)*). In 1981, the basics of reliability analysis of structures in Germany were assembled in the second draft of *GruSiBau (1981)*. In 2001, *Six (2001)* applied the methods of structural reliability to nonlinear problems in concrete design.

Due to the significant improvement in computational capacity, even complex reliability problems can be solved by Monte Carlo simulation. This method is mathematically exact and simple to use though time-consuming. However, with the development of faster computers, this method has already become very important in practice.

Reliability analysis is strongly linked to socio-economic problems since reliability of structures always represents a compromise of safety and efficiency. *Rosenblueth & Mendoza (1971)* suggested a probabilistic optimization including benefit, structural cost and failure consequences (risk) for the derivation of proper target reliabilities (see section 2.6). The modelling of failure consequences is difficult, especially the modelling of fatalities in monetary units. For this purpose, an approach was developed by use of the *Life Quality Index* (*LQI*; see *Pandey et al. (2006)*). Certainly, probabilistic optimization is

complex and thus, most codes have been calibrated on the previous code if this code had proven good. Consequently, a proper evaluation of the reliability of most design codes has not been carried out.

Nevertheless, fully-probabilistic methods are more amd more frequently finding their way into practice and are already standard techniques in some fields of engineering, such as the design of nuclear power plants or in offshore engineering. Probabilistic methods are, however, not common in classical structural engineering, although their use has been permitted in special cases since the introduction of EN 1990.

2.5.2 Limit States and Basic Variables

Before a probability of failure can be calculated, failure has to be defined. This is done by definition of the limit state. Several limit states are known in structural engineering:

- Ultimate limit state (ULS)

  Exceeding of the ultimate limit state refers to failure of the member or structure. This will likely lead to serious injury or loss of human life. This limit state therefore represents the idea of safety. ULS can be subdivided into various other limit states, such as loss of the global equilibrium (tip over), buckling, cross-sectional failure, fatigue and loss of function of a structure that is combined with severe danger to human life, e.g. imperviousness of gas tanks.

- Serviceability limit state (SLS)

  In serviceability limit state, failure refers to mostly monetary losses. Structures that are not serviceable anymore will lose their value and therefore have a strong impact on economy. The largest number of legal suits that are filed related to construction, deal with issues of serviceability. However, danger to life and limb is normally not existent. A typical example of SLS failure is intolerable deformation.

Limit states can refer to the entire structure or to the single member and can be applied to every part of the structure, from slabs to foundation. Typically, several limit states apply to one structure. Limit states require definition by giving limit values for the respective criterion. This may be allowable stresses or crack widths as well as allowable deformations. These values are commonly provided in codes. Thus, codes define limit states and differences occur from code to code.

Codes do not only provide limit values for certain criteria, they also provide mechanical models that make it possible to formulate the limit state mathematically. This is a necessary requirement. The provided models depend on random variables – in reliability analysis referred to as *basic variables*. Obvious basic variables in structural engineering are e.g. compressive strength, dimensions and loads. Besides these, other important basic variables, so-called model uncertainties, have to be taken into account. These represent

the uncertainty of the prediction models for strength and loads and will be discussed in later sections.

In structural engineering, limit states can be commonly formulated in a general form as follows

$$g(x) = R - E = Z = 0 \qquad \text{Eq. 2-58}$$

where x is the vector of basic variables, R is resistance and E is load effect.

The limit state is reached for $g(x) = 0$. For values $Z < 0$ or $Z > 0$, it has to be defined whether this is "safe" or "unsafe". Herein, the limit state function will be formulated in such a way that values $Z > 0$ will be "safe" while values $Z < 0$ will be considered "unsafe". The limit state itself will still be considered safe. This assumption aligns with the Eurocodes and the ISO codes.

The formulation of the limit state function according to Eq. 2-58 requires basic variables that can clearly be defined as acting on either the side of the resistance or the load effect. In some cases this might be difficult; for example all materials with a strong interaction between axial load and flexural capacity, such as unreinforced masonry.

In most cases, resistance and load effect are independent random variables with continuous densities $f_R(r)$ and $f_E(e)$. In this case, Z also becomes a random variable with PDF F_Z.

$$F_Z = \int_{-\infty}^{\infty} f_E(e) \cdot F_R(z+e) de \qquad \text{Eq. 2-59}$$

The probability of failure P_f can be determined by solution of the following integral.

$$P_f = \int_{-\infty}^{\infty} \int_{-\infty}^{\infty} f_R(r) \cdot f_E(e) dr de = \int_{-\infty}^{\infty} F_R(e) \cdot f_E(e) de \qquad \text{Eq. 2-60}$$

Figure 2-4 shows this integral for a two-dimensional case for normally distributed random variables R and E.

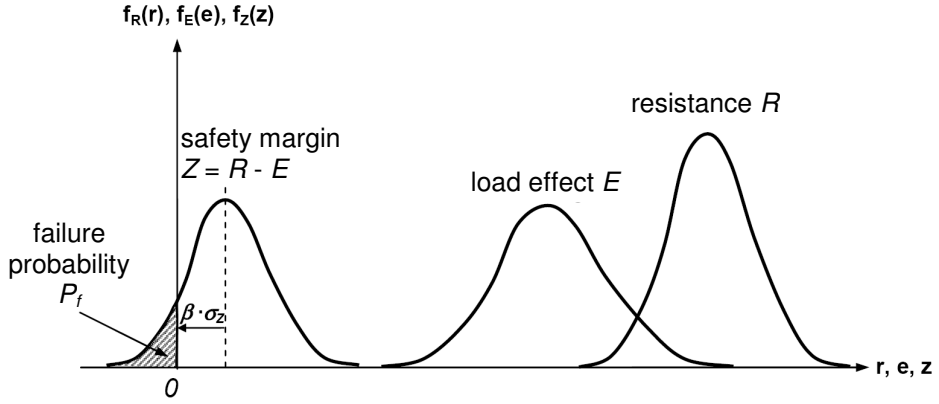

Figure 2-4 *Limit state function and probability of failure in a two-dimensional case (Glowienka (2007))*

The corresponding probability of survival R_f is

$$R_f = 1 - P_f \qquad \text{Eq. 2-61}$$

The integral in Eq. 2-60 can only be solved in closed form for a few cases. In most cases, the solution of the integral requires special methods of analysis, see section 2.5.3. For the special case of normally distributed basic variables, Z is also normally distributed and thus the moments can be calculated from

$$m_Z = m_R - m_E \qquad \text{Eq. 2-62}$$

$$\sigma_Z = \sqrt{\sigma_R^2 + \sigma_E^2} \qquad \text{Eq. 2-63}$$

The probability of failure then becomes

$$P_f = \Phi\left(-\frac{m_Z}{\sigma_Z}\right) \qquad \text{Eq. 2-64}$$

The term in parenthesis has been used by *Cornell (1969)* for the definition of the reliability index β. The advantage of this definition is the independence from the type of distribution of Z and is a measure of the distance between the design point and the mean (see Figure 2-4).

$$\beta_{Cornell} = \frac{m_Z}{\sigma_Z} = -\Phi^{-1}\left(P_f\right) \qquad \text{Eq. 2-65}$$

and thus

$$\beta_{Cornell} = \frac{1}{CoV_Z} \qquad \text{Eq. 2-66}$$

Another advantage is that only a small amount of data about the basic variables is required to determine $\beta_{Cornell}$. The stochastic moments, i.e. the mean m_i and standard deviation σ_i, of the basic variables are sufficient for approximate calculation of the structural reliability. However, it must be noted that the distribution type, the missing parameter in Eq. 2-65, can have significant influence on the failure probability especially for structural engineering problems. Failure probability is very small in structural engineering so that the upper and lower "tails" of the distribution become very important.

The more important shortcoming of this formulation is the influence of the formulation of the limit state function, as reported and discussed by *Madsen et al. (1986)*. The reason for this stems from the mathematical treatment of the limit state function. *Hasofer & Lind (1974)* proposed a modified formulation, here referred to as β. They suggested that the basic variables be transformed into the standard normal space and then defined β as the shortest distance between the failure point and the origin, as shown in Figure 2-5.

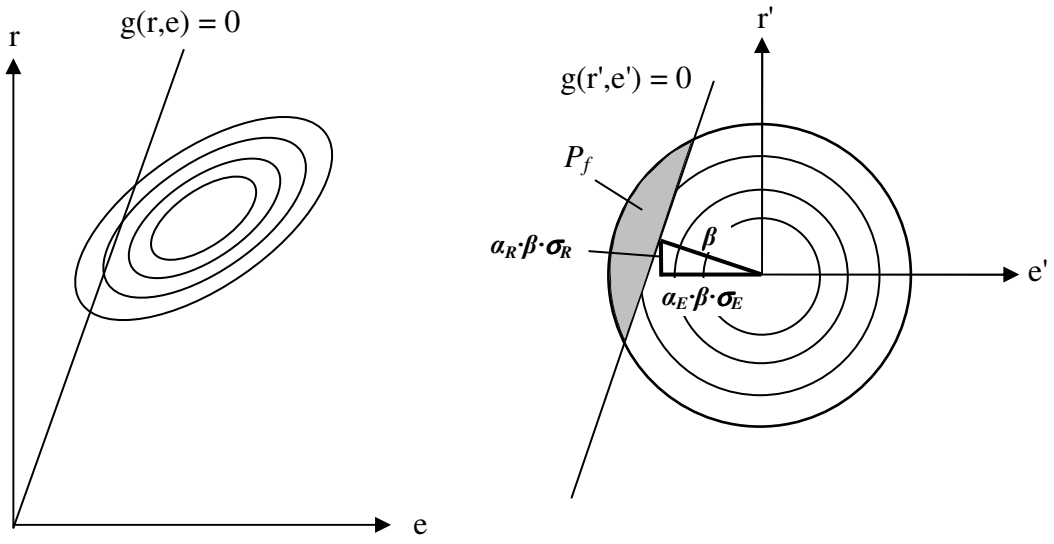

Figure 2-5 Transformation of global and transformed basic variables and definition of β

As can be seen from Figure 2-5, two new parameters, α_R and α_E, are introduced with this definition. These are referred to as sensitivity factors and can be determined for every basic variable. They represent the influence of the basic variable on the structural reliability; the larger α_i, the larger the influence. Because of the geometrical definition of α_i, the following condition has to be fulfilled.

$$\sum_{i=1}^{n} \alpha_i^2 = 1 \qquad \text{Eq. 2-67}$$

To determine the coordinates of the design point, the point that gives the largest probability of failure, the basic variables have to be retransformed. This gives the quantiles of the normal distribution.

$$e = m_E + \alpha_E \cdot \beta \cdot \sigma_E \qquad \text{Eq. 2-68}$$

$$r = m_R - \alpha_R \cdot \beta \cdot \sigma_R \qquad \text{Eq. 2-69}$$

2.5.3 Methods of Analysis

2.5.3.1 General

For the solution of the integral in Eq. 2-60, several methods are possible. These methods can generally be divided into two groups: the mathematical exact approaches and the simplified approaches. While the exact approaches require considerable computational capacity, simplified approaches are more efficient but do not provide "exact" results. *Glowienka (2007)* compared the common techniques as presented in Table 2.5-1. In the following sections, the methods will be explained briefly. For detailed information, see *Melchers (1999)* or *Rackwitz (2004)*.

Table 2.5-1 Classification of Probabilistic Methods (Glowienka (2007))

Level		Solution	PDF	LSF	Result
1	semi-probabilistic	calibration on previous codes	not required	-	partial safety factors
2	simplified	FOSM[a]	only normal	linear approximation	approximate failure probability
		FORM, SORM	all types	linear/square approximation	
3	exact	NI and MCS	all types	any	theoretical exact failure probability
4	probabilistic optimization	Level 2 and 3	all types	Any under consideration of economic data	stochastically optimized structures

[a]First Order Second Moment, a method that only works with normally-distributed basic variables.

2.5.3.2 Mathematical Exact Approaches

The most typical, mathematical exact approaches are the Monte Carlo simulation (MCS) and the method of numerical integration (NI). Both obtain the exact failure probability but require very powerful computers, especially for cases involving large numbers of variables.

Performing a MCS comprises generating random values corresponding to the statistical distributions of the basic variables. The failure probability then is determined from the number of samples *x* that do not fulfil the limit state and the total number of samples *n*.

$$P_f = \frac{x}{n} \qquad \text{Eq. 2-70}$$

This simple method is used in many scientific fields. In structural design, the application can be difficult due to the fact that the failure probabilities are very small. Typical values of P_f are in the range of 10^{-6} and so a sample size of at least a million is required. Therefore, and especially if this method is linked to Finite Element simulations with large computation time, the method becomes quite cumbersome. Therefore other methods, based on MCS, have been developed that limit the bandwidth of samples, such as Adaptive Importance Sampling (AIS). These procedures generate random values close to the limit state function (LSF) and thus reduce the total number of samples (see Figure 2-6). For further information see *Melchers (1999)*.

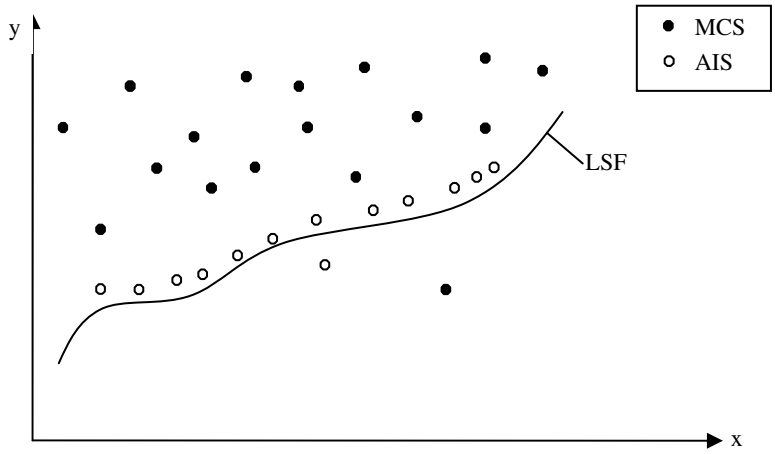

Figure 2-6 *Simplified comparison of Crude Monte Carlo Simulation and Adaptive Importance Sampling*

According to *Rackwitz (2004)*, the coefficient of variation in case of analysis by MCS can be calculated from

$$CoV\left(P_f\right) \approx \frac{1}{\sqrt{n \cdot P_f}} \qquad \text{Eq. 2-71}$$

As can be seen, large numbers of simulations are required ($n >> 1/P_f$). In case of numerical integration, the multi-dimensional integral is calculated numerically. The shortcoming is again the large required computational capacity.

2.5.3.3 Simplified Approaches

As mentioned before, problems of reliability often lead to complicated integrals that cannot be solved analytically. To avoid time-consuming numerical analysis as described in the previous section, simplified methods have been developed (see Table 2.5-1). One major advantage, besides the time-efficiency, is the smaller amount of required data.

FOSM is useful when only the stochastic moments of the basic variables are known. The method is handy due to two main simplifications. The first is the assumption of every basic variable being Gaussian normal distributed and the second is the transforming of non-linear limit state functions to linear. This can be done by applying a first-order Taylor series approximation at the design point which has to be determined by iteration. The determination of the failure probability can happen in normal space. The reliability index β is defined as the minimum distance between the design point and the origin.

The disadvantages of this method are the imprecise results in case of basic variables that do not come close to Gaussian distribution, such as live loads, and the increasing error for larger probabilities of failure.

The next level of the simplified approaches is represented by FORM. FORM is similar to FOSM but includes information about the kind of distributions. The transformation of the limit state function to a Taylor series stays the same as in FOSM. Only the first members are included so that the limit state function remains linear. The determination of the reliability index β leads to an optimization problem since the smallest value for β has to be derived. To solve this problem, the so-called *Rackwitz-Fießler* algorithm can be applied (see *Rackwitz and Fießler 1978).* In this algorithm, the basic variables that are not normally distributed are transformed into normally distributed quantities with a best match in the region of the design point. For more information, see *Melchers (1999)* and *Spaethe (1992).* An advantage of this method, besides the more exact results, is that sensitivity values α_i are obtained which allow for calculation of the design values of the basic variables in normal space and provide information about the influence of the respective basic variable on the failure probability P_f.

The most advanced simplified method is SORM. Within SORM, the limit state function is not transformed to a linear LSF but the quadratic members of the Taylor series are used as well. This leads to better results and is more time-consuming. The results obtained from SORM almost equal the results of the exact methods explained in the previous section. However, the differences in the results compared to FORM are only large in the case of LSFs with large slope.

2.6 Target Reliability and Risk-Based Optimization

2.6.1 General

In the previous sections, the idea and the determination of reliability was explained. Now, what can we gain from this? What is the concept of reliability analysis implemented in design codes?

These questions again lead to the term of "target reliability". Some international design codes (see EN 1990 and ISO 2394) give a target reliability on which the design equations should be calibrated. These values are often derived empirically and are not based on scientific methods.

Other approaches try to give the target reliability dependant on the failure consequences. It is obvious that large failure consequences in the sense of fatalities or major impact on society (just consider large infrastructure projects) should be designed to a higher degree of safety than less "dangerous" structures.

In the following, the definition of target reliability will be discussed and the method of determination by fully-probabilistic analysis will be explained.

2.6.2 Optimization of the Target Reliability

Although probabilities of failure in structural engineering are small, failure can always happen. Therefore, the question of acceptable risk arises. But what is risk and which risk is acceptable?

Many definitions of the term risk can be found in the literature. Here, "risk" refers to the product of failure consequences H and failure probability P_f and will be denoted as $D(p)$.

$$D(p) = P_f \cdot H \qquad \text{Eq. 2-72}$$

Over the centuries, structural design was subject to an empirical optimization process ("trial and error"). Structures were designed and were considered oversized if no failure occurred. The next structure was then made more efficient; meaning the cross-sections of the members decreased, and the cycle continued until eventually failure occurred. Then the opposite effect happens and cross-sections become larger again in the following structures. The procedure is schematically displayed in Figure 2-3.

This method has significant disadvantages: it requires a lot of time and experience and also requires structures that are being built repeatedly. In times of new kinds of structures – consider nuclear power plants - and building methods, this method is rather inappropriate and impractical to derive target reliabilities.

Another way of deriving the target reliability is fully-probabilistic economic optimization which was first suggested by *Rosenblueth & Mendoza (1971)*. Here, the target reliability is regarded as a compromise between benefit, costs and risk related to a structure. Therefore, it represents an economical optimization problem as formulated in the following equation.

$$Z(p) = B(p) - C(p) - D(p) \qquad \text{Eq. 2-73}$$

B(p) is the benefit derived from a structure. Note that the benefit does not necessarily have to be constant; it can depend on the vector of the optimization parameters *p*. For example, if the optimization parameter is the wall thickness (for residential and office buildings), thinner walls will lead to more area that can be rented and accordingly to larger benefit. *C(p)* represents the structural cost. The risk *D(p)* (see Eq. 2-72) should include every possible consequence of the structural failure and therefore consists of loss of material as well as loss of life. The targeting function may be expanded with other summands accounting for e.g. costs of maintenance. A typical example for a target function is presented in Figure 2-7. One major task in this method is quantification of these abstract aspects in monetary units, which will be discussed in chapter 7.

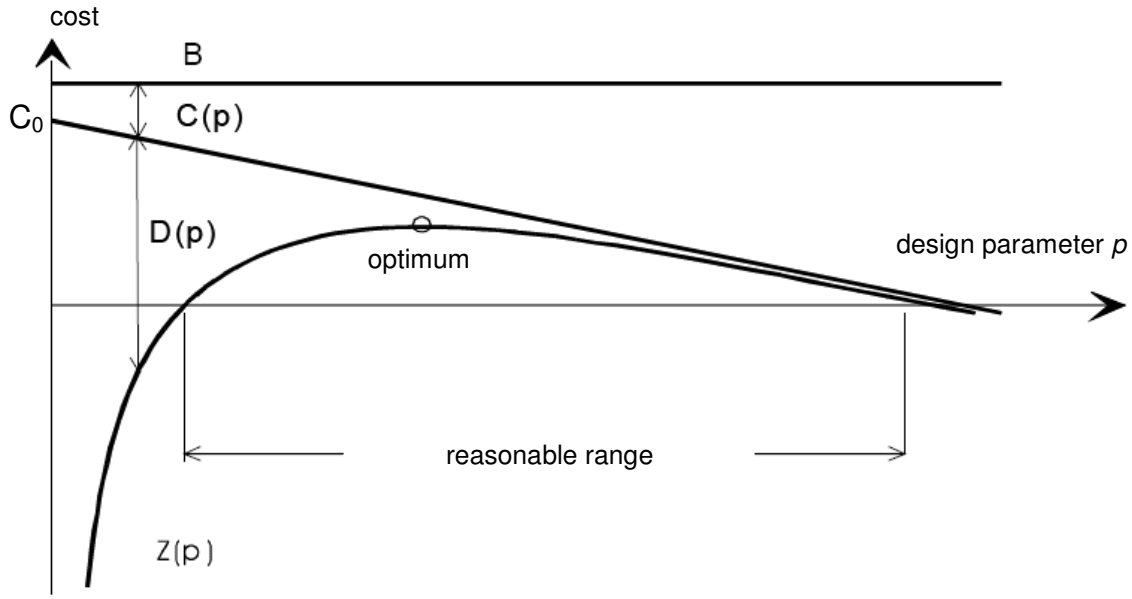

Figure 2-7 Targeting function (Rackwitz (2004))

Eq. 2-73 is formulated in a general way and can be modified to better suit structural engineering problems. In most cases, the benefit *B(p)* is constant. Hence, *B(p)* becomes the constant benefit referred to as *b*.

The structural cost *C(p)* consists of a structural cost independent of *p* and a part that depends on *p* since costs for on-site facilities, tools and even labour will not change significantly with *p*. This gives

$$C(p) = C_0 + \sum c_i \cdot p_i \qquad \text{Eq. 2-74}$$

where c_i is the cost for the single structural element. Usually, C_0 is large compared to $\Sigma c_i \cdot p_i$.

A very important aspect in fully-probabilistic optimization is discounting. The decision for or against a project has to be made at a certain point in time ($t = 0$). The optimization has to account for the service life t_s of a structure and therefore discounting effects are important. Hence, every aspect that is related to $t = t_s$ has to be discounted. This applies to the benefit b and the risk $D(p)$. The structural cost $C(p)$ occurs at $t = 0$. For simplicity, a continuous discounting function $\delta(t)$ should be used (*Rackwitz (2008)*).

$$\delta(t) = e^{-\varphi \cdot t} \qquad \text{Eq. 2-75}$$

with φ being the discount rate.

The discount rate should represent the mean real discount rate over the observation period. In the literature, values ranging from 2% to 5% can be found (see *Rackwitz (2004)*). Applying Eq. 2-75 to the benefit b yields

$$B(p) = \frac{b}{\varphi} \cdot e^{-\varphi \cdot t} \qquad \text{Eq. 2-76}$$

The same function can be applied to the risk $D(p)$. According to *JCSS (2001)*, this gives

$$D(p) = D_0 \cdot e^{-\varphi \cdot t} \qquad \text{Eq. 2-77}$$

Note that the discount rates are valid for the observation period t. If annual discount rates φ' are supposed to be applied, these have to be converted, Eq. 2-76.

$$\varphi = \ln(1 + \varphi') \qquad \text{Eq. 2-78}$$

Of course, every structure has a different setting. Some will be rebuilt directly after failure, others probably will not. Therefore, the target function has to be modified for different scenarios. The modifications mainly affect the risk concerning term. For failure of the structure directly after completion, the targeting function becomes:

$$Z(p) = B(p) - C(p) - D(p) = B(p) - C(p) - (B(p) + H) \cdot P_f(p) \qquad \text{Eq. 2-79}$$

Note that the risk $D(p)$ includes the benefit. The reason for this is that the structure is not supposed to be reconstructed and therefore no structural cost applies but the expected benefit is part of the loss. In case of systematic reconstruction, the failure cost D_0 as introduced in Eq. 2-77, includes structural cost $C(p)$ and cost due to failure consequences H.

$$D_0 = C(p) + H \qquad \text{Eq. 2-80}$$

The cost due to failure consequences H should include all possible failure consequences in monetary unit and can be derived from an event tree (for example). Ideally, the failure consequences do not only include the direct cost occurring at the point of failure but also the impact on larger systems such as society. Note, that the structural cost is equal to the structural cost at the time of the original construction. Therefore, design in the first case is considered optimal. Of course, a structure that failed will unlikely be reconstructed in the same way. However, the increase in structural cost is considered negligible.

The important case of time-invariant failure during the service life of the structure can be modelled according to Eq. 2-81 (*JCSS (2001)*):

$$Z(p) = B(p) - C(p) - (C(p) + H) \cdot \frac{P_f(p)}{1 - P_f(p)} \qquad \text{Eq. 2-81}$$

Since failure becomes more probable for a longer observation period, failure probability can be linked to a Poisson process. Time-variant actions are often modelled by a Poisson process (see e.g. *Spaethe (1992)*) since this corresponds to increasing probability of occurrence with time. Other processes may also be used, as explained by *Rackwitz (2004)*. However, a Poisson process is commonly used in structural engineering for the modelling of time-dependent events.

Introducing the intensity $\lambda(p)$ of the Poisson process – often referred to as failure rate - into the targeting function, gives Eq. 2-82 for structures without systematic reconstruction and Eq. 2-83 in the complimentary case.

$$Z(p) = \frac{b}{\varphi} - C(p) - \left(\frac{b}{\varphi} + H\right) \cdot \frac{\lambda(p)}{\varphi - \lambda(p)} \quad \text{without reconstruction} \qquad \text{Eq. 2-82}$$

$$Z(p) = \frac{b}{\varphi} - C(p) - (C(p) + H) \cdot \frac{\lambda(p)}{\varphi} \quad \text{with reconstruction} \qquad \text{Eq. 2-83}$$

In the case of reconstruction, the discrete reconstruction period has to be considered since during this period, the structure can neither produce benefit nor fail. *Rackwitz (2004)* recommended the following factor A_w to take this into account.

$$A_w = \frac{E_R}{E_t + E_R} \qquad \text{Eq. 2-84}$$

with E_t being the service life of the structure and E_R representing the reconstruction time.

2.6.3 Societal Risk Acceptance and Life Quality Index

Risk acceptance is an intensively discussed matter with strong philosophical issues. Within the scope of this thesis, the following will only give a brief introduction into the topic. For further information, the reader is referred to *Rackwitz (2004)*.

In the optimization of the target reliability, a unified standard to account for all aspects is required. In the literature, it is common to use a monetary unit as the basis of optimization (e.g. *Rackwitz (2004)*). However, when it comes to failure and loss of human life, a monetary approach is questionable. Is it ethically correct to rate life in such a way? And if so, how can this be done?

Current approaches to risk of human life do not define a monetary value for a human life. Instead, there is often reference to a "cost to reduce risk to human life". The most detailed and probably best definition has been derived by *Tengs et al. (1995)* who define the cost to "*reduce the probability of premature death by some intervention changing the behaviour and/or technology of individuals or organizations*". However, a definition like this still has to maintain the limits of society's ethics and moral principles which are commonly established in the constitutions of the respective states.

One major issue in risk assessment is risk perception. It is a well-known fact that risks are perceived differently from the actual importance. Just consider the fact that smoking is a known cause of cancer and the authorities even attempt to make people realize this by different methods. However, the number of smokers is still increasing. On the other hand, terrorist attacks are a major concern among the public, although the probability of dying in a terrorist attack is essentially smaller than the probability of dying because of smoking-related cancer. This subjective risk perception is an important issue in risk assessment since it may lead to irrational risk controlling measures, something that society cannot afford. Only a reasonable judgement of risk in the context of all risks associated with society's financial power will lead to material prosperity which is the basis for a gain in life quality. Studies showed (see *Tengs et al. (1995)*) that only 10% to 20% of the gross domestic product is spent on public health and risk reduction while a large part is wasted. This shows the necessity of reasonable public risk management.

Several concepts for the rating of risk to human life have been developed that mostly link the cost associated with a fatality to values of economy, such as the gross national product. The most common approach is based on the *Life Quality Index* (*LQI)* as suggested by *Nathwani et al. (1997)*. The *LQI* can be seen as a social indicator representing the quality of life in a respective country. *LQI* is a function of the gross domestic product per capita g and other parameters like the life expectancy at birth e and the fraction of life devoted to earning a living (*Pandey et al. (2005)* and *Pandey et al. (2006))*.

$$LQI = g^{w} \cdot e^{(1-w)} \qquad \text{Eq. 2-85}$$

In this equation, e is the life expectancy at birth (in years) and w is the percentage of time that is spent earning a living. In industrialized countries, w ranges from 15% to over 20%. The *LQI* is an indicator that includes basic human needs and concerns: wealth, life expectancy and free time to enjoy life. These concerns are linked, as it can be seen in Figure 2-8. The industrial nations are located in the right half of the figure equalling high g and large e. The *LQI* can be interpreted in many ways; an extensive discussion can be found in *Rackwitz & Streicher (2002)*. Essentially, one has to understand that many aspects cannot be part of the *LQI* since the *LQI* has been formulated to be able to judge investments toward saving lives. Aspects other than the mentioned ones, for example loss of cultural heritage, are hard to account for directly and do not contribute to the idea of the *LQI*.

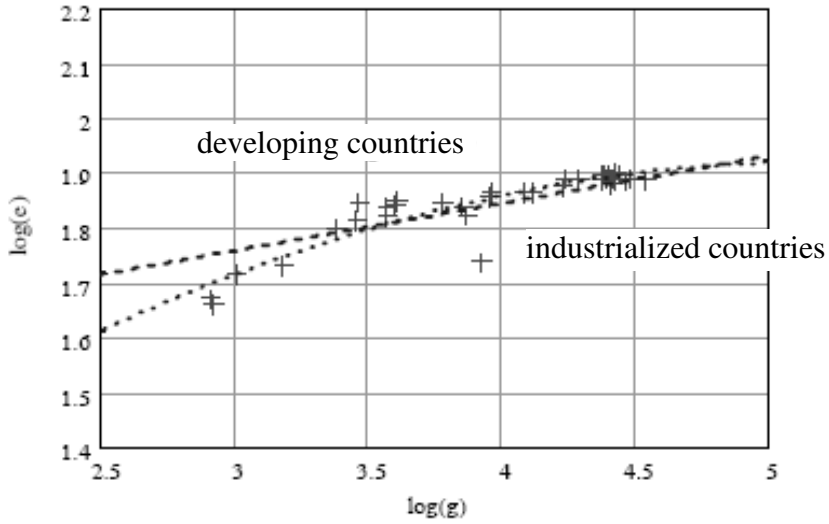

Figure 2-8 Life expectancy e over gross domestic product g (Rackwitz (2004))

From the idea of the *LQI*, *Skjong & Ronold (1998)* developed a concept to account for cost related to risk to human life and limb. With this concept the "societal life saving cost" (*SLSC*) (sometimes also referred to as "**i**mplied **c**osts of **a**verting a **f**atality" (*ICAF*)) can be computed. The idea behind the derivation of *SLSC* is to find the cost $-\Delta g$ per year required to extend a person's life by Δe. This gives

$$-\Delta g = g \cdot \left[1 - \left(1 + \frac{\Delta e}{e} \right)^{1-\frac{1}{w}} \right] \qquad \text{Eq. 2-86}$$

Due to the fact that $-\Delta g$ is an annual cost and the *SLSC* has to be invested at the decision point in time $t = 0$, Eq. 2-86 should be multiplied with $e_r = e/2$ corresponding to using half the life expectancy e to derive the SLSC. It is therefore assumed that the average fatality in case of structural failure happens after having lived half the average life expectancy.

This yields

$$SLSC(e_r) = |\Delta g| \cdot e_r \qquad \text{Eq. 2-87}$$

A selection of values for *SLSC* is presented in the following table.

Table 2.6-1 Selected social indicators and SLSC according to Rackwitz (2004)

Country	g[a]	e[b]	w	*SLSC*
Canada	27330.16	78.84	0.13	$1.3 \cdot 10^6$
USA	34260.22	77.86	0.15	$1.6 \cdot 10^6$
Germany	25010.15	78.87	0.12	$1.1 \cdot 10^6$
Czech Rep.	12900.67	73.77	0.17	$4.6 \cdot 10^5$
[a]private consumption in PPP in US$ [b]quality life expectancy in years				

2.6.4 Classification of Failure Consequences

Failure consequences are the sum of the monetary equivalent of all the aspects that are related to a certain failure scenario. The failure consequences of a scenario can be classified by relating the structural cost *C(p)* to the costs in case of failure *H*. *JCSS (2001)* suggests the use of the following ratio.

$$f(p) = \frac{C(p) + H}{C(p)} \qquad \text{Eq. 2-88}$$

The cost in case of failure *H* is governed by the cost associated with fatalities. So, *H* becomes

$$H = n \cdot k \cdot SLSC \qquad \text{Eq. 2-89}$$

with *n* being the number of people in the building at the time of failure, *k* being the parameter representing the ratio of fatalities-per-person according to Table 2.6-2 and *SLSC* being the "Societal Life Saving Cost" as defined in the previous section.

Table 2.6-2 Estimates for k according to Rackwitz (2004)

Type and cause of failure	*k*
Earthquake	0.01-1.0
Avalanches, rock fall, explosions, impact etc.	0.01-1.0
Floods and storms	0.0001-0.01
Sudden structural failure in places of public entertainment	0.1-0.5
Fire in buildings	0.0005-0.002
Fire in road tunnels	0.01-1.0

This yields

$$f(p) = \frac{C_0 + n \cdot k \cdot SLSC}{C_0} \qquad \text{Eq. 2-90}$$

for the indicator *f(p)*. *JCSS (2001)* gives reference values for this criterion summarized in Table 2.6-3.

Table 2.6-3 Reference values for f(p) according to JCSS (2001)

Range of *f(p)*	Failure consequences	Examples of structures
$f(p) \leq 2$	small	agricultural structures, silos, masts
$2 < f(p) \leq 5$	medium	office, residential, industrial
$5 < f(p) \leq 10$	large	highway bridges, theatres, hospitals
$10 < f(p)$	catastrophic	-

Structures with $f(p) > 10$ should be subject to detailed cost-benefit analysis. Generally, it should be questioned whether the structure should be built at all. In most cases, masonry structures are residential or office buildings and therefore should be categorized into the medium failure consequences category ($\beta_t = 3.2$ for 50 years).

2.6.5 Target Reliability in the Literature

Target reliabilities for structures are independent of the materials or construction methods used. They are provided in some codes (e.g. ISO 2394, EN 1990). Since 2001, DIN 1055-100 defined the target reliabilities for Germany depending on the limit state and the observation period but independent from the failure consequences and risk. This is surprising since the *GruSiBau (1981)* already defined consequence class to categorize the failure consequences and linked these to the reliability index β for an observation period of 50 years.

Table 2.6-4 Target reliabilities according to DIN EN 1990/NA for commonly monitored structures

Limit state	Target reliability	
	1 yrs[a]	50 yrs[a]
Ultimate	4.7	3.8
Fatigue	-	1.5 - 3.8[b]
Serviceability	3.0	1.5
[a]observation period [b]depending on accessibility, tolerance and maintainability		

In December 2010, DIN 1055-100 was withdrawn and replaced by DIN EN 1990/NA. The regulations of DIN EN 1990/NA adopt the approach of *GruSiBau (1981)* and define similar consequence classes. For these consequence classes, the target reliability for different kinds of structures is provided.

Table 2.6-5 Consequence classes according to GruSiBau (1981) for observation period of 1 year

Consequence class	Ultimate limit state	Serviceability limit state[a]
1	No danger for human life and only small economical impact $\beta_t = 4.2$	Small economical impact and only short interference with use $\beta_t = 2.5$
2	Danger for human life and significant impact on economy $\beta_t = 4.7$	Significant impact on economy, significant interference with use $\beta_t = 3.0$
3	Large meaning of the structure to society $\beta_t = 5.2$	Large economical impact, large interference with use $\beta_t = 3.5$
[a]If exceeding SLS results in danger for human life, the case should be treated as ULS.		

A different approach is suggested by the *JCSS (2001)*. Not only the risk to human life and limb but also the risk of investment is taken into account by linking the target reliability to the relative cost of enhancing the structural reliability. The required target reliability can then be determined from the following table.

Table 2.6-6 Target reliabilities according to JCSS (2001) for an observation period of 50 years

Relative cost for enhancing the structural reliability	Failure consequences		
	Minor[a]	Average[b]	Major[c]
large	$\beta = 1.7$ ($P_f \approx 5 \cdot 10^{-2}$)	$\beta = 2.0$ ($P_f \approx 3 \cdot 10^{-2}$)	$\beta = 2.6$ ($P_f \approx 5 \cdot 10^{-3}$)
medium	$\beta = 2.6$ ($P_f \approx 5 \cdot 10^{-3}$)	$\boldsymbol{\beta = 3.2}$ **($\boldsymbol{P_f \approx 7 \cdot 10^{-4}}$)**[d]	$\beta = 3.5$ ($P_f \approx 3 \cdot 10^{-4}$)
small	$\beta = 3.2$ ($P_f \approx 7 \cdot 10^{-4}$)	$\beta = 3.5$ ($P_f \approx 3 \cdot 10^{-4}$)	$\beta = 3.8$ ($P_f \approx 10^{-5}$)
[a]e.g. agricultural buildings [b]e.g. office buildings, residential buildings or industrial buildings [c]e.g. bridges, stadiums or high-rise buildings [d]recommendation for regular cases			

2.7 Safety Concepts in Structural Design

The reliability aspect has to be implemented into every day practice. In general, there are two different options: either applying fully-probabilistic methods or using simplified approaches.

Fully-probabilistic approaches are complex as has been shown in the preceding sections. They require a large amount of available data and computation capacity and thus are expensive and time-consuming. Currently, fully-probabilistic analyses are only appropriate in cases of out-of-the-ordinary structures.

Therefore, simplified methods are more common and are a part of every structural code. In the past, the so-called global safety factor concept has mainly been used. In this safety concept, just one single factor is applied to either increase the load effect or reduce the strength. In case of masonry structures, this makes a difference due to the nonlinear inte-

raction of load effect and resistance. A typical form of a design check according to the global safety factor concept is shown in Eq. 2-91.

$$\gamma_{gl} \cdot E = R \qquad \text{Eq. 2-91}$$

On the one hand, this concept is easy to apply. On the other hand, the global safety factor concept cannot lead to very efficient design since it does not take into account different scatter of the basic variables or different load combinations and configurations. Hence, the semi-probabilistic safety concept with partial safety factors has been developed. In this safety concept, every main basic variable has its own partial safety factor. This makes it possible to account for different properties of the separate basic variables but also makes design more difficult. Load combinations have to be considered thoroughly. The number of load configurations can easily reach double digit numbers. In *Graubner & Brehm (2009)*, the typical number of load configurations was determined for a typical masonry building. It was shown that although the number of load combinations to be investigated is large, only a small number can govern the design. A typical expression for a design check following the concept of partial safety factors, as it is used in e.g. the German codes, is presented in Eq. 2-92.

$$\gamma_E \cdot E_k \leq \frac{R_k}{\gamma_R} \qquad \text{Eq. 2-92}$$

Note that the characteristic values are now included in the equation. Characteristic values have to be defined by the codes and are normally a percentile of the distribution of a basic variable. For the typical characteristic values of various basic variables in masonry design see chapters 3 and 0. For details on the determination of partial safety factors, see *Pottharst (1977)* and *Melchers (1999)*.

The currently applied partial safety factors in Germany are mainly based on *Schobbe (1982)* and the first draft of *GruSiBau (1981)*. Risk-based approaches have not been used explicitly. The target value of the failure probability for an observation period of 1 year was defined as $P_f = 10^{-6}$ following the recommendations of the available version of ISO 2394 at that time.

2.8 Summary

In this chapter the idea of reliability analysis is explained. Since this includes stochastic modelling of engineering problems, which are commonly modelled deterministically, the stochastic background that is required for the study in the following chapters is presented.

Functional relations between stochastic distribution as well as a number of concepts for the proper estimation of stochastic moments are introduced and explained. The concept of data updating based on the theorem of *Bayes* is explained.

After the presentation of the stochastic background, the concept of structural reliability is introduced with a brief outline of the historical development. Possible determination procedures for the failure probability are discussed and the term reliability is defined. Subsequently, the definition of the target reliability and its determination by fully-probabilistic analysis is presented. A possible targeting function is shown and the contributions of the benefit derived from a structure, the structural cost and the costs related to failure of the structure are analysed. The latter requires the quantification of abstract aspects such as loss of human life. In a reliability analysis, the concept of the Life Quality Index is a possible way of deriving the costs related to fatalities. From this index, equivalent costs, referred to as "*Societal Life saving Costs*" (*SLSC*) can be determined which make it possible to account for fatalities in a fully-probabilistic optimization.

3 LOADS ON MASONRY SHEAR WALLS

3.1 Introduction

Members in construction have to be designed to carry their respective loads over their service life. The term “load” commonly refers to actions that cause stresses in the member. Additionally, effects that may influence a member’s capacity, e. g. corrosion, are also often referred to as “loads”. Here, the term “loads” refers to acting forces on the member, such as self-weight or wind load; effects like corrosion are not part of this thesis.

As explained in chapter 2, the reliability of a member is derived from a limit state function taking into account the resistance and loads. Therefore, the modelling of the loads is as important as the modelling of the resistance to be able to obtain proper and realistic results especially if a probability of failure has to be calculated.

The field of application of masonry in Germany is mostly residential or office buildings. Additionally, Germany is not likely to be subjected to severe seismic events although earthquakes can occur. Even so, the wind load still governs the design in most cases. Furthermore, only some regions in the south of Germany experience heavy snowfall. Therefore, the governing loads on a typical masonry structure are self-weight and live load as the main vertical loads and wind load as the main horizontal load. In case of basement walls, earth pressure must also be taken into account. However, this thesis deals with bracing shear walls in masonry buildings which are not usually subject to earth pressure since nowadays basement walls (including bracing walls at this level) are constructed using reinforced concrete. Thus, masonry shear walls usually serve their bracing function above ground and consequently, wind load is the governing load case.

In this chapter, prediction models for the relevant load effects will be described and explained. The necessary stochastic parameters for the determination of the reliability in chapter 6 will be derived and provided.

3.2 Methods for the Stochastic Modelling of Load Actions

Normally, loads are variable over time and space. Additionally, their occurrence can only be predicted by deterministic methods in very few cases and so, stochastic methods have to be applied. Loads can be described as a stochastic random variable, a random process or a random field. The stochastic assessment of the loads is complex and cannot be efficient for every design case. Thus, simple design models have been derived such as uniformly distributed loads that are actually a special case of a time-dependent random function.

The modelling of load actions depends on the kind of load. Loads are commonly classified into three categories:

Dead loads are loads that act permanently on a member, i.e. the scatter around the mean is small and the variation is low. The term dead load mainly refers to self-weight of the structure.

Live loads are loads that change significantly and often with time. In common construction the term live load refers mainly to loads related to the occupancy of a structure. However other loads such as wind load, snow load and temperature loads are actually live loads as well. For clarity, only loads due to the use of a structure will be referred to as live loads herein.

Accidental loads are loads of large quantity but small probability of occurrence over the observation period. Additionally, the duration of occurrence is short. Typical accidental loads are earthquakes, impact, explosions, avalanches and debris.

However, in structural modelling, loads lead to structural responses which are actually the main interest of the designer. Every load event is a chain of basically four events: the cause of the load event, the load action, the load effect and the structural response. For illustration, consider snow load on a roof. The load event is freezing of water in clouds, the load action is snow fall, the load effect is snow load on the roof and the corresponding structural response is the bending moment in the girders and the corresponding deflection.

This chain is difficult to model due to its three-dimensional variability. In reliability analysis, stochastic processes are the most common approach. For matters of simplification it has proven effective to convert the distributions derived from the stochastic process and stochastic fields to distributions of extremes.

Current load modelling codes define characteristic values of loads that are then used for design in combination with safety factors. The characteristic values are quantiles of the stochastic distribution of the loads and consequently correspond to a certain probability of exceedance. Dead loads are normally only slightly variable and can act favourably or unfavourably on a structure. Thus, the characteristic value is defined as the mean (50%-quantile) in most codes.

In contrast, live loads and especially wind and snow loads are heavily scattered and are defined as the 98%-quantile of a distribution of extremes in *DIN EN 1990/NA* for an observation period of 1 year. A conversion to other observation periods can occur by applying the theory of extremes, as explained, for example, in *Spaethe (1992)*. Another possible way of defining the characteristic value of live loads is definition by probability of occurrence, e.g. the design wind load is the wind load that would only be exceeded once in 50 years.

Structural design is carried out for limit states representing scenarios with extreme loads, normally maximum and minimum loads have to be considered. These values represent extreme values over a relatively long observation period. While instantaneous values can

be determined by measurement, extremes normally have to be predicted and the use of distributions of extremes has proven effective for this purpose. A popular method was developed by *Gumbel (1958).* The load amplitude is considered stationary and the load events are assumed to be independent. Then it is assumed that the instantaneous values are distributed with $F_x(x)$. The amplitudes change suddenly from one point in time t_i (i = 1, 2, 3…, n) to another and follow a stepped pattern with constant impulse duration d. The recurrence period of amplitude with a value of r is referred to as T_R (see Figure 3-1).

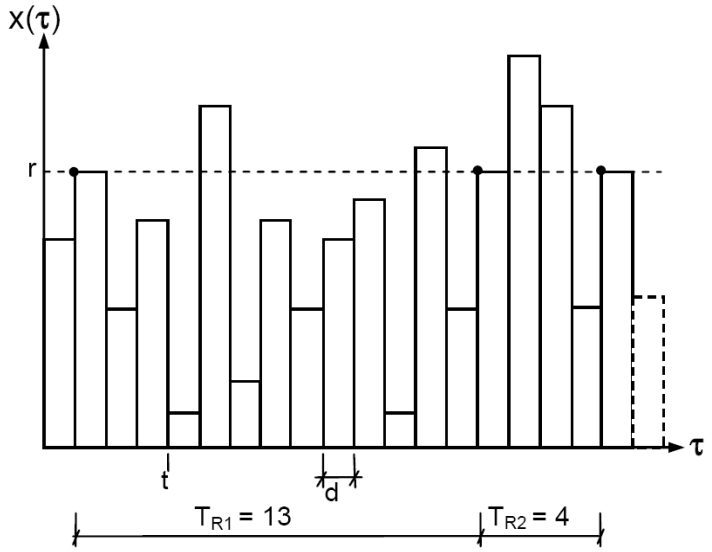

Figure 3-1 Approximation of a load process according to Glowienka (2007)

The distribution of the independent maximum values $F_y(x)$ over the observation period [0, T] with the discrete parameter $n = T/d$ adds up to

$$F_Y(x) = F_{\max}(x) = \left(F_X(x)\right)^n \qquad \text{Eq. 3-1}$$

$$f_Y(x) = n \cdot \left(F_X(x)\right)^{n-1} \cdot f_X(x) \qquad \text{Eq. 3-2}$$

For the independent minimum values the distribution can be derived in an analogous way.

$$F_Z(x) = 1 - \left(1 - F_X(x)\right)^n \qquad \text{Eq. 3-3}$$

$$f_Z(x) = n \cdot \left(1 - F_X(x)\right)^{n-1} \cdot f_X(x) \qquad \text{Eq. 3-4}$$

Gumbel (1958) showed that the distributions of extremes converge to basically 3 kinds of distribution referred to as *Gumbel*-, *Frêchet*- and *Weibull*-distribution (also referred to as Type I, Type II and Type III). *Frêchet*- and *Weibull*-distributions are different from the *Gumbel*-distribution due to their slope, as can be seen in Figure 3-2. Another main difference is the upper and lower limits; while Type I distributions are unlimited in both direc-

tions, Type II distributions provide a lower limit and Type III distribution provide an upper limit.

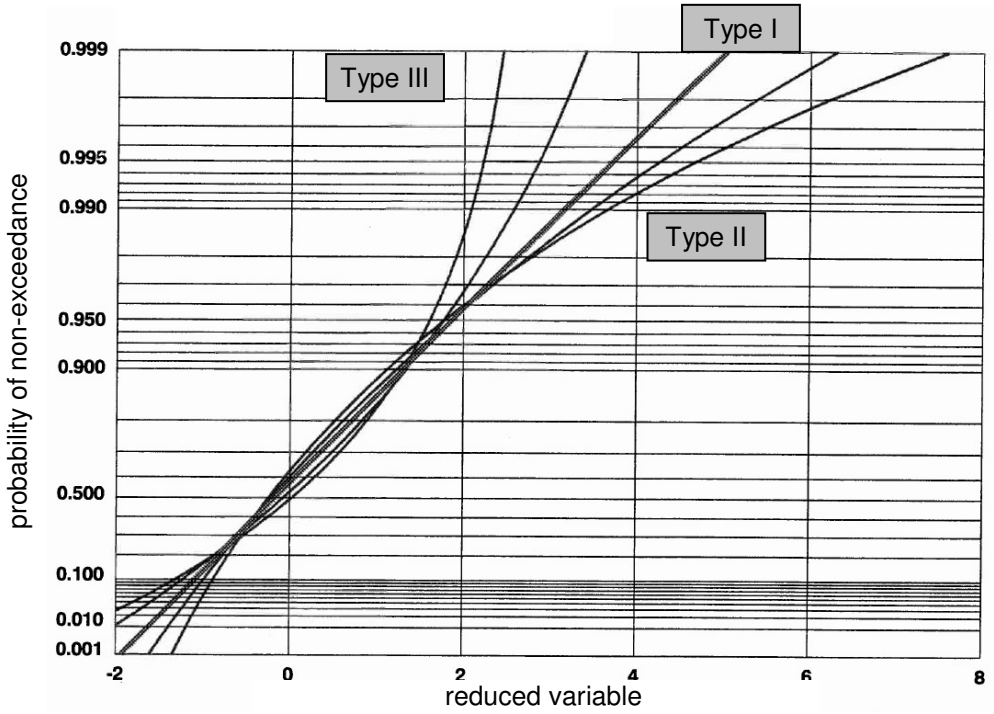

Figure 3-2 Different kinds of distributions of extremes on Gumbel grid (Kasperski (2000))

This thesis aims at the determination of the reliability of masonry shear walls in common masonry buildings. Thus, the horizontal (wind) load is most important. Considering the fact that wind load has an actual physical upper limit, the *Weibull*-distribution seems the most appropriate for the modelling of the wind load although *Gumbel*-distributions have been widely used in the literature since the application is simple and only a few parameters have to be known. However, the *Weibull*-distribution was suggested by *Kasperski (2000)*.

The general formulation of distributions of extremes can be defined according to the following equation.

$$F(x) = \exp\left[-\left(f_1 - f_2 \cdot \frac{x-m}{\sigma}\right)^{1/\tau}\right] \qquad \text{Eq. 3-5}$$

where m is the mean, σ is the standard deviation and τ is the shape parameter. To obtain *Weibull*-distributions, the shape parameter must be $\tau > 0$. *Gumbel*-distributions are derived from $\tau = 0$ and consequently, *Frêchet*-distributions fulfil $\tau < 0$. The parameters f_1 and f_2 depend on the shape parameter.

$$f_1 = \Gamma(1+\tau) \qquad \text{Eq. 3-6}$$

$$f_2 = \sqrt{\Gamma(1+2\cdot\tau) - f_1^2} \qquad \text{Eq. 3-7}$$

where Γ is the Gamma function.

A very important aspect about distributions of extremes is their dependence on the observation period. With increasing observation period, i.e. increasing number of observations *n*, the mean of all three distributions increases significantly. The difference between *Gumbel*, *Frêchet* and *Weibull* distributions is with regard to the standard deviation. With increasing observation period, the standard deviation of *Gumbel* distribution stays constant; consequently, the coefficient of variation decreases. In case of *Frêchet* distributions, the standard deviation increases; in case of *Weibull* distributions, the standard deviation decreases which results in a significant reduction of the coefficient of variation of *Weibull* distributions.

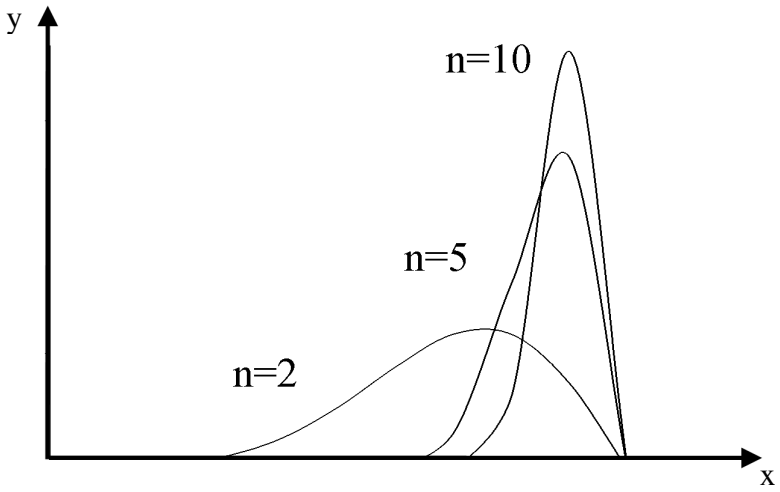

Figure 3-3 Weibull distribution for different numbers of observations n

3.3 Dead Load

In masonry construction, the dead load primarily consists of the self-weight of the structural system. Hence, slabs and walls represent the largest contribution. The contribution of the dead load to the total load is about 70% for common residential and office structures.

Dead loads act almost permanently on a member. They provide constant axial force to the masonry members which is favourable to the lateral load-carrying capacity in most cases. This makes dead load a very important aspect in design. In *DIN EN 1990/NA*, the corresponding partial safety factor is $\gamma_G = 1.0$ for favourable action of the dead load. Most other codes, e.g. *CSA S304.1 (2004)*, stipulate a partial safety factor of $\gamma_G < 1.0$ in this case.

Glowienka (2007) showed that the dead load does not affect the failure probability of centrically compressed masonry members significantly due to the small scatter (see Figure 3-4) and the corresponding small sensitivity value α_i.

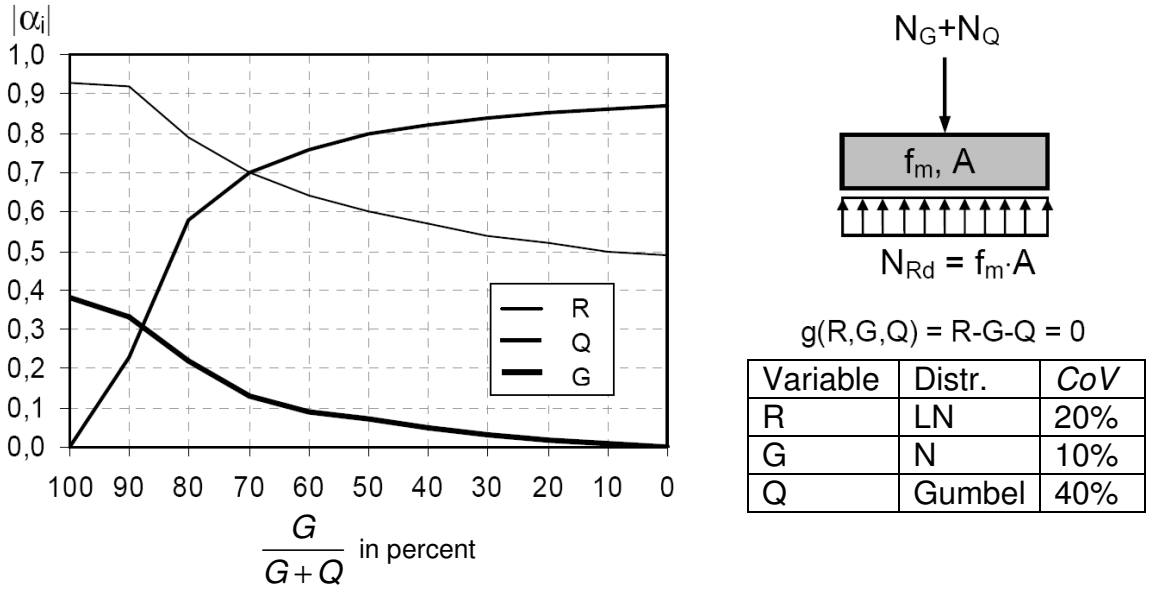

Variable	Distr.	*CoV*
R	LN	20%
G	N	10%
Q	Gumbel	40%

Figure 3-4 Sensitivity values α_i depending on the ratio of dead-to-live load (Glowienka (2007))

For shear walls, a larger sensitivity of the dead load is expected because shear failure occurs more frequently under minimum axial load. Consequently, detailed assessment of the dead load is required.

Dead load is determined from the density of the material and the volume of the member. Although density scatters over the member, e. g. due to concentration of reinforcement or aggregate in case of RC, this can not be taken into account in this thesis. Therefore, the influence of spatial scatter on the resulting dead load will be considered negligible and members are assumed to be homogeneous. Thus, the distribution of the dead load over a member is assumed to be constant.

The dimensions of the member will scatter and so will the volume of the members. This is influenced by the workmanship (e.g. accuracy of formwork) amongst other things. Due to this, the scatter of the self-weight of precast members is normally smaller than the scatter of cast-in-place members. Since masonry units are produced in plants and factories, the scatter of the unit dimensions is small and will be neglected here.

As mentioned, the self-weight of the walls can be derived from the density ρ and volume V_i of every respective layer of the wall.

$$g_i = \rho_i \cdot V_i \qquad \text{Eq. 3-8}$$

The layers are formed by the masonry units, the mortar joints and other possible materials, e.g. plaster. In most cases, the densities of the mortar and units are not treated separately. Rather, the masonry assembly is treated as a homogenous material. Particularly in the case of masonry with thin layer mortar (TLM), the weight of the mortar does not require separate consideration. The discontinuity because of the mortar layers can be neg-

lected. In the case of general purpose mortar (GPM), the layers are thicker and may have an effect on the self-weight especially in case of filled head joints. Nevertheless, the density of the mortar is similar to the density of the masonry units and so the effect even for thicker joints is negligible.

The main influence parameter of the self-weight of the masonry walls is the density of the masonry units. According to *Graubner & Glowienka (2007)*, the scatter of the density of the units is small. A value of $V_{unit} \approx 3\%$ is provided.

The volume of masonry walls is also variable even if quality control is good. *CIB (1989.a)* gives a coefficient of variation for the geometry of about 5%. This seems to be conservative; it would equal a deviation in thickness of up to one centimetre in case of a typical 20 cm thick wall. Nevertheless, the total scatter of the self-weight of masonry walls can be determined from the aforementioned influencing factors.

$$V_{wall} = \sqrt{V_{unit}^2 + V_{geometry}^2} \qquad \text{Eq. 3-9}$$

With $V_{unit} = 5\%$ and $V_{geometry} = 3\%$, the coefficient of variation of the self-weight of the masonry wall V_{wall} is 6%.

The largest contribution to the self-weight of a structure is the self-weight of the concrete slabs. *Graubner & Glowienka (2005b)* assessed the corresponding stochastic properties. They found that the governing parameters are the concrete density and the thickness. Other parameters like reinforcement ratio or density of the steel can be neglected in case of slabs. The influence of variation in the dimensions on the self-weight of columns and beams is stronger. However, this contribution to the dead load of the entire structure is small and thus this influence can be neglected.

Glowienka (2007) analysed the influence of the thickness of the slab and the coefficient of variation of the density of the concrete on the scatter of the self-weight of the slab, as shown in Figure 3-5. It can be seen that changes in thickness have a significant effect on the scatter of the weight of the RC slabs but only up to a point with little influence evident for thicker slabs. The major influence for thick slabs is the coefficient of variation of the density. According to *Graubner & Glowienka (2005b)*, the concrete density has a coefficient of variation of 2.5%. The reinforcement ratio of the slab was found to only affect the mean of the self-weight but not the scatter due to the small scatter of the self-weight of the reinforcement. However, the reinforcement ratio is important. *DIN EN 1990/NA* provides a characteristic value of the specific weight of RC of $\gamma_{concrete} = 25$ kN/m³. This corresponds to a reinforcement ratio of 3% taking into account a typical value of the specific weight of concrete of 23.1 kN/m³). For typical thickness of the concrete slabs in masonry buildings of about 16-18 cm, the coefficient of variation was determined to be 4% by *Graubner & Glowienka (2005b)*. *Glowienka (2007)* also accounted for the contributions

of the finishings and determined a coefficient of variation of the self-weight of the concrete slabs of 6%.

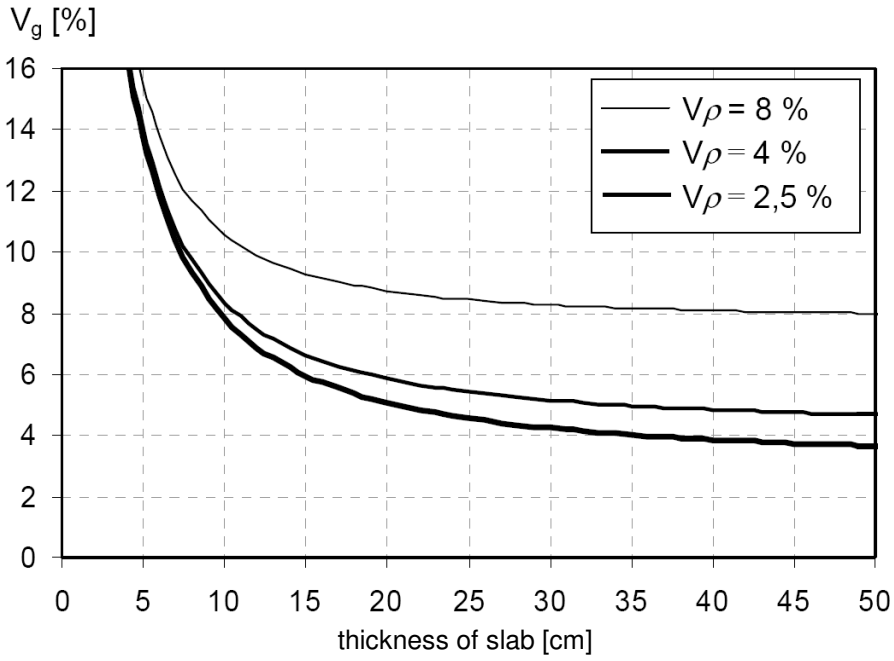

Figure 3-5 *Coefficient of variation of an RC slab vs. slab thickness for different values of the coefficient of variation of the density of the concrete (Glowienka (2007))*

In the end, the coefficient of variation of the self-weight of the walls and slabs is equal and represents the coefficient of variation of the dead load of the structure. The stochastic model appropriate for the dead load can be found in Table 3.3-1. Dead load is commonly assumed to be normally distributed. In some cases, a lognormal distribution can also be an appropriate choice.

Table 3.3-1 *Stochastic model of the dead load*

Type of distribution	mean (m_x/X_k)	σ	*CoV*
N or LN	1.0	0.06	6%

3.4 Live Load

The determination of a stochastic model for the live load is complex due to the large variation in the loads and especially because of the spatial variation. Stochastic fields have to be used to derive a useful model for practice. A detailed description would go beyond the scope of this thesis, however, the theory of live load modelling will be presented briefly. For more detailed information see *Rackwitz (1996)*, *Glowienka (2007)* or *Schmidt (2003)*.

Live load in typical masonry buildings comes from the use of the building and is essential to the structural integrity of masonry buildings. As explained in section 3.2, live loads are variable over time and location. Considering the live load in a building, it becomes clear that the live load can be divided into several contributions. Some live load will act more

or less permanently, e.g. furnishings, however, since they are removable, they are still considered live loads. In addition, there are loads that act only over a short time and lead to peaks in the total live load, e.g. groups of people or agglomeration of furniture due to renovation. See Figure 3-6 for illustration. The total load that is the basis for design is the sum of the different contributions.

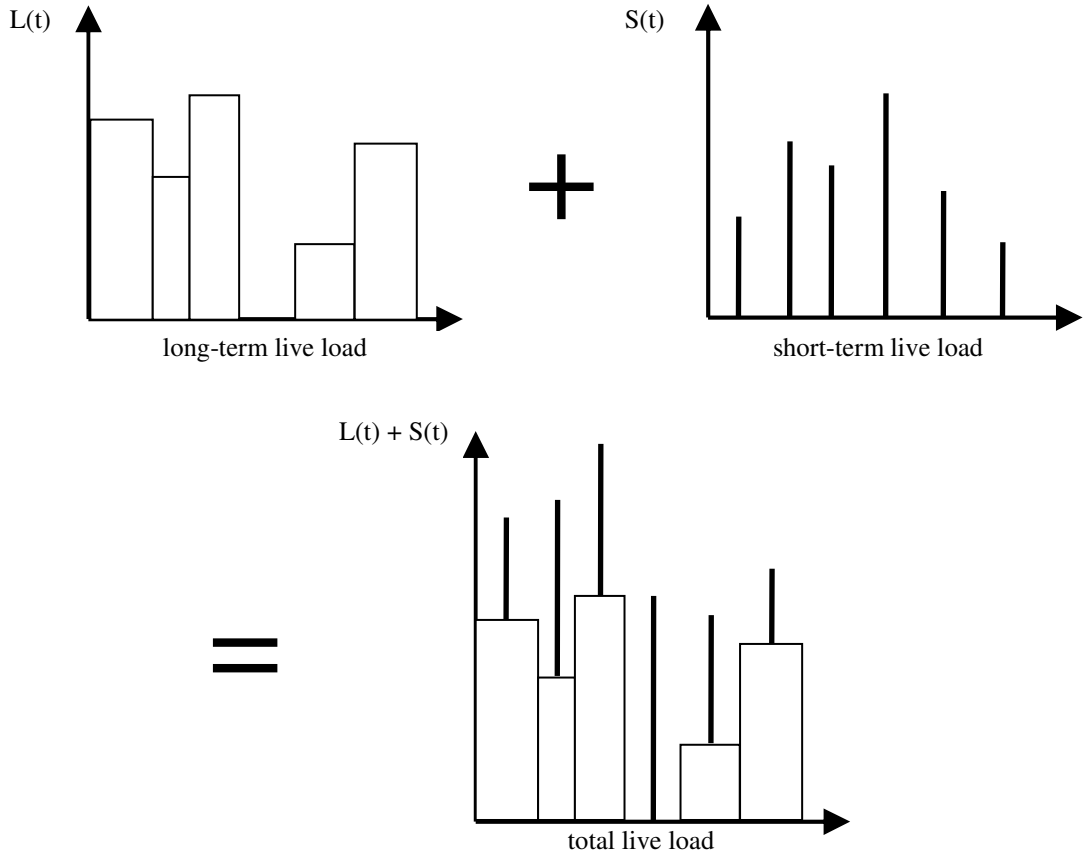

Figure 3-6 Typical representation of live load

The most popular model for the modelling of the live loads can be found in *CIB (1989.b)*. It is the basis used in most German and international codes.

$$W(x,y) = m + V + U(x,y) \qquad \text{Eq. 3-10}$$

In this equation, m represents the deterministic mean of the live load which depends on the kind of use (residential, office, archive etc.). V is a random variable with mean zero that accounts for load variation between two independent areas A_1 and A_2 on one floor or between floors. $U(x,y)$ is a random field accounting for spatial variation of the load.

The corresponding structural responses (bending moment, axial force, shear) can be calculated by multiplication with the ordinates of the influence area $i(x,y)$.

$$S(A_j) = \int_A W(x,y) \cdot i(x,y)\, dA \qquad \text{Eq. 3-11}$$

In structural design, a determination of the structural response by evaluation of every load increment according to Eq. 3-11 is too complex. A preferred solution is the definition of an equivalent uniformly distributed load q, i.e. a uniformly distributed load that leads to the same load effect. This can be derived from the following equation.

$$\int_A q \cdot i(x,y)\,dA = \int_A W(x,y) \cdot i(x,y)\,dA \qquad \text{Eq. 3-12}$$

This yields the following equation for the uniformly distributed load:

$$q = \frac{\int_A W(x,y) \cdot i(x,y)\,dA}{\int_A i(x,y)\,dA} \qquad \text{Eq. 3-13}$$

Rackwitz (1996) determined the stochastic moments of the live load in general form.

$$E[q] = E\left[W(x,y)\right] = m_q \qquad \text{Eq. 3-14}$$

$$VAR[q] \approx \sigma_V^2 + \sigma_U^2 \cdot \frac{A_0}{A} \cdot \kappa \qquad \text{Eq. 3-15}$$

$$\kappa \approx \frac{\int_A i^2(x,y)\,dA}{\left(\int_A i(x,y)\,dA\right)^2} \qquad \text{Eq. 3-16}$$

where m_q is the mean of the live load, σ_V is the standard deviation of V, σ_U is the standard deviation of U. The parameter κ depends on the required stress resultants and the structural system, A_0 is the reference area of the load measure and A is the effective area. Recommendations for the value of κ can be found in various sources, e.g. see *JCSS (2003)*, *Melchers (1999)* and *Hausmann (2007)*. The recommended type of distribution for q is the Γ-distribution according to *JCSS (2003)*. The required stochastic moments should be derived from load measures. Estimates can also be found in *CIB (1989b)* as well as in *JCSS (2003)*.

A similar model can be applied for the short-term live loads. It has to be noted that short-term live loads are modelled by a stochastic field due to the large scatter. Thus, the contribution σ_V in Eq. 3-11 can be set to 0. Consequently, the short-term load is especially important in case of small values of the influence area A, i.e. for balconies or stairs. This aligns with the larger characteristic values of the live load for these members in most design codes. Currently, there is still a lack of realistic data from load measures. However, *Rackwitz (1996)* stated that mean and standard deviation are almost of equal quantity. Hence, an exponential distribution such as the Gamma distribution is recommended.

The variation in live load over time can be modelled by stochastic processes. Commonly, a Poisson-process is applied. *Glowienka (2007)* gives the following equation for the trans-

formation of the maximum point-in-time load to a permanent load based on *Marten (1975)*.

$$F_{qt,\max}(x) = \frac{\lambda_S}{\lambda_S + \lambda_t \cdot \left(1 - F_{qt}(x)\right)} \qquad \text{Eq. 3-17}$$

where λ_S is the average load fluctuation rate, λ_t is the occurrence rate of the maximum load and $F_{qt}(x)$ is the distribution of the load. For minimum load, *Arteaga (2004)* gives

$$F_{qt,\min}(x) = 1 - \exp\left(\lambda_S \cdot T \cdot F_{qs}(x)\right) \qquad \text{Eq. 3-18}$$

For further information see *Marten (1975)* and *Rackwitz (1996)*.

Now, the two contributions for the point-in-time load (permanent and short-term load) have been defined. According to *Ferry Borges & Castanheta (1971)*, the total live load is the sum of the contributions. The required parameters can be found in *JCSS (2003)* and are displayed in Table 3.4-1.

Table 3.4-1 Parameters for the live load model according to JCSS (2003)

Type of use	Ref. area	permanent load				short-term load			
	A_0 in m²	m_{perm} in kN/m²	$\sigma_{V,perm}$ in kN/m²	$\sigma_{U,perm}$ in kN/m²	$1/\lambda^a$ in a	$m_{s\text{-}t}$ in kN/m²	$\sigma_{U,s\text{-}t}$ in kN/m²	$1/\lambda^a$ in a	d[b]
office	20	0.5	0.30	0.60	5	0.20	0.40	0.3	1-3
lobby	20	0.2	0.15	0.30	10	0.40	0.60	1.0	1-3
residential	20	0.3	0.15	0.30	7	0.30	0.40	1.0	1-3
hotel	20	0.3	0.05	0.10	10	0.20	0.40	0.1	1-3
hospital	20	0.4	0.30	0.60	5-10	0.20	0.40	1.0	1-3
laboratory	20	0.7	0.40	0.80	5-10	-	-	-	-
library	20	1.7	0.50	1.00	>10	-	-	-	-
classroom	100	0.6	0.15	0.40	>10	0.50	1.40	0.3	1-5
sales room	100	0.9	0.60	1.60	1-5	0.40	1.10	1.1	1-14
factories									
light duty	100	1.0	1.00	2.80	5-10	-	-	-	-
heavy duty	100	3.0	1.50	4.10	5-10	-	-	-	-

[a] load fluctuation rate
[b] average load duration

The application of these values makes it possible to determine the point-in-time load for almost all typical masonry buildings. However, for design purposes the design load over an observation period is required. Consequently, the point-in-time load has to be converted. This can be done by application of the distributions of extremes (see section 3.2). For live loads, a *Gumbel*-distribution is a common approach. The stochastic parameters for the live load have been determined by various authors; a comparison is presented in Table 3.4-2.

Table 3.4-2 Comparison of recommended stochastic parameters reported in the literature

Type of use	*CIB (1989)*[a]			*Rackwitz (1996)*			*Glowienka (2007)*		
	m_q[b]	V_q	q_k[b]	m_q[b]	V_q	q_k[b]	m_q[b]	V_q	q_k[b]
office	2.64	0.19	2.42	1.81	0.20	1.64	2.51	0.37	2.09

residential	1.73	0.20	1.57	1.52	0.29	1.32	1.81	0.28	1.59
classroom	1.63	0.12	1.54	2.65	0.36	2.23	3.61	0.22	3.49
[a]based on load measures according to *Chalk & Corotis (1980)* [b]kN/m²									

As can be seen, the recommendations vary significantly. The coefficients of variation, as well as the means, have a wide range of values. An important observation is the inconsistency with the characteristic values provided in the German code *DIN 1055-3*.

Table 3.4-3 Characteristic values of the live load according to DIN 1055-3

Type of use	q_k in kN/m²
office	2.00
residential	1.50
classroom	3.00

It can only be assumed that the characteristic value of the live load as provided in *DIN 1055-3* does not represent the 98%-quantile (for an observation period of 1 year) as stated by *Grünberg (2004)*. However, the characteristic values provided in Table 3.4-2 are also not in agreement. *Glowienka (2007)* found that the models match the code values much better if they are considered modes for an observation period of 50 years rather than 98%-quantiles for 1 year. The reason is logical; a sample over 1 year is not representative due to the small load fluctuation rate. From the presented information, a stochastic model for the reliability analysis in chapter 6 has to be derived. Considering the fact that the parameters of *CIB (1989b)* are based on load measures and are scientifically accepted, a coefficient of variation of 20% seems justified. This is consistent with the recommendations of *Sørensen (2002)* and *Gayton et al. (2004)*. With this coefficient of variation the ratio of mean-to-mode of a *Gumbel* distribution becomes 1.1.

Table 3.4-4 Chosen stochastic model for the live load

Type of distribution	m (m_x/X_k)[a]	σ	*CoV*
Gumbel	1.1	0.22	20%
[a]The characteristic value for 1 yr is considered to be the mode for 50 yrs.			

3.5 Wind Load

Wind is a natural phenomenon and is caused by temperature differences in the atmosphere that lead to differences in the air-pressure. In addition, the rotation of the earth also contributes to increase the wind pressure. The main parameters affecting the wind load are the wind velocity v and the gust intensity which are determined from annual extremes and normally classified in design codes. Unlike self-weight and live load, wind load strongly depends on the location of a structure. Coast regions are commonly subjected to higher wind velocity and more likely to experience massive storms.

In structural design, the natural phenomenon of wind load refers to the stress/force on a member due to wind. Wind loads represent the main horizontal loads on typical masonry

buildings and act on every outer wall and every bracing wall. The wind load not only depends on the wind velocity; but many other parameters as well. The main influences are the shape of the member or structure, roughness of the surroundings as well as the dynamic behaviour of the structure. These influences are also spatially, locally and time-dependently correlated. The altitude above ground has an especially strong influence. To account for this influence, the reference value of the wind load normally refers to the load at an altitude of 10 m above ground.

In Germany, wind velocities are measured at many locations. Typically, prominent places like roofs of high-rise structures or large bridges are equipped with wind-monitoring units for scientific assessment.In addition, the German Weather Agency (Deutscher Wetterdienst) gathers data which are available to the public. However, all these data only represent the wind velocity at a certain time at a certain location and must be converted to a wind load by appropriate models. Effects of resonance can increase the structural response significantly. Therefore, the response strongly depends on the structure. Dynamic effects are normally taken into account by a dynamic blast factor which is multiplied with the static wind load. Since this thesis deals with common masonry structures in Germany, only structures with a height of less than 25 m, and are therefore insensitive to dynamic effects, will be considered. Structures with an increase of the wind load of less than 10% due to dynamic effects are considered to be insensitive. In these cases, a permanent, static load can be calculated to represent the wind load. Although, the wind blast is a local phenomenon it can be considered to act on the entire structure at the same time in the case of small structures. For more information see *Schuëller (1981).*

The aim of the following section is the derivation of the distribution and stochastic moments for the wind load. As mentioned before, this thesis deals with structures that are insensitive to dynamic effects. In this case, a simplified stochastic model for the wind load can be applied. More detailed models can be found in *Rackwitz (1996)* and *JCSS (2003).*

The model used herein has been developed by *König & Hosser (1982)* and is assumed to sufficiently represent the wind load in Germany. It also forms the basis of *DIN 1055-4*. In this model, the wind load w is the product of the wind pressure q and a factor c_p that accounts for the geometry of the structure.

$$w = c_p \cdot q \qquad \text{Eq. 3-19}$$

The wind pressure q is normally derived by application of *Bernoulli's* rule to the wind velocity.

$$q = \frac{1}{2} \cdot \rho \cdot v_z^2 \qquad \text{Eq. 3-20}$$

where ρ is density of the air and v_z represents the wind velocity at altitude z. The density of the air is strongly influenced by the temperature of the air; the lower the temperature, the higher the density. A value of $\rho = 1.25$ kg/m² can be assumed for average conditions. This gives

$$q \approx \frac{v_z^2}{1600} \qquad \text{Eq. 3-21}$$

The wind velocity v_z can be split into a slowly deviating part $\bar{v}_z$ and the blast v_z'.

$$v_z = \bar{v}_z + v_z' \qquad \text{Eq. 3-22}$$

The contribution $\bar{v}_z$ depends on the roughness of the terrain which is normally taken into account by the factor α_w in civil engineering.

$$\bar{v}_z = \bar{v}_G \cdot \left(\frac{z}{z_G} \right)^{\alpha_w} \qquad \text{Eq. 3-23}$$

The wind velocity $\bar{v}_G$ is the velocity at the so-called gradient altitude at which the velocity is independent from the roughness of the terrain. The gradient altitude increases with increasing roughness. The annual extremes of $\bar{v}_G$ are usually modelled by a *Gumbel* distribution (see *JCSS (2003)*). *König & Hosser (1982)* provide the following values for the 10 min. average for regular settings in Germany and an observation period of 1 year.

$$m_{\bar{v}_G} = 29.6 \ \ m/s \qquad \text{Eq. 3-24}$$

$$CoV_{\bar{v}_G} = 12 \ \ \% \qquad \text{Eq. 3-25}$$

The contribution of the blast v_z' to the wind velocity can also be calculated on the basis of the gradient velocity and the blast factor ξ. The blast factor has to be related to the reference altitude of 10 m.

$$v_z' = \bar{v}_G \cdot \xi \cdot \left(\frac{z_1}{z_G} \right)^{\alpha_w} \qquad \text{Eq. 3-26}$$

Substituting Eq. 3-23 and Eq. 3-26 into Eq. 3-22 yields the final expression for the wind velocity v_z.

$$v_z = \bar{v}_G \left(\left(\frac{z}{z_G} \right)^{\alpha_w} + \xi \cdot \left(\frac{z_1}{z_G} \right)^{\alpha_w} \right) \qquad \text{Eq. 3-27}$$

DIN 1055-4 provides values for the parameters α_w, ξ and z_G. These values have a large range, however, the most common values have been recommended by *König & Hosser*

(1982) and are provided in Table 3.5-1. Please note that these values are only valid if the velocity is inserted in kN/m² and the altitudes in m because of the regression parameters.

Table 3.5-1 Parameters of the wind model according to König & Hosser(1982)

Terrain	α_w	ξ	z_G
open	0.16	0.56	200
city	0.28	0.98	400

The mean wind load can finally be derived from Eq. 3-21 and Eq. 3-27.

$$v_z = \frac{c_p}{1600} \cdot \left(\overline{v}_G \left(\left(\frac{z}{z_G} \right)^{\alpha} + \xi \cdot \left(\frac{z_1}{z_G} \right)^{\alpha} \right) \right)^2 \quad [\text{kN/m²}] \qquad \text{Eq. 3-28}$$

According to *JCSS (2003)*, the resulting wind pressure q should also be modelled by *Gumbel* distribution and the coefficient of variation should be double the coefficient of variation of the wind velocity. This gives

$$CoV_q \approx 2 \cdot CoV_{\overline{v}_G} = 24\% \qquad \text{Eq. 3-29}$$

The coefficient of variation of the wind load $CoV_{w,1}$ can then be determined from the vector sum of CoV_q and the coefficient of variation of the aerodynamic parameter c_p to account for the uncertainty in the modelling of c_p. According to *JCSS (2003)*, the coefficient of variation of c_p is estimated to be 10%. Note that the index "1" refers to the observation period of 1 year.

$$CoV_{w,1} = \sqrt{CoV_q^2 + CoV_{c_p}^2} = 26\% \qquad \text{Eq. 3-30}$$

For design purposes, characteristic values have to be defined and determined from the database. As mentioned previously, in *DIN 1055-4*, the characteristic value of the design wind load is defined to be the wind load that is only exceeded once in 50 years, however, the number of extreme values measured over an observation period of 50 years is limited. However, the amount of data for 1 year periods is relatively large. This makes it possible to generate extreme values for large observation periods by MCS.

The first step herein is the determination of the 1 year PDF. Since extreme values are the subject, a PDF of extremes should be chosen (see section 3.2). In the literature, *Gumbel* distributions are commonly used (see *Grünberg (2004)* and *JCSS (2003)*). The *Gumbel* distribution is not considered to be the best choice due to the missing upper limit. *Kasperski (2000)* recommended the use of a *Weibull* distribution instead. In the *Weibull* distribution, a third parameter τ is required in addition to the moments. This parameter defines the upper limit and is also referred to as the shape parameter (see Figure 3-2). This important parameter was determined by use of a test database provided with the software ProGumbel (*Niemann (2009)*). The parameters determined for various locations were with-

in a range of 0.04-0.4. This is consistent with other values reported in the literature. *Kasperski (2000)* gives a similar range for τ and recommends a value of $\tau = 0.2$ for further investigations. This value will be used in the following study.

The 50 year distribution was derived from MCS. Random values were generated based on the 1 year distribution with the coefficient of variation as defined by Eq. 3-30. Subsequently, the maximum values of every set of 50 values were determined and collected. From there a new set of data of 50 year extremes was obtained. In the last step, a *Weibull* distribution was fit to the new set of data. The number of simulations was large (n = 100,000) corresponding to a new set of 2000 50 year extremes. The results of this study are presented in Table 3.5-2.

Table 3.5-2 Stochastic Properties of the Wind Load

Observation period	Distribution type	m (v_m / v_k)	σ	τ	*CoV*
1 yr	Weibull	0.6375	0.1658	0.200	26%
50 yrs	Weibull	1.0300	0.0759	0.073	7.4%

Note, that the mean represents the ratio of the mean to the characteristic value of *DIN 1055-4*. This ratio is nearly 1.0 for an observation period of 50 years. This highlights the appropriateness of the characteristic values of *DIN 1055-4* because the 98%-quantile of the 1 year distribution is assumed to almost equal the mean of the 50 year distribution. It can also be seen that the standard deviation decreases significantly with larger observation periods which is expected for *Weibull* distributions (see Figure 3-3). This is contrary to a *Gumbel* distribution where the standard deviation stays equal and only the mean increases for larger observation periods.

3.6 Model Uncertainty in the Determination of the Load Effects

In the previous sections, the models for the determination of the stochastic parameters for dead load, live load and wind load were explained. From these models, the coefficient of variation of the load itself was derived. For design purposes, the structural response, i.e. the load effects, has to be calculated. Further models are required which are also uncertain to a some extent due to inevitable simplifications of the structural system. One example of a typical simplification in masonry design is the application of a linear-elastic stress-strain relationship in the determination of the stress resultants. Masonry still has plastic potentials in the load-carrying capacity and so stress transfer will happen over the structure. Thus, the load effect derived from linear-elastic analysis will likely be different from the actual one.

These uncertainties are referred to as model uncertainties and have to be included in a reliability analysis. Since model uncertainties of the load model can generally be taken into account by increasing the coefficient of variation of the load, the term model uncertainty will be used for the model uncertainties in the determination of the stress resultants.

In this thesis, the model uncertainty will be included in the reliability analysis by introducing it as basic variable. It could also be included by increasing the scatter of the load actions. But since model uncertainties for shear as well as for axial forces are required, two basic variables will be introduced due to matters of transparency. This corresponds to the recommendation according to *JCSS (2003)*. There, also prior values for the stochastic parameters of the model uncertainty on the determination of the load effect are provided.

Table 3.6-1 Recommended stochastic models for the model uncertainty according to JCSS (2003)

Model type	Distr.	*m*	*CoV*
moments in frames	LN	1.0	0.10
axial forces in frames			0.05
shear forces in frames			0.10
moments in plates			0.20
forces in plates			0.10
stresses in 2D solids	N	0	0.05
stresses in 3D solids		0	0.05

According to *JCSS (2003)*, the model uncertainty can either be applied as a summand or as a multiplier. Due to the more efficient stochastic modelling, the latter seem more useful.

The model uncertainty strongly depends on the structural system. Especially masonry shear walls are generally reduced to simple models because many aspects, such as the coupling moment of the slabs or the contribution of non-load bearing walls, cannot be easily quantified. It can only be assumed that the shear force that really acts on the shear wall is less than the design load. However, how much less cannot be quantified. Consequently, the mean of the model uncertainty on the shear load will be set to 1.0. Since no other data is available, the recommendation of the *JCSS (2003)* will be used and so the coefficient of variation of the model uncertainty on the shear load will be 10%.

The axial load is commonly determined from multiplying the influence area A_0 by the acting vertical loads. This model is considered to be almost exact, the only uncertainty lies within the determination of the influence area. In the past, the slabs were mostly modelled as beams with one-way span in common masonry design. With the spread of FE software, the uncertainty in the determination of the axial load decreased. However, the recommended coefficient of variation according to JCSS (2003) of 5% for axial loads is already small and will not be reduced further. The chosen stochastic model is summarized in the following table.

Table 3.6-2 Chosen stochastic model for model uncertainty on the loads

Basic variable	Distribution	m (v_m / v_k)	σ	*CoV*
Model uncertainty on the shear load	LN	1.0	0.10	10%
Model uncertainty on the axial load			0.05	5%

3.7 Summary

In this chapter, the typical loads that act on masonry shear walls are discussed. These are dead load due to the self-weight of the structure, live load due to use of the building and wind load.

The general concept of distributions of extremes is explained. These distributions are essential for the modelling of the live and wind load. The general formulation is presented and it is shown that three basic kinds of extreme distribution exist: *Gumbel*, *Frêchet* and *Weibull* distribution. These differ in their curvature and their limits. While *Gumbel* distributions are unlimited in both directions, *Frêchet* and *Gumbel* distribution have a lower or upper limit, respectively.

Axial load in general, can act favourably and unfavourably on the load-carrying capacity of the wall. Dead load represents the largest contribution of the axial load; the typical dead-to-live load ratio in masonry buildings is 70:30. Therefore, the dead load is essential to the shear capacity of masonry members. The stochastic model for the dead load is derived from the contributions of walls and slabs.

Modelling the live load is significantly more complex than modelling the dead load due to the variability over time and location. Stochastic fields and processes must be applied. From there, the different contributions to the live load, the permanent and short-term load, can be determined. For design purposes the point-in-time load is converted to the distribution of extremes for an observation period of 50 years by using a *Gumbel* distribution.

The wind load is a load action that strongly depends on the structure. The wind load mainly depends on the wind speed which is a function of many parameters, e.g. altitude or geographical location. The model presented by *König & Hosser (1982)* includes these parameters and makes it possible to derive a wind load acting on the structure. For the stochastic modelling of the wind load a *Weibull* distribution is chosen due to its upper limit, since wind load is limited by a physical maximum. To derive the 50 year distribution of extremes, the stochastic shape parameter is determined from a database of wind measurements for an observation period of 1 year. Then, an MCS is conducted and the distribution of the wind load is obtained. It was shown that the characteristic values of the wind load according to *DIN 1055-4* are within an acceptable range.

In the last step, the model uncertainties for axial and shear load are defined following the recommendations of *JCSS (2003)*. In the end, the full stochastic model for the loads as required for the reliability analysis in chapter 6 are defined.

4 LOAD-CARRYING BEHAVIOUR AND MATERIAL PROPERTIES OF MASONRY

4.1 General

Masonry is a composite material consisting of units, often referred to as “brick”, and mortar. Therefore, the material properties of masonry are a combination of the properties of both components. Since masonry is one of the oldest and most traditional construction materials, the number of different kinds of units and mortar that have been used in the past is quite large. The history of application of masonry reaches back several thousand years. While in the beginning natural units (e.g. cut stone) were common, today, mainly manufactured units are used due to the efficiency of industrial manufacturing. Contemporary masonry consists of a large variety of different unit materials, formats and mortar types which all differ significantly in their properties. For example, large-sized units made of calcium silicate and smaller-sized clay bricks for double-leaf walls. Mortars have also undergone many changes. Hydraulic lime mortars have been replaced by Portland cement mortars which are available today as general purpose mortar (GPM) applied in joints of approximately one centimetre thickness, thin layer mortar (TLM), and also as lightweight mortar for special applications such as thermal insulation.

In structural design, masonry is mainly considered homogeneous. Therefore, the properties of units and mortars are used to derive the properties of masonry. Even if discrete micro-modelling of masonry can be useful, it is only scarcely used in practice due to its complexity and uncertainty.

In general, this thesis deals with unreinforced masonry (URM) as it is executed in Western Europe with a special focus on Germany. In this chapter, the load-carrying behaviour of masonry will be explained and the corresponding material properties will be discussed. Since this thesis deals with the reliability of shear walls, the stochastic models for every required material property will also be provided within this chapter.

4.2 Typology

Masonry units differ in size and format, perforation and most important, material. Different materials exhibit different stress-strain relationships, as shown in Figure 4-1. Thus, masonry made of clay brick units with general purpose mortar (GPM) behaves differently from masonry made of calcium silicate with thin layer mortar.

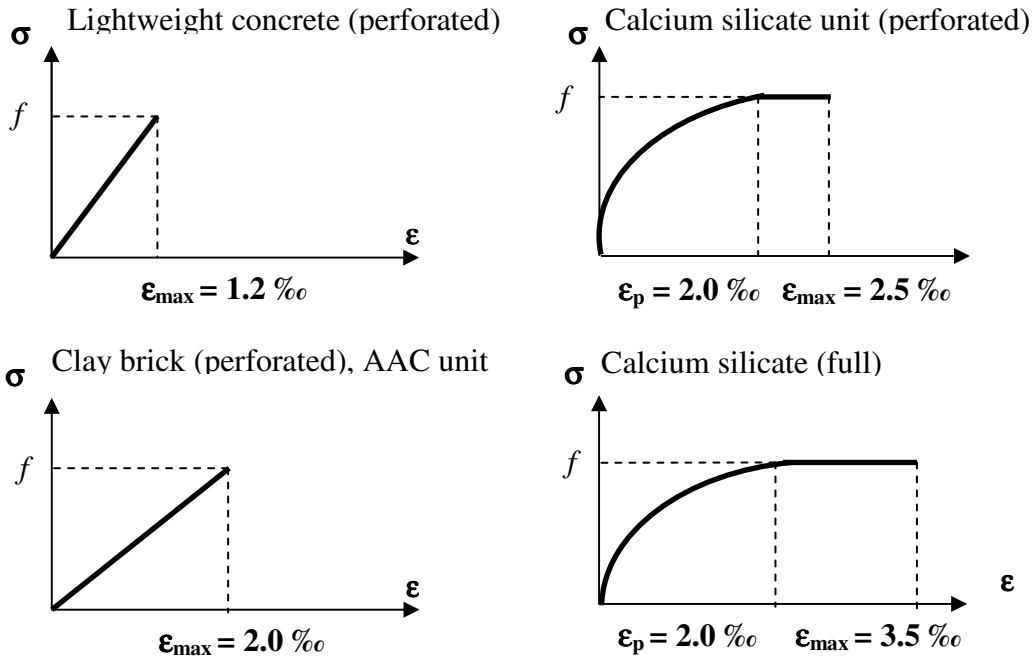

Figure 4-1 Stress-strain relationships of different kinds of masonry units

In Germany, five materials are currently approved for production of masonry units: clay bricks (CB), calcium silicate (CS), autoclave aerated concrete (AAC) as well as standard and lightweight concrete (LC). The large variety of units comes from the optimization of the units to suit various purposes from building envelope properties to load-carrying capacity. Therefore, even within Germany, strong regional differences in application and typology exist; just consider the extreme climates at the coast compared to the Alpine region.

When it comes to size and formatting, regular and large-sized units have to be differentiated. Large-sized units are those longer than 250 mm and higher than 500 mm. However, they also have to keep within maximum limits which are presented in Table 4.2-1. Large-sized clay bricks only play a minor role on the German market and are therefore not included in the following.

Table 4.2-1 Maximum dimensions for large-sized units

Material of unit	Maximum height of unit h_b [mm]	Maximum length of unit l_b [mm]
CS	623	998
AAC	624	1499
LC	623	997

Large-sized units are getting more and more popular due to the increased efficiency in consruction. Until now, they were subject to general technical approvals since they were not included in the German design codes. However, DIN EN 1996-1-1/NA which will be released in 2011, includes the design of masonry structures using large-sized masonry units.

In addition, many different kinds of perforation patterns exist. The types of units range from full AAC blocks without perforation to CB units with a void area of up to 45% of the cross sectional area. The variety of available units is significant with new products being developed and approved constantly.

Not only are there many different kinds of units, the variety of mortars is also considerable. In masonry, mortar is used bind the units together, to account for slight variations in unit sizes, and most importantly, to eliminate stress concentrations that would occur if masonry units were laid directly on top of each other due to imperfections in their surfaces. The units can be combined with different kinds of mortars. Mortars can be classified as General Purpose Mortar (GPM; in German codes often only denoted by a Roman numeral), Thin Layer Mortar (TLM) and Lightweight Mortar (LM). In Germany, GPM is additionally divided into 5 different types depending on the compressive strength (see Table 4.2-2). While GPM is usually applied with a bed joint thickness of about 1 cm, TLM layers are within the range of 2-3 mm and therefore require units with a higher degree of tolerance on the surface imperfections. TLM provides higher compressive strength to the masonry and also provides better cohesion compared to GPM. Large-sized units are mostly used in combination with TLM. Lightweight mortar has advantages in terms of thermal insulation but limits the masonry compressive strength. All mortar types influence the shrinkage and creep of the masonry assemblage.

Table 4.2-2 Compressive strength of mortar according to DIN EN 998-2 in MN/m²

Mortar kind	GPM					LM		TLM
DIN 1053	I	II	IIa	III	IIIa	LM 21	LM 36	TLM
DIN EN 1996	M 1	M 2.5	M 5	M 10	M 20	M 5	M 5	M 10
Compressive strength (DIN EN 998-2)[a]	1	2.5	5	10	20	5	5	10
[a]in N/mm²								

An important characteristic, especially for the shear capacity, is the treatment of the head joints. The head joints can be filled with mortar, or they can be unfilled with either a small gap remaining between the units or with the units laid in contact with each other. In Germany, head joints are usually left unfilled because of better construction efficiency, with the exception being special applications, e.g. in masonry beams above windows, where head joints are required to be filled. In other European countries, such as Switzerland, head joints generally have to be filled.

4.3 Load-Carrying Capacity of Masonry Subjected to Axial Compression

In this section, the general load-carrying behaviour of masonry subjected to axial stress will be explained. It will be necessary to mention some masonry properties. Detailed information on the masonry properties is provided in section 4.5.

Units and mortar in a masonry wall under axial compression are subjected to a triaxial state of stress due to the different *Poisson's* ratio of the unit and mortar and the bond between them. This leads to different horizontal strain of the units and the mortar. When masonry is subjected to compression, the mortar is compressed in all directions since it is confined by the units, while unit is subject to tension in the lateral direction. Failure therefore occurs when the tensile strength of the units is exceeded. Figure 4-2 illustrates this behaviour. Since the tensile strength of the units is always smaller than their compressive strength, the compressive strength of the masonry assemblage is smaller than the unit compressive strength.

As mentioned above, the lateral strain of the mortar is responsible for the tensile stresses in the unit. The lateral strain depends on the thickness of the mortar layer. Therefore, although the compressive strength of TLM can be smaller than the compressive strength of GPM, the use of TLM enhances the masonry compressive strength significantly. For more information refer to *Glock (2004)* and *Kickler (2003)*.

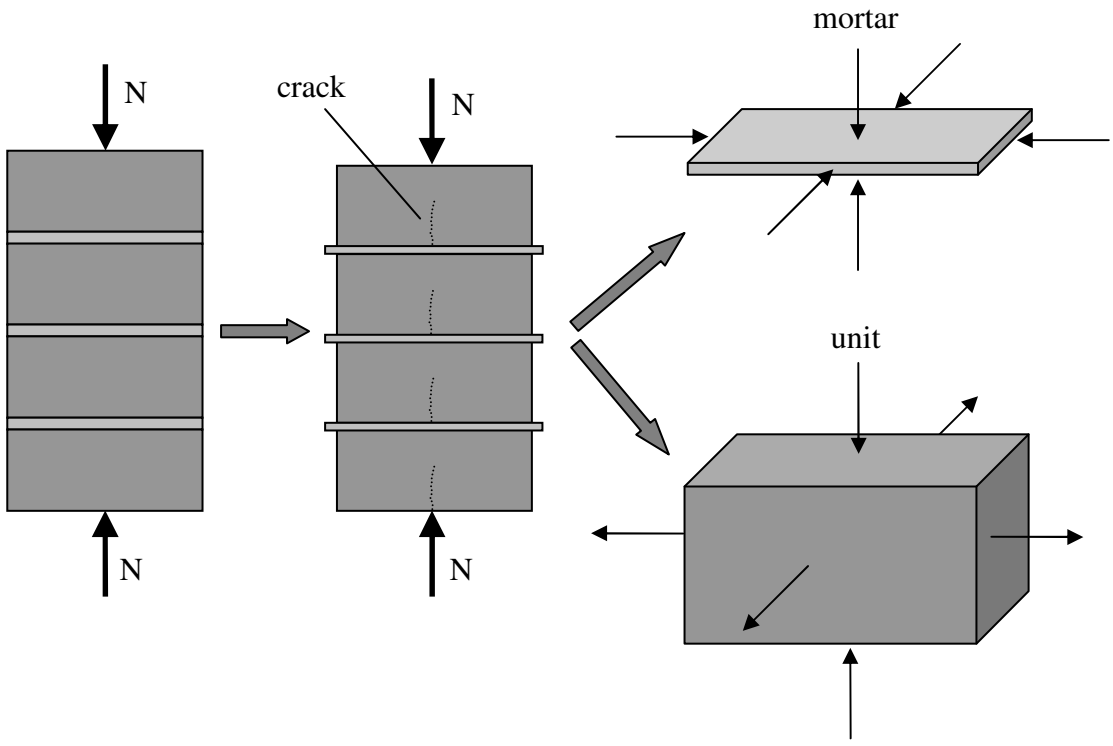

Figure 4-2 Load-carrying behaviour of masonry subjected to axial stress

The load carrying capacity of unreinforced masonry members subjected to axial compression strongly depends on the eccentricity of the axial load. Large eccentricities will lead to cracking of the cross section due to the low flexural tensile strength of the masonry. This leads to a redistribution of the compressive stress and an increase in the stress at the edge of the cross-section. The eccentricity of the load is defined as the ratio of bending moment to axial load, see Eq. 4-1.

$$e = \frac{M}{N} \qquad \text{Eq. 4-1}$$

This leads to a very important fact about unreinforced masonry (URM): resistance and load are not independent, the loading can affect the strength.

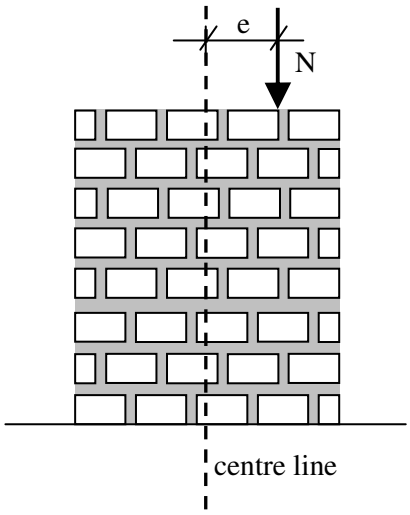

Figure 4-3 Eccentricity of axial load

Figure 4-4 shows the load-carrying capacity of an URM cross-section for different values of the eccentricity-to-thickness ratio *e/t* assuming linear elastic material behaviour.

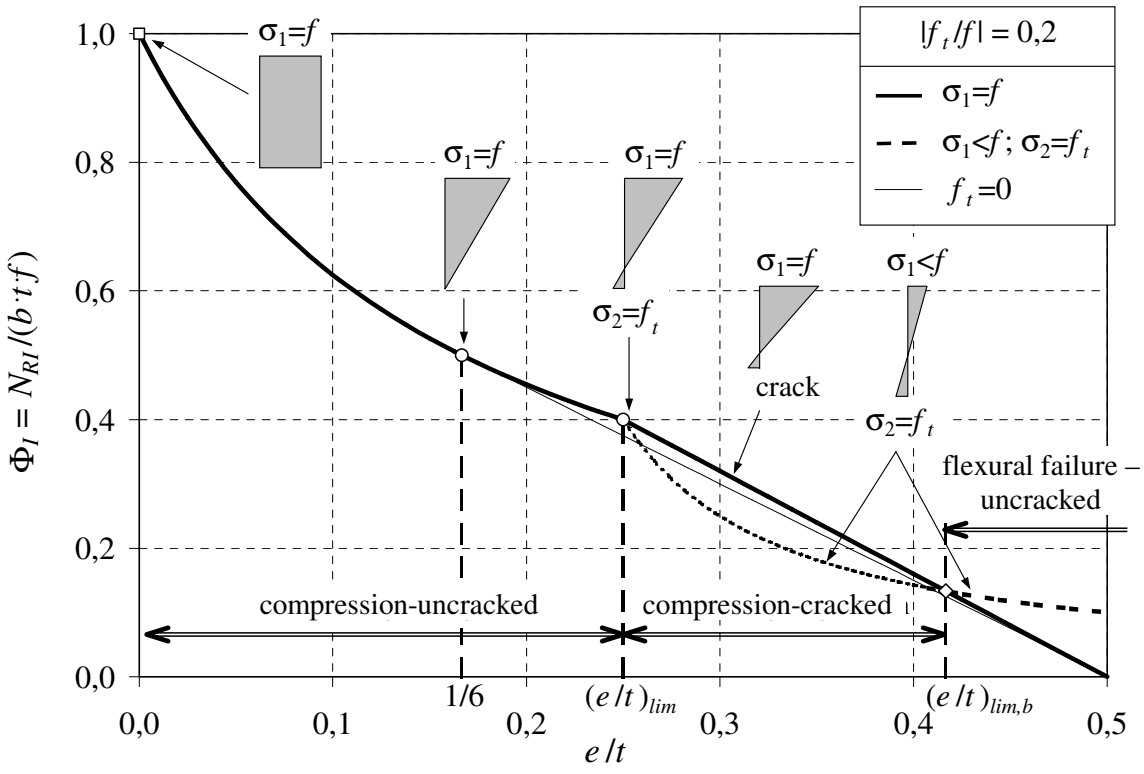

Figure 4-4 Load-carrying capacity of the cross-section for linear-elastic stress-strain-relationship and different values of eccentricity-to- thickness ratio e/t (Glock (2004))

It becomes obvious that the flexural tensile strength f_t strongly influences the load-carrying capacity for large eccentricities. However, it is not taken into account in common design models due to its large scatter. Figure 4-4 is based on a linear-elastic stress-strain relationship though this is not representative of all kinds of masonry. Clay brick masonry exhibits linear-elastic behaviour and therefore fails as soon as the stress at the edge reaches the compressive strength of the masonry. Calcium silicate masonry shows distinctly plastic behaviour and can reach higher utilization of the cross-section.

4.4 Load-Carrying Capacity of Masonry Subjected to In-Plane Loads

4.4.1 General

In general, shear stress is divided into two kinds depending on the direction of the shear stress: in-plane and out-of-plane shear. While in-plane shear, as it occurs e. g. in bracing walls, leads to a number of failure modes and exhibits complex load-carrying behaviour, out-of-plane shear is significantly less complex since only one failure mode is likely to occur. In the following chapters, the focus will be set on in-plane shear.

The failure modes of masonry subjected to in-plane loads can generally be divided into "global" failure, flexural failure and shear failure. Shear failure itself consists of another number of failure modes. The following sections provide information about the general load-carrying behaviour of masonry walls subjected to in-plane shear to be able to relate the material properties to the load-carrying behaviour. For detailed information on the determination of the shear capacity, see chapter 5.

4.4.2 Load-Carrying Behaviour and Failure Modes

The failure mode that occurs depends on the combination of axial and shear stress, and the material properties. The dimensions of the wall, represented by the slenderness ratio $h/l_{w,}$ also influence the failure mode significantly. In this section, the failure modes will be described and explained.

The first failure mode to be discussed is **tip over of the entire wall** which belongs to the group of "global" failures. This failure mode occurs when the resultant of the vertical stress is located outside of the cross-section, i.e. in case of large eccentricities ($e > l_w/2$). For smaller values of the eccentricity, tensile stresses in the bottom layer occur which may exceed the cohesion. This will lead to cracking but is not followed by tip over of the entire wall as long as the resultant of the vertical stress stays within the cross section ($e \leq l_w/2$) and the vertical stress does not exceed the masonry compressive strength. The failure mode itself can be identified from one large crack in the bottom bed joint. This failure is likely to occur for slender walls and walls with low axial loads. Figure 4-5 illustrates this failure mode.

Relevant:
dimensions
eccentricity

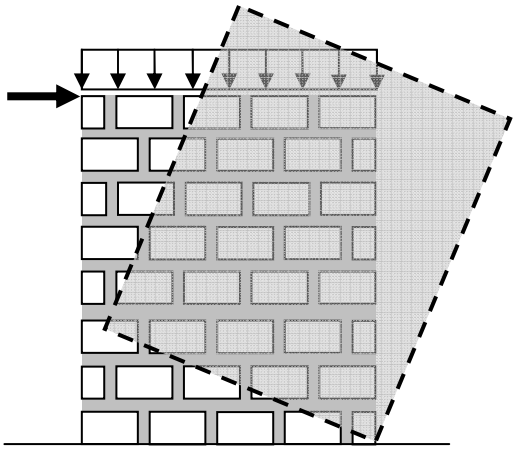

Figure 4-5 Tip over of the entire wall

The second failure mode is **flexural failure**. This failure occurs when the vertical stress at the toe of the wall exceeds the masonry compressive strength causing crushing of the unit in the bottom corner. The reason for this high stress is the large eccentricity which leads to a short length subjected to compression, consequently the vertical stress gets concentrated and the compressive strength f_m is exceeded. The appearance of this failure mode is very similar to shear crushing failure which will be explained later in this section. This failure mode can govern the load-carrying capacity under both minimum and maximum loads and therefore has to be considered in both cases. This failure mode is shown in Figure 4-6 . It is also likely to occur for slender walls.

Relevant:
eccentricity,
compressive strength f_m

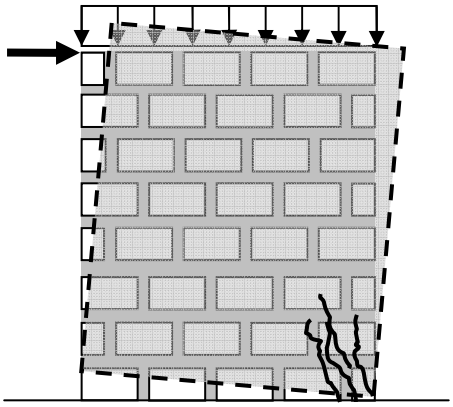

Figure 4-6 Flexural failure

The next failure mode is **sliding failure** (see Figure 4-7). Large horizontal forces and low vertical stress lead to exceedance of the sliding strength in the bed joints. The sliding capacity is governed by *Coulomb's* friction law ($V = \mu \cdot N$). This failure mode normally only occurs for squat walls. This failure mode should be differentiated from sliding shear failure, which is explained next.

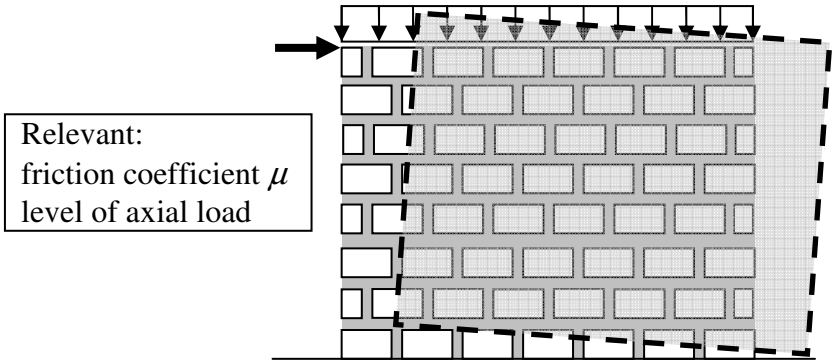

Figure 4-7 Sliding failure

The fourth failure mode, **shear failure**, actually consists of a set of possible failure modes. One difference to the previously mentioned failure modes are the cracks that occur in the wall over different courses. Shear failure describes the failure due to a combination of the principal stresses and can be subdivided into four failure modes: **sliding shear**, **diagonal tension**, **tip over of the separate unit** and **shear crushing**. The failure modes are shown in Figure 4-8.

Tip over of the separate units is a failure mode that only occurs if the head joints are unfilled and depends on the dimensions of the units, represented by the ratio h_b/l_b. Material strength is not involved. This failure mode is unlikely to occur except in the rare case of modern, large-sized masonry units with $h_b/l_b \geq 1.0$.

Sliding shear failure leads to the typical stepped crack pattern as shown in Figure 4-8. The horizontal shear strength, consisting of cohesion f_{v0} and the contribution of the axial load, in the bed joints is exceeded and therefore several bed joints fail which leads to the stepped crack pattern. This failure mode is likely to occur under low axial load since the axial force increases the shear capacity of the bed joints.

Diagonal tension failure occurs when the tensile strength of the units is exceeded. The main diagonal compressive strut generates tensile stress perpendicular to the compression which ruptures the unit. These cracks generally initiate near mid-height of the wall and propagate to the corners of the wall.

Shear crushing is similar to flexural (compression) failure in terms of crack formation. However, the cause is different: while in the case of flexural failure the maximum vertical stress is exceeded, shear compression failure happens when the compressive strength is exceeded in the diagonal strut. The overlap of the units is very important for this failure mode since it determines the angle of the diagonal compression.

For further information on the shear strength of unreinforced masonry refer to *Mann & Müller (1973), Simon (2002)* and *Kranzler (2008)*.

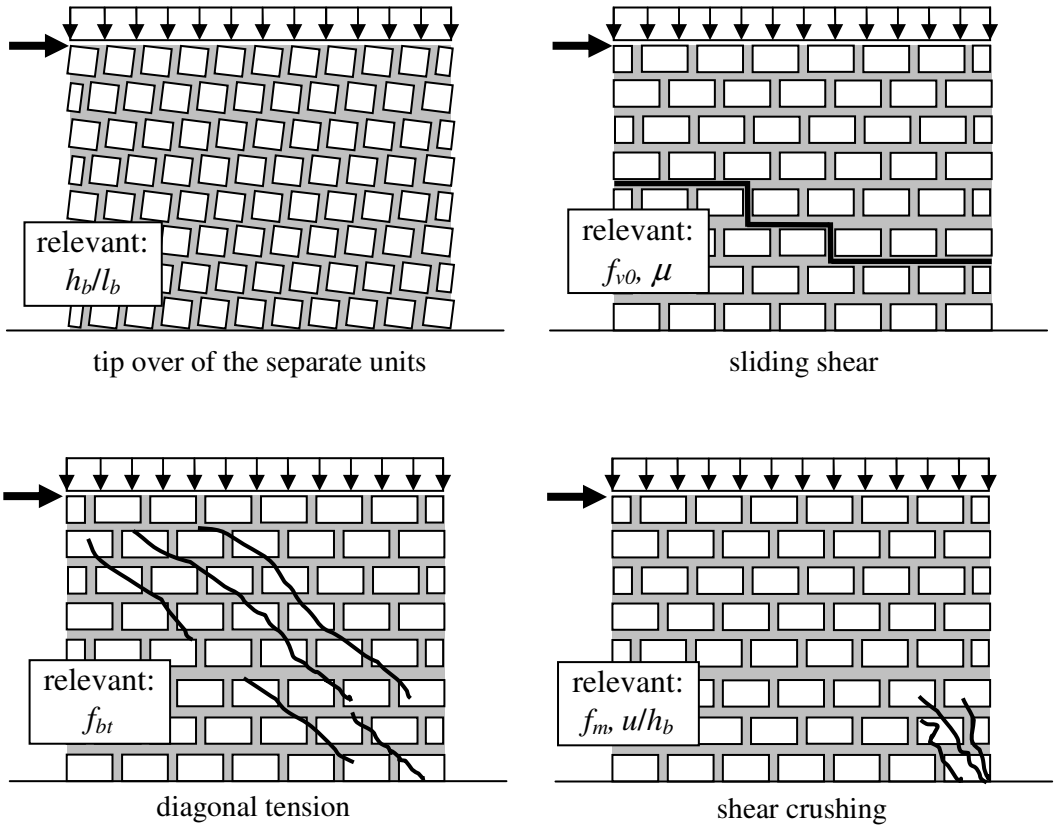

Figure 4-8 Shear failure

4.5 Material Properties

4.5.1 General

Material properties, mainly material strengths, are provided within the national design codes. Most codes are based on the concept of partial safety factors, as explained in section 2.7. The partial safety factors for the strength have to be applied to so-called characteristic values which are determined from tests by use of standardized methods. Because of the long tradition of masonry in practise, characteristic values have been derived empirically in the past, based on only a few tests due to the large variety of unit-mortar-combinations. With growing acceptance of probabilistic techniques, the characteristic values have been defined as quantiles of the stochastic distribution of a material property. For material strength, the recommended value is the 5%-quantile (see DIN EN 1990/NA). In the following sections, the material properties influencing the shear capacity of URM members will be discussed and stochastic models defined by distribution type, mean and standard deviation, will be derived for each property as the basis for the reliability analysis in chapter 6.

4.5.2 Compressive Strength of the Unit

In Germany, the compressive strength of the units is determined according to DIN EN 772-1. However, this code refers to the specific testing procedures for any material. For the three main materials, specific codes are: DIN EN 771-2 for calcium silicate, DIN EN 771-4 and DIN EN V 4165 for autoclave aerated concrete, DIN EN 771-1 for clay bricks.

The characteristic value of the compressive strength is defined as the mean compressive strength of six specimens of 100 mm length and 100 mm width. The value that can be found in the codes also accounts for a size factor that depends on the height and width of the units. The size factor increases with the unit height and can be obtained from DIN EN 772-1. Note that this value does not represent a 5%-quantile.

The test method is relatively simple as shown in Figure 4-9. The unit is loaded up to failure in the hydraulic press. Special attention has to be paid to the interface between the unit and compression plates: a layer of high-strength mortar of about 5 cm thickness is laid in between the plates and the unit and the plates will either be coated with oil or a thin sheet of paper to reduce adhesion.

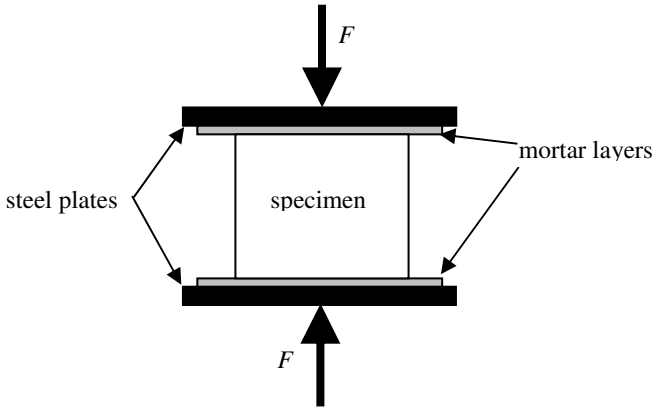

Figure 4-9 Determination of the compressive strength of the units

Commonly the compressive strength is determined from entire units but in case of large-sized units it may also be determined from smaller samples (prisms). The compressive strength of the units is used to classify the masonry compressive strength. Therefore, classes of unit compressive strength have to be determined. For stochastic analysis the mean values of these classes have to be known. DIN EN 1996-1-1/NA provides such values, presented in Table 4.5-1.

Table 4.5-1 *Mean values of f_b depending on the class of compressive strength according to DIN EN 1996-1-1/NA*

Class of compressive strength of units (minimum value)	2	4	6	8	10	12	16	20	28	36	48	60
Mean value of class of compressive strength f_b in N/mm²	2.5	5.0	7.5	10.0	12.5	15.0	20.0	25.0	35.0	45.0	60.0	75.0

Actually, the existent number of compressive tests on masonry units is large since every masonry producer performs tests in the process of quality control. Accessing test data however is difficult; most data is not available due to marketing reasons. However, in the research project of *Graubner & Glowienka (2007)* a large database provided by the masonry industry was assessed and average coefficients of variation depending on the unit material were provided, see Table 4.5-2, which can be used as prior information for further investigations.

Table 4.5-2 *Average coefficient of variation V_m of the compressive strength of the unit according to Graubner & Glowienka (2007)*

Unit material	Range of *CoV* in %	*n*	*CoV*
CS	6-10	693	8%
CB	4-17	434	9%
AAC	5-11	140	8%
LC, NC	6-17	69	12%

Due to the large number of available tests, especially in the case of CS, CB and AAC, the sample is considered reliable. It was also found from the database that the mean values provided in DIN EN 1996-1-1/NA match the means obtained from the database very well. The applied stochastic model for the compressive strength of the various units is summarized in Table 4.5-3.

Table 4.5-3 *Stochastic model for the compressive strength of the unit*

Unit material	Distr.	m ($f_{b,m}/f_{b,DIN\ EN\ 1996}$)	*CoV*	$f_{b,m}/f_{b,5\%}$
CS	LN	1.1	8%	1.09
CB		1.1	9%	1.07
AAC		1.2	8%	1.09
LC, NC		1.1	12%	1.02

The mean values represent the ratio of the mean f_m to the compressive strength of unit f_b according to DIN EN 1996-1-1 and are average values over all classes of compressive strength.

4.5.3 Compressive Strength of Mortar

As mentioned in section 4.2, three major groups of mortars are available in Germany which differ in compressive strength, density and application (joint thickness). These groups are GPM, LM and TLM. Testing of the compressive strength of mortar is simple; prisms are produced and loaded until failure in a hydraulic press. The corresponding test methods are based upon DIN 18555 (DIN 1053-1, DIN 1053-100) and DIN EN 998 (DIN EN 1996).

Commonly, mortars are classified by their compressive strength. Although the reference names of the groups according to DIN 1053 and DIN EN 1996 are different, the mortars are equivalent. Table 4.5-4 relates the mortar types to the mortar groups.

Table 4.5-4 Compressive strength of mortar according to DIN 18555-5 and DIN EN 998-2

Mortar group according to DIN 1053-1	GPM I	GPM II	GPM IIa	GPM III	GPM IIIa	LM 21	LM 36	TLM
DIN EN 1996-1-1	M 1	M 2.5	M 5	M 10	M20	M 5	M 5	M 10
f_{mo} [a] according to DIN EN 998-2	≥ 1	≥ 2.5	≥ 5	≥ 10	≥ 20	≥ 5	≥ 5	≥ 10
[a] in N/mm²								

Besides the contribution to the masonry compressive strength, mortar provides initial shear strength referred to as cohesion (see section 4.5.6). From assessment of a test data-base available to the author, suitable stochastic models of the mortar compressive strength for different kinds of mortar groups could be derived

Table 4.5-5 Stochastic models for the compressive strength of mortar

Mortar type	n	Distr.	m ($f_{m,mo}/f_{mo,EN\ 998\text{-}2}$)	CoV
TLM	87	LN	1.29	33%
LM	34		1.48	35%
II	115		1.46	29%
IIa	142		1.34	22%
III	61		1.28	25%
IIIa	22		1.65	33%

Mortar group I is no longer in use and thus is not included in the table. The scatter of the mortar strength is significant compared to the scatter of the compressive strength of the units. It must be noted that the values according to DIN EN 998-2 represent characteristic values but are defined as minimum values and not as a percentile. Thus, a comparison of a quantile with the minimum values is not useful.

4.5.4 Compressive Strength of Masonry

4.5.4.1 General

The important property of masonry is its compressive strength referred to as f_m. Other properties, such as the modulus of elasticity are correlated with the compressive strength and thus it is a common approach to relate these properties to the compressive strength. In shear design, masonry compressive strength is the relevant material property for the flexure and shear crushing failure modes.

4.5.4.2 Experimental Determination of the Compressive Strength of Masonry

Compressive strength of masonry f_m is commonly determined on so-called RILEM specimens according to DIN EN 1052-1 (1998). These specimens have to be 5 units tall; this is equal to a slenderness $\lambda = h_{ef}/t$ between 3 and 5. If a specimen exceeds the maximum height of 1000 mm, the topmost and the lowest layer of bricks may be sliced plane. The minimum length of the specimens is 400 mm. A typical test configuration is shown in Figure 4-10.

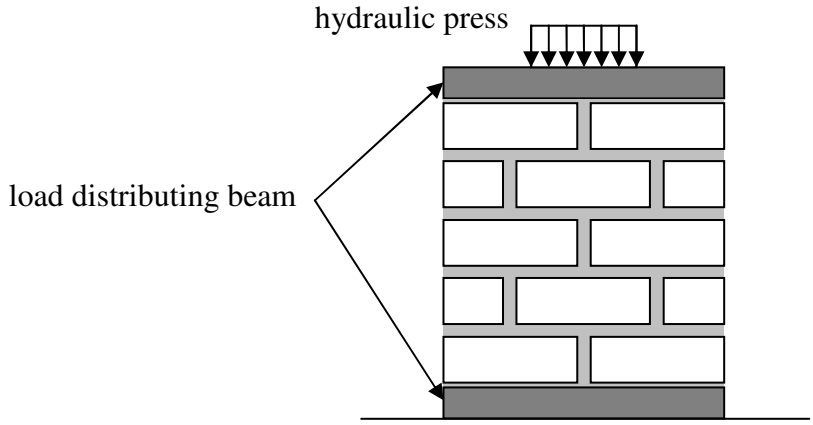

Figure 4-10 Testing of masonry compressive strength on RILEM specimen

This test can also be used to determine the modulus of elasticity of the masonry. The strains are measured at 4 locations over the height of the prism at a load level of approximately $0.33 \cdot f_m$. Eq. 4-2 then gives the secant modulus of elasticity. The compressive strength of the respective specimen can easily be determined by dividing the applied failure load in the test by the cross-sectional area of the specimen, Eq. 4-3.

$$E_i = \frac{F_{i,\max}}{3 \cdot \varepsilon_i \cdot A_i} \qquad \text{Eq. 4-2}$$

$$f_i = \frac{F_{i,\max}}{A_i} \qquad \text{Eq. 4-3}$$

A minimum number of 3 specimens have to be tested to obtain the masonry compressive strength. The characteristic value according to DIN EN 1052-1 can then be determined using Eq. 4-4.

$$f_{mk} = \frac{f_{m,m}}{1.2} \leq f_{mi,m} = \frac{1}{3} \cdot \sum_{i=1}^{3} f_{m,i} \qquad \text{Eq. 4-4}$$

The factor 1.2 in Eq. 4-4 results in a characteristic value that is about 80% of the mean value. This is a common estimate when it comes to masonry compressive strength. Considering the compressive strength lognormally distributed and assuming the characteristic value to represent a 5%-quantile, the corresponding coefficient of variation is determined to be 11%. This seems rather unconservative considering the larger scatter of compressive strength for units and mortar. The characteristic value as determined represents the short-term strength of the masonry.

Since a number of 3 specimens is not a representative sample, more specimens may be tested. If so, the characteristic value of the masonry compressive strength has to be determined to represent the 5%-quantile on a confidence level of 95% according to DIN EN 1052-1. This matches the requirements of the German National Annex to DIN EN 1990. However, it must be noted that the masonry compressive strength as tested is not a constant material property since it strongly depends on the plane strain constraint in the test (see *Probst (1981)*).

4.5.4.3 Analytical Prediction of the Compressive Strength of Masonry

Due to the large variety of possible unit-mortar combinations, it has often been attempted to determine the masonry compressive strength analytically from the properties of both components. Direct testing of the masonry compressive strength is not often conducted due to cost effectiveness; testing mainly happens in the process of quality control of the masonry producers and in the process of technical approval of new masonry products. Therefore, tests are normally performed on the components rather than on the composite.

Mann (1983) developed an approach for the determination of the masonry compressive strength based on the properties of the two components. DIN EN 1996 is based on this approach as well.

$$f_m = a \cdot f_b^b \cdot f_{mo}^c \quad f_b \text{ and } f_m \text{ in N/mm²; valid only for GPM} \qquad \text{Eq. 4-5}$$

where f_b and f_{mo} have to be inserted in N/mm².

In this equation a, b and c represent empirical factors derived from tests by regression analysis. These values have been determined in the past and for many new masonry products and are undergoing permanent updating. Table 4.5-6 gives some values for a, b and c for the determination of mean values. Please note that references to the units in the first

column are chosen to represent the common ones in Germany. The resulting compressive strength is valid for a slenderness of the specimen of $\lambda = 10$. However, more detailed values for the determination of characteristic values can be found in DIN EN 1996-1-1/NA, for example.

In case of masonry with TLM, the influence of the mortar compressive strength on the masonry compressive strength is negligible. This yields the following equation for TLM.

$$f_m = a \cdot f_b^b \qquad f_b \text{ and } f_m \text{ in N/mm²; valid only for TLM} \qquad \text{Eq. 4-6}$$

Table 4.5-6 Parameters a, b and c for the determination of the mean masonry compressive strength for a slenderness of λ = 10 according to Schubert (2010)

Masonry			n	a	b	c
Units		Mortar				
Material	Unit type					
LC	V, Vbl, Hbl	TLM	35	0.85	0.84	0
		LWM	80	0.85	0.58	0.15
		GPM	167	0.85	0.73	0.07
	Hbl	LWM	59	0.86	0.57	0.14
	V, Vbl	GPM	61	0.85	0.72	0.09
	Hbl	GPM	106	0.89	0.69	0.05
	V, Vbl	TLM	20	0.63	1.00	0
AAC	PB	NM	140	0.98	0.68	0.02
				0.99	0.69	0
		LM	17	0.80	0.64	0.09
				0.99	0.64	0
	PP	DM	162	0.63	1.00	0
				0.83	0.86	0
NC	Hbn	GPM	15	0.03	1.82	0.23
CS	CS full	GPM	276	0.70	0.74	0.21
	CS block	GPM	24	0.44	0.92	0.17
	CS perforated	GPM	108	0.85	0.57	0.20
	CS hollow	GPM	70	0.99	0.64	0.05
	CS elements	TLM	66	0.53	1.00	0
CB	full	GPM	55	0.73	0.73	0.16
	perforated		342	0.55	0.56	0.46
	lightweight perforated	TLM	9	0.75	0.72	0
		LWM 21	17	0.67	0.50	0.05
		LWM 21	17	0.18	1.00	0
		LWM 36	13	0.47	0.82	0
		LWM 36	13	0.28	1.00	0
		GPM	28	0.26	0.82	0.42

The slenderness of the specimens plays a major role in the determination of the masonry compressive strength. In order to compare the values predicted by Eq. 4-5 and Eq. 4-6 to test data for the assessment of the accuracy of the equations, the masonry compressive strengths have to be converted to the same reference slenderness $\lambda = h_k/t$. This can be done by multiplication with the factor $k_{\lambda=5}$ according to *Mann (1983)*. This factor converts the masonry compressive strength to the reference slenderness of $\lambda = 5$.

$$k_{\lambda=5} = \left(0.966 + 0.00136 \cdot \lambda_{specimen}^2\right) \qquad \text{Eq. 4-7}$$

In *Graubner & Glowienka (2007)*, a large database with hundreds of tests on units, mortar and RILEM specimens was evaluated. Table 4.5-7 provides the coefficients of variation obtained depending on unit material and type of mortar.

Table 4.5-7 Coefficients of variation of masonry compressive strength for various unit-mortar-combinations according to Graubner & Glowienka (2007)

Unit	Mortar	Range of *CoV*	*n*	$CoV_{,recommended}$
CS	TLM	11% - 33%	60	20%
	GPM	9% - 28%	339	20%
CB	TLM	17% - 26%	44	20%
	GPM	8% - 32%	348	20%
	LWM	15% - 25%	42	21%
AAC	TLM	8% - 23%	98	16%
LC	TLM	16% - 25%	33	22%
	GPM	14% - 20%	36	17%

It can be seen that although the range of scatter is large, the average coefficient of variation comes close to 20% in every case. This corresponds to other values obtained from the literature, as shown in Table 4.5-8.

Table 4.5-8 Values for the coefficient of variation found in the literature

Source	$f_m/f_{k,5\%}$	$CoV_{,average}$	Comment
Kirtschig & Kasten (1980)	1.34	17%	average value over various unit materials
Galambos et al. (1982)	1.36	18%	derived for the axial capacity of masonry walls
Tschötschel (1989)	1.55	25%	-
Holicky & Markova (2002)	1.41	20%	-
Schueremans (2001)	1.36	19%	for historical masonry

Glowienka (2007) derived the stochastic properties for the masonry compressive strength of large-sized AAC and CS units from test data and performed a Bayesian update to eliminate stochastic uncertainties. The derived stochastic properties show smaller scatter of the masonry compressive strength due to the presence of fewer mortar joints.

Table 4.5-9 Stochastic model for the compressive strength of masonry for URM made of large-sized units according to Glowienka (2007)

Unit material	Distr.	$f_m/f_{k,5\%}$	*CoV*
CS	LN	1.32 N/mm²	16%
AAC		1.27 N/mm²	14%

Assessment of the test database of *Graubner & Glowienka (2007),* which was available to the author, allowed determination of the stochastic properties of mean-to-characteristic masonry compressive strength. In the assessment, the ratio of the masonry compressive strength in the test to the characteristic value according to DIN EN 1996 was determined and the stochastic moments of this ratio were derived. The characteristic values according to DIN EN 1996 are presented in Table 4.5-10 to Table 4.5-12.

Table 4.5-10 Characteristic values of the masonry compressive strength for hollow clay brick masonry according to DIN EN 1996

Class of compressive strength of unit according to DIN EN 1996	f_k in N/mm²			
	GPM II	GPM IIa	GPM III	GPM IIIa
2	1.4	1.6	1.9	2.2
4	2.1	2.4	2.9	3.3
6	2.7	3.1	3.7	4.2
8	3.1	3.9	4.4	4.9
10	3.5	45	5.0	5.6
12	3.9	5.0	5.6	6.3
16	4.6	5.9	6.6	7.4
20	5.3	6.7	7.5	8.4
28	5.3	6.7	9.2	10.3
36	5.3	6.7	10.2	11.9
48	5.3	6.7	12.2	14.1
60	5.3	6.7	14.3	16.0

Table 4.5-11 Characteristic values of the masonry compressive strength for calcium silicate masonry with TLM according to DIN EN 1996

Class of compressive strength of unit according to DIN EN 1996	f_k in N/mm²			
	Large-size units		Regular size units	
	CS XL	CS XL-N, CS XL-E	CS P	CS L-P
2	-	-	-	-
4	4.7	2.9	2.9	2.9
6	6.0	4.0	4.0	3.7
8	7.3	5.0	5.0	4.4
10	8.3	6.0	6.0	5.0
12	9.4	7.0	7.0	5.6
16	11.2	8.8	8.8	6.6
20	12.9	10.5	10.5	7.6
28	16.0	13.8	13.8	7.6
36	16.0	13.8	13.8	7.6
48	16.0	13.8	13.8	7.6
60	16.0	13.8	13.8	7.6

Table 4.5-12 Characteristic values of the masonry compressive strength for AAC masonry with TLM according to DIN EN 1996

Class of compressive strength of unit according to DIN EN 1996	f_k in N/mm²
	full units with TLM
2	1.8
4	3.2
6	4.5
8	5.7

The results of the assessment are displayed in Table 4.5-13. The numbers represent weighted results depending on the number of tests. Note that the characteristic values in the right column have been determined on the basis of a lognormal distribution which has showed good fit with the test data by χ^2-test.

Table 4.5-13 Results of the assessment of the test database

Unit	Mortar	n	$f_m/f_{k,EN}$	CoV	$f_m/f_{k,5\%}$
CS	TLM	60	1.55	19%	1.33
AAC		98	1.81	16%	1.32
CB	GPM	334	1.43	17%	1.34

Comparing these numbers to the literature, the test-to-characteristic ratios are larger. It becomes obvious that the code values do not represent the 5%-quantiles of the distribution in every case. The characteristic values provided by the code are smaller than intended by the definition of a 5%-quantile and therefore the code values are conservative. In the assessment, a general tendency for conservativism in the characteristic values, especially for AAC, was detected.

4.5.5 Tensile Strength of Units

The tensile strength of the unit f_{bt} is important to the prediction of the load-bearing capacity because unreinforced masonry under compression fails due to tension and shear failure is also often governed by the tensile strength. When it comes to tensile strength, the tensile strength of the units must be differentiated from the tensile strength of the masonry. Especially in the case of modern masonry that is mostly constructed with TLM, the cohesion of the mortar is sometimes so strong that tensile failure is likely to occur in the unit (especially in case of AAC) and thus, detailed knowledge about the tensile strength of the unit gains importance.

Testing of the tensile strength is difficult and expensive; various methods exist which all determine different kinds of tensile strength. Depending on the test method, the obtained tensile strength represents the splitting tensile strength or the direct tensile strength in the longitudinal direction of the unit. Both kinds of tensile strength are illustrated in the following figure.

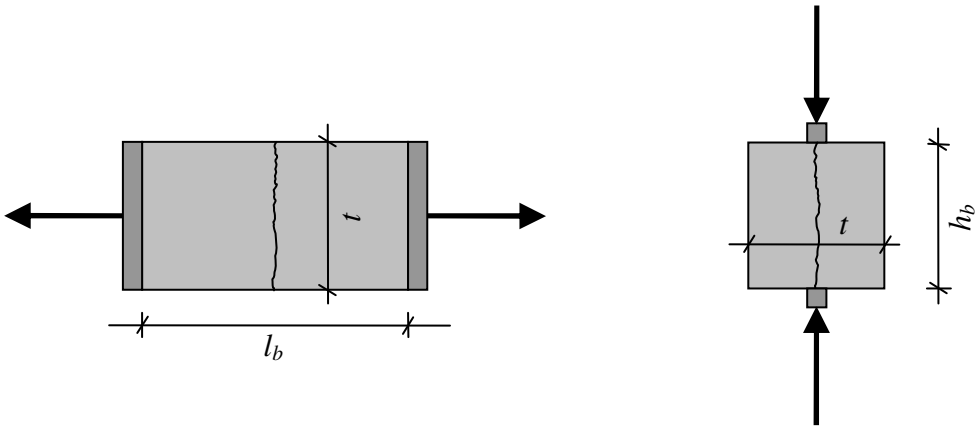

Direct tensile strength in the longitudinal direction of the unit

Splitting tensile strength

Figure 4-11 Direct tensile strength in longitudinal direction of the unit and splitting tensile strength

Thus, tensile strength strongly depends on the direction of investigation. Considering a wall under vertical and horizontal loading, the tensile stresses do not occur only in the vertical or horizontal directions but in the diagonal direction and the resultant stress is inclined. However, in most codes, e.g. DIN 1053-1, the term tensile strength refers to the tensile strength in longitudinal direction of the unit. It is obvious that the influence of the direction is larger in case of perforated units, e.g. typical clay bricks, and smaller for full units such as common AAC or CS blocks. *Kranzler (2008)* found that the tensile strength of clay bricks is best characterized by the splitting tensile strength while in the case of CS and AAC units, the direct tensile strength in the longitudinal direction proved more appropriate.

As in the case of concrete, the tensile strength of masonry units can be correlated with the compressive strength of the unit. Therefore, the most common approach for the analytical determination of the tensile strength of the unit is to multiply the compressive strength by a factor that depends on the type of unit as in Eq. 4-8.

$$f_{bt,i} = a_z \cdot f_b \qquad \text{Eq. 4-8}$$

This approach has been established in every generation of DIN 1053 since 1990. The factor a_z represents the ratio of tensile-to-compressive strength of the unit. In this equation, the compressive strength of the unit f_b refers to the class of compressive strength according to the German code. Values for this ratio according to DIN 1053 can be taken from Table 4.5-14. These values determine the characteristic value of the tensile strength in the longitudinal direction of the unit. Note that f_b in DIN EN 1996-1-1/NA is larger than f_b according to DIN 1053 (see section 4.5.2).

Table 4.5-14 *Factors $a_{z,k}$ according to DIN 1053-1, -100 and DIN EN 1996-1-1/NA for the characteristic value f_{btk} of the tensile strength in the longitudinal direction of the unit*

Unit	$a_{z,k}$	
	DIN 1053-1 and -100	DIN EN 1996-1-1/NA
Hollow blocks	0.025	0.025
Perforated units; units with grip holes	0.033	0.033
Full blocks	0.040	0.040
AAC	no special factor	0.082

As can be seen, DIN 1053-1 and DIN 1053-100 do not differentiate between the different unit materials. DIN EN 1996-1-1/NA copies the factors from DIN 1053-1 but adds another factor to account for the larger tensile strength of AAC due to the homogeneity of the units. *Schubert (2010)* determined the factors a_z depending on the unit material as presented in Table 4.5-15. These factors are more detailed than the values according to the codes and were derived to represent the mean of the series. Factors are available for the direct tensile strength in the longitudinal direction of the unit and for the splitting tensile strength.

Table 4.5-15 *Factors a_z for the determination of the tensile strength of unit in longitudinal direction according to Schubert (2010)*

Unit	a_z
CS full block (2 DF[a])	0.06
CS full block (2 DF[a]) with grip holes	0.05
CS perforated brick (2 DF[a])	0.04
Clay bricks	0.026
LC full 2, full block 2	0.105
LC full unit, full block and hollow block ≥ 4	0.062
LC hollow block 2	0.086
AAC 2	0.180
AAC 4, 6, 8	0.090
AAC all	0.100
[a]DF is a format of the units with 240 × 115 × 52 mm.	

To derive proper stochastic properties, test data from the literature was assessed and then updated using Bayes' theorem (see section 2.4.4). The test data was obtained from specimens of the relevant unit materials (CS, CB, AAC) so that an absolute value for the mean could be derived. The assessment is summarized in Table 4.5-16. The values for CS presented in the table were derived from tests on prisms that were cut from full units. This leads to larger values of the tensile strength. According to *Schubert (2010)*, the difference between tensile strength derived from tests on prisms and derived from tests on the unit is approximately 35%. Hence, the mean value of the tensile strength of CS units was multiplied with the factor 0.65.

Table 4.5-16 Likelihood parameters for the tensile strength of units derived from tests

Material	*m*	σ	*CoV*	*n*	Source
CS (f_k = 20 N/mm²)	1.78[a]	0.09	5%	11	Gunkler et al. (2009)
CB[b] (f_k = 12 N/mm²)	0.38	0.03	8%	4	Zilch & Krauns (2004)
AAC (f_k = 4 N/mm²)	0.57	0.07	12%	35	Höveling et al. (2009)
[a]converted from prisms; [b]splitting tensile strength					

The scatter of the tensile strength is astonishingly small. The main reason for this is that all tests were performed on the same kind of unit from the same batch. In reality, larger scatter is expected due to different manufacturers and plants. To reduce the stochastic uncertainty or correlation and to obtain more realistic values, the Likelihood parameters have to be updated using prior information. Only summaries of additional tests were available as prior information; detailed data about each single test could not be found. The prior information is summarized in the following table.

Table 4.5-17 Prior parameters for the update

Unit	*m*	σ	*CoV*	*n*	Source	Comment
CS 20	1.26	0.290	23%	18	Schubert (2010)	-
	1.50	0.45	30%	10	JCSS (2003)	Estimated on basis of experience with concrete
CB 12[a]	0.48	0.120	25%	29	Schubert (2010)	-
	0.54	0.124	23%	6	Schubert (2003)	Derived for lightweight CB 12 at incline direction of 30°
	0.96	0.103	11%	4		Derived for perforated CB 12 at incline direction of 30°
AAC 4[b]	0.44	0.080	9%	8	Schubert (2010)	-
	0.48	0.034	7%	24	Parker et al. (2007)	Weighted average values from series of AAC 4
[a]lightweight perforated [b]plane element						

The parameters of the prior distributions were derived by linear weighting depending on the number of tests. The parameters were then updated with the Likelihood information derived from test data and can be found in Table 4.5-18.

Table 4.5-18 Transformed stochastic Parameters of the unit tensile strength

Unit	Prior				Likelihood				Posterior			
	m'	*s'*	*v'*	*n'*	*m*	*s*	*v*	*n*	*m''*	*s''*	*v''*	*n''*
CS	0.265	0.251	27	28	0.575	0.050	10	11	0.353	0.256	38	39
CB	-0.646	0.229	38	39	-0.971	0.080	3	4	-0.677	0.239	42	43
AAC	-0.793	0.109	32	33	-0.570	0.120	34	35	-0.678	0.160	67	68

The required stochastic model for the unit tensile strength is then obtained by conversion of the posterior parameters to lognormal space. The values provided in Table 4.5-18 are valid for the approximation of a lognormal distribution to the *log-t*-distribution of the updating procedure. The stochastic uncertainties due to the sample size are included in the update process. Table 4.5-19 gives the stochastic models for the unit tensile strength.

It can be seen that the model for calcium silicate units shows the largest coefficient of variation. The reason for this is the large difference between the mean values of the Likelihood and prior parameters. Additionally, by comparing the ratio of $f_{bt,m}/f_{btk,EN}$ to the values in the right column, it can be seen that the values provided within the European code are conservative for CS and AAC. In case of CB, the values are not conservative for the provided stochastic model.

Table 4.5-19 Stochastic model for the tensile strength of units

Material	Distr.	m in N/mm²	$f_{bt,m}/f_{btk,EN}$	CoV	$f_{bt,m}/f_{btk,5\%}$
CS (20/TLM)	LN	1.47	1.84[b]	26%	1.57
CB (12/GPM)		0.52[a]	1.31[a,c]	24%[a]	1.52
AAC (4/TLM)		0.51	1.55[d]	16%	1.32
[a]splitting tensile strength [b]$f_{bt,cal}$ according to DIN EN 1996-1-1 ($f_{bt,cal}$ = 0.800 N/mm²) [c]$f_{bt,cal}$ according to DIN EN 1996-1-1 ($f_{bt,cal}$ = 0.396 N/mm²) [d]$f_{bt,cal}$ according to DIN EN 1996-1-1 ($f_{bt,cal}$ = 0.328 N/mm²)					

4.5.6 Cohesion and Friction Coefficient

The cohesion f_{v0} refers to the adhesion of the mortar. The mortar acts as the bonding agent and provides masonry with shear strength even without vertical compression. Therefore, cohesion is often referred to as "initial" shear strength. In the determination of the sliding shear strength and the flexural tensile strength of masonry walls, cohesion is a governing parameter.

The friction coefficient μ links the axial load to the corresponding contribution of the shear strength according to *Coulomb's* law (*Coulomb (1776)*). It represents the internal angle of friction and relates the shear force to the vertical force proportionally. In masonry design according to the German design codes, the cohesion is determined from the test method according to DIN 18555-5 (tests of mortar) on a two-unit specimen from a minimum number of 9 specimens. DIN EN 1996 refers to the test method according to DIN EN 1052-3 which is part of the European code harmonization. It is significantly different from the German procedure but bears the advantage of being mostly independent of the unit size and format. Figure 4-12 displays the two test setups schematically.

The values obtained from the two tests for the cohesion differ significantly, with values determined according to DIN 18555-5 being twice as large as the values according to DIN EN 1052-3 (*Schubert (2003)*). In *Schubert & Caballero (1995)* a factor of $f_{vk0,DIN\ 1052\text{-}3} / f_{vk0,DIN\ 18555\text{-}5} = 2.0$ was verified. Currently, test methods that will provide more reliable values are being developed (see *Popal & Lissel (2010)*).

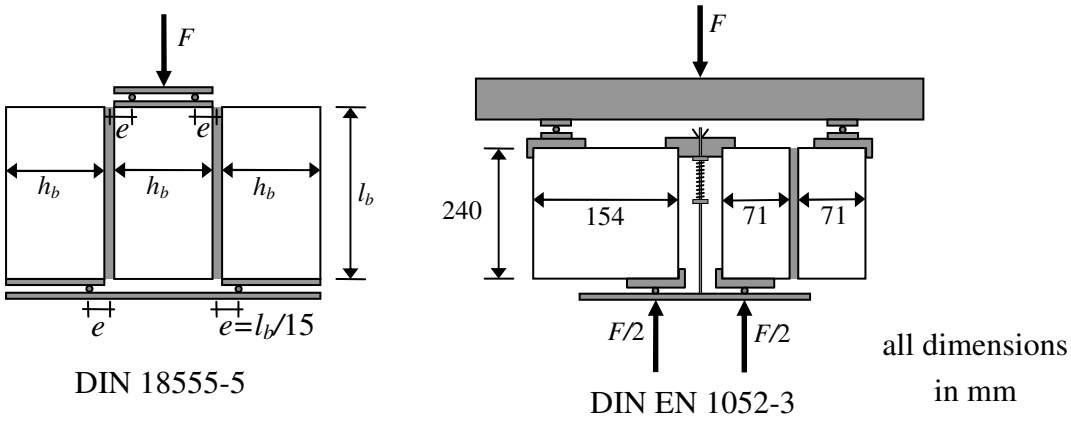

Figure 4-12 *Test setup for the determination of cohesion according to DIN 18555-5 and DIN EN 1052-3*

Cohesion depends on three main parameters: type of mortar, kind of unit and strength of the unit-mortar-interface. Large differences only occur in case of GPM. If TLM is applied, cohesion is similar for different kinds of units. This corresponds to the values according to DIN EN 1996-1-1/NA given in Table 4.5-20.

Table 4.5-20 *Characteristic values of the cohesion according to DIN EN 1996-1-1/NA (determined according to DIN 18555-5) without axial compression*

f_{vk0} in N/mm²			
GPM		TLM	LM
20 and higher	0.21	0.35[a]	0.14
10 - 19	0.18		
5 - 9	0.14		
2.5 - 4.5	0.07		
1 - 2	0.02		
[a]divide by 2 if the void area is more than 15% of the cross-section			

Brameshuber et al. (2006) and *Schubert et al. (2003)* report the stochastic parameters of the cohesion for large-sized CS and AAC units with TLM. These values were derived for large-sized units in "plane quality" (very even surface of the units) which represent the common masonry in Germany. In the case of clay bricks, only a few tests for the determination of the cohesion of GPM are available in the literature. One single test can be found in *Schubert et al. (2003)* giving a value of 0.55 N/mm² for CB 12/IIa and 3 tests in *Ötes & Löring (2003)* give a mean value of 0.50 N/mm² for the same kind of masonry. According to *Schubert (2010)*, the cohesion of clay bricks (all kinds) with GPM lies within the range of 0.4-1.0 N/mm² providing a mean value of 0.50 N/mm² for GPM IIa. This corresponds to the values found in the mentioned tests. No data about the scatter could be found and so the scatter will be assumed to be larger than in case of CS and AAC units. The stochastic models for the cohesion are summarized in Table 4.5-21. It can be seen from the determination of the 5%-quantiles that the values provided within the code are

conservative, even for the large scatter assumed. In case of GPM IIa and CB units, the value seems overly conservative.

Table 4.5-21 Stochastic models of the cohesion for large-sized AAC and CS units with TLM and CB units with GPM IIa according to Brameshuber et al. (2006) and Schubert (2010)

Unit	Mortar	Dist.	m	$f_{v0m}/f_{v0k,EN}$	CoV	$f_{v0m}/f_{v0k,5\%}$
AAC large-sized	TLM	LN	0.75 N/mm²	2.14	35%	1.16
CS large-sized						
CB	IIa		0.50 N/mm²	3.57	40%	1.76

The database of tests of the friction coefficient μ is poor since a determination of these parameters was not stipulated in DIN 18555-5. Because nearly all tests of the cohesion were carried out on the basis of DIN 18555-5, there is a significant lack of data. Nevertheless, some recommendations can be found in the literature and usually range from 0.51 (*Mann & Müller (1973)*) to 0.86 *König et al. (1988)*. *Schueremans (2001)* derived the friction coefficient independently from material and unit type by means of a lognormal distribution with a mean of 0.8 and *CoV* of 19%. This model gives a characteristic value of $\mu_k = 0.6$ as the 5%-quantile which corresponds to the value provided in the German code. This stochastic model will be used herein.

4.6 Summary

In this chapter, the basic knowledge about the load-carrying behaviour of URM walls subjected to axial load and in-plane shear is explained. Additionally, the relevant material properties are presented.

Unreinforced masonry walls exhibit complex load-carrying behaviour; various failure modes are possible depending on the geometry of the wall, the absolute value of stress and the masonry properties, among other influences. The corresponding material properties are explained and assessed. Typical test procedures are displayed and the status and numbers from design codes are analysed for each material property so that stochastic models could be derived. The stochastic models are derived by use of test data and values available in the literature. For more realistic results, some properties are updated with prior information by use of Bayesian techniques. In this way, appropriate stochastic models are derived for all required material properties assuming homogeneous material properties and smeared stress-strain relationships. The stochastic models for the material properties are summarized in Table 4.6-1.

Table 4.6-1 Summary of the stochastic models of the material properties

Basic variable	Unit	Dist.	m [N/mm²]	$X_{k.EN}$[a] [N/mm²]	$f_{m,i}/f_{k,i}$	CoV	Comment
Compressive strength f_m	CS	LN	-	10.5	1.55	19%	-
	AAC		-	3.2	1.81	16%	-
	CB		-	5.0	1.43	17%	-
Cohesion f_{v0}	CS		0.75	0.35	2.14	35%	TLM
	AAC						
	CB		0.50	0.14	3.57	40%	GPM
Friction coefficient μ	all		0.8	0.6	1.33	19%	-
Tensile strength of unit f_{bt}	CS		1.47	0.80	1.84	26%	-
	AAC		0.51	0.33	1.55	16%	
	CB		0.52	0.40	1.31	24%	splitting tensile strength

[a]for CS 20/TLM, AAC 4/TLM and CB 12/GPM IIa

5 PREDICTION OF THE LOAD-CARRYING CAPACITY

5.1 General

In comparison to the prediction of the flexural capacity, the prediction of the shear capacity is much more difficult. The reason for this is the very complex load-carrying behaviour of unreinforced masonry subjected to shear. Due to the nonhomogeneous and orthotropic nature of the material, several failure modes are likely to occur, as was described in section 4.4. Summarizing, the critical failure modes are

- tip over of the entire wall
- flexural failure
- sliding shear
- diagonal tension
- crushing

Figure 5-1 shows the load-carrying capacities v_R versus the axial load n. Note that the location and possibility of the failure envelope intersections depend on dimensions, material properties and loading. The figure only illustrates the general situation.

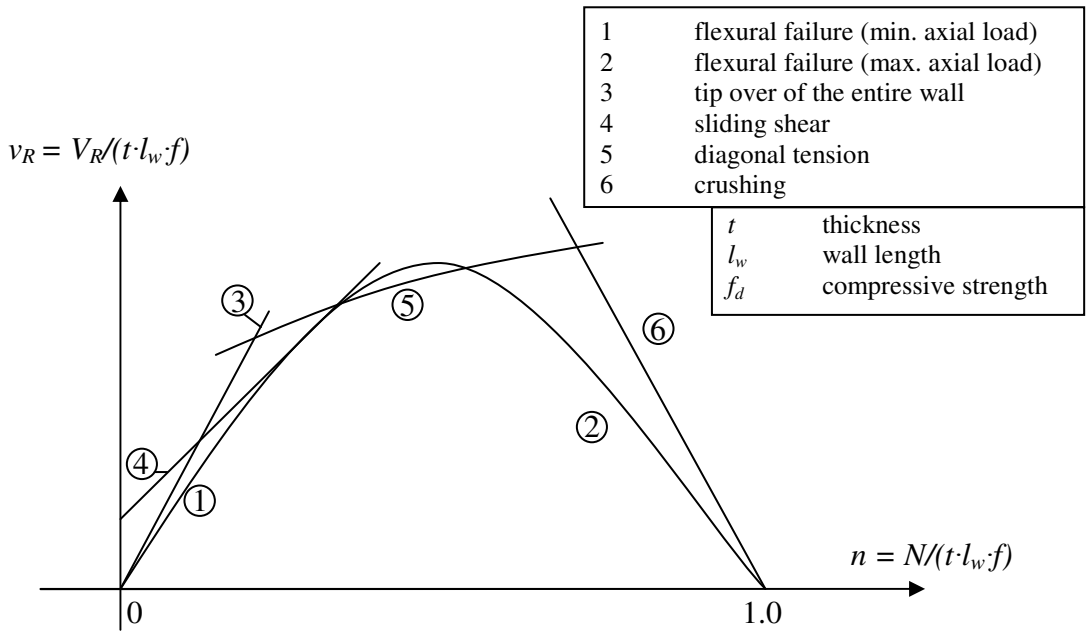

Figure 5-1 Shear capacity v_R vs. axial load n and failure modes

The idea of different ranges for different failure modes forms the basis for most common shear models, such as *Mann & Müller (1973)*. Although, this thesis focusses on the reliability of masonry shear walls, a general understanding of shear in masonry is required. Thus, a brief overview of shear models will be presented here. Subsequently, the models will be assessed by comparison with a test database so that the most realistic model can be identified. For more detailed information on the shear models, refer to *Kranzler*

(2008). All the models presented model the masonry with a smeared stress-strain relationship; discrete modelling of unit and mortar is not useful for reliability analysis.

5.2 Notation

A normalized, non-dimensional notation for the axial and shear force will be used in the following. The main advantage of this notation is the assessment being independent from the compressive strength and dimensions of the analysed wall.

$$n_i = \frac{N_i}{t \cdot l_w \cdot f_i} \qquad \text{Eq. 5-1}$$

$$v_i = \frac{V_i}{t \cdot l_w \cdot f_i} \qquad \text{Eq. 5-2}$$

where n_i and v_i are the non-dimensional axial and shear force, N_i and V_i are dimensional axial and shear force, t is the thickness of the wall, l_w is the length of the wall and f_i is the compressive strength. This notation will be used for consistency in the following discussion. Note, that the subscripts of N_i and V_i may be different (e.g. $V_i = V_{Rk}$ or $V_i = V_{Ek}$).

For the reliability analysis in chapter 6, a realistic prediction model is required. Thus, the models presented in this chapter will be assessed with test data to identify the best model and derive the required stochastic parameters for the model uncertainty.

5.3 Classical Beam Theory

5.3.1 Pre-Assumptions and Structural System

In the following sections, the prediction of the shear capacity of a URM wall will be explained. Here, the term “shear capacity” refers to the horizontal load that can be sustained by the wall. This load is limited by a number of possible failure modes of the wall which were described in section 4.4.2. In general, the limiting failure modes can be divided into failure related to axial stress (and flexure) and failure related to shear. Commonly, the shear capacity related to axial stress is determined from either classical beam theory which will be explained in this section or from theory of plastic limit analysis which will not be the focus of this thesis but be briefly discussed in section 5.4.

A number of simplifications in modeling of the realistic load-carrying behaviour are made in the application of classical beam theory. The hypothesis of Bernoulli, i.e. cross-sections remaining plane, is assumed valid and the influence of shear on the deformations is neglected.

Typical masonry walls subjected to in-plane shear can be modelled as walls with centric axial load and horizontal load at the top of the wall by using the shear slenderness ratio λ_v as proposed by *Kranzler (2008)*. The parameter λ_v can be calculated from Eq. 5-3. The

parameter ψ in this equation accounts for the structural system of the wall and is illustrated in Figure 5-2. In chapter 6, the shear slenderness will be the main parameter in the reliability analysis.

$$\lambda_v = \psi \cdot h_w / l_w \qquad \text{Eq. 5-3}$$

$$\psi = \frac{1}{\left(1 - \frac{e_o}{e_u}\right)} > 0 \quad for\ |e_u| > |e_o|$$

$$\psi = \frac{1}{\left(1 - \frac{e_u}{e_o}\right)} > 0 \quad for\ |e_u| \leq |e_o| \qquad \text{Eq. 5-4}$$

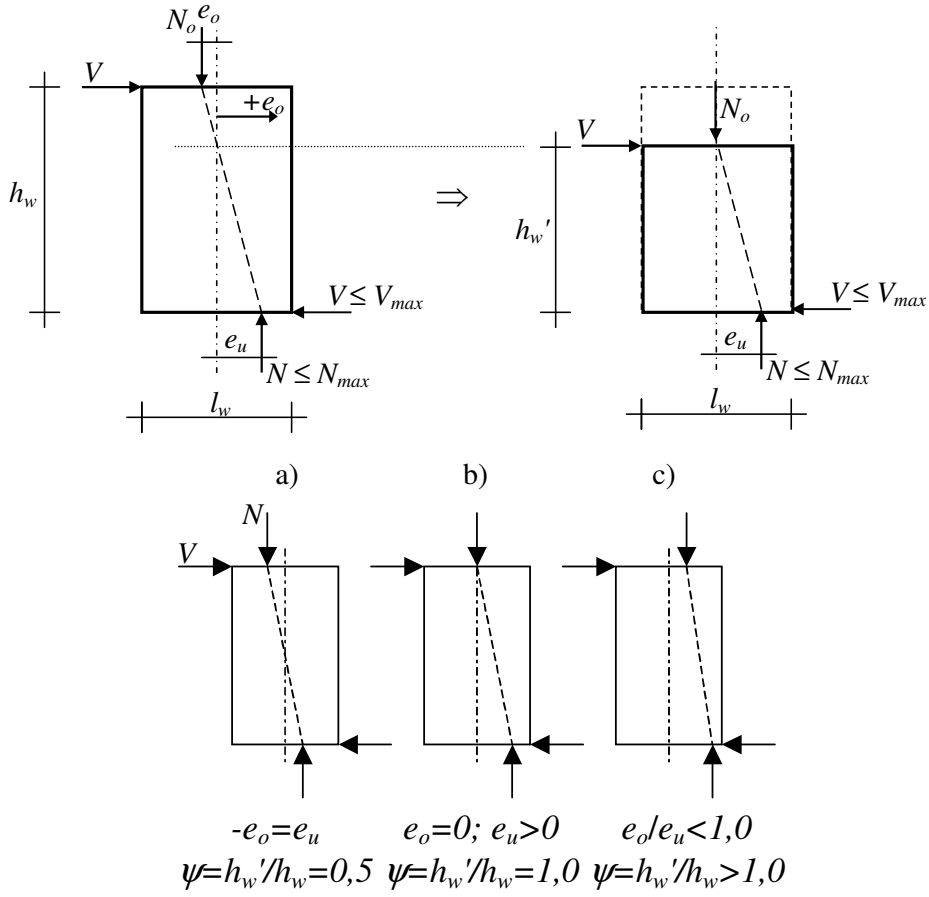

Figure 5-2 Conversion of the structural system of a Shear Wall according to Kranzler (2008)

The shear slenderness λ_v can also be seen as a measure of the eccentricity, since

$$\frac{e}{l_w} = \frac{V}{N} \cdot \frac{h_w}{l_w} \cdot \psi = \frac{V}{N} \cdot \lambda_v \qquad \text{Eq. 5-5}$$

Consequently, for constant *V/N*, the eccentricity increases with increasing λ_v resulting in a larger moment arm in the structural system.

5.3.2 Tip over of the Entire Wall

Besides the typical failure modes that occur due to exceeding the material strength, another failure mode has to be considered in case of URM: the tip over (index "to") of the entire wall (see section 4.4). In this failure mode, the wall itself remains "undamaged", theoretically. This failure happens for eccentricities $e_u/l_w > 0.5$, i.e. when the resultant of the axial stress is located outside the cross section and when tensile strength in the bottom layer is non-existent.

$$\nu_{R,to} = \frac{n}{2 \cdot \lambda_v} \qquad \text{Eq. 5-6}$$

This failure mode represents an upper limit of the shear capacity and can only govern in case of large values of the shear slenderness in combination with large eccentricities. Normally, the other failure modes lead to significantly smaller shear capacities.

5.3.3 Flexural Failure

The flexural capacity depends on the assumed stress-strain relationship. In general, two limit cases are possible: linear-elastic or fully-plastic. The realistic stress-strain relationship of course lies in between these two cases. For information on the prediction of the flexural capacity based on an arbitrary stress-strain relationship, refer to *Glock* (2004).

If a linear-elastic stress-strain relationship is assumed, cracked (denoted by "c" in the index) and uncracked ("uc") cross-sections have to be differentiated. Possible failure modes are then flexural failure ("fl") of the uncracked cross-section corresponding to the axial stress exceeding the compressive strength and compression failure of the cracked cross-section. The latter happens if the stress at the edge of the cross-section exceeds the compressive strength. Because of the eccentricity, the length under compression decreases and thus the stress at the edge increases. If tensile strength f_{x1} of the cross-section in the vertical direction is taken into account, a third failure mode can occur. However, such tensile strength will not be taken into account here as it is not in most design guidelines and codes. The reason is the strong influence of workmanship and the large uncertainty in the tensile strength. Using a linear-elastic stress-strain relationship leads to:

$$\nu_{R,fl,uc} = \frac{1-n}{6 \cdot \lambda_v} \quad n > 0.5 \qquad \text{Eq. 5-7}$$

$$\nu_{R,fl,c} = \frac{3 \cdot n - 4 \cdot n^2}{6 \cdot \lambda_v} \; n \le 0.5 \qquad \text{Eq. 5-8}$$

If the stress-strain relationship is assumed fully-plastic, a differentiation between cracked and uncracked cross-sections is unnecessary due to the use of the stress block and thus the shape of the stress distribution does not change from uncracked to cracked state. In this

case, the shear capacity for a fully-plastic stress-strain relationship is equal to $v_{f,cr}$ according to Eq. 5-9.

$$v_{R,fl,plastic} = \frac{1}{2 \cdot \lambda_v} \cdot \left(n - n^2\right) \qquad \text{Eq. 5-9}$$

5.3.4 Shear Capacity

5.3.4.1 Historical development

The first studies on masonry shear strength (see *Kelch & Norman (1931)*, *Benjamin & Williams (1958)*, *Vogt (1961)*, *Zelger (1964)*) focused on recalculation of experimental data and derived a shear strength f_v directly from the test data.

$$V_R = f_v \cdot A' \qquad \text{Eq. 5-10}$$

where V_R is the shear capacity, A' is the corresponding cross-sectional area (which is equal to the cross-sectional area subjected to compression).

The fact that shear capacity of unreinforced masonry depends on the axial stress was verified in every study. *Hendry & Sinha* (1969, 1971) reasoned an almost linear relationship of axial stress and shear capacity from their test results, see Figure 5-3.

In most tests, a failure of the mortar-unit interface due to the low cohesion of the old mortars was observed. This leads to the common approach to predict the shear capacity using the *Mohr-Coulomb* criterion.

$$f_v = f_{v0} - \mu \cdot \sigma_x \qquad \text{Eq. 5-11}$$

Today's mortars provide much better cohesion, especially TLM. Additionally, today's shear walls are much more slender so that other failure modes become likely. However, Eq. 5-11 is still the only design model available in a large number of codes.

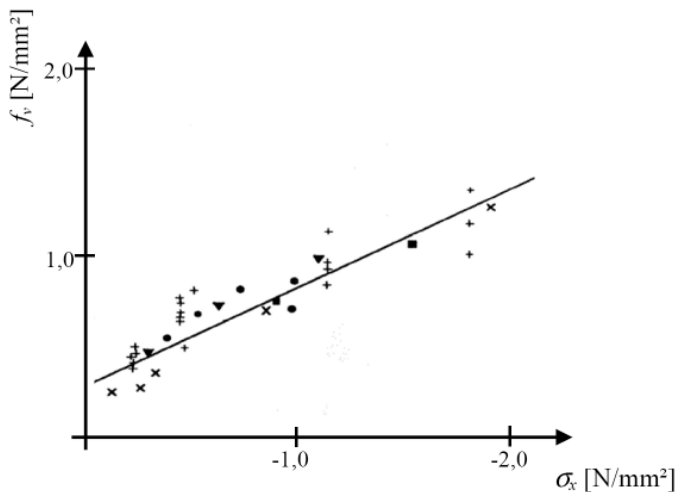

Figure 5-3 Influence of the axial stress on the shear capacity (Hendry & Sinha (1969, 1971))

In subsequent years it was found that the linear approach is not appropriate (see *Stafford-Smith & Carter (1971)*) especially for large axial loads. *Tomazevic (1982)* proposed the use of a general limit stress depending on the geometry of the wall. This gave a new equation for the shear strength corresponding to diagonal tension failure (see section 4.4.2).

$$f_v = \frac{\sigma_{1,t}}{c} \cdot \sqrt{1 - \frac{\sigma_x}{\sigma_{1,t}}} \qquad \text{Eq. 5-12}$$

where σ_x is axial stress, $\sigma_{1,t}$ is the resulting principal tensile stress and c is a parameter that represents the distribution of the axial stress over the cross-section. The parameter c has entered the German design codes in similar form.

From there, *Mann & Müller (1973, 1978)* developed a model for the shear strength that includes tensile and compressive strength of the unit as well as the cohesion. The model neglects shear transfer through the head joints which applies for unfilled head joints and represents the common situation in Germany where head joints are usually unfilled. Taking into account the shrinkage of the units and mortar, shear transfer through the head joints has to be questioned even in case of filled head joints. *Mann & Müller's* model has been derived from the single unit instead from the wall. Overall, *Mann & Müller* accounted for four failure modes: tip over of the separate unit, sliding shear, diagonal tension and (shear) crushing as explained in section 4.4. The occurrence of these failure modes depends on the level of axial stress as presented in Figure 5-1.

Mann & Müller's model has formed the basis for the German design codes since its development. Therefore, it is described in more detail in section 5.3.4.2.

Using *Mann & Müller's* work as a basis, many authors went on developing shear models. Here, only models that brought significant new knowledge will be explained, for more detailed information see *Simon (2002)* and *Kranzler (2008)*. A significant shortcoming of *Mann & Müller's* model is that is does not account for small overlaps *u/h* which have

become more and more common due to the application of large-size masonry units. *Graubner & Simon* (2001), *Simon* (2002) as well as *Jäger & Schöps (2004)* therefore included the overlap in their models. The model of *Jäger & Schöps* forms the basis for some parts of the new German National Annex to Eurocode 6 and thus will be discussed in more detail in section 5.3.4.3. *Page (1978, 1980, 1982)* conducted a large test series on biaxially stressed masonry specimens with inclined bed joints and therefore was able to define failure modes for different combinations of principal stresses (tension-tension, tension-compression, compression-compression). Figure 5-4 shows the typical results for the tension-compression combination. Every point of the failure envelope shown represents failure. As it can be seen from this figure, an analytical formulation of the envelope area in an efficient and practical way is not possible.

Ganz (1985) developed a failure envelope for biaxially stressed URM based on *Page (1978, 1980, 1981, 1982)*. He formulated five failure modes for masonry without tensile strength and thirteen failure modes for masonry with tensile strength. This model is special since it is based on theory of plasticity instead of following a linear-elastic approach. The failure envelope according to *Ganz* (1985) is presented in Figure 5-5.

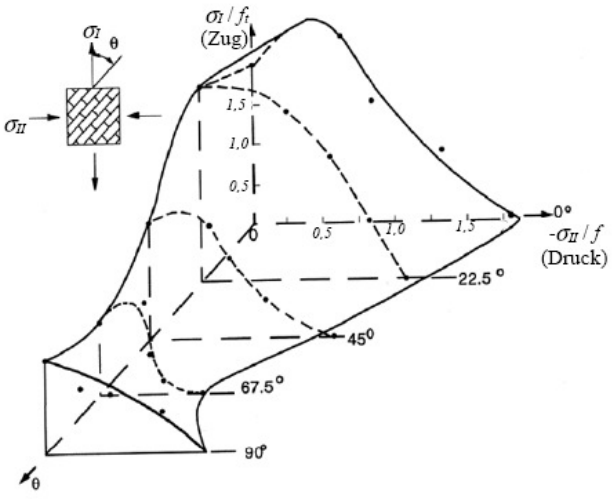

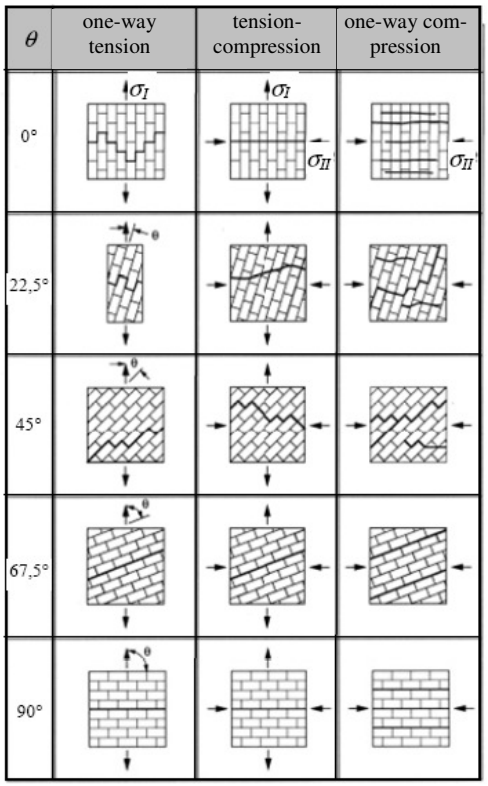

Figure 5-4 *Failure envelope and failure modes occurring for tension-compression combination (Page (1982))*

Mojsilovic (1995) and *Mojsilovic & Marti (1997)* developed their model on the basis of *Ganz*'s work. They added another failure mode for masonry without tensile strength that covered typical failure of CS masonry along the head joints. However, the required material and strength parameters for this model are very difficult to determine. The model of

Mojsilovic and Marti forms the basis of the Swiss design code but will not be taken into account for probabilistic analysis in this thesis because it has been derived for filled head joints which are mandatory in Switzerland but uncommon in Germany.

A relatively new model is the model according to *Schermer* (2004). It is based on the theory of plasticity and the model of *Mann & Müller (1973)*.

The newest approach to shear strength prediction comes from *Kranzler (2008)*. His approach is based on the models of *Mann & Müller (1973)* and *Jäger & Schöps (2004)*. From there, he formulated a minimum value of the sliding shear strength and calibrated the approach of *Jäger & Schöps (2004)* for diagonal tension.

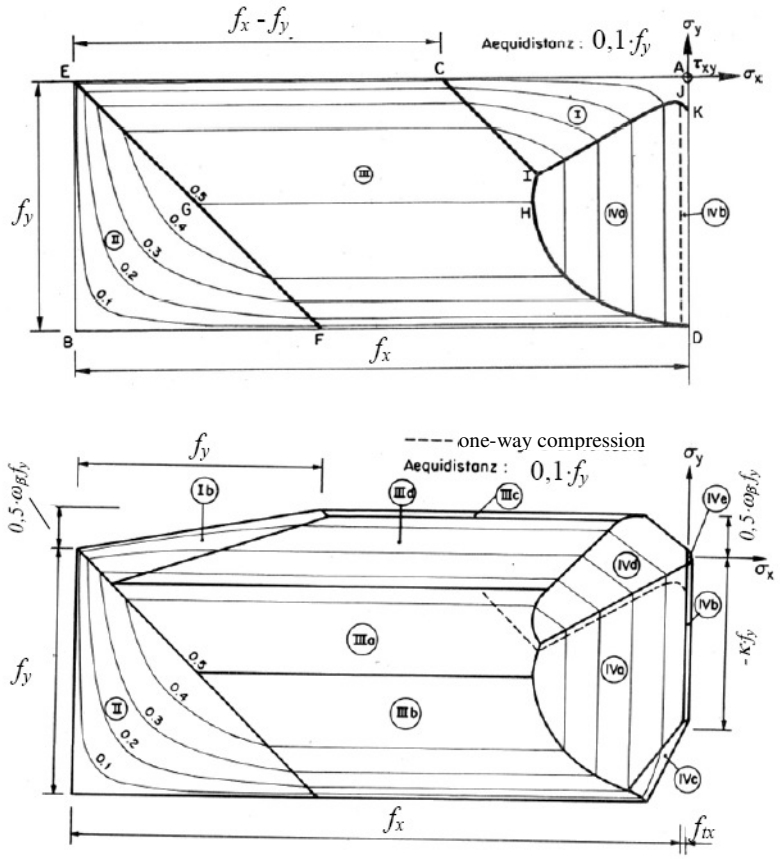

Figure 5-5 Failure envelope for masonry with and without tensile strength (Ganz (1985))

5.3.4.2 Shear Model according to *Mann & Müller* (1973)

Mann & Müller (1973) derived their model from an idealized, separate unit in a wall with regular running bond corresponding to an overlap $u/l_b = 0.5$. The stresses in consideration are shown in the following figure.

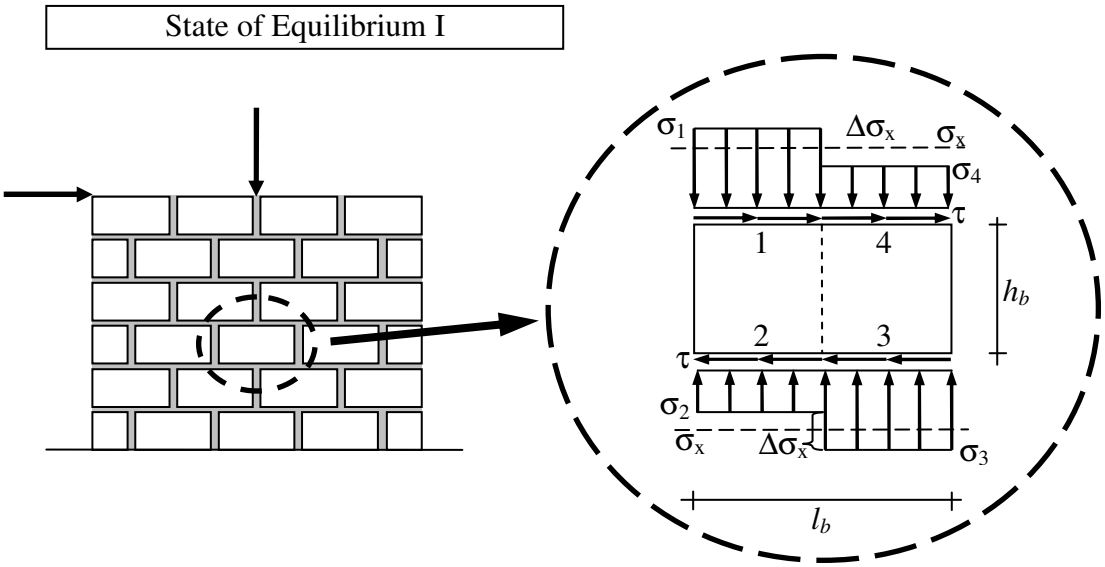

Figure 5-6 Stress model and state of equilibrium according to Mann & Müller (1973)

In the stress model, the stress transfer over the head joints is neglected so that only the shear stress τ and the axial stresses σ_i occur. The shear stress generates a rotating moment that has to be equalized by another moment due to the axial stresses. This leads to different axial stress in the areas 1 and 4 (and 2 and 3, respectively). This model is considered to be valid for every unit. From equilibrium at the unit, the axial stresses σ_1 and σ_2 can be determined:

$$\tau \cdot l_b \cdot \frac{h_b}{2} \cdot 2 = \Delta\sigma_x \cdot \frac{l_b}{2} \cdot \frac{l_b}{4} \cdot 4 \qquad \text{Eq. 5-13}$$

$$\Delta\sigma_x = 2 \cdot \tau \cdot \frac{h_b}{l_b} \qquad \text{Eq. 5-14}$$

$$\sigma_{1,2} = \sigma_x \pm 2 \cdot \tau \cdot \frac{h_b}{l_b} \qquad \text{Eq. 5-15}$$

Mann & Müller (1973) defined further failure criteria for the partial areas (1 - 4) of the unit. These failure criteria match the failure modes presented in section 4.4. The failure mode “tip over of the separate unit” occurs when the initial tensile strength f_{x1} in the bed joint is exceeded which could be the case for very tall units and small axial stress resulting in tensile stress in the areas 2 and 4,. The corresponding shear strength $f_{v,tsu}$ is then:

$$f_{v,tsu} = \left(f_{x1} - \sigma_x\right) \cdot \frac{l_b}{2 \cdot h_b} \qquad \text{Eq. 5-16}$$

Sliding shear failure (s) is thought to occur when the shear strength in the areas 2 and 4 is exceeded.

$$\tau \le f_{v,s} = f_{v0} - \mu \cdot \sigma_2 \qquad \text{Eq. 5-17}$$

Note that σ_2 is positive when tensile. By substituting Eq. 5-15 into the above equation, the shear strength due to sliding shear can be determined from

$$f_{v,s} = \frac{f_{v0} - \mu \cdot \sigma_x}{1 + \mu \cdot \dfrac{2 \cdot h_b}{l_b}} \qquad \text{Eq. 5-18}$$

It becomes obvious that it is not the maximum stress σ_I but rather the minimum axial stress σ_2 that governs. This stress occurs in the areas 2 and 4 (see Figure 5-6) and failure happens there at the same time. *Mann & Müller* used this fact to explain the stepped crack formation.

With growing axial compression, tensile stresses in the diagonal direction of the unit occur. Cracking occurs when the tensile strength of the unit is exceeded. *Mann & Müller* calculated the corresponding shear stress τ_b inside the unit assuming that only unidirectional axial stress σ_x is available. The principal tensile stress σ_I can then be determined from Eq. 5-19.

$$\sigma_I = \frac{\sigma_x}{2} + \frac{1}{2} \cdot \sqrt{\left(\sigma_x^2 + 4 \cdot \tau_b^2\right)} \qquad \text{Eq. 5-19}$$

$$\tau_b = \sigma_I \cdot \sqrt{1 - \frac{\sigma_x}{\sigma_I}} \qquad \text{Eq. 5-20}$$

Introducing the tensile strength of the unit f_{bt} and setting $f_{bt} = \sigma_I$ yields

$$\tau_b = f_{bt} \cdot \sqrt{1 - \frac{\sigma_x}{f_{bt}}} \qquad \text{Eq. 5-21}$$

Note that τ_b is still the shear stress *inside* the unit and is not equal to the shear stress τ. *Mann & Müller (1978)* gave a value of $\tau_b = 2.3 \cdot \tau$. However, this value is only valid for units with $h_b/l_b = 0.5$.

$$f_{v,dt} = \frac{1}{2.3} \cdot f_{bt} \cdot \sqrt{1 - \frac{\sigma_x}{f_{bt}}} \qquad \text{Eq. 5-22}$$

Exceeding this shear strength will lead to the failure mode “diagonal tension” (dt), as shown in Figure 4-8. In case of very large axial stress σ_x, the areas 1 and 3 will fail due to exceeding the masonry strength f_m. From Eq. 5-24, the corresponding shear strength can be derived. The failure mode is referred to as “crushing” (c).

$$f_{v,c} = \left(f_m + \sigma_x\right) \cdot \frac{u}{h_b} \qquad \text{Eq. 5-23}$$

For the typical case of running bond and unit format of $l_b/h_b = 2$, the equation becomes:

$$f_{v,c} = \left(f_m + \sigma_x\right) \cdot \frac{l_b}{2 \cdot h_b} \qquad \text{Eq. 5-24}$$

Note that compressive stress is negative in the equation.

Shear failure will occur if any of the mentioned shear strengths is exceeded at a given load stage. *Kranzler (2008)* calculated the failure envelope for various unit formats, as presented in Figure 5-7.

It can be seen that the slope of the curve for sliding shear failure changes. The reason is that the stress redistribution into less stressed areas is neglected because of the discrete partition of the unit into four areas in the stress model. Therefore, tip over of the separate unit hardly ever governs and can be neglected according to *Mann & Müller (1973)* in common masonry design.

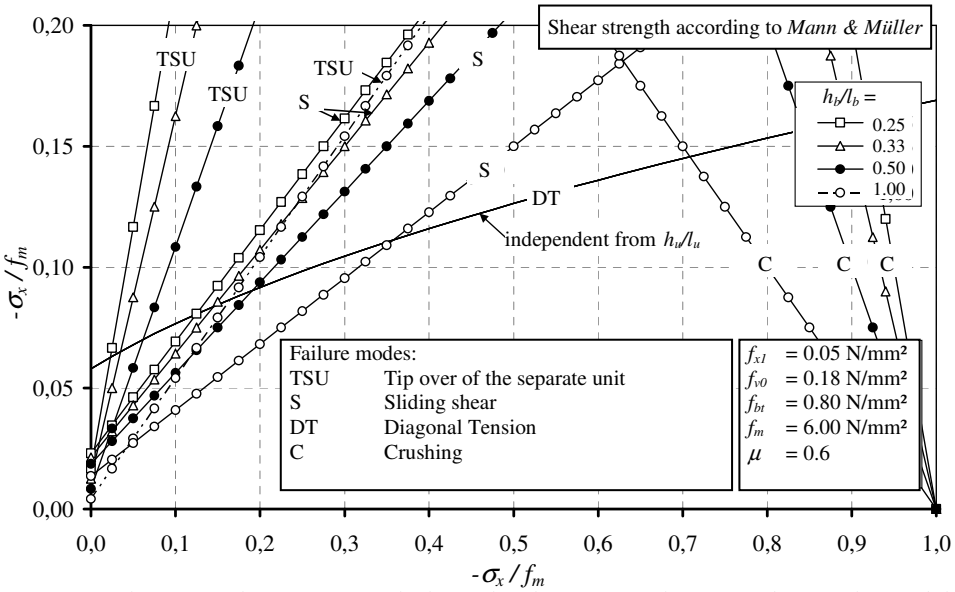

Figure 5-7 *Influence of the unit format h_b/l_b on the shear strength f_v according to the model of Mann & Müller (figure taken from Kranzler (2008))*

5.3.4.3 Shear Model according to *Jäger & Schöps (2004)*

While the model of *Mann & Müller (1973)* considers failure to happen when one partial area of the unit fails, *Jäger & Schöps (2004)* follow a different approach by considering stress redistribution over the unit. This leads to two new possible states of equilibrium besides the state defined by *Mann & Müller* (see Figure 5-6). In addition, new equations for diagonal tension failure were derived by fitting an empirical model to the shear stress distributions found in FE simulations. However, their investigations were simplified since

the normal and shear stress were considered to be constant in the respective area of the unit. A probable partial cracking inside the single areas is not taken into account.

As long as failure does not occur in one of the areas, the stress model is equal to the model of *Mann & Müller (1973)*, here further referred to as state of equilibrium I (see Figure 5-6). When failure occurs, stress redistribution to less stressed areas can occur and so *Jäger & Schöps (2004)* defined the states of equilibrium presented in the following figure.

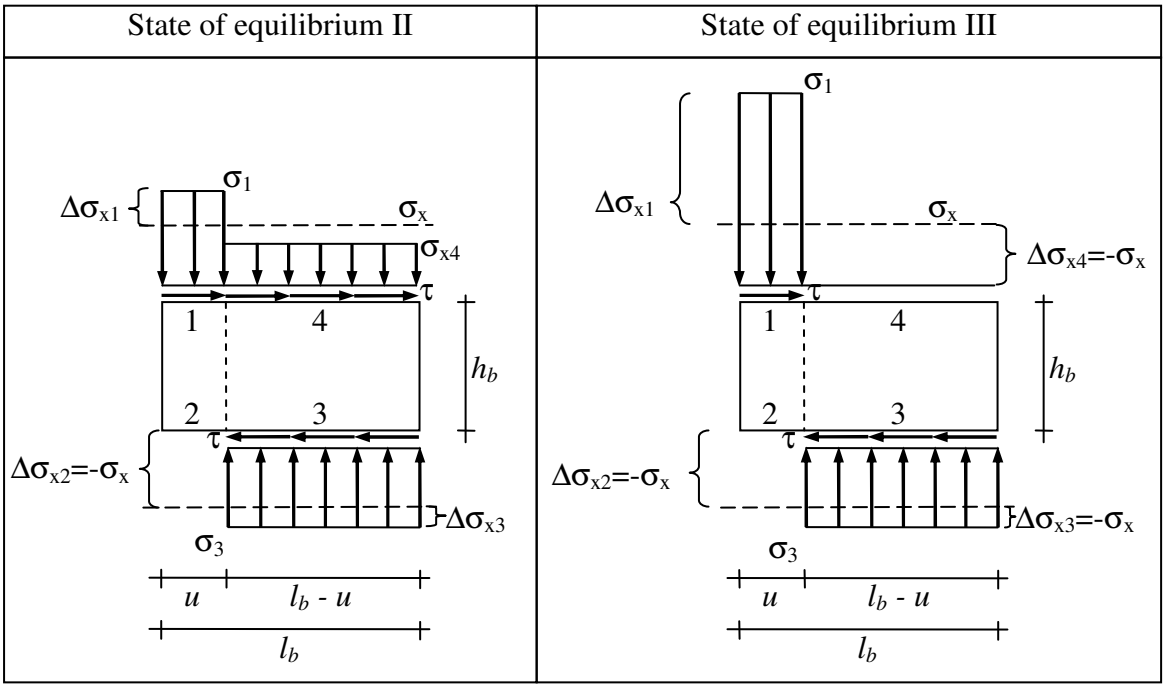

Figure 5-8 States of equilibrium II (left) and III (right) according to Jäger & Schöps (2004)

The stresses can be determined from moment equilibrium. For state of equilibrium II, this yields

$$\tau \cdot l_b \cdot \frac{h_b}{2} \cdot 2 = \Delta\sigma_{x1} \cdot \frac{u^2}{2} + \Delta\sigma_{x2} \cdot \frac{u^2}{2} + \Delta\sigma_{x3} \cdot \frac{(l_b - u)^2}{2} + \Delta\sigma_{x4} \cdot \frac{(l_b - u)^2}{2} \qquad \text{Eq. 5-25}$$

$$\frac{\Delta\sigma_{x1}}{\Delta\sigma_{x4}} = \frac{l_b - u}{u} \qquad \text{Eq. 5-26}$$

$$\Delta\sigma_{x2} = -\sigma_x \qquad \text{Eq. 5-27}$$

$$\Delta\sigma_{x3} = -\sigma_x \cdot \frac{u}{l_b - u} \qquad \text{Eq. 5-28}$$

$$\sigma_1 = -2 \cdot \tau \cdot \frac{h_b}{u} \qquad \text{Eq. 5-29}$$

$$\sigma_2 = 0 \qquad \text{Eq. 5-30}$$

$$\sigma_3 = \sigma_x \cdot \left(1 + \frac{u}{l_b - u}\right) \qquad \text{Eq. 5-31}$$

$$\sigma_4 = \sigma_x \cdot \left(1 + \frac{u}{l_b - u}\right) + 2 \cdot \tau \cdot \frac{h_b}{l_b - u} \qquad \text{Eq. 5-32}$$

The state of equilibrium III can only occur for a certain ratio of axial and shear stress. For larger shear, the system will then fail by tip over of the entire wall, for smaller shear, state of equilibrium II governs. In case of tip over, the shear can be calculated from the following equation.

$$\tau = -\frac{1}{2} \cdot \sigma_x \cdot \frac{l_b}{h_b} \qquad \text{Eq. 5-33}$$

The corresponding axial stresses in the areas 1 and 3 are then independent from the shear and become

$$\sigma_1 = \sigma_x \cdot \left(1 + \frac{l_b - u}{u}\right) \qquad \text{Eq. 5-34}$$

$$\sigma_3 = \sigma_x \cdot \left(1 + \frac{u}{l_b - u}\right) \qquad \text{Eq. 5-35}$$

Jäger & Schöps (2004) derived the shear strengths for the four failure modes as defined by *Mann & Müller (1973)* by defining further limit states for every state of equilibrium depending on the stress distribution, on the first area that fails and other conditions. This leads to a large number of possible limit states. A description of every limit state goes beyond the scope of this thesis; detailed information and analysis can be found in *Kranzler (2008)*.

It can, however, be stated that tip over of the separate units can become relevant in the model according the *Jäger & Schöps (2004)* due to the stress distribution and the corresponding constant value of the friction coefficient μ for different unit formats. This differs from the model of *Mann & Müller (1973)*.

The sliding shear strength is generally larger according to *Jäger & Schöps* than *Mann & Müller* due to the plasticity of the cross-section and the corresponding stress distribution being accounted for. For diagonal tension failure, *Jäger & Schöps (2004)* showed that the maximum shear stress always occurs at the edges of the units and not in the centre as assumed by previous authors. This was verified by FE simulations. The ratio of maximum shear stress to average shear stress $F = \tau_b / \tau$ was found to depend on the

thickness of the bed joints and was determined to be $F = 1.7$ for GPM and $F = 2.0$ for TLM and tall units (see Figure 5-9).

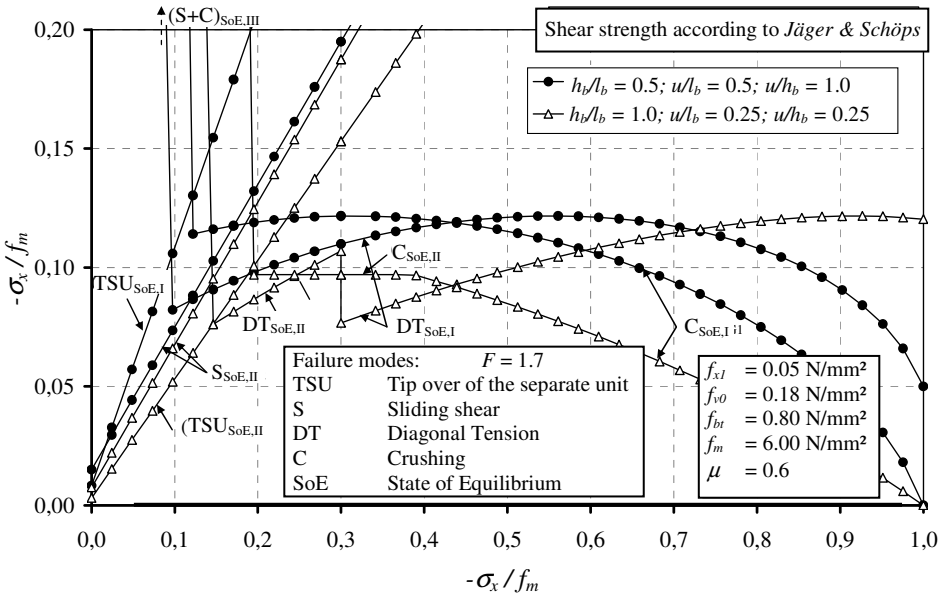

Figure 5-9 Failure envelope of the model according to Jäger & Schöps (Kranzler (2008))

5.3.4.4 Shear Model according to *Kranzler (2008)*

Kranzler (2008) based his work on the models of *Mann & Müller (1973)* and *Jäger & Schöps (2004)*. He was able to start his work from a large number of tests which were conducted to study modern large-sized masonry. *Kranzler (2008)* developed a new prediction model in which a minimum value of the sliding shear strength *min* v_s based on the second law of *Amontons* was introduced.

$$\min v_s = \mu \cdot n \qquad \text{Eq. 5-36}$$

For diagonal tensile failure (dt), *Kranzler (2008)* provides an equation based on *Jäger & Schöps (2004). Kranzler (2008)* modified the original factor F used to account for different thickness of the bed joints to a factor F' for better fit with the data.

$$v_{dt} = \frac{1}{c} \cdot \frac{f_{bt}}{f_m} \cdot \left(F'\right)^{-2} \cdot \left(\sqrt{1 + \left(F'\right)^2 \cdot \frac{n}{f_{bt}/f_m}} - 1 \right) \quad \text{for } h_w/h_b > 5 \qquad \text{Eq. 5-37}$$

$$v_{dt} = \frac{1}{c} \cdot \frac{f_{bt}}{f_m} \cdot \left(2 \cdot F' \cdot \frac{u}{h_b} \right)^{-2} \cdot \left(\sqrt{1 + \left(2 \cdot F' \cdot \frac{u}{h_b} \right)^2 \cdot \frac{n}{f_{bt}/f_m}} - 1 \right) \quad \text{for } h_w/h_b \le 5 \qquad \text{Eq. 5-38}$$

$$F' = F \cdot \left(0.63 + 0.45 \cdot f_{bt}\right) \quad f_{bt} \text{ in N/mm²} \qquad \text{Eq. 5-39}$$

with $F = 2.0$ for masonry with TLM and 1.7 for masonry with GPM. In addition, *Kranzler (2008)* recommended the use of the equation for flexural strength for very large axial forces (e.g. as in Eq. 5-8) instead of application of the shear crushing models.

5.4 Plastic Limit Analysis

A determination of the load-carrying capacity can also be carried out by plastic limit analysis. This is significantly more complex than the application of classical beam theory. This theory will not be used for the reliability analysis in the following chapter but will be explained briefly as a matter of completeness.

Plastic limit analysis was introduced into masonry design by *Ganz (1985)* and further developed by *Mojsilovic & Schwartz (2006)*. The latter divided their approach into simplified and exact methods. The difference between the two methods is the modelling of the stresses: while the simplified method only considers a single stress field due to the load, the exact method considers several stress fields. However, both methods require the determination of an inclined compressive strength f_θ. *Kranzler (2008)* gives a closed form solution for the shear capacity according to the simplified method.

$$v_{pl} = \lambda_v \cdot \frac{f_y}{f_x} \cdot \left(\sqrt{1 + \frac{\left(f_y / f_x\right) \cdot n - n^2}{\lambda_v^2 \cdot \left(f_y / f_x\right)^2}} - 1 \right) \qquad \text{Eq. 5-40}$$

where f_x is masonry compressive strength in the vertical direction and f_y is masonry compressive strength in the horizontal direction. The influence of the ratio f_y/f_x increases with increasing axial force n, see Figure 5-10.

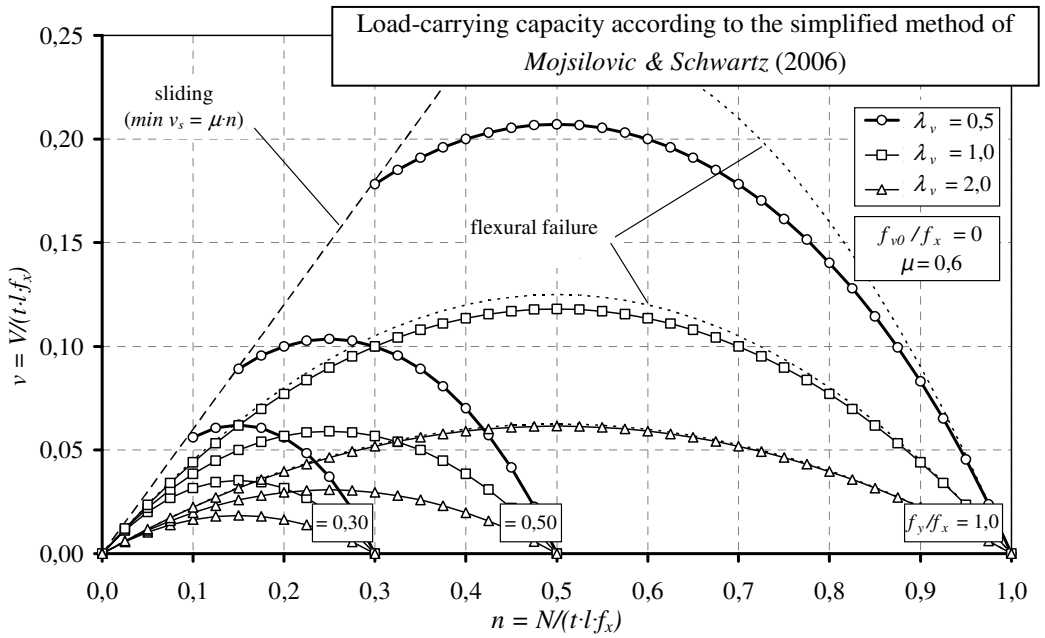

Figure 5-10 *Load-carrying capacity according to the simplified method of Mojsilovic & Schwartz (2006) (figure taken from Kranzler (2008))*

It can be seen that the load-carrying capacity is low for small values of f_y/f_x and can even be zero for $n > f_y/f_x$. Using the exact procedure is recommended in these cases since it leads to significantly larger capacities.

The exact procedure superimposes the diagonal stress field with the vertical stress field. A closed-form solution is not possible; iteration of the load-carrying capacity is required. The iteration has to be carried out over the inclination of the struts in the inclined stress field and the corresponding combination of axial and horizontal load have to be computed. For more detailed information, the reader is referred to *Kranzler (2008)*, however, the capacities according to the exact method are presented in Figure 5-11.

The plateau is reached for the respective maximum value of the angle of the struts. The capacities determined with the exact method are significantly larger than compared to the simplified method for small values of the ratio f_y/f_x. For large values of this ratio, the simplified method leads to larger capacities. The reason for this is related to the axial force that is required to determine $v = \mu \cdot n$. However, a simplified design model should never yield larger capacities than an "exact" method.

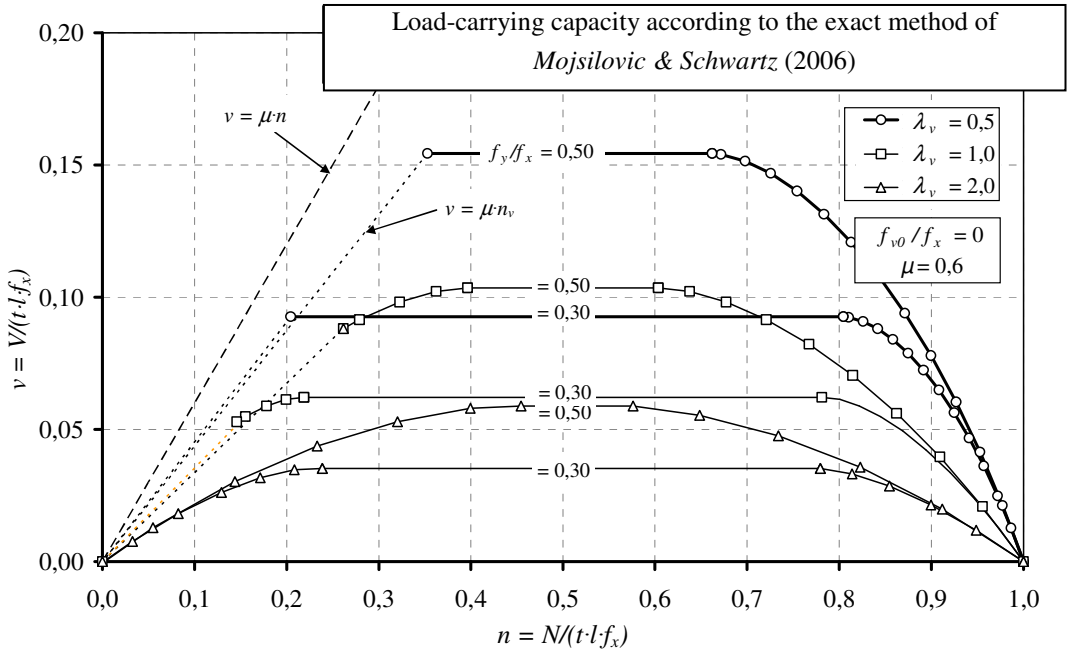

Figure 5-11 *Load-carrying capacity according to the exact method of Mojsilovic & Schwartz (2006) (figure taken from Kranzler (2008))*

5.5 Design models

5.5.1 Notation

In the following sections the non-dimensional definition of the forces as explained in section 5.2 will be used again. However, to refer to the corresponding loads and strengths from the codes, the definition will be presented again in the actual form.

$$n_{Gk} = \frac{N_{Gk}}{t \cdot l_w \cdot f_k} \qquad \text{Eq. 5-41}$$

$$v_{Ek} = \frac{V_{Ek}}{t \cdot l_w \cdot f_k} \qquad \text{Eq. 5-42}$$

Note that the masonry compressive strength f_k is the characteristic value according to DIN 1053-100 or DIN EN 1996. N_{Gk} is the characteristic value of the axial dead load. V_{Ek} is the maximum sustainable characteristic shear load in ultimate limit state. It was decided to use V_{Ek} instead of V_{Rk} due to better handling in the reliability analysis in chapter 6 where the mean of the shear load v_E will be determined from the characteristic value v_{Ek} (also see section 2.7). So, the normalized design equations as presented in the following sections can be used directly for the reliability analysis.

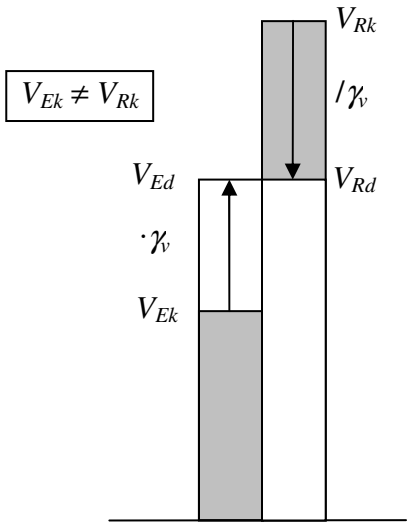

Figure 5-12 Relationship of V_{Ek} and V_{Rk} in semi-probabilistic design

5.5.2 Design Model according to DIN 1053-1 and DIN 1053-100

DIN 1053-1 (1996) and DIN 1053-100 (2007) include both simplified and exact design methods for shear walls. Since this thesis is about reliability assessment which requires exact prediction of the shear capacity, only the exact methods will be explained. For further information see *Simon (2002)* and *Kranzler (2008)*.

In contrast to DIN 1053-100, DIN 1053-1 applies the global safety concept to account for the inevitable uncertainties in the design. In this safety concept, the stresses due to the loads are multiplied by a safety factor $\gamma_{gl} = 2.0$ and checked with the strength. This is actually not correct because the stresses are determined based on the cross-sectional area subjected to compression and consequently an interaction between the load effect and resistance is inherent. It would have been correct to apply the safety factor directly to the loads, then obtain the corresponding cross-sectional area subjected to compression and in the next step calculate the stresses. However, DIN 1053-1 does not clearly insist on this procedure and thus, the formally wrong application of γ_{gl} on the resistance has become common in practice.

To align the design of masonry members with the design of concrete and steel members where the semi-probabilistic safety concept was already adopted, DIN 1053-100 was developed. The shear concept remains similar in both codes; the same failure modes are taken into account. However, the change in the safety concept revealed the aforementioned shortcoming of the old code. Figure 5-13 illustrates the effect of the safety concept on the length subjected to compression of the cross-section. Due to the smaller design value of the horizontal load according to DIN 1053-1, the length subjected to compression is larger than according to DIN 1053-100 (see Figure 5-13). This leads to smaller, allowable stresses. Hence, the design stress according to DIN 1053-1 is smaller than according to DIN 1053-100 and the estimated safety margin of $\gamma_{gl} = 2.0$ is not provided. In addition, the method of partial safety factors is state-of-the-art since it allows for consideration of the uncertainties of every parameter. Applying the global safety factor entirely on the resistance, as in the old code, does not differentiate between the different scatters of the respective parameters and load combinations.

The design according to DIN 1053-1 had, however, proven good in the past and so, a factor α_s was introduced in DIN 1053-100 that set the new capacities almost back to the level of DIN 1053-1, which were bigger. This factor increases the length of the wall under compression and so increases the load-carrying capacity. The factor is different in case of uncracked and cracked cross-sections. In case of an uncracked cross-section, the factor leads to the exact capacities as given by DIN 1053-1; in the cracked state, the new capacities come closer but still do not reach the capacities of DIN 1053-1.

The following non-dimensional equations have been derived from the code equations. To derive the values for DIN 1053-1, set $\gamma_{gl} = 2.0$. In case of DIN 1053-100, $\gamma_v = 1.5$, $\gamma_M = 1.5$, $\alpha_{uncr} = 1.125$ and $\alpha_{cr} = 1.333$. Note that the compressive strength was defined differently in both codes. The compressive strength β_R according to DIN 1053-1 already included the factor η accounting for long-term reduction of the compressive strength.

$$\beta_R = \eta \cdot f_k \qquad \text{Eq. 5-43}$$

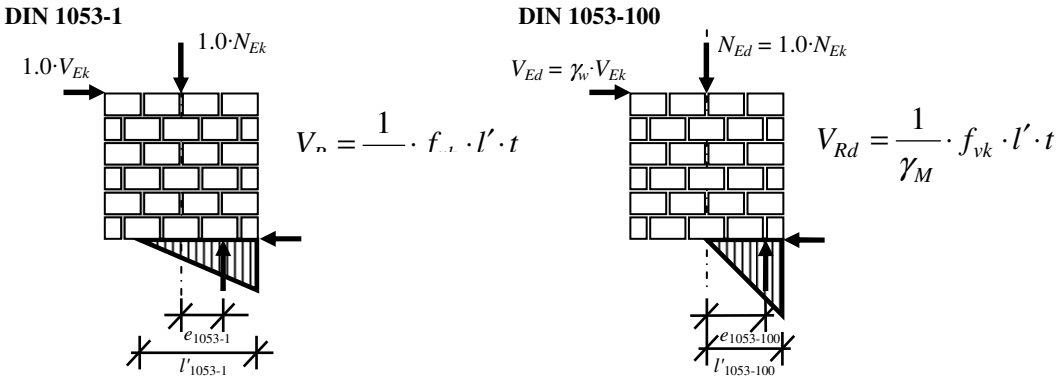

Figure 5-13 *Effect of the different safety concepts in DIN 1053-1 and -100 on the length subjected to compression*

Both design codes stipulate that at least half the cross-section remains under compression for service loads. This check actually belongs to the serviceability limit state but the criterion also serves as a check against the tip over of the entire wall (see section 5.3.2) with a safety margin. Tip over happens when the resultant of the axial stress is located outside of the cross-section. The limit state is given when $e/l_w = 1/2$. In general, DIN 1053-100 requires a safety factor of 1.5 for this kind of failure. Thus, the maximum eccentricity according to DIN 1053-1 is $e/l_w = 1/3$.

Tip Over in DIN 1053-1

$$v_{Ek,to} = \frac{1}{3} \cdot \frac{n_{Gk}}{\lambda_v} \qquad \text{Eq. 5-44}$$

Tip Over in DIN 1053-100

In DIN 1053-100, the check was modified. DIN 1053-100, clause 5.4 stipulates a limitation on the length under compression to at least half the length of the cross section under the frequent load situation according to DIN 1055-100. For the case of dead load and wind load, the frequent load situation is defined as follows

$$E_{d,frequ} = E_{Gk} \oplus \psi_1 \cdot E_{wk} \qquad \text{Eq. 5-45}$$

where $E_{d,frequ}$ is the design load effect, E_{Gk} is the characteristic value of load effect due to dead load, E_{wk} is the characteristic value of the load effect due to wind load and ψ_1 is the combination factor according to DIN 1055-100. For wind load, a value of $\psi_1 = 0.5$ is provided. In DIN 1053-100, the assumed stress-strain relationship is fully-plastic for the check against flexural failure. This leads to

$$v_{to,Ek,DIN1053-100,plastic} = \frac{1}{2} \cdot \frac{n_{Gk}}{\lambda_v} \qquad \text{Eq. 5-46}$$

However, it is questionable whether the material actually follows fully-plastic behaviour under minimum axial load. Thus, although not clearly stated in the code, linear-elastic stress-strain behaviour should be assumed for this check and consequently the shear load due to tip over of the entire wall should be calculated from

$$v_{to,Ek,DIN1053\text{–}100,elastic} = \frac{2}{3} \cdot \frac{n_{Gk}}{\lambda_v} \qquad \text{Eq. 5-47}$$

Flexural Failure in DIN 1053-1

The checks against flexural failure for both codes are different because of the assumed stress-strain relationships. Due to the assumed linear-elastic relationship in DIN 1053-1, the cracked and uncracked states have to be differentiated. Additionally, the stress at the edge of the cross-section may be increased by 1/3 due to the possibility of stress redistribution from the edge to less stressed regions of the cross-section due to plastic capacity. Applying the same normalized formulation as before, the design equations for flexural failure can be written as follows.

$$v_{Ek,fl,uc} = \frac{\frac{4}{3} \cdot \frac{\eta}{\gamma_{gl}} - n_{Ed}}{6 \cdot \lambda_v} \quad \text{for } 0.283 < n_{Ed} < 0.425 \qquad \text{Eq. 5-48}$$

$$v_{Ek,fl,c} = \frac{1}{2 \cdot \lambda_v} \cdot \left(n_{Ed} - \frac{\gamma_{gl}}{\eta} n_{Ed}^2 \right) \quad \text{for } n_{Ed} \leq 0.283 \qquad \text{Eq. 5-49}$$

where η is the durability factor with a value of $\eta = 0.85$. The second equation is similar to Eq. 5-8. Note that the provided ranges of n_{Ed} are only valid for a ratio of live-to-dead load of 3:7.

Flexural Failure in DIN 1053-100

For the fully-plastic stress-strain relationship as used in DIN 1053-100, the following equation can be derived.

$$v_{Ek,fl} = \frac{1}{\gamma_v \cdot 2 \cdot \lambda_v} \cdot \left(n_{Ed} - \frac{\gamma_M}{\eta} \cdot n_{Ed}^2 \right) \qquad \text{Eq. 5-50}$$

Note that n_{Ed} can be the maximum or minimum axial load. From here it can be seen that in case of DIN 1053-100, the check against tip over of the entire wall cannot govern.

$$v_{Ek,to,elastic} = \frac{2}{3 \cdot \lambda_v} \cdot n_{Gk} > v_{Ek,fl} = \frac{1}{\gamma_v \cdot 2 \cdot \lambda_v} \cdot \left(n_{Gk} - \frac{\gamma_M}{\eta} \cdot n_{Gk}^2 \right) \qquad \text{Eq. 5-51}$$

where $\gamma_v = 1.5$ for wind load.

In Eq. 5-50, a possible combination factor ψ as provided by DIN 1055-100 is not taken into account since the governing load action for masonry shear walls in Germany is al-

most always the wind load. Earthquake, if considered at all, is secondary for the design of typical masonry buildings.

In case of shear failure (sliding, diagonal tension, crushing) both German codes are based on *Mann & Müller (1973)*. Due to the common masonry units in Germany, the parameters of the model were modified so that a typical unit with $h_b/l_b = 0.5$ is generally considered. Additionally, regular stretcher bond with a minimum overlap of $0.4 \cdot h_b$ is assumed. The failure mode "tip over of the separate units" was not included in either code. However, following the aforementioned assumptions, the failure mode did not govern and thus did not need to be checked. In the calculation of the shear stress, the shear distribution over the cross-section is taken into account by the factor c which depends on the slenderness h_w/l_w of the wall (see Eq. 5-52).

$$1 \le c = 0.5 \cdot \left(1 + \frac{h_w}{l_w}\right) \le 1.5 \qquad \text{Eq. 5-52}$$

Sliding Shear in DIN 1053-1

Unlike the checks for the flexural capacity, both codes use a linear-elastic stress-strain relationship for the checks against shear failure under minimum load. Thus, the design equations are similar. For sliding shear, the sustainable shear load according to DIN 1053-1 can be calculated from the following equations.

$$v_{Ek,s,uc} = \frac{1}{\gamma_{gl} \cdot c} \cdot \left(\frac{f_{vk0}}{f_k} + \frac{\mu}{1+\mu} \cdot n_{Gk}\right) \qquad \text{Eq. 5-53}$$

$$v_{Ek,s,c} = \frac{\frac{3}{2} \cdot \frac{f_{vk0}}{f_k} + \frac{\mu}{1+\mu} \cdot n_{Gk}}{\gamma_{gl} \cdot c + \frac{3}{n_{Gk}} \cdot \frac{f_{vk0}}{f_k} \cdot \lambda_v} \qquad \text{Eq. 5-54}$$

where $\mu = 0.6$ and f_{vk0} is cohesion which is referred to as β_{RHS} in DIN 1053-1 ($f_{vk0} = \beta_{RHS}$).

Sliding Shear in DIN 1053-100

The sliding shear capacity according to DIN 1053-100 can be determined as follows:

$$v_{Ek,s,uc} = \frac{\alpha_{S,uncr}}{\gamma_v \cdot \gamma_M \cdot c} \cdot \left(\frac{f_{vk0}}{f_k} + \frac{\mu}{1+\mu} \cdot n_{Gk}\right) \qquad \text{Eq. 5-55}$$

$$v_{Ek,s,c} = \frac{\frac{3}{2} \cdot \frac{f_{vk0}}{f_d} + \frac{\mu}{1+\mu} \cdot n_{Gk}}{\gamma_v \cdot \left(\frac{\gamma_M \cdot c}{\alpha_{S,cr}} + \frac{3}{n_{Gk}} \cdot \frac{f_{vk0}}{f_k} \cdot \lambda_v\right)} \qquad \text{Eq. 5-56}$$

The values for the cohesion are equal in both codes and depend on the mortar type and whether the head joints are filled or unfilled to take into account the larger shear capacity of a wall with filled head joints according to the model of *Mann & Müller (1973).* The friction coefficient μ is generally considered to be 0.6 in the codes but is reduced by the factor $1/(1+\mu)$ to account for possible rotation of the units as identified by *Mann & Müller (1973).*

Diagonal Tension in (DIN 1053-1, -100)

The following equations can be used to determine the shear capacity due to diagonal tension failure according to DIN 1053-100 and are based on Eq. 5-22. To convert these equations to DIN 1053-1, set $\alpha_{s,uncr} = \alpha_{s,cr} = \gamma_v = 1.0$ and $\gamma_M = \gamma_{gl} = 2.0$. The tensile strength of the unit f_{bt} according to DIN 1053-100 is equal to β_{RZ} in DIN 1053-1. Both depend on the perforation pattern of the units (see Table 4.5-14).

$$A = 0.45 \cdot \frac{f_{bt}/f_k}{\gamma_M \cdot c} \qquad \text{Eq. 5-57}$$

$$B = \frac{3 \cdot A}{n_{Gk}} \cdot \alpha_{S,cr} \cdot \lambda_v \qquad \text{Eq. 5-58}$$

$$v_{Ek,dt,uc} = \frac{\alpha_{S,uncr}}{\gamma_v} \cdot A \cdot \sqrt{1 + \frac{n_{Gk}}{f_{bt}/f_k}} \qquad \text{Eq. 5-59}$$

$$v_{Ek,dt,c} = \frac{\alpha_{S,cr}}{2 \cdot \gamma_v} \cdot \frac{A \cdot B}{1 - B^2} \cdot \left(3 + \frac{n_{Gk}}{f_{bt}/f_k} \right) \cdot \left[-1 + \sqrt{1 + \frac{1 - B^2}{B^2} \cdot \frac{3 \cdot \left(3 + \frac{2 \cdot n_{Gk}}{f_{bt}/f_k} \right)}{\left(3 + \frac{n_{Gk}}{f_{bt}/f_k} \right)^2}} \right] \qquad \text{Eq. 5-60}$$

Shear Crushing in DIN 1053-1

For shear crushing, Eq. 5-61 and Eq. 5-62 can be used to compute the shear capacity according to DIN 1053-1.

$$v_{Ek,cr,c} = \frac{1}{c} \cdot \left(\frac{\eta}{\gamma_{gl}} - n_{Ed} \right) \qquad \text{Eq. 5-61}$$

$$v_{Ek,cr,c} = \frac{\frac{3}{2} \cdot \frac{\eta}{\gamma_{gl}} - n_{Ed}}{c + \frac{\eta}{\gamma_{gl}} \cdot \frac{3}{n_{Ed}} \cdot \lambda_v} \qquad \text{Eq. 5-62}$$

Shear Crushing in DIN 1053-100

For design according to DIN 1053-100, the following equations apply.

$$v_{Ek,cr,uc} = \frac{\alpha_{S,uncr}}{\gamma_v \cdot \gamma_M \cdot c} \cdot \left(\frac{\eta}{\gamma_M} - n_{Ed} \right) \qquad \text{Eq. 5-63}$$

$$v_{Ek,cr,c} = \frac{\frac{3}{2} \cdot \frac{\eta}{\gamma_M} - n_{Ed}}{\gamma_v \cdot \left(\frac{\gamma_M \cdot c}{\alpha_{S,cr}} + \frac{3}{n_{Ed}} \cdot \lambda_v \cdot \frac{\eta}{\gamma_M} \right)} \qquad \text{Eq. 5-64}$$

Actually, this failure mode can only occur for very large axial loads and small overlap ($u/h_b < 0.4$). Due to the pre-assumption of $u/h_b = 0.5$, the overlap ratio was not included in the design of either DIN code. For masonry constructed of large-sized units, the regulation for the overlap can be found in the general technical approvals. Generally, the check against shear crushing was not explicitly included in analytical form in both codes but was mentioned in figures. Nowadays, it can govern especially for large-sized masonry units because of the small overlap; that is why the overlap ratio is now supposed to be included in DIN EN 1996-1-1/NA which is also valid for small overlap ratios ($u/h_b \geq 0.2$) which will be explained in the following section. Another fact that makes this failure mode more important in the design according to more recent codes using the semi-probabilistic safety concept are the larger design loads that are reached.

5.5.3 Design Model according to DIN EN 1996-1-1/NA

Although the Eurocode 6, in Germany referred to as DIN EN 1996, was released in 2005, there are currently two masonry design codes valid in Germany: DIN 1053-1 (1996) and DIN 1053-100 (2007), as dicussed in section 5.5.2. Recently, the code committees have been working on development of a new generation of the German design code DIN 1053 (E DIN 1053-11, -12, -13) which, according to the latest information, will not become mandatory. Instead, some of the rules, especially the shear design, will be incorporated in the National Annex to Eurocode 6, DIN EN 1996-1-1/NA. The National Annex will be finalized and introduced in 2011. Thus, this section refers to the current version of DIN EN 1996-1-1 (2010) and the current draft of the National Annex DIN EN 1996-1-1/NA (2011-01). However, further changes could still occur and it cannot be guaranteed that the the final version will be the same as what it used in the following study. In the following, the most current design model will be presented in the same normalized, non-dimensional format as in the previous sections.

Tip Over

In case of tip over of the entire wall, the check was modified. DIN EN 1996-1-1/NA, clause 7.2 (4) stipulates a limitation on the resulting eccentricity e/l_w to $1/3 \cdot l_w$ for slender

walls with $h_w/l_w \geq 2.0$ under the common load combination (see Eq. 5-45). The definition of the load combination is identical in DIN EN 1990 and DIN 1055-100. Consequently, the shear capacity according to DIN EN 1996-1-1/NA and DIN 1053-100 due to tip over of the entire wall are also identical and the limitation of the eccentricity to one third of the cross-sectional length is a clear indication that a linear-elastic stress-strain relationship is supposed to be assumed because this equals the maximum eccentricity of $e/l_w = 0.5$ divided by a safety factor of 1.5.

$$v_{Ek,to} = \frac{2}{3} \cdot \frac{n_{Gk}}{\lambda_v} \qquad \text{Eq. 5-65}$$

The shear design concept is based on the semi-probabilistic concept and the shear design model differentiates between the four possible modes of failure: tip over of the separate units, sliding shear, diagonal tension and crushing.

Flexural Failure

In addtion, a check against flexural failure of the wall has to be carried out; this check is identical to the check according to DIN 1053-100.

The procedure for the check of the shear capacity in DIN EN 1996-1-1/NA is a little different to the DIN codes. Instead of always checking all failure modes, limits for the single failure modes are provided so that not all failure modes need to necessarily be considered.

Sliding Shear

Sliding shear is the only one that has to be checked in every case. The sliding shear capacity can be determined from

$$v_{S,Ek,\min} = \mu \cdot \frac{n_{Gk}}{\gamma_M \cdot \gamma_v} \qquad \text{Eq. 5-66}$$

This is equal to the minimum value of the sliding shear resistance as suggested by *Kranzler (2008)*. The friction coefficient μ equals 0.6 since the minimum value refers to a sliding failure of the entire wall and thus no slip of the units along the bed joints can occur.

If larger values of the shear capacity are required, the sliding shear capacity may be determined from a different equation. This equation is based on the model of *Mann & Müller (1973)* and was included similarly in the previous German code. Assuming that sliding shear failure will occur under minimum load, the stress distribution is assumed linear-elastic. Thus, the length under compression can be calculated from Eq. 5-67.

$$l'_{w,lin} = \frac{3}{2} \cdot \left(1 - 2 \cdot \left(\frac{e_0}{l_w} + \frac{V_{Ed}}{N_{Dd}} \cdot \lambda_v\right)\right) \cdot l_w \leq \left(1 - 2 \cdot \frac{e_0}{l_w}\right) \cdot l_w \qquad \text{Eq. 5-67}$$

From Eq. 5-67, we can derive the design equations for sliding shear failure in non-dimensional, closed form.

$$v_{Ek,s,uc} = \frac{1}{\gamma_v \cdot \gamma_M \cdot c \cdot (1+\mu)} \cdot \left(\frac{f_{vk1}}{f_k} + \mu \cdot n_{Dk} \right) \quad \text{cross-section uncracked} \qquad \text{Eq. 5-68}$$

$$v_{Ek,s,c} = \frac{\frac{3}{2} \cdot \frac{f_{vk1}}{f_k} + \frac{\mu}{1+\mu} \cdot n_{Dk}}{\gamma_v \cdot \gamma_M \cdot \left(c + 3 \cdot \lambda_v \cdot \frac{f_{vk1}}{f_d \cdot n_{Dk}} \right)} \quad \text{cross-section cracked} \qquad \text{Eq. 5-69}$$

$$f_{vk1} = 1.25 \cdot f_{vk0} \qquad \text{Eq. 5-70}$$

This value can be greater than the shear capacity according to Eq. 5-66, especially in case of large values of the cohesion f_{vk1}, as it is the case for TLM. Consequently, application of this design equation can lead to more efficient design.

Diagonal Tension

The equation for diagonal tension failure is based on *Jäger & Schöps (2004)*. Diagonal tension failure only has to be checked for squat and somewhat slender walls with $\lambda_v \leq 1.5$ for all kinds of masonry except AAC (Eq. 5-71) and for squat walls with $\lambda_v \leq 1.0$ in case of AAC masonry. This differentiation is based on the different behaviour of AAC walls subjected to diagonal tension.

$$v_{Ek,dt} = \frac{1}{c} \cdot \frac{f_{bt}}{f_k} \cdot \frac{1}{(F')^2} \cdot \left(\sqrt{1 + (F')^2 \cdot \left(1 + \frac{n_{Gk}}{\frac{f_{bt}}{f_k}} \right)} - 1 \right) \quad \text{all materials except AAC} \qquad \text{Eq. 5-71}$$

$$v_{Ek,dt} = \frac{1}{c} \cdot \frac{f_{bt}}{f_k} \cdot \frac{2}{(F')^2} \cdot \left(\sqrt{1 + \frac{(F')^2}{4} \cdot \left(1 + \frac{n_{Gk}}{\frac{f_{bt}}{f_k}} \right)} - 1 \right) \quad \text{for AAC} \qquad \text{Eq. 5-72}$$

$$F' = 1.2 + 0.85 \cdot f_{bt} \quad f_{bt} \text{ in N/mm²} \qquad \text{Eq. 5-73}$$

In case of AAC masonry with filled head joints, the capacity according to Eq. 5-72 may be increased by 15%. However, these equations were part of the latest draft of E DIN 1053-13 and were supposed to be included in DIN EN 1996-1-1/NA. Currently, a simplified formulation according to *Jäger et al. (2011)* is being discussed, as in Eq. 5-74.

$$v_{Ek,dt} = \frac{\alpha}{\gamma_M \cdot \gamma_v \cdot c} \frac{f_{bt,cal}}{f_k} \cdot \sqrt{1 + \frac{n_{Gk}}{\beta} \cdot \frac{f_k}{f_{bt,cal}}} \qquad \text{Eq. 5-74}$$

$$f_{bt,cal} = \frac{\delta_i \cdot f_b}{1.25} \qquad \text{Eq. 5-75}$$

where α, β and δ_i are the parameters presented in Table 5.5-1 and f_b is the mean compressive strength of the unit as provided in Table 4.5-1.

Table 5.5-1 Parameters α, β and δ_i for the design according to DIN EN 1996-1-1/NA

Type of unit	α	β	δ_i
hollow block unit	0.24	0.2	0.025
perforated unit			0.033
units with grip holes	0.22		
full blocks without grip holes			0.040
AAC	0.21	0.32	0.082

Shear Crushing

Shear crushing failure has to be checked only if the overlap ratio $u/h_b \leq 0.4$, which is the case for most kinds of large-sized masonry, and if the axial force is considered large. Since this failure is most likely to happen under maximum load, the corresponding stress-strain relationship is assumed fully-plastic. Eq. 5-77 represents the case with the entire cross-section being subjected to compression while Eq. 5-78 is valid for partially compressed cross-sections.

$$l'_{w,pla} = \left(1 - 2 \cdot \left(\frac{V_{Ed}}{N_{Dd}} \cdot \lambda_v\right)\right) \cdot l_w \leq l_w \qquad \text{Eq. 5-76}$$

With this relationship, the following equations for shear crushing can be derived.

$$v_{c,Ek,uncr} = \frac{1}{\gamma_v \cdot \gamma_M \cdot c} \cdot \frac{u}{h_b} \cdot \left(1 - \gamma_M \cdot n_{Ed}\right) \qquad \text{Eq. 5-77}$$

$$v_{c,Ek,cr} = \frac{u}{h_b} \frac{1 - \gamma_M \cdot n_{Ed}}{1 + \frac{2}{\gamma_M \cdot c} \cdot \frac{u}{h_b} \cdot \frac{\lambda_v}{n_{Ed}}} \qquad \text{Eq. 5-78}$$

Note the similarity to *Mann & Müller's* model (see section 5.3.4.2). The main difference is the accounting for the overlap u/h_b.

Tip Over of the Separate Units

This failure mode must only be checked if the units are tall ($h_b \geq l_b$). This kind of unit is not very common but large-sized units with $h_b/l_b \leq 1.0$ are available. In such cases, the shear capacity due to tip over of the separate units can be determined from the following equation.

$$v_{TSU,Ek} = \frac{K_1}{\gamma_v} \cdot \frac{1}{2} \cdot \left(\frac{l_b}{h_b} + \frac{l_b}{h_w} \right) \cdot n_{Gk} \qquad \text{Eq. 5-79}$$

This failure mode depends only on dimensions; material strength is not included and thus uncertainties linked to the material strength do not have to be taken into account. Hence, the factor $K_1 = 1.3$ was included to account for this fact. The value of $K_1 = 1.3$ comes from the definition of the partial safety factor $\gamma_M = 1.5$ in the German codes which is supposed to be the product of a safety factor accounting for the model uncertainty and a safety factor for the material ($\gamma_M = \gamma_{model} \cdot \gamma_{material} = 1.2 \cdot 1.3 \approx 1.5$).

5.5.4 Comparison of DIN 1053-1, -100 and DIN EN 1996-1-1/NA

The models explained above yield different shear capacities. In the following, the capacities derived according to each model will be compared. In the study, the value of the axial dead load n_{Gk} was increased in steps of 0.01 to a value of $n_{Gk,max}$. This value depends on the safety factors of the respective code and the ratio of live-to-dead load. The ratio of live-to-dead load is $q/g = 3/7$ in every case; representing typical residential structures in Germany. The definition of $n_{Gk,max}$, normalized on the basis of f_k, is presented in Eq. 5-80 and Eq. 5-81 and the resulting values are shown in Table 5.5-2.

$$n_{Gk,\max} \cdot \left(\gamma_G + \frac{q}{g} \cdot \gamma_Q \right) = \frac{f_d}{f_k} = \frac{\eta}{\gamma_M} \quad \text{in case of partial safety concept} \qquad \text{Eq. 5-80}$$

$$n_{Gk,\max} \cdot \left(1 + \frac{q}{g} \right) = \frac{\beta_R}{f_k} = \frac{\eta}{\gamma_{gl}} \quad \text{in case of global safety concept} \qquad \text{Eq. 5-81}$$

Table 5.5-2 Values of $n_{G,max}$

Code	$n_{G,max}$
DIN 1053-1	0.298
DIN 1053-100	0.284
DIN EN 1996-1-1/NA	

For every value of the axial force, a corresponding *maximum sustainable* value of the horizontal force v_{Ek} is determined; this corresponds to changing the eccentricity of the axial force from maximum to minimum.

The first wall that is examined is a squat ($\lambda_v = 0.5$) AAC wall. It can be seen that the distributions of the derived capacities are different. The reason for this is the predicted failure mode which is different according to every code. DIN EN 1996-1-1/NA predicts sliding shear failure while the DIN 1053 codes predict diagonal tension for small axial load. The DIN 1053 codes lead to equal shear capacities in the case of diagonal tension failure. The equation for diagonal tension according to DIN EN 1996-1-1/NA gives larger shear capacities. The reason is the larger value of the tensile strength of the unit which is almost

double the value of DIN 1053-1 and DIN 1053-100. Figure 5-14 shows the distribution of v_{Ek} versus the axial force n_{Gk} according to the three codes.

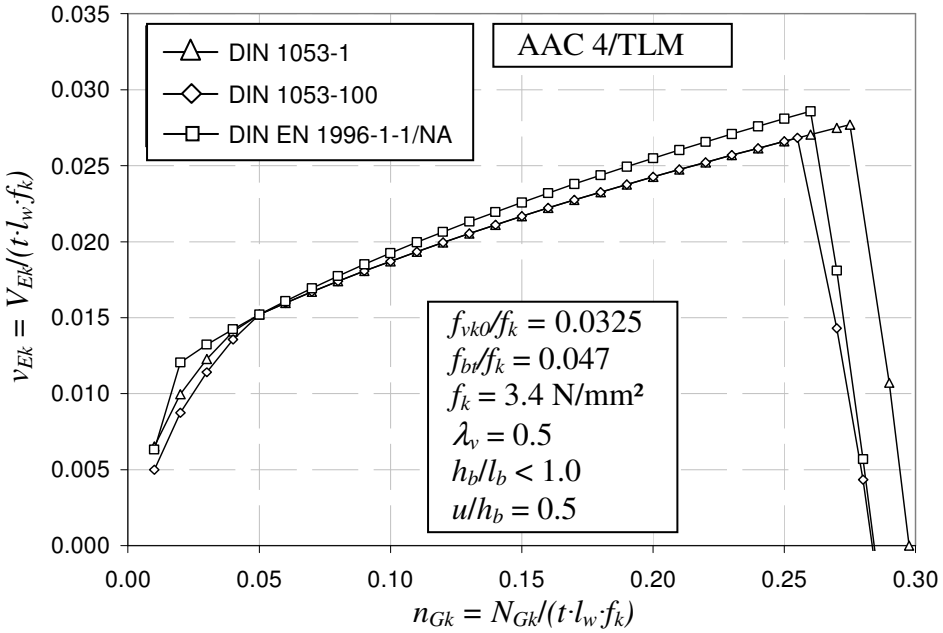

Figure 5-14 Shear capacity v_{Ek} vs. axial dead load n_{Gk} for a squat AAC wall (λ_v = 0.5)

In case of CB (Figure 5-15), the tensile strength of the unit is underestimated in DIN EN 1996-1-1/NA (not the case in both DIN 1053 codes). Thus, the capacity due to diagonal tension according to DIN EN 1996-1-1/NA is smaller than the capacity according to both DIN 1053 codes because of the conservative calibration.

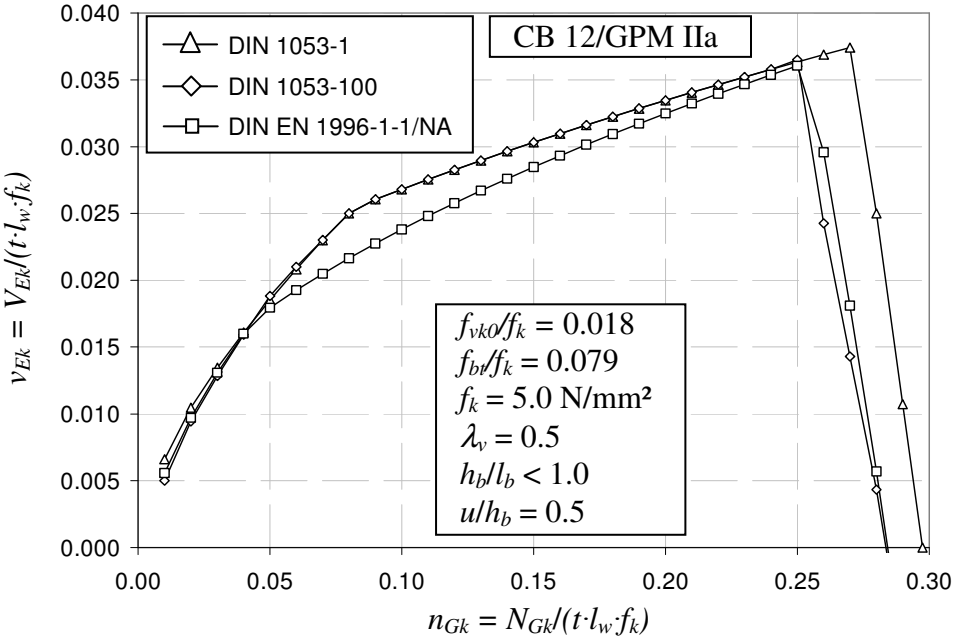

Figure 5-15 Shear capacity v_{Ek} vs. axial dead load n_{Gk} for a squat CB wall (λ_v = 0.5)

A similar plot is drawn for CS walls (see Figure 5-16). For small axial load, the capacity of DIN EN 1996-1-1/NA is slightly larger, the reason being the larger value of the cohe-

sion f_{vk1} ($f_{vk1} = 1.25 \cdot f_{vk0}$). However, the design equation for diagonal tension failure leads to smaller capacities with the DIN EN 1996-1-1/NA for all materials except AAC.

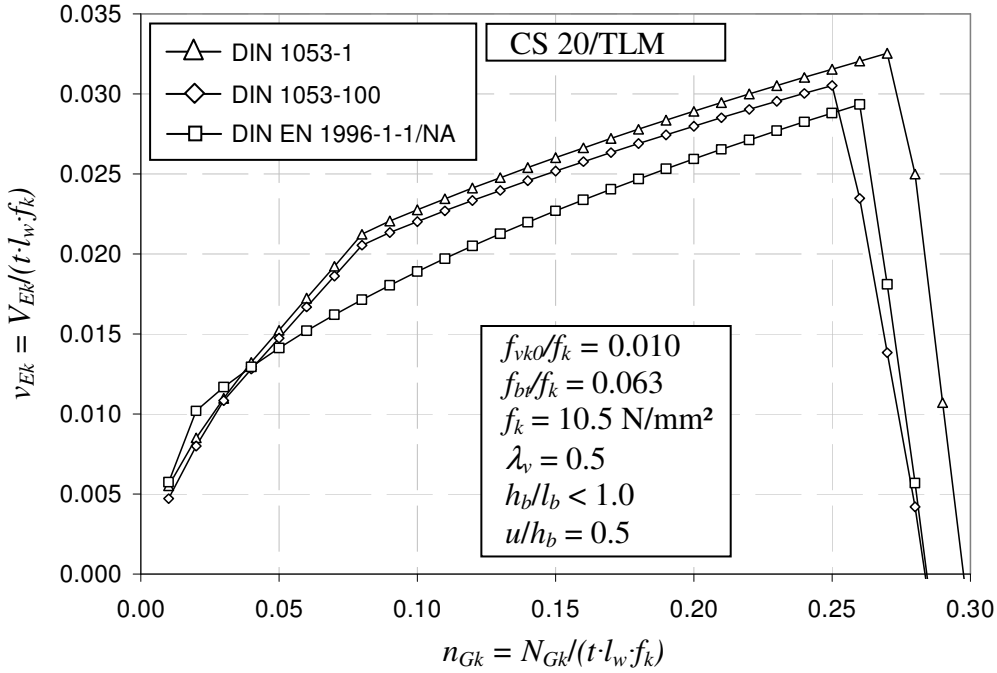

Figure 5-16 Shear capacity v_{Ek} vs. axial dead load n_{Gk} for a squat CS wall ($\lambda_v = 0.5$)

In case of slender walls, flexural failure governs in most cases. The design according to DIN 1053-100 and DIN EN 1996-1-1/NA is equal for flexural failure and so are the obtained capacities. However, for AAC (see Figure 5-17) and cases of low axial load, diagonal tension governs in case of DIN 1053-100 due to the aforementioned underestimation of the tensile strength of the unit. The capacities determined from the National Annex lie in between the capacities of the German design codes. The linear slope of the line for low axial load corresponds to the failure mode tip over of the entire wall which governs in the case of DIN 1053-1. For high axial load, two failure modes limit the shear capacity according to DIN 1053-1: flexural failure under maximum axial load and shear crushing. This is the reason for the two sudden changes at $n_{Gk} = 0.21$ and $n_{Gk} = 0.28$. The generally greater capacity according to DIN 1053-1 is due to the application of the global safety factor on the strength, as discussed in section 5.5.2

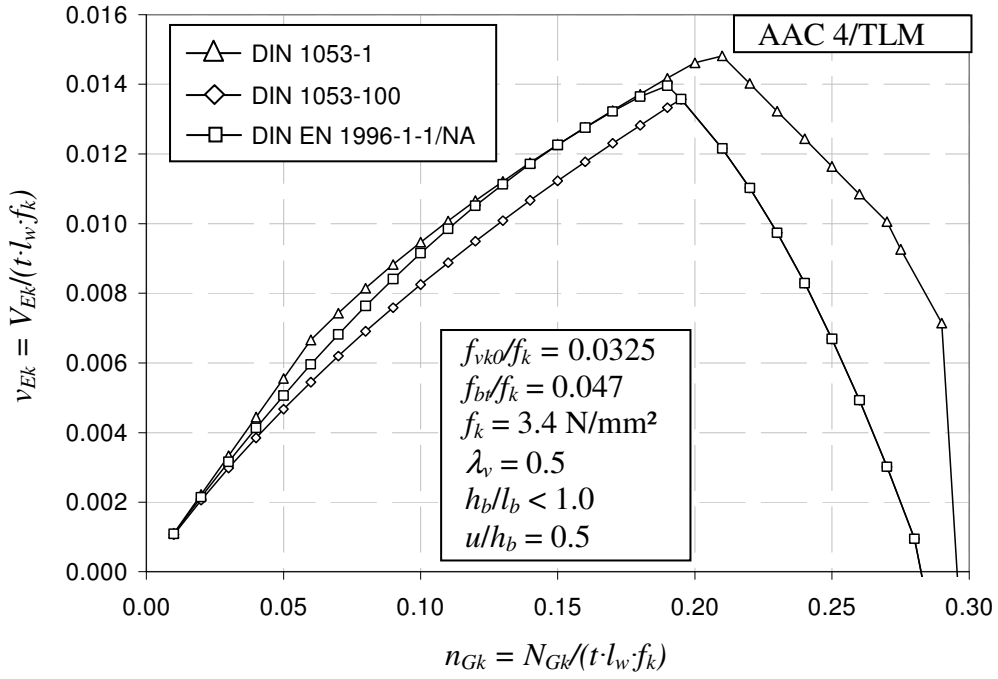

Figure 5-17 Shear capacity v_{Ek} vs. axial dead load n_{Gk} for a slender AAC wall (λ_v = 3.0)

In case of CB and CS walls, diagonal tension does not govern over a large range of the axial load for slender walls; here, flexural failure governs for all three codes. This is illustrated in Figure 5-18 and Figure 5-19.

It can be concluded that DIN 1053-1 generally leads to larger capacities than DIN 1053-100. The capacities are similar when diagonal tension governs. DIN EN 1996-1-1/NA leads to larger capacities for sliding shear and - in case of AAC – for diagonal tension. However, DIN 1053-1 provides the highest capacities due to the application of the global safety factor on the strength.

It is important to note the different idealisations of the structural system according to the codes. In DIN 1053-1 and -100, the shear wall is normally modelled as a building-high cantilever while in DIN EN 1996-1-1/NA, an overturning moment from the RC slabs can be taken into account and the shear wall can be modelled as a storey-high cantilever. Thus, in the DIN 1053 codes, larger values of the shear slenderness are likely to be considered in design than in DIN EN 1996-1-1/NA. However, the determination of an overturning moment will unlikely happen in practice. Since $\lambda_v = h_w/l_w$ in this study, differences in the structural system are incorporated in the non-dimensional formulation of the comparison.

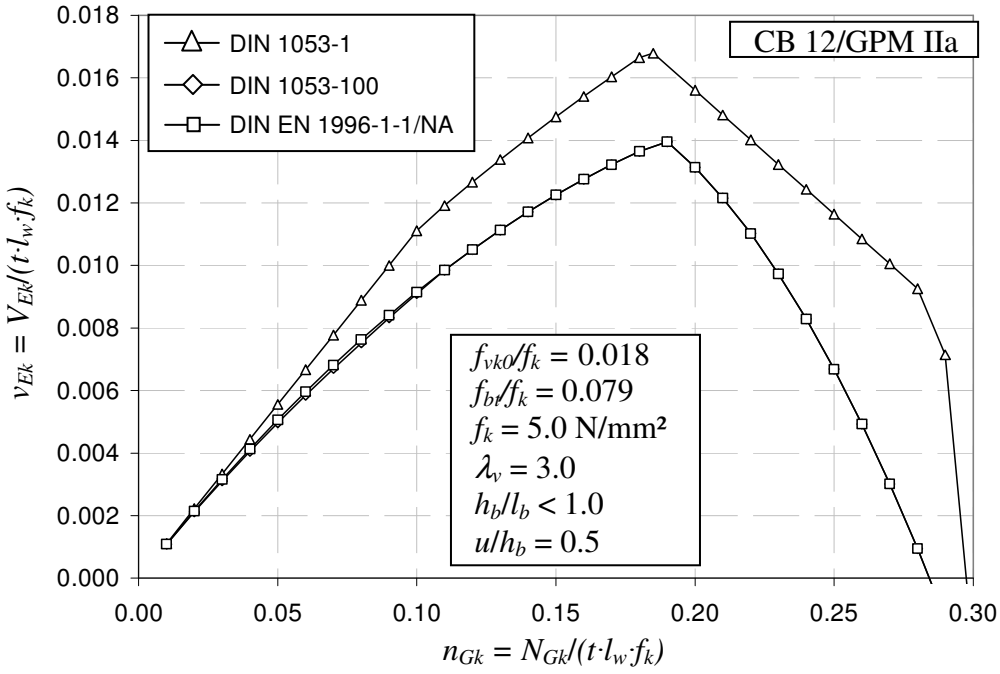

Figure 5-18 *Shear capacity v_{Ek} vs. axial dead load n_{Gk} for a slender CB wall (λ_v = 3.0)*

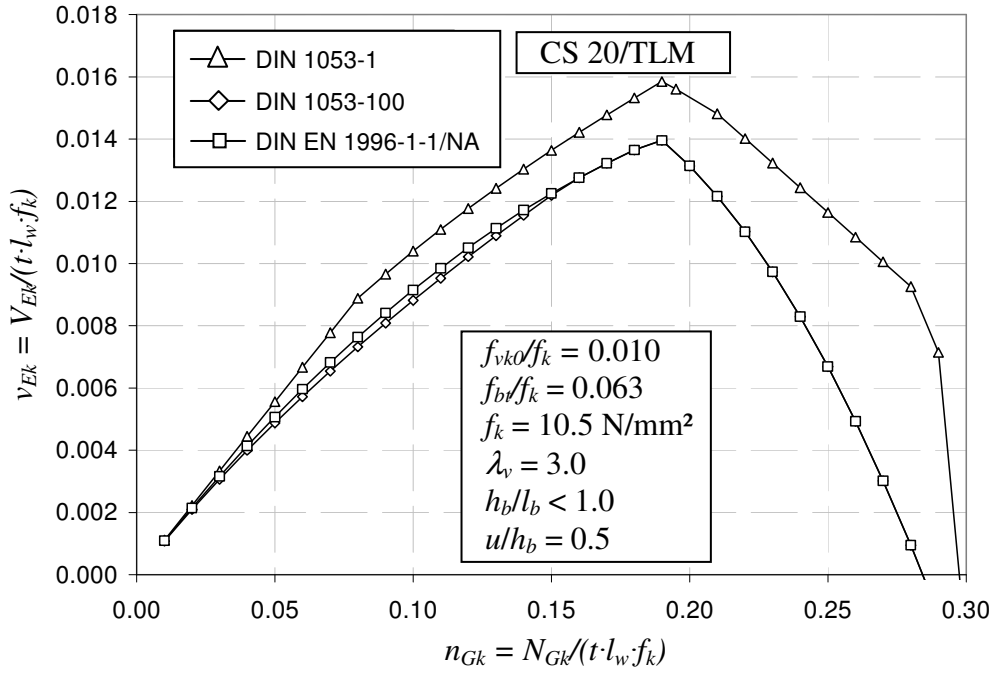

Figure 5-19 *Shear capacity v_{Ek} vs. axial dead load n_{Gk} for a slender CS wall (λ_v = 3.0)*

In Figure 5-20, the influence of small overlap u/h_b on the shear capacity according to DIN EN 1996-1-1/NA is shown. Small overlap leads to significant loss of capacity for large axial load. In the figure the shear capacity v_{Ek} versus the axial dead load n_{GK} are plotted for the minimum required overlap of $u/h_b = 0.2$ and $u/h_b \geq 0.4$. A reduction in capacity of about 50% is possible.

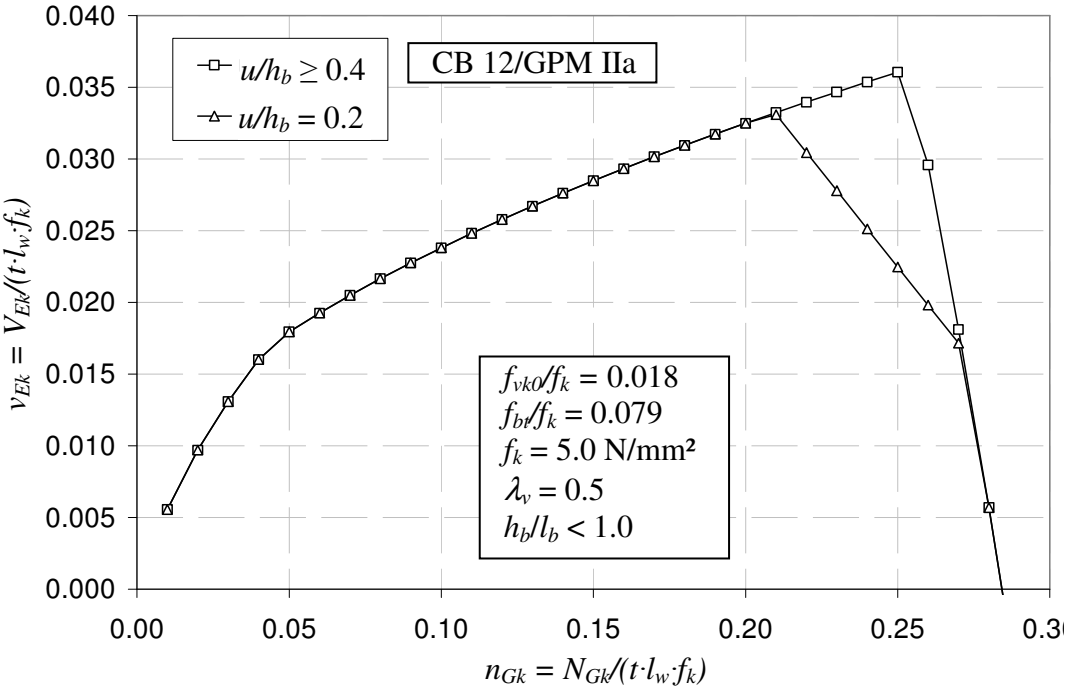

Figure 5-20 *Shear capacity v_{Ek} vs. axial dead load n_{Gk} for a squat CB wall ($\lambda_v = 0.5$) for different overlap ratios u/h_b*

5.5.5 Design Model according to SIA 866

For completeness, the design model according to the Swiss design code SIA 866 will be explained briefly in this section. SIA 866 gives design rules for URM, reinforced masonry and prestressed masonry. It is based on the concept of partial safety factors. The corresponding load combinations are similar to the ones in the DIN codes and the Eurocode 6. It is noteworthy that favourably acting dead load has to multiplied by a safety factor of $\gamma_G = 0.8$ while for unfavourably acting dead load the same safety factor as in the German and European codes ($\gamma_G = 1.35$) has to be applied. The safety factor on the material $\gamma_M = 2.0$ is significantly larger than in the German codes. In shear design, a major difference is that the cohesion is disregarded due to its large scatter and the large friction coefficient $\mu_d = 0.6$. Note, that the friction coefficient is already a design value incorporating a partial safety factor of 1.2.

The Swiss code, however, represents an exception because the design model is based on a plastic stress-strain relationship. The method was proposed by *Mojsilovic & Schwartz (2006)* and is also based on *Ganz (1985)*, as discussed in section 5.3.4.1. Thus, the shear capacity v_{Ed} has to be determined from design diagrams provided in the code. Design equations are not provided. The parameters for the diagrams are the axial load n_{Ed}, the aspect ratio h_w/l_w and the horizontal compressive strength which depends on the unit and mortar type.

5.6 Assessment and Model Uncertainties

5.6.1 General

Besides the applied loads, dimensions and strength parameters, the predicted load-carrying capacity of a structural member depends on the prediction model used. For example, consider the models for the determination of the compressive strength; as discussed in section 4.5.4, or the model for the wind load explained in section 3.5. No model can exactly represent and predict reality. Uncertainties, either resulting from effects that are not included in the model due to lack of knowledge or due to matters of simplification, have to be assessed and quantified in an appropriate way and must be included in the reliability analysis in the next chapter as basic variables. The best way to quantify the stochastic properties is to compare the model to test data (see *JCSS (2003)*) by assessment of the test-to-prediction ratio Θ (Eq. 5-82).

$$\Theta = \frac{v_{test}}{v_{prediction}} \qquad \text{Eq. 5-82}$$

where v_{test} is the ultimate shear obtained in the test and $v_{prediction}$ is the maximum allowable shear force predicted by the respective model.

In case of the assessed design models, all safety factors will be set to 1.0 and the measured properties are used, not the characteristic or design values according to the code.

To eliminate stochastic uncertainties and obtain more realistic results although the sample size is limited, a Bayesian update will be performed subsequently. In the following sections, the model uncertainties for shear capacity prediction of URM walls will be determined.

5.6.2 Test Data

To determine the shear capacity of masonry walls, several test arrangements have been reported in the literature. A standard test arrangement is not available. However, tests are usually similar to some extent. A typical test setup is presented in Figure 5-21.

The control of the axial force is very important. Due to overturning of the wall, the initial axial load increases significantly. Hence, the hydraulic actuators in the vertical direction need to be adjusted permanently to provide constant total axial load. This leads to different forces in each actuator and so eccentricities can result on top of the wall. However, test data reported usually only includes the axial force at the point of failure and the corresponding horizontal load.

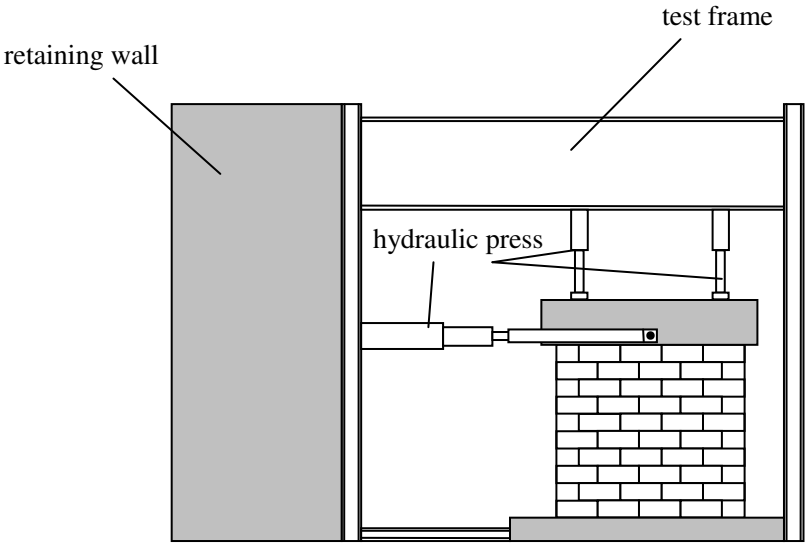

Figure 5-21 Typical test setup for shear capacity

Normally, shear tests are conducted within the application process for technical approval and these tests aim at efficiency. Therefore, the test data reported is often lacking the required detail for a proper stochastic assessment; in many cases only the masonry compressive strength is reported, while the cohesion, friction coefficient and tensile strengths are not determined due to the laborious testing. Another important aspect is the small number of tests on identical specimens. Often only one single test on a wall specimen is carried out for a given masonry typology. In addition, material strengths of the units and mortar are rarely determined for every specimen but rather are determined once per batch of units. Other parameters like cohesion or friction coefficient are not determined in many cases. Therefore, only tests where the cohesion and tensile strength of the units were documented are included in the assessment of the model performance. The test data used herein for assessment of the model performance were taken from various sources (see Table 5.6-1). In total, 43 tests on CB specimens, 51 on AAC and 15 on CS were evaluated. A summary of the test data is provided in the Appendix.

Besides the forces and material properties reported, the governing failure mode has to be identified. This is difficult, since the failure modes are not clear. The typical, theoretical crack patterns related to a failure mode do not necessarily show in the test. Normally, the failure modes are combined, e.g. cracks occur in the centre of the wall (diagonal tension) and propagate toward the corners of the wall. Therefore, failure modes have to be questioned and defined clearly. For example, *Kranzler (2008)* considered failure modes as sliding shear only if there was not a single crack through the unit.

Table 5.6-1 Overview of test database

Author	Number of tests	Material	Comments
Löring (2005)	10	3 on CB, 3 on CS, 2 on AAC, 2 on LDC	-
Jäger & Schöps (2004)	2 (1)[a]	CS	-
Costa (2007)	4	AAC	-
Jäger & Schöps (2005)	18	AAC	-
Bojsilikov & Tomazevic (2005)	7	CB	-
Bojsilikov et al. (2004)	18	CB	-
Fehling & Stürz (2006a)	18	15 on CB, 2 on CS	-
Schermer (2007)	1	CS	-
Magenes (2007)	8	CS	-
Fehling & Stürz (2006b)	9 (8)[a]	AAC	-
Höveling et al.(2009)	26 (18)[a,b]	AAC	2 different test setups
Gunkler et al. (2009)	10 (7)[a]	KS	-

[a]Number in parenthesis is the actual used number of tests in the assessment.
[b]Tests by the "alternative" test method could not be assessed.

Here, failure modes had to be determined from the pictures of the specimens. This leads to more uncertainty that will be dealt with within the assessment. It was attempted to achieve more realistic modelling by comparing the test results with the prediction for a certain failure mode instead of the minimum value obtained from the prediction model. The reason for this is that the goal of the assessment is to identify the most realistic model for application in the reliability analysis in the next chapter. Therefore, the best partial models for single failure modes will be assembled into the model for the reliability analysis. The test data indicated three failure modes: sliding shear, diagonal tension and flexure. Shear crushing in terms of large diagonal compression exceeding the compressive strength of the masonry did not occur in the tests due to the low levels of axial loading.

5.6.3 Comparison and Assessment

For the reliability analysis in the next chapter, the best model - in terms of realistic prediction of the shear capacity – has to be chosen. To assess the models, the data is clustered into different groups, depending on the unit material and the failure modes in the test. Then the predicted shear capacity of the various models is compared to the test result. This gives a set of data for the test-to-prediction ratio.

A model is thought to show good performance if it neither under- nor overestimates the strength substantially and additionally exhibits small scatter. Overestimation of the shear capacity is indicated by test-to-prediction ratios smaller than 1.0 while values larger than 1.0 denote underestimation of the capacity. *CoV* is again taken as the indicator for scatter. It becomes apparent that the models of *Mann & Müller (1973)* and the model according to

DIN EN 1996-1-1/NA show the best performance due to the smallest resulting *CoV* and means reasonably close to unity. The derived stochastic moments of the test-to-prediction ratio are summarized in the following table. These were determined by the method of moments described in section 2.4.2.

Table 5.6-2 Stochastic properties of the test-to-prediction ratio by comparison with test data

Failure	Model	Unit	*n*	*m*	σ	*CoV*
Diagonal tension	Mann & Müller[a]	CS	3	1.01	0.17	16%
		AAC	39	1.09	0.20	19%
		CB	20	1.41	0.22	15%
	DIN EN 1996-1-1/NA	CS	3	0.86	0.12	14%
		AAC	39	1.11	0.18	16%
		CB	20	0.96	0.08	9%
	Kranzler	CS	3	0.80	0.12	16%
		AAC	39	1.15	0.28	24%
		CB	20	0.91	0.07	8%
	DIN 1053-100[b]	CS	3	1.06	0.28	26%
		AAC	39	1.13	0.31	27%
		CB	20	1.39	0.121	15%
Sliding shear	Mann & Müller[a]	CS	6	1.20	0.12	10%
		AAC	3	1.05	0.06	6%
		CB	3	1.47	0.10	6%
	DIN EN 1996-1-1/NA & Kranzler	CS	6	1.00[c]	0.12	14%
		AAC	3	1.00[c]	0.08	9%
		CB	3	1.06	0.14	13%
	DIN 1053-100[b]	CS	6	1.00	0.06	6%
		AAC	3	0.97	0.20	21%
		CB	3	1.45	0.10	7%
Flexure	ideal-plastic	CS	5	0.93	0.07	7%
		AAC	7	1.04	0.09	9%
		CB	18	1.09	0.12	11%

[a]ideal-plastic stress-strain relationship
[b]ideal-plastic stress-strain relationship and no shear modification factor
[c]set to 1.0 due to physical reasons

Figure 5-22 and Figure 5-23 show the test-to-prediction ratio for every test grouped by unit material and failure mode. A list of all tests and required data can be found in the Appendix.

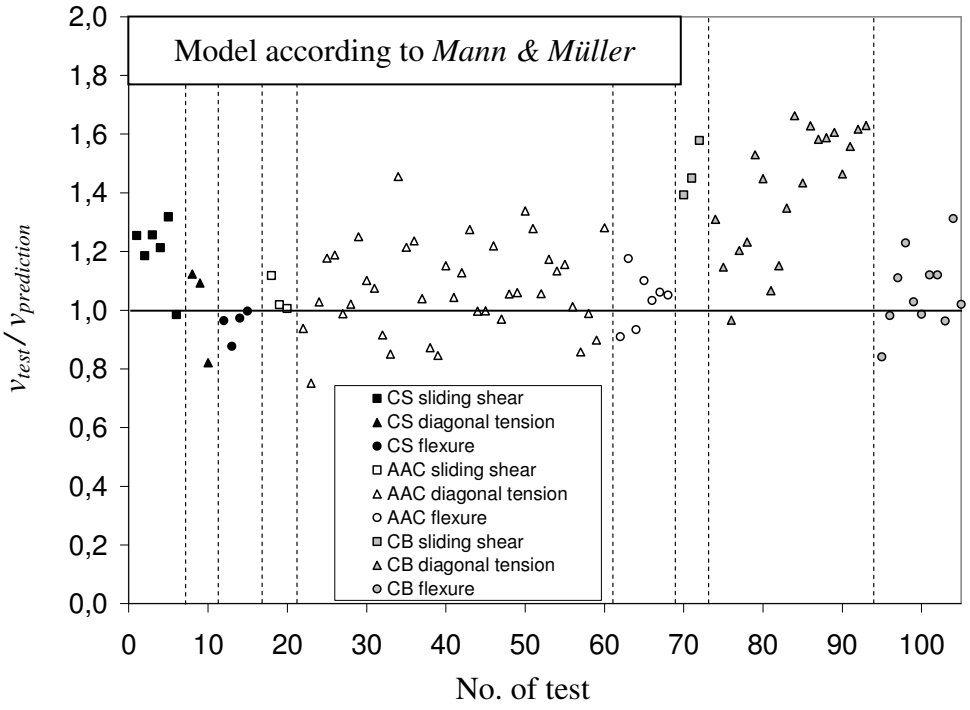

Figure 5-22 Assessment of the Model according to Mann & Müller with test data

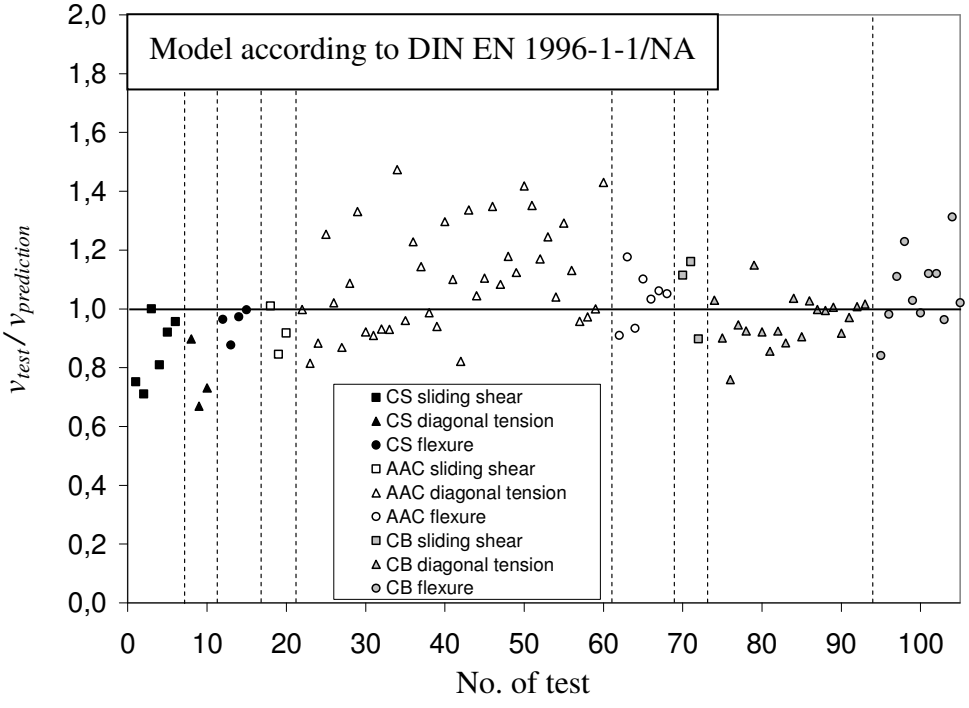

Figure 5-23 Assessment of the Model according to DIN EN 1996-1-1 with test data

In the assessment of the results, the failure modes that occurred in the test had to be identified. This is difficult since crack formations are not distinct; most tests show a combination of failure modes and thus the failure modes cannot be identified clearly. In addition, not every required material property and parameter was determined in every test. Therefore, some parameters had to be estimated. A detailed summary of the obtained values can be found in the Appendix.

In the assessment of the tests, the number of available tests plays a major role. In case of diagonal tension failure of AAC and CB walls, a sufficient number of test results was found. In case of CS walls, only 3 walls that failed due to diagonal tension were reported. The number of tests reported for walls that failed in flexure can be considered sufficient for all materials while sliding shear only occurred in 3 tests on AAC and CB specimens and 6 tests on CS specimens. The uncertainties due to the small sample size make an update necessary.

As can be seen from the results in Table 5.6-2, diagonal tension of CS and AAC is modelled best by the model of *Mann & Müller (1973)*. The mean of the test-to-prediction ratio is close to 1.0 and the scatter is reasonable. The models of DIN EN 1996-1-1/NA and *Kranzler (2008)* overestimate the capacity. Keeping in mind that these numbers are based on only 3 tests, the reason is a shortcoming of the model of *Mann & Müller*: the effect of filled head joints is not taken into account. This leads to smaller capacities. Thus, it can be considered a coincidence that the model of *Mann & Müller* fits the results of these 3 tests well. In fact, 2 tests are underestimated while 1 test is overestimated. The model of DIN EN 1996-1-1/NA overestimates the capacity but has smaller scatter. The same holds for *Kranzler's* model. At this point, it has to be mentioned that "under- and overestimation" are not necessarily equal to smaller or larger design capacities according to the corresponding design methods since the important effects of the safety concepts as well as differently defined characteristic values do not affect this assessment.

In case of sliding shear, the model of *Mann & Müller* shows good fit for AAC units, providing a mean of 1.05 and a very small coefficient of variation of 6%. It underestimates the capacity for CS and especially CB units. The reason for this lies in the calculation of the length under compression. In the assessment, the model of *Mann & Müller* was used taking into account a stress block, while the model of DIN EN 1996-1-1/NA uses a linear-elastic stress distribution. This results in longer length under compression. The model of DIN EN 1996-1-1/NA shows overestimation of the test results for CS and AAC. The reason for this is the minimum value of the sliding shear capacity in Eq. 5-66 ($v = \mu \cdot N$) that leads to overestimation of the shear capacity. Considering the fact that this minimum value is based on a physical axiom, it becomes clear that the overestimation must come from the friction coefficient. The friction coefficient is normally derived from small-scale tests and thus does not represent the situation in a full-scale wall. In the tests on CS, especially the tests that were part of the *ESECMaSE* project (*ESECMaSE (2004)*), the friction coefficient was not determined for every wall. Instead, the material properties were determined on small-scale specimens before performing the tests in different labs. Therefore, accuracy of this parameter cannot be expected. Accordingly, the mean for the model of DIN EN 1996-1-1/NA for sliding shear will be set to 1.0. The coefficient of variation remains unchanged; the standard deviation increases to a value of 0.14 for CS and 0.09 for AAC. The model of DIN 1053-100 gives good results for CS and AAC as seen in Table

5.6-2. Since it is based on the model of *Mann & Müller*, the results are similar for both models. The underestimation of the shear capacity for CS units by the *Mann & Müller* model is not detected for the DIN 1053-100 model and the scatter is smaller (6%). The difference to the model according to *Mann & Müller* comes from the influence of the unit format that is not taken into account in the DIN 1053-100 model. Note, that the shear modification factor according to DIN 1053-100 has not been applied since it is not a scientifically based factor.

For the assessment of the tests that failed due to flexure, the capacity was calculated on the basis of a stress block corresponding to fully-plastic material behaviour. This model shows good performance for all materials.

5.6.4 Determination of Model Uncertainties

In the previous section, prediction models for the shear capacities related to the different failure modes were assessed and shown to fit quite well with test data. However, this assessment did not include some important aspects and the uncertainty is different from the numbers in Table 5.6-2 indicate. The main sources of uncertainty are the estimates of the material properties and the identification of the failure mode. Other potential sources for greater uncertainty are e.g. different production quality from lab to lab and differences between the material properties converted from small scale to large scale and, most importantly, the uncertainties due to the limited amount of test data. Therefore, updating becomes necessary and hence, prior information is required. Prior information derived from a specified number of tests, as was used for the update of the tensile strength of the unit in section 4.5.5, is not available. However, prior values derived from expert opinions are available based on experience with similar materials or similar models and will be used to determine the prior distribution. The prior information is summarized in the following table.

Table 5.6-3 Prior information for the update of the model uncertainties

Material	Failure mode	m	CoV	Source
all	shear in general	1.20[a]	25%[a]	JCSS (2003)
		1.35[b]	16%[b]	Löring (2005)
	flexure	1.20[a]	20%[a]	JCSS (2003)
CS	flexure	1.00	18%	Glowienka(2007)
AAC		1.00	14%	
CB		1.00[c]	20%[c]	

[a]estimated from experience with concrete
[b]estimated from experience with reinforced masonry
[c]estimated based on CS and AAC units

In the next step the update is performed for all models and the parameters provided in Table 5.6-2. The values for the shear failure modes were updated using the same prior information. The model for flexure was updated for all materials using different prior

information. The updated and converted stochastic parameters are presented in Table 5.6-4.

Table 5.6-4 Stochastic properties of the models, converted to normal space, after the update

Failure mode	Model	Unit	m	σ	CoV
Diagonal tension	Mann & Müller[a]	CS	1.21	0.25	21%
		AAC	1.12	0.22	20%
		CB	1.40	0.23	16%
	DIN EN 1996-1-1/NA	CS	1.15	0.28	24%
		AAC	1.14	0.20	18%
		CB	1.03	0.18	18%
	Kranzler	CS	1.12	0.30	27%
		AAC	1.17	0.27	23%
		CB	0.99	0.19	19%
	DIN 1053-100	CS	1.23	0.27	22%
		AAC	1.15	0.30	26%
		CB	1.39	0.23	16%
Sliding shear	Mann & Müller[a]	CS	1.27	0.21	17%
		AAC	1.23	0.24	19%
		CB	1.41	0.24	17%
	DIN EN 1996-1-1/NA	CS	1.15[b]	0.24	21%
		AAC	1.21[b]	0.25	20%
		CB	1.24	0.24	20%
	DIN 1053-100	CS	1.15	0.22	19%
		AAC	1.12	0.27	23%
		CB	1.40	0.24	17%
Flexure	ideal-plastic	CS	1.00	0.18	18%
		AAC	1.05	0.16	15%
		CB	1.10	0.20	18%

[a]ideal-plastic stress-strain relationship
[b]updated with a mean of 1.0 (Likelihood)

It can be seen that the scatter of all models for sliding shear is within a range of 17%-23% while most models give a scatter of about 20%. The mean values are larger than 1.0. Due to the large differences in the number of available tests (see Table 5.6-1), the influence of the prior information was different in every case. There was a large influence on the results derived from a small numbers of tests and vice versa.

In general, the stochastic properties indicate that the models give reasonable results and are appropriate for reliability analysis. However, the stochastic properties are similar for many models which makes choosing models for the reliability analysis in chapter 6 difficult. On the other hand since the models all showed good performance, with little exception, the choice will not result in major differences in the reliabilities obtained.

From here, the model uncertainties for sliding shear, diagonal tension and flexure can be determined. Only the model uncertainty for the prediction of the shear capacity due to shear crushing remains unknown. Tests that exhibited this failure mode are not available

because of the large axial loads that have to be applied to cause this failure mode. Therefore, the model uncertainty has to be estimated. Considering the similarity to flexural failure, the stochastic moments of the model uncertainty for shear crushing are estimated with a mean of 1.0 and a standard deviation of 0.2. Also, the DIN EN 1996-1-1/NA (2010-10) model is considered to be appropriate because it is basically *Mann & Müller's* model but includes consideration of the overlap.

5.7 Summary

Chapter 5 introduces the reader to the methods of shear capacity prediction of masonry walls subjected to in-plane shear. In the first sections, the most common approaches assuming linear-elastic stress-strain distribution are presented. The failure modes that are related to shear failure and the corresponding models are explained. Models based on plastic limit analysis are also mentioned and briefly discussed but are not considered useful for the subject of this thesis.

The models presented range from scientific models such as *Mann & Müller (1973)* and *Jäger & Schöps (2004)* to design models from various codes. The models are introduced and non-dimensional design equations are provided.

For the reliability analysis in chapter 6, a realistic prediction model is required. Prediction models come with uncertainty since not every influence or aspect can be included in a model and every model is subject to a certain degree of simplification. A variety of prediction models for the shear capacity are provided and discussed; German and international design models are part of the assessment as well as scientific models. The models are assessed with test data in order to identify the most realistic model. The model of *Mann & Müller* and the model of DIN EN 1996-1-1/NA are found to match the test data most accurately in case of sliding shear and diagonal tension depending on the unit material. For flexural failure, prediction on the basis of an ideal-plastic stress-strain relationship showed good agreement with the test data. Since the assessment of the tests is very uncertain due to limited number of samples and further sources of uncertainty, a Bayesian update is performed applying prior information in the form of expert opinions. By performing the update, the stochastic properties of the prediction models could be specified and enhanced.

From the obtained stochastic parameters, the model for the reliability analysis that follows was assembled by choosing the parts of the investigated models that showed best performance. Thus, different models are used for every unit material and failure mode. Table 5.7-1 summarizes the results. However, the stochastic model for shear crushing had to be estimated since test data is not available. The new set of prediction equations is believed to represent the behaviour of URM shear walls realistically and consequently is an appropriate basis for reliability analysis in chapter 6.

Table 5.7-1 Summary of the stochastic models of the model uncertainties

Failure mode	Unit	Model	Dist.	m	σ	CoV
Diagonal tension Θ_{dt}	CS	*Mann & Müller*	LN	1.21	0.25	21%
	AAC	DIN EN 1996-1-1/NA		1.14	0.20	17%
	CB			1.03	0.18	17%
Sliding shear Θ_s	CS	DIN EN 1996-1-1/NA		1.15	0.24	21%
	AAC	*Mann & Müller*		1.23	0.24	20%
	CB	DIN EN 1996-1-1/NA		1.24	0.24	19%
Flexure Θ_f	CS	fully-plastic[a]		1.00	0.18	18%
	AAC			1.05	0.16	15%
	CB			1.10	0.20	18%
Shear crushing Θ_c	all	DIN EN 1996-1-1/NA		1.00	0.20	20%

[a]stress-strain relationship

6 RELIABILITY OF URM WALLS SUBJECTED TO IN-PLANE SHEAR

6.1 Introduction

In the design process of structures, many uncertainties in the form of basic variables are involved. Due to matters of simplicity, the uncertainties are taken into account by using supposedly conservative design values of loads and material properties. In contrast to this deterministic design approach, the basic variables can be formulated by means of stochastic methods. If the stochastic properties of the basic variables are known, the theoretical failure probability and thus the structural reliability of the single member and the entire structure can be computed with the methods described in section 2.5. The failure probability is only theoretical since human errors and deviations in execution are not taken into account. In addition, the stochastic quantification of the basic variables is difficult and not all influences can be included in the limit state function, such as e.g. the quality of the design process or workmanship. Therefore the term “structural reliability” refers to an operative value that is only influenced by material, loads and design models. It only represents a quantity to evaluate and compare different structures and construction methods.

While failure of walls subjected to out-of-plane flexure is not necessarily followed by collapse of the structure, failure of the bracing shear walls possibly is. Masonry shear walls are the major lateral load-carrying elements in masonry structures. In this chapter, the reliability of masonry shear walls designed according to DIN 1053 and DIN EN 1996-1-1/NA will be determined using analytical models. The goal is the determination of the provided reliability of masonry shear walls in the past as a measure for the societally accepted minimum reliability.

6.2 General

To be able to assess the reliability of a member, the reliability must be related to design according to standards. DIN EN 1990 provides target reliabilities for all members independent of the material. According to this, members designed following the German design codes must exhibit the defined target reliabilities in their limit state. In the following study, members will be designed in such a way that the cross-section is completely utilized. For flexural members, this is an overly conservative assumption since walls are commonly thicker than necessary to satisfy non-structural building envelope requirements. In case of shear walls, this is not the case since the length of the members - which is not affected by building envelope issues – is the governing parameter and consequently slender walls might be utilized to 100%.

Since the application and typology of masonry members is extremely varied, a representative sample of masonry members has to be chosen. The chosen members are summarized and presented in section 6.4. The reliability will be determined for the design according to the two currently available codes in Germany (DIN 1053-1, DIN 1053-100) and the current draft of the upcoming National Annex to Eurocode 6, DIN EN 1996-1-1/NA. This will make it possible to compare the currently available level of reliability of masonry shear walls and the probable future level. However, the draft has not been finalized yet; changes are still possible.

For the reliability analysis, limit state functions for the respective failure modes (see chapter 5) were derived and will subsequently be used to determine the reliability of the respective members. Figure 6-1 outlines the procedure for the reliability analysis. The reliabilities obtained will then be assessed and analysed.

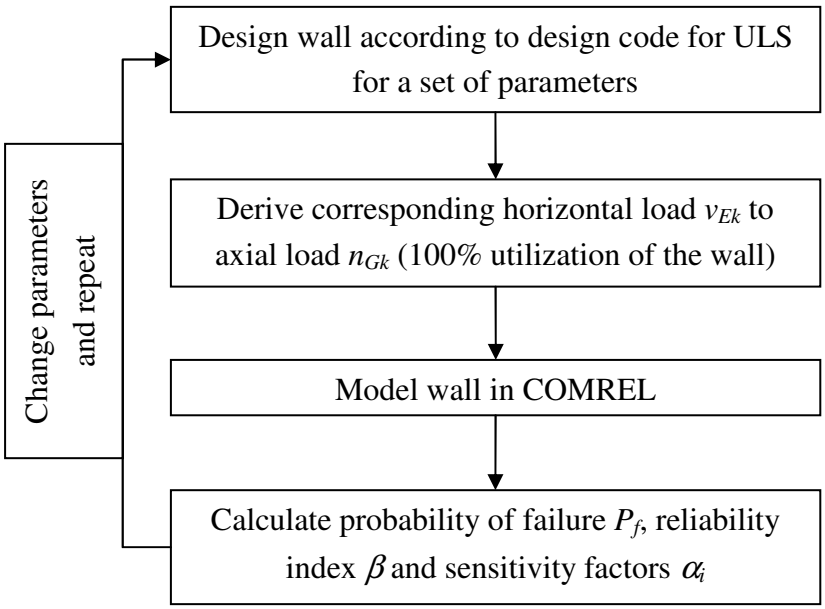

Figure 6-1 Procedure forReliability Analysis

The calculation of the failure probability and reliability will be carried out using COMREL (*RCP (2004)*), a commercial software for reliability analysis. For more information on the method of analysis see section 6.6.4.

The reliability analysis will be conducted for single members. It is assumed that failure of the single member is directly followed by failure of the entire structure. This is a conservative assumption since masonry structures usually have some structural redundancy and the potential for redistribution of loads to less utilized members. Even if the bracing system is assumed to be statically determinate, there will be members that contribute to the bracing that were not considered in the structural model. Even the loss of entire members can possibly be compensated for if the remaining structure can carry the loads because of plastic reserves in the load-carrying capacity. Therefore, the reliability determined in this

chapter gives the lower limit of the reliability; true reliability of the structure will likely be larger. A general quantification of these effects is difficult and impossible at this point.

6.3 Structural System

The structural system plays a major role in the stochastic modelling. The most common approach to modelling the bracing system in practice is the simplifying assumption of considering each wall as a building-high cantilever that is subjected to horizontal load at the top of the wall. This was the preferred system according to DIN 1053-1 and DIN 1053-100. However, this does not account for a possible over-turning moment from the concrete slabs. *Kranzler (2008)* therefore converted the shear wall with an eccentricity of the axial load at the top of the wall to an equivalent wall without eccentricity as shown in Figure 5-2. This approach is part of the design model of DIN EN 1996-1-1/NA and was described in more detail in section 5.5.3.

For the reliability analysis, the relevant range of λ_v has to be known; especially the maximum value, since representing very slender walls is important. It is assumed that the most critical situation is present in the case of townhouse complexes. The reason for this is the fact that normally windows cannot be inserted in the two shared walls of a typical town house. Thus, large windows have to be inserted into the two other walls including a large window/door-opening at the ground floor. This leads to little space for bracing walls, and inside the house usually only the staircase walls can actually be considered as bracing elements in the lateral direction. Figure 6-2 shows the typical dimensions of a townhouse in Germany and the corresponding values of $\lambda_v = h_w/l_w$. The shortest walls are about 1.0 m long. Estimating the typical storey height to be approx. 3.0 m, the upper value of $\lambda_v = h_w/l_w$ becomes $\lambda_v = 3.0$. However, this requires concentric axial loads at the top of every wall. Slender members will likely fail in flexure and flexural failure will also govern the design. In this case, the eccentricity is limited and thus no changes in the reliability distribution for very slender walls are expected. This will be verified in section 6.7. However, this upper limit is thought to represent all common cases of slender walls in residential and office masonry buildings. The minimum value, $\lambda_v = 0.25$ corresponds to a wall with a length of four times the height.

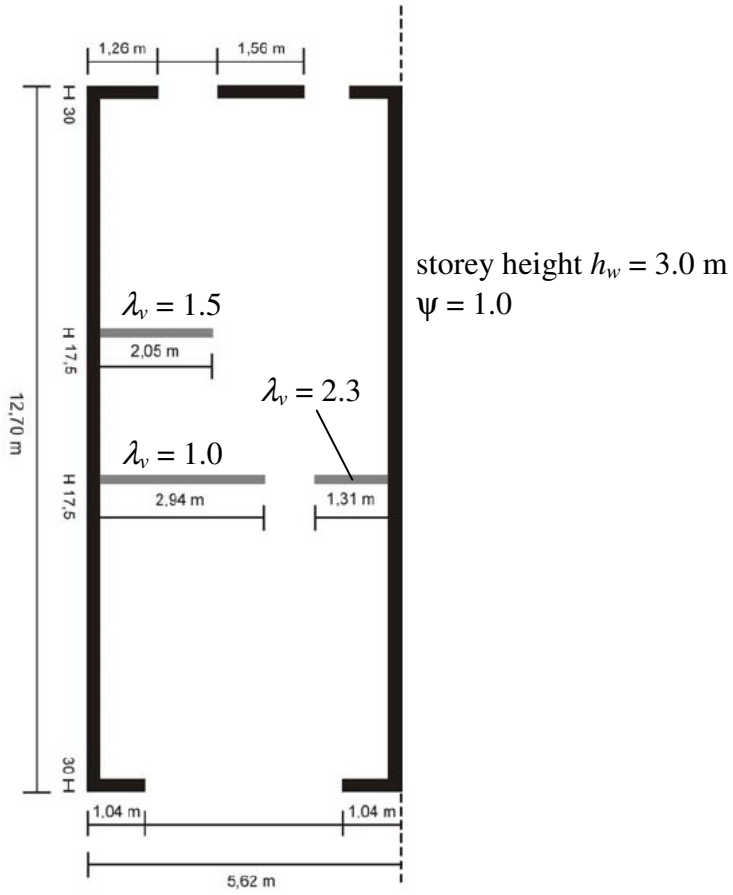

Figure 6-2 Typical floor plan dimensions of a townhouse in Germany according to Meyer (2005)

6.4 Masonry Members to be Examined

A survey of masonry designers, producers and experts revealed that although the range of typology of masonry is large, there are actually only a small number of unit-mortar-combinations with practical relevance in Germany. These will form the basis for this study. In addition, the range in wall geometry must also be limited to a certain extent. By performing the analysis using a non-dimensional probabilistic model (see section 6.6.2), the geometry can be reduced to one single parameter, the shear slenderness ratio λ_v. This parameter will be studied in the range of $\lambda_v = \{0.25; 0.5; 1.0; 2.0; 3.0\}$ to account for common masonry design practice. The study parameters are presented in Table 6.4-1.

Table 6.4-1 Reliability Study Parameters

Unit	Compressive Strength of unit[a]	Mortar	Comments	Range
CS	20	TLM	full block (grip holes)	λ_v = {0.25;0.5;1.0;2.0;3.0} $n_{Gk} = 0.01\text{-}n_{Gk,max}$
AAC	4	TLM	full block	
CB	12	GPM[b]	hollow brick	
[a]corresponding to the categories of compressive strength according to DIN 1053-1 [b]GPM IIa according to DIN 1053-1				

In total, 425 walls are examined. In addition, walls with special properties, e.g. small overlap u/h_b, will complete the study.

6.5 Design Check

All walls will be designed according to DIN 1053-1, DIN 1053-100 and DIN EN 1996-1-1/NA, respectively. The design models were described and analysed in sections 5.5.2 and 5.5.3. However, the following table summarizes some of the properties and differences of the design models that affect the load-carrying capacity.

Table 6.5-1 Comparison of the design models

Aspect	DIN 1053-1	DIN 1053-100	DIN EN 1996-1-1/NA[a]
safety format	global	partial factors	partial factors
length under compression	linear-elastic	linear-elastic with modification factor	linear-elastic and fully-plastic[1]
level of check	stress	force	force
diagonal tension model	based on *Mann & Müller (1973)*	based on *Mann & Müller (1973)*	based on *Jäger & Schöps (2004)*
location of check	toe of the wall	toe of the wall	toe and mid-height of the wall[b]
application of the safety factors	on strength[c]	on load and strength	on load and strength
cohesion	$\beta_{RHS} = f_{vk0}$	f_{vk0}	$f_{vk1} = 1.25 \cdot f_{vk0}$

[a]current draft
[b]depending on the failure mode
[c]formally wrong but common in design practice

Different load combinations have to be considered in the design due to the fact that axial load can act favourably and unfavourably. In case of sliding shear and diagonal tension, axial load acts favourably. Hence, only dead load is considered for these failure modes since the sustained live load which can be considered in ultimate limtit state design is small (see *Glowienka (2007)*). In case of shear crushing, axial loads act unfavourably, so both dead and live loads are considered. For flexural failure, two load combinations representing minimum axial load (only dead load) and maximum load (dead and live load) have to be considered. Of course, wind load always acts unfavourably because it is independent from the axial load and thus the maximum wind load can always occur at any level of axial load and increase the bending moment. The matrix of partial safety factors considered in the design according to DIN 1053-100 for the reliability analysis is displayed in Table 6.5-2.

Table 6.5-2 Failure modes and corresponding partial safety factors in the design according to DIN 1053-100

Failure mode	γ_G	γ_Q	γ_w
Sliding shear	1.0	0	1.5
Diagonal tension	1.0	0	1.5
Shear crushing	1.35	1.5	1.5
Flexure (min)	1.0	0	1.5
Flexure (max)	1.35	1.5	1.5
Tip over[a]	1.0	0	1.0
[a]serviceability limit state			

6.6 Reliability Analysis

6.6.1 General

The equations used in the following are normalized to give comparable, non-dimensional results. The normalization is carried out by the same method as described and applied in section 5.5.1. The axial and horizontal force will be divided by the characteristic value of the masonry compressive strength. Since the level of reliability according to the three codes will be determined and compared, the same strength has to be used in every case. Here, the characteristic value of the compressive strength according to DIN EN 1996-1-1/NA is used. The absolute value of this quantity does not have an influence on the findings of the study; it only represents a mutual standard. In general, the quantities are formulated as in Eq. 5-41 and Eq. 5-42.

6.6.2 Limit State Function and Probability of Failure

The analytical prediction model for the shear capacity that forms the basis of the limit state function has to be the most realistic model available. The best model is the model that provides the model uncertainty, with the smallest coefficient of variation and, ideally, a mean close to 1. It does not have to be similar to the chosen design models.

The available models were described and assessed in chapter 5. In section 5.6, the models were assessed against test data and the corresponding model uncertainties were determined. It was found that the models of *Mann & Müller (1973)* and DIN EN 1996-1-1/NA show the most agreement with the test data depending on the unit material and failure mode (see Table 5.7-1). Thus, the limit state function has to be formulated differently for every unit material and every failure mode. The failure modes considered are:

- Sliding shear (minimum axial load)
- Diagonal tension (minimum axial load)
- Crushing (maximum axial load)
- Flexural failure (minimum and maximum axial load)

The main difference between the prediction models described in chapter 5 and the probabilistic model is the insertion of the model uncertainties Θ_i as basic variables. In general, model uncertainties can be applied as factors or summands (see *JCSS (2003)*). Here, the model uncertainties will be inserted as factors. The limit state function in the general form according to Eq. 2-58, can be formulated as in Eq. 6-1.

$$g(x) = \begin{cases} v_{R,sliding} - \Theta_E \cdot v_E \\ v_{R,diagonal} - \Theta_E \cdot v_E \\ v_{R,crushing} - \Theta_E \cdot v_E \\ v_{R,flexure,\min} - \Theta_E \cdot v_E \\ v_{R,flexure,\max} - \Theta_E \cdot v_E \end{cases} \qquad \text{Eq. 6-1}$$

In this equation, v_E refers to the mean sustainable shear load at the ultimate limit state derived from the shear loads v_{Ek} according to the different codes (see chapter 5). The mean shear resistances v_R are calculated using Eq. 6-2 through Eq. 6-11.

As previously mentioned, the most appropriate model for the prediction of the shear capacity $v_{R,i}$ has to be applied in each particular case. The best models for every failure mode and every material were identified in the previous chapter and were summarized in Table 5.7-1. The relevant limit state functions for every case follow in Eq. 6-2 through Eq. 6-11.

First, the model for flexural failure based on a fully-plastic stress-strain relationship is presented which is equal for all unit materials investigated.

$$v_{R,flexure,\min} = \Theta_{R,flexure} \cdot \frac{1}{2 \cdot \lambda_v} \cdot \left(\Theta_E \cdot n_G - \frac{f_k}{f} \left(\Theta_E \cdot n_G \right)^2 \right) \qquad \text{Eq. 6-2}$$

$$v_{R,flexure,\max} = \eta \cdot \Theta_{R,flexure} \cdot \frac{1}{2 \cdot \lambda_v} \cdot \left(\Theta_E \cdot \left(n_G + n_Q \right) - \frac{f_k}{f} \left(\Theta_E \cdot \left(n_G + n_Q \right) \right)^2 \right) \qquad \text{Eq. 6-3}$$

As determined in section 5.6, the models of *Mann & Müller (1973)* and DIN EN 1996-1-1/NA describe the capacities due to sliding shear and diagonal tension quite well. The minimum shear strength $v = \mu \cdot n$, as suggested by *Kranzler (2008)* based on the second law of *Amontons*, was also included to account for this physical limit. This gives:

$$v_{R,sliding} = \max \begin{cases} \Theta_{R,sliding,M\&M} \cdot \dfrac{\frac{3}{2} \cdot \frac{f_{v0}}{f_k} + \mu \cdot \Theta_E \cdot n_G}{c \cdot \left(1 + 2 \cdot \mu \cdot \frac{h_b}{l_b} \right) + 3 \cdot \frac{f_{v0}}{f_k} \cdot \frac{\lambda_v}{\Theta_E \cdot n_G}} \\ \Theta_{R,sliding,M\&M} \cdot \mu \cdot \Theta_E \cdot n_G \end{cases} \qquad \text{Eq. 6-4}$$

$$v_{R,diagonal} = \Theta_{R,diagonal,M\&M} \cdot \frac{1}{2} \cdot \frac{A \cdot B}{1-B^2} \cdot \left(2 + \frac{\Theta_E \cdot n_G}{\frac{f_{bt}}{f_k}} \right) \cdot \left[-1 + \sqrt{1 + \frac{1-B^2}{B^2} \cdot \frac{4 \cdot \left(1 + \frac{\Theta_E \cdot n_G}{f_{bt}/f_k} \right)}{\left(2 + \frac{\Theta_E \cdot n_G}{f_{bt}/f_k} \right)^2}} \right]$$

Eq. 6-5

$$A = \frac{f_{bt}/f_k}{2.3 \cdot c}$$ Eq. 6-6

$$B = \frac{2 \cdot A}{\Theta_E \cdot n_G} \cdot \lambda_v$$ Eq. 6-7

Likewise, the equations for the capacities due to sliding shear and diagonal tension based on DIN EN 1996-1-1/NA can be obtained.

$$v_{R,sliding} = \max \begin{cases} \Theta_{R,sliding,EN} \cdot \dfrac{\frac{3}{2} \cdot \frac{f_{v0}}{f_k} + \mu \cdot \Theta_E \cdot n_G}{c \cdot (1+\mu) + 3 \cdot \frac{f_{v0}}{f_k} \cdot \frac{\lambda_v}{\Theta_E \cdot n_G}} \\ \Theta_{R,sliding,EN} \cdot \mu \cdot \Theta_E \cdot n_G \end{cases}$$ Eq. 6-8

$$v_{R,diagonal} = \Theta_{R,diagonal,EN} \cdot \frac{1}{c} \cdot \frac{f_{bt}}{f_k} \cdot \frac{1}{F^{*2}} \cdot \left(\sqrt{1 + F^{*2} \cdot \left[1 + \frac{\Theta_E \cdot n_G}{\frac{f_{bt}}{f_k}} \right]} - 1 \right)$$ Eq. 6-9

$$F^* = 1.2 + 0.85 \cdot f_{bt} \qquad f_{bt} \text{ in N/mm²}$$ Eq. 6-10

The final equation is the equation for shear crushing. It is based on the model of *Mann & Müller* and takes into account different values of the overlap u/h_b. The corresponding stress-strain relationship is fully-plastic.

$$v_{R,crushing} = \Theta_{R,crushing} \cdot \frac{u}{h_b} \cdot \frac{\frac{f_m}{f_k} - \Theta_E \cdot \left(n_G + n_Q \right)}{c + \frac{2}{f_k} \cdot \frac{u}{h_b} \cdot \frac{\lambda_v}{\Theta_E \cdot \left(n_G + n_Q \right)}}$$ Eq. 6-11

6.6.3 Stochastic Model

The stochastic properties of the basic variables were determined in the previous chapters. For clarity, the entire stochastic model is summarized in Table 6.6-1.

Note that the mean of the basic variables is the ratio of mean-to-characteristic of the actual quantity. To derive the actual quantity, this ratio must be multiplied by the characteristic value. For example, the means of the shear load v_E and the dead load n_G can be computed from Eq. 6-12 and Eq. 6-13.

$$v_E = v_{Ek} \cdot \left(\frac{m_v}{X_{Vk}} \right) \qquad \text{Eq. 6-12}$$

$$n_G = n_{Gk} \cdot \left(\frac{m_G}{X_{Gk}} \right) \qquad \text{Eq. 6-13}$$

where n_{Gk} is the deterministic characteristic value of the axial dead load and the ratio in parenthesis is a random variable and can be taken from Table 6.6-1.

Table 6.6-1 Summary of the stochastic model

	Basic variable	Material	Distr.	$m_{X,i}/X_{k,i}$	*CoV*
Resistance	Compressive strength of masonry f_m	CS	LN	1.55	19%
		AAC		1.81	16%
		CB		1.43	17%
	Tensile strength of unit f_{bt}	CS		1.84	26%
		AAC		1.55	16%
		CB		1.31	24%
	Cohesion f_{v0}	TLM		2.14	35%
		GPM		3.57	40%
	Friction Coefficient μ	all		1.33	19%
	Model uncertainty sliding shear Θ_s	CS		1.15	21%
		AAC		1.23	20%
		CB		1.24	19%
	Model uncertainty diagonal tension Θ_{dt}	CS		1.21	21%
		AAC		1.14	17%
		CB		1.03	17%
	Model uncertainty crushing Θ_c	all		1.00	20%
	Model uncertainty flexure Θ_f	CS		1.00	18%
		AAC		1.05	15%
		CB		1.10	18%
Load	Model uncertainty on the shear load $\Theta_{E,v}$	all		1.00	10%
	Model uncertainty on the axial load $\Theta_{E,a}$			1.00	5%
	Wind load v[a,b]		Weibull	1.03	7%
	Live load n_Q[a]		Gumbel	1.10	20%
	Dead load n_G		N	1.00	6%

[a] observation period of 50 yrs
[b] $\tau = 0.073$

6.6.4 Method of Analysis

Generally, several methods of analysis are possible (see section 2.5.3), however, the simplified methods, FORM and SORM, are very efficient and less time-consuming than numerical procedures such as MCS. They also allow for the determination of sensitivity factors which simplify the sensitivity analysis. However, in this case a system of limit state functions is existent; one for every possible failure mode. This requires a special procedure for the determination of the failure probability.

For a system of 4 limit state functions $g(x)_i = \{g(x)_1,\ldots, g(x)_4\}$, Figure 6-3 illustrates the situation by use of a tree diagram and also shows the typical functions and corresponding overlaps in normal space, (also see Figure 2-4).

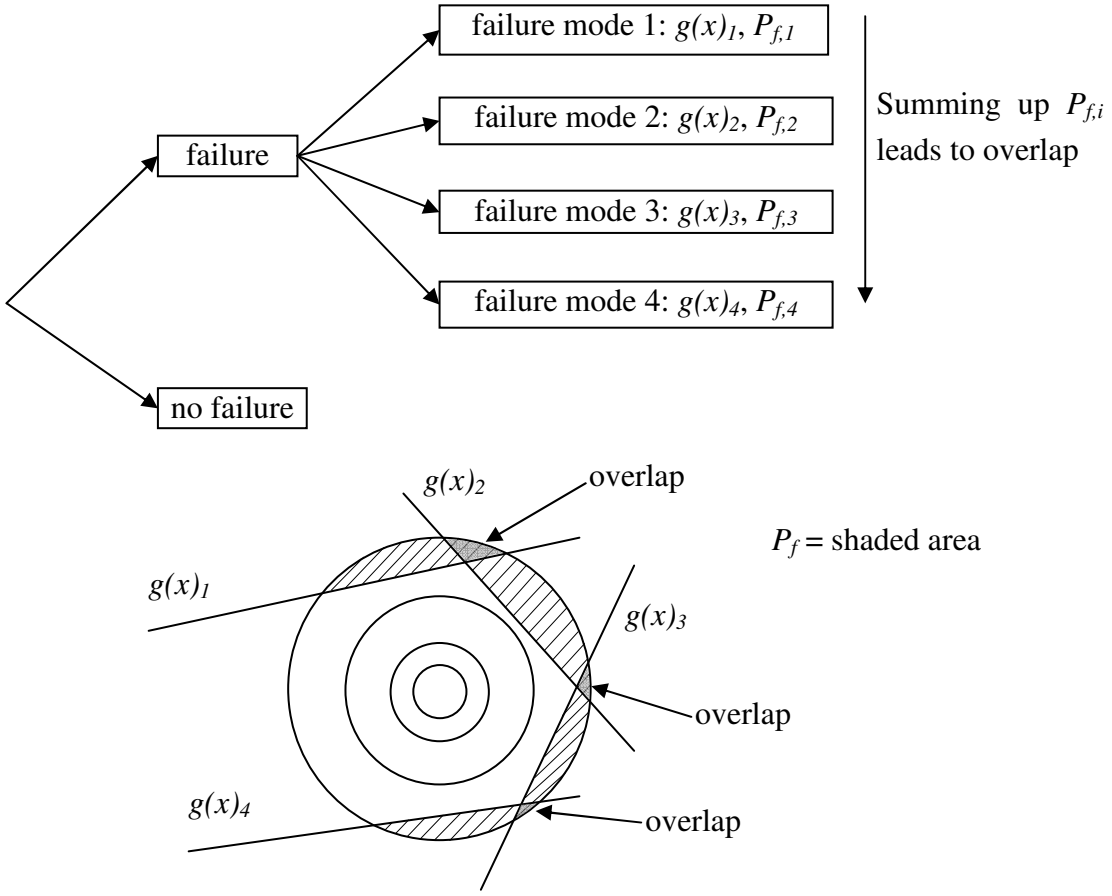

Figure 6-3 System of Limit State Functions

Ideally, MCS should be used to account for the different limit state functions at the same time and to exclude the overlap of the functions. Here, a different approach is chosen to save computation time and to obtain sensitivity values. SORM is used for every single limit state function, so that the probability of exceeding the limit state for every single failure mode is determined. The probabilities of failure for each load situation are then added as shown in Eq. 6-14.

$$P_f = P_{f,sliding} + P_{f,diagonal} + P_{f,flexure} + P_{f,crushing} \quad \text{Eq. 6-14}$$

This gives a maximum value of the probability of failure of the system of limit state functions since the overlap of the different limit state functions is not deducted from the sum of failure probabilities. A comparison with MCS where the overlap is deducted for selected cases showed only negligible differences to the results obtained with SORM. Consequently, the obtained failure probabilities represent the failure probability of the system very well and SORM was chosen as method of analysis. The probability of failure $P_f = \Sigma P_{f,i}$ is then used for calculation of the reliability index β according to Eq. 2-65.

6.7 Theoretical Reliability of Masonry Shear Walls Subjected to Wind Load

6.7.1 General

In the following, the reliability of typical masonry used in practice in Germany, past and present, will be determined. Therefore, unless otherwise noted, the overlap will be set to $u/h_b \geq 0.4$ and the unit format is $h_b/l_b \leq 1.0$. Here, the term reliability refers to the theoretical reliability assuming full (100%) utilization of the cross-section.

6.7.2 DIN 1053-1

The reliability of masonry walls generally depends on a large number of basic variables which are related to resistance, loads and model uncertainties. In the previous chapters, the basic variables were determined and stochastic models were derived. These models will not be varied in the following study since they are valid for every wall. The main parameter of the study is the deterministic shear slenderness λ_v (see section 6.3). Variation of this parameter allows for the modelling of squat and slender walls. The formulation of the structural system using the parameter λ_v has another positive effect on the reliability analysis: the wall gets converted into a wall with concentric axial load and horizontal load acting on top of the wall so that the bending moment at the toe of the wall is independent of the axial load. Bending moment and axial load are therefore uncorrelated since they are caused by different physical effects that act perpendicularly to each other.

In Figure 6-4, the reliability index β determined in the probabilistic analysis and the sustainable shear load v_{Ek} according to DIN 1053-1are plotted versus the axial dead load n_{Gk} and the expected failure mode is indicated. Since the axial dead load n_G can be computed from the characteristic value n_{Gk}, it is possible to use the latter as mutual parameter and to plot it on the x-axis in order to compare the code design and the results obtained for the reliability. The failure mode predicted from the reliability analysis is the failure mode that yielded the largest probability of failure. The slenderness of the wall is $\lambda_v = 3.0$.

The target region of reliability is in between the recommended values of $\beta_t = 3.8$ (DIN EN 1990) and $\beta_t = 3.2$ (*JCSS (2001)*). It can be seen that the reliability falls below the minimum target value for all values of n_{Gk} in the practically relevant range (further referred to as "practical range") from $n_{Gk} = 0.05 - 0.20$.

$$n_{Gk,relevant} = 0.05 - 0.20 \qquad \text{Eq. 6-15}$$

Considering the corresponding partial safety factors, durability factor and a ratio of live-to-dead load of 3/7, a value of $n_{Gk} = 0.2$ corresponds to a utilization of the axial (fully-plastic) capacity of the cross-section of 70% (dead and live load) or 50% (dead load only). These values are almost never reached in common masonry construction. Most members will actually be within the range of $n_{Gk} = 0.05 - 0.15$. For high axial load, the reliability increases suddenly to values of over $\beta = 5.0$. The reason for the sudden rise lies in the design according to the code; while the code predicts that the capacity due to flexural failure governs for $n_{Gk} = 0.19–0.28$, according to the probabilistic model, diagonal tension governs in this region. The reason for this difference is the relatively conservative approach to diagonal tension capacity in DIN 1053-1. When the capacity according to the code starts to decrease, the capacity according to the probabilistic model is still increasing due to the less conservative approach to the tensile strength of the unit and the decreasing design wind load.

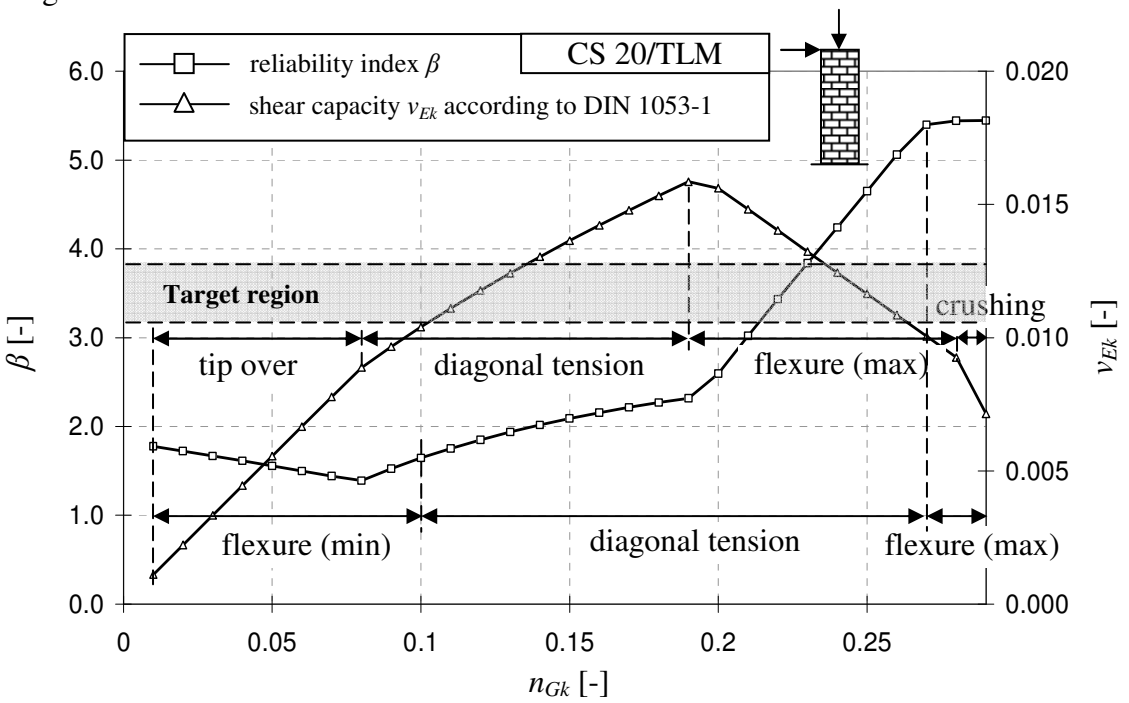

Figure 6-4 *Reliability index β and sustainable shear load v_{Ek} vs. axial dead load n_{Gk} for a CS wall with $\lambda_v = 3.0$ (designed according to DIN 1053-1)*

Note, that different failure modes are predicted according to the code design and the reliability analysis. The reason for this is the stochastic treatment of the variables in the reliability analysis. For example, the tensile strength of the unit f_{bt} is estimated to be

smaller in the reliability analysis than the characteristic value in the code due to the large scatter. This leads a larger range where diagonal tension governs in the reliability analysis compared to the code design. In addition, the model uncertainties influence the derived capacities and thus change the relevant ranges for the failure modes.

The distribution of the reliability index β and the corresponding distribution of the eccentricities e/l_w are plotted versus the axial dead load n_{Gk} in Figure 6-5. The eccentricity e/l_w represents the effect of slenderness and the ratio of horizontal to axial load and thus is a measure for the length under compression. In the following, the term "eccentricity" refers to the deterministic value obtained from the code design according to Eq. 6-16.

$$\frac{e}{l_w} = \frac{V_{Ek}}{N_{Gk}} \cdot \lambda_v \qquad \text{Eq. 6-16}$$

It is observed that large eccentricities generally lead to low reliability. It can also be seen that the slope of the distribution of reliability changes with the slope of the distribution of eccentricity. The range of n_{Gk} where tip over of the entire wall governs occurs for constant eccentricity while the other failure modes lead to varying slope of the distribution. In general, large values of n_{Gk} correspond to small eccentricity and vice versa.

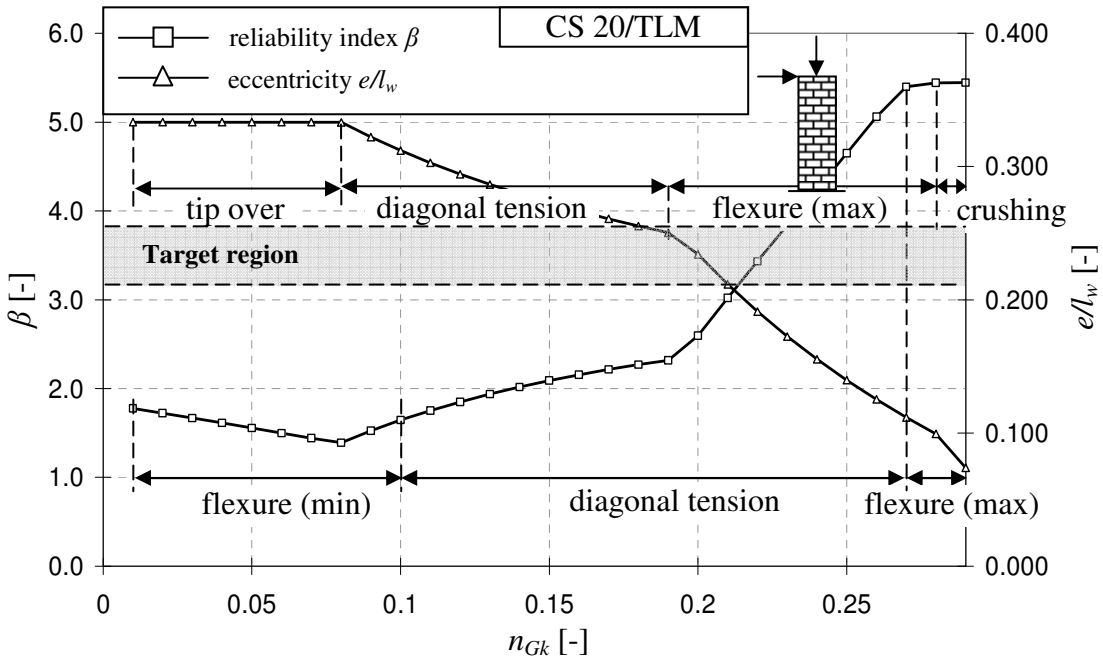

Figure 6-5 *Reliability index β and eccentricity e/l_w vs. axial dead load n_{Gk} for a CS wall with λ_v = 3.0 (designed according to DIN 1053-1)*

Table 6.7-1 shows a selection of sensitivity values for the slender CS wall. It can be seen that the model uncertainties are the important basic variables for minimum axial load. In case of maximum axial load, the model uncertainty is unimportant; the corresponding failure modes are governed by the compressive strength of the masonry. The results are sensitive to the wind load in every case of minimum axial load but not in the case of maximum load. The reason is the eccentricity; in case of maximum load the cross-section re-

mains under compression and thus the horizontal load is less influential. In this case, the axial load is the most important load and thus the live load becomes important due to the large scatter. However, the jump occurs in a region of very high axial stress due to dead load which does not represent common conditions in masonry construction.

Table 6.7-1 Select sensitivity values for a CS wall with $\lambda_v = 3.0$

n_{Gk}	e/l_w	FM[a]	β	$\alpha_{\Theta s}$	$\alpha_{\Theta dt}$	$\alpha_{\Theta c}$	$\alpha_{\Theta f}$	$\alpha_{\Theta E}$	α_{nG}	α_{nQ}	α_v	α_{fm}	α_{ft}	α_{fv0}	α_μ
0.01	0.33	F	1.97	-	-	-	0.84	-0.00	0.33	-	-0.44	0.01	-	-	-
0.10	0.31	F	1.70	-	-	-	0.84	-0.04	0.31	-	-0.44	0.07	-	-	-
0.19	0.25	DT	2.35	-	0.87	-	-	-0.09	0.21	-	-0.36	-	0.23	-	-
0.20	0.23	DT	2.55	-	0.87	-	-	-0.09	0.21	-	-0.36	-	0.24	-	-
0.28	0.10	F	5.50	-	-	-	0.14	-0.37	0.13	-0.34	-0.07	0.82	-	-	-
0.29	0.07	F	5.90	-	-	-	0.10	-0.37	-0.13	-0.39	-0.04	0.83	-	-	-

[a]FM=Failure Mode (S = sliding; DT = diagonal tension; C = crushing; F = flexure)

As expected for a slender wall, flexural failure under minimum load limits the reliability for low levels of axial load. The reliability obtained is significantly less than $\beta = 2.0$ for $n_{Gk} \leq 0.1$. However, the average value within the practical range is $\beta \approx 2.0$.

For squat walls, a change of the failure modes is expected. Flexural failure is unlikely to occur while sliding shear and especially diagonal tension are expected to govern. The reliability for a squat CS wall with $\lambda_v = 0.5$ is presented in Figure 6-6. In contrast to the slender wall, the reliability of the squat wall is within or above the target region over the practical range. Sliding shear failure governs in the code design but in the probabilistic analysis, diagonal tension mostly governs. This leads to a curved reliability distribution in the range of $n_{Gk} = 0.01–0.10$. The average reliability over the practical range is $\beta = 3.9$.

In Figure 6-7, the distribution of eccentricity is compared to the distribution of reliability for a squat CS wall in the same way as in Figure 6-5. Again, it can be seen that large eccentricity leads to small reliability. However, the eccentricity is generally smaller than in the case of slender walls; large values of the shear slenderness λ_v lead to higher eccentricity.

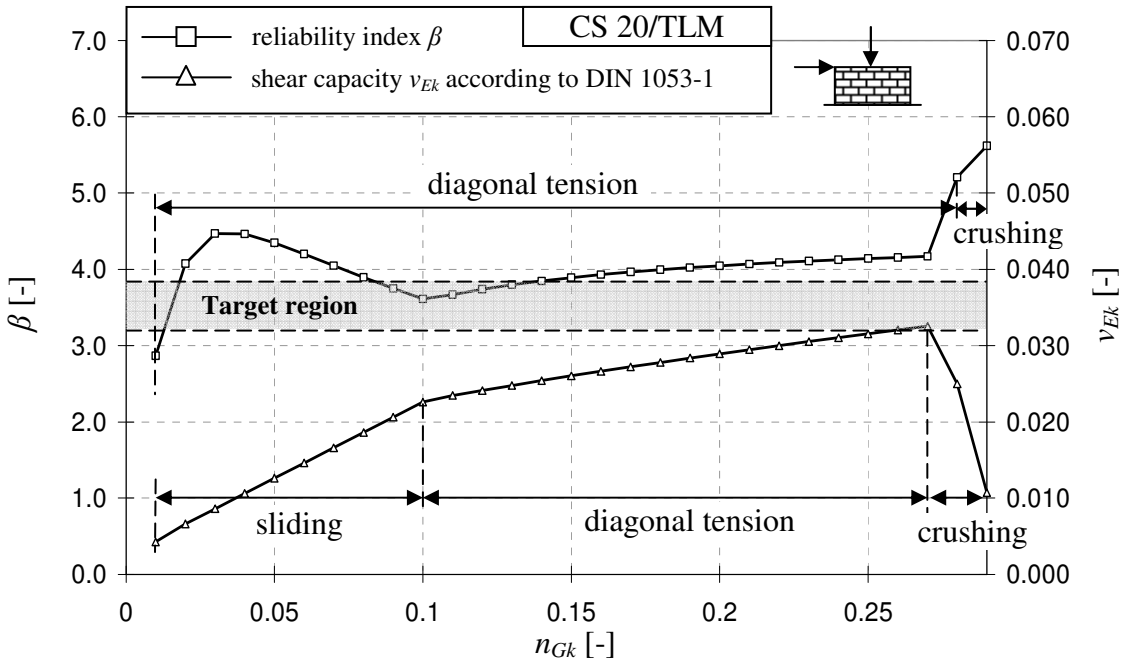

Figure 6-6 *Reliability index β and shear resistance v_{Ek} vs. axial dead load n_{Gk} for a CS wall with λ_v = 0.5 (designed according to DIN 1053-1)*

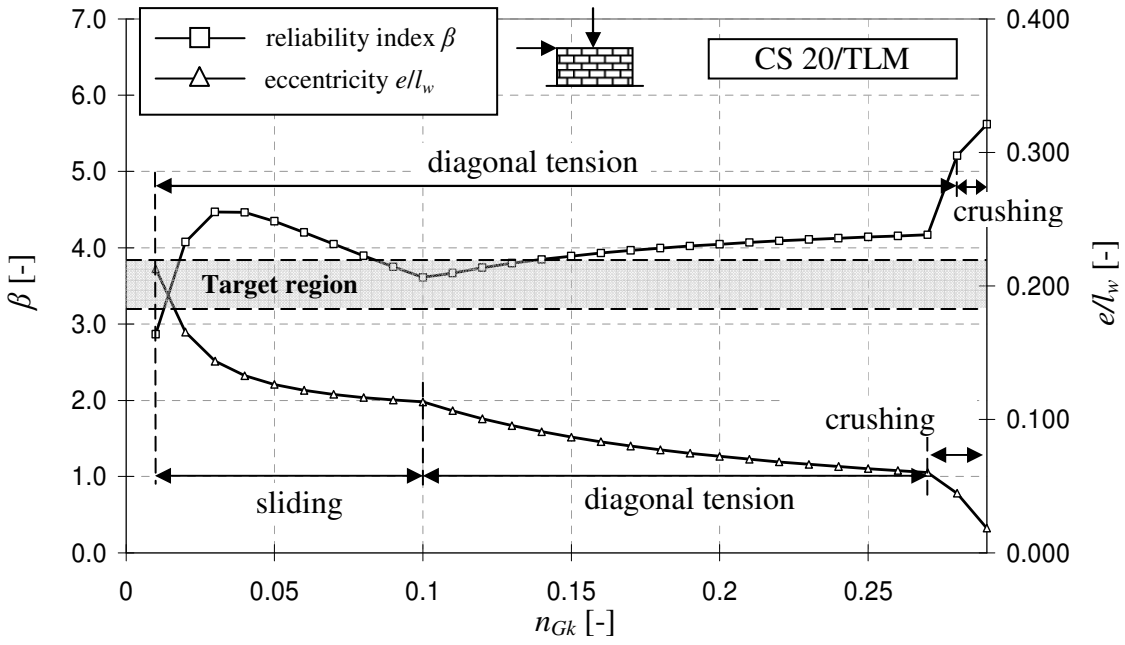

Figure 6-7 *Reliability index β and eccentricity e/l_w vs. axial dead load n_{Gk} for a CS wall with λ_v = 0.5 (designed according to DIN 1053-1)*

Figure 6-8 shows the reliability versus the axial load for various values of the shear slenderness λ_v. The tendency for higher reliability in squat walls is obvious (λ_v small → β large). A jump in reliability can be detected at the change from slender to squat walls. The cause for this jump is the increasing influence of the wind load on the eccentricity due to the large value of λ_v which represents the slope of the eccentricity (see Figure 6-9). This

means, the eccentricity for a given combination of horizontal and axial load is larger for a larger value of λ_v than for a small λ_v.

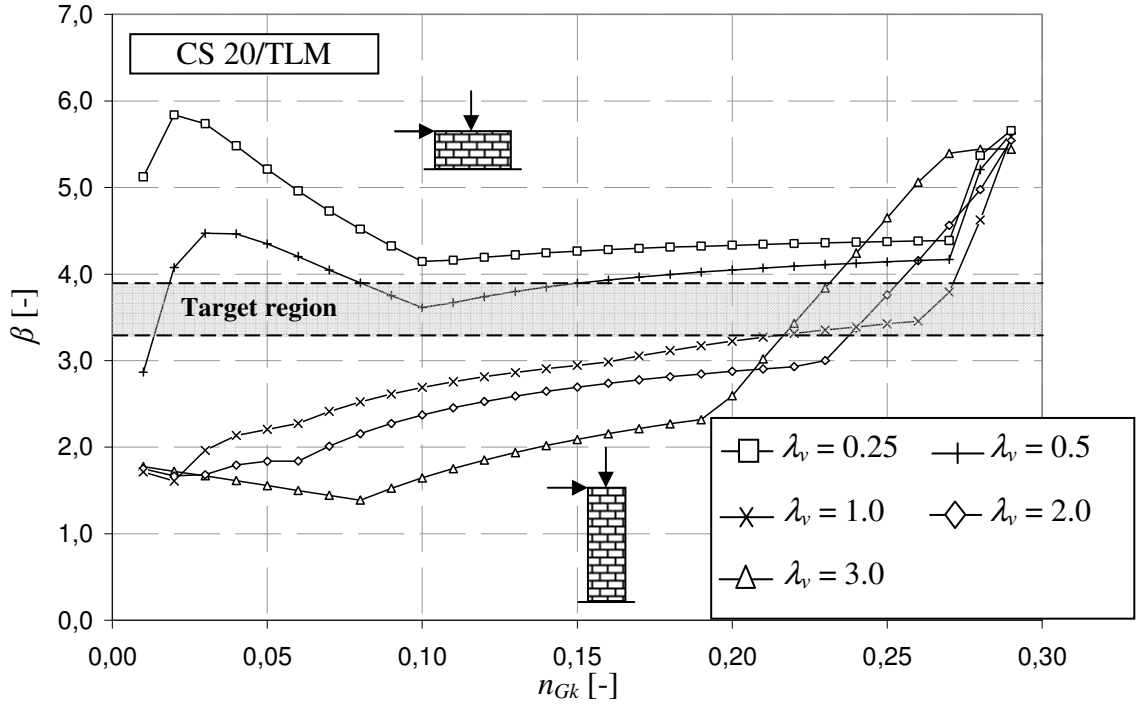

Figure 6-8 *Reliability index β vs. dead load n_{Gk} for different values of the shear slenderness λ_v for CS walls (designed according to DIN 1053-1)*

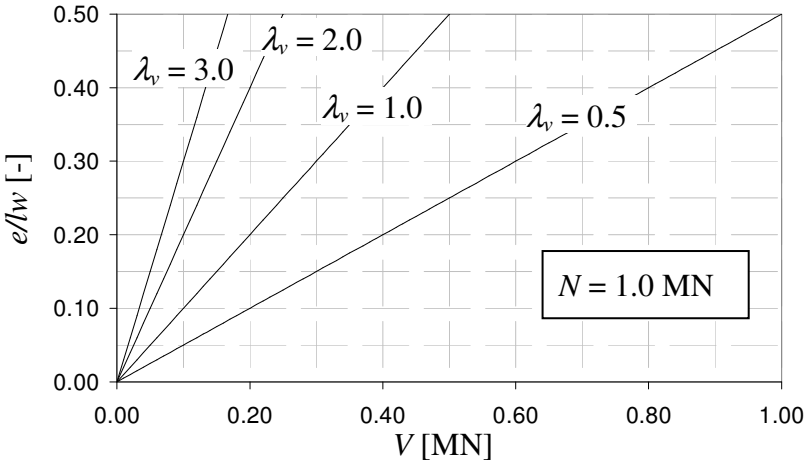

Figure 6-9 *Eccentricity e/l_w for different values of $\lambda_v = h_w/l_w$*

Figure 6-10 shows the reliability index β versus the eccentricity e/l_w for various CS walls with different values of the shear slenderness. It can be seen that for one value of the eccentricity the reliability can vary dependent on the slenderness ratio (other values of reliability for the same eccentricity). This occurs in case of slender walls when tip over of the entire wall governs. At an eccentricity of $e/l_w = 0.33$, several values of the reliability for $\lambda_v = 3.0$ can be obtained. The eccentricity for these values is equal, just the absolute amount of dead load is larger. Consequently, the reliability is different although eccentric-

ity and failure mode remain unchanged. Furthermore, it can be seen that there is a "preferred" range of eccentricity for every slenderness λ_v, indicated by the higher density of markers on every curve. In general, the "preferred" eccentricity is higher for slender walls.

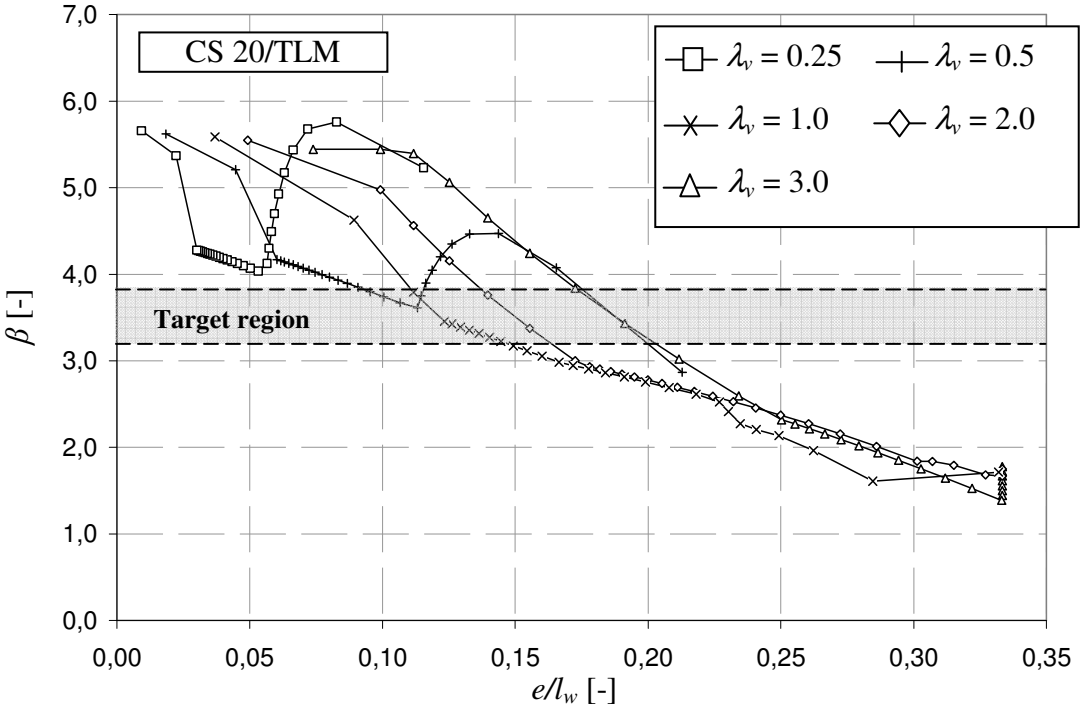

Figure 6-10 *Reliability index β vs. eccentricity ratio e/l_w for different values of the shear slenderness λ_v for CS walls (designed according to DIN 1053-1)*

In the case of the other unit materials, similar results are obtained. The distribution of the reliability versus the axial dead load for CB walls is similar to the CS walls (see Figure 6-11). However, the average level of reliability for the slender CB wall is $\beta \approx 2.1$ in the practical range. The reason for the more constant distribution is the relatively large tensile strength of the unit compared to the compressive strength: Diagonal tension does not govern in the reliability analysis; flexural failure (min and max) is governing.

The squat CB wall with $\lambda_v = 0.5$ provides a reliability above the target region for almost every axial load. The value stays almost constant at $\beta \approx 4.3$. The tendency for higher reliability in squat walls is also observed for CB walls as seen in Figure 6-13. However, the diagonal tension governs the design (and thus the tensile strength of the unit) for $\lambda_v = 1.0$ in the range of $n_{Gk} = 0.16$–0.24 and leads to the same reliabilities as for $\lambda_v = 0.5$ since the increase of the self-weight of the walls over the member height is neglected in the analysis.

The reliability versus the eccentricity is shown in Figure 6-14. The findings are similar to those for the CS walls.

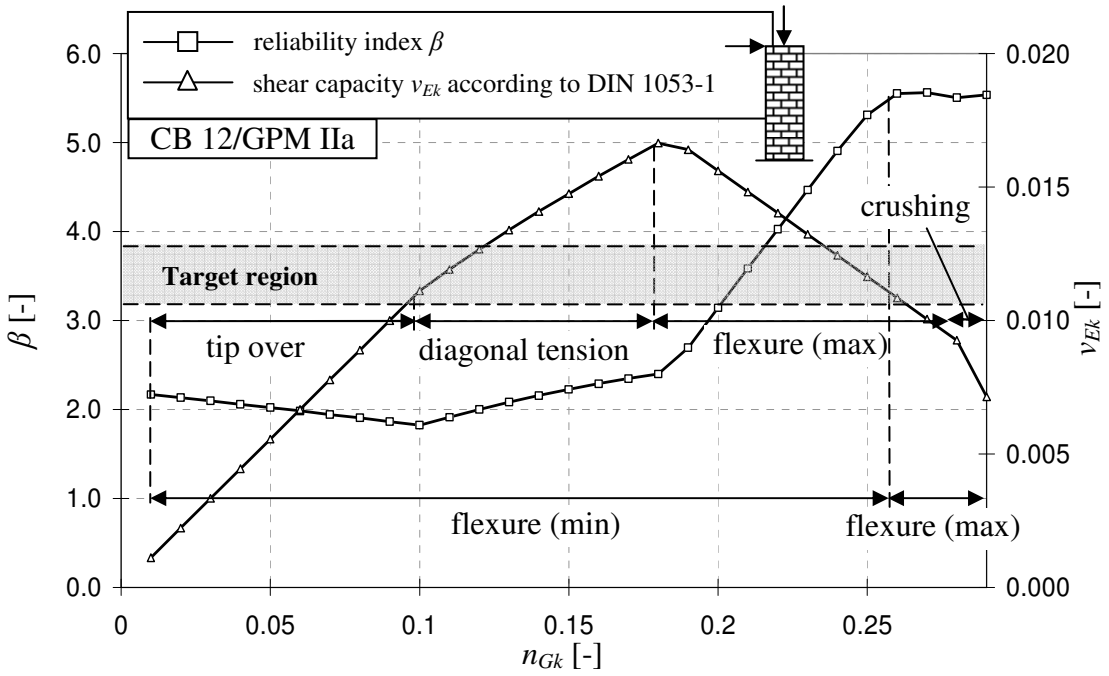

Figure 6-11 *Reliability index β and shear resistance v_{Ek} vs. axial dead load n_{Gk} for a CB wall with λ_v = 3.0 (designed according to DIN 1053-1)*

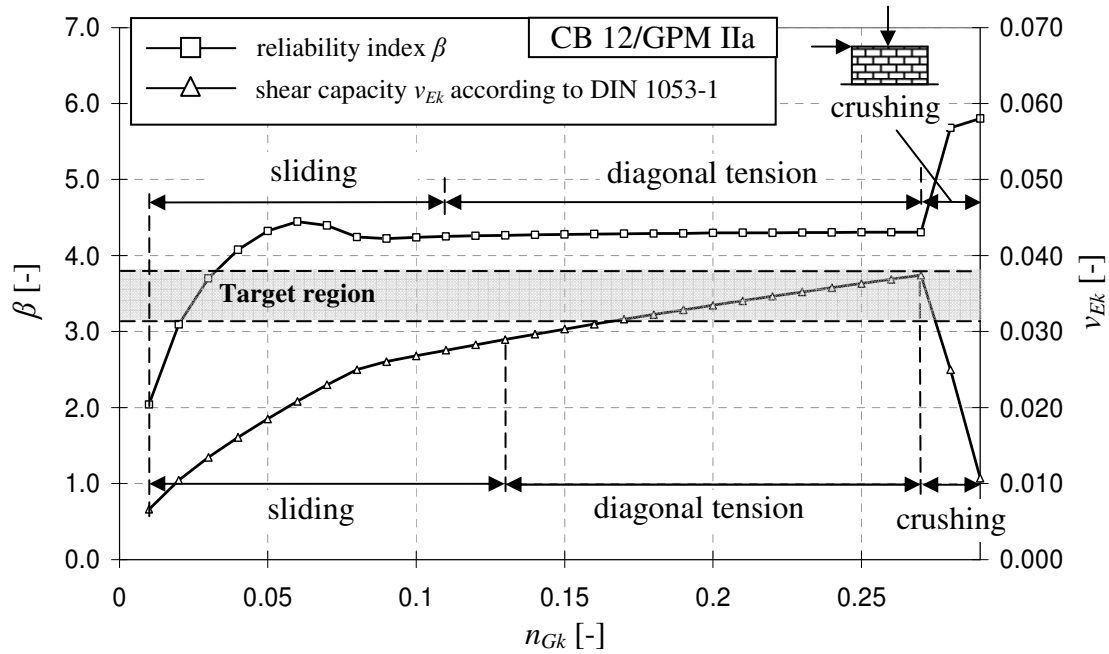

Figure 6-12 *Reliability index β and shear resistance v_{Ek} vs. axial dead load n_{Gk} for a CB wall with λ_v = 0.5 (designed according to DIN 1053-1)*

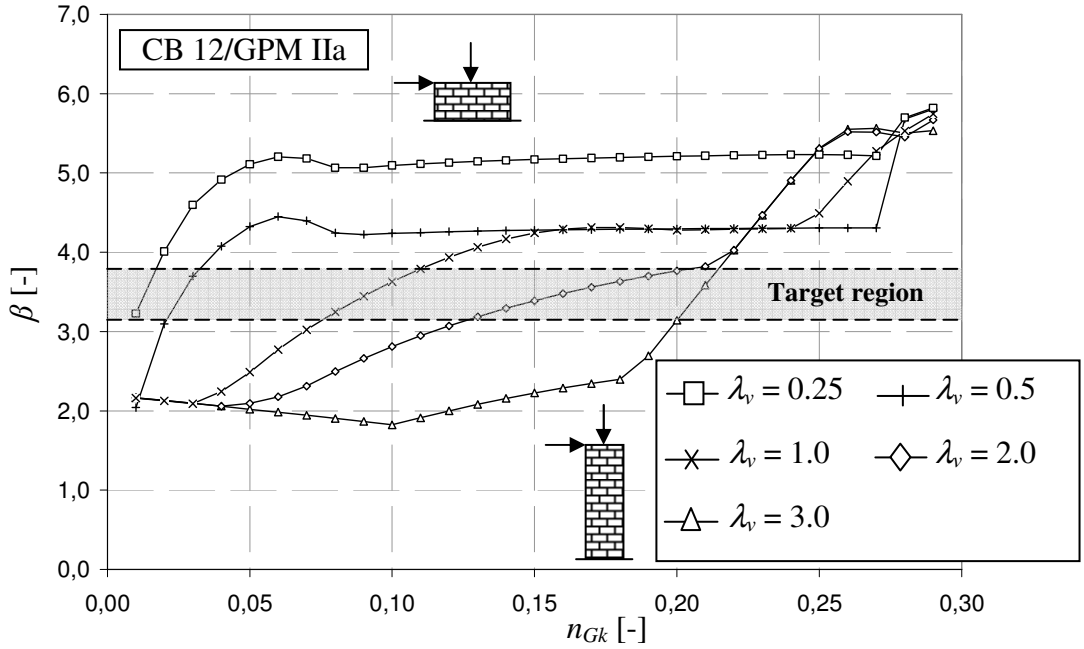

Figure 6-13 *Reliability index β vs. dead load n_{Gk} for different values of the shear slenderness λ_v for CB walls (designed according to DIN 1053-1)*

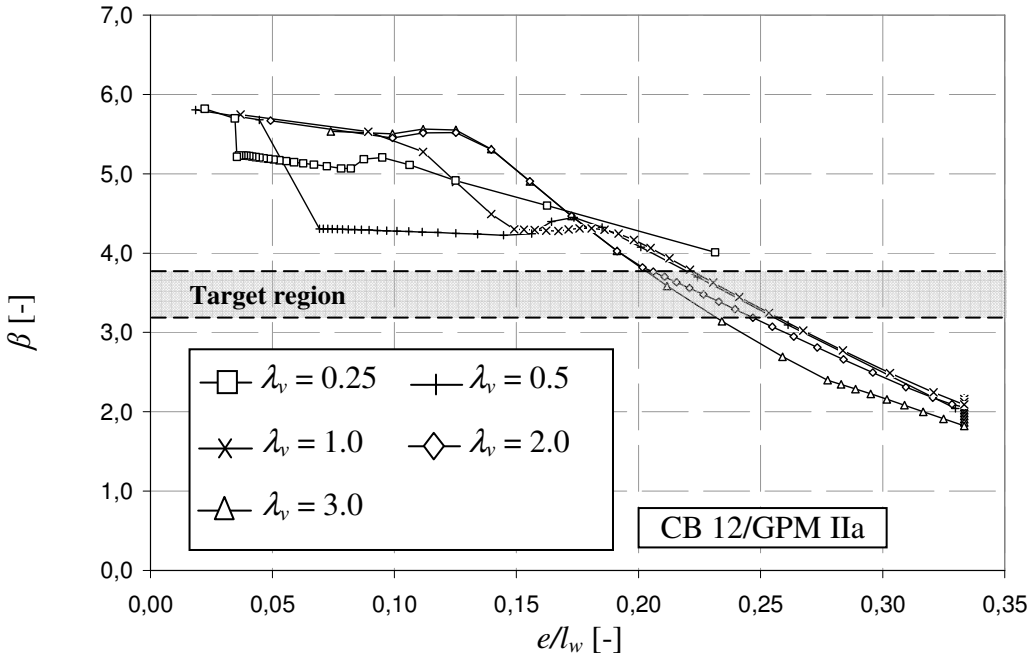

Figure 6-14 *Reliability index β vs. eccentricity ratio e/l_w for different values of the shear slenderness λ_v for CB walls (designed according to DIN 1053-1)*

The highest reliability of the three materials is obtained in case of AAC walls. Even slender walls reach reliabilities within the target region due to the underestimation of the tensile strength of the AAC unit in DIN 1053-1 (see Figure 6-15). Thus, the calculated capacities are significantly larger than the ones predicted by the code. The average value of β within the practical range is approximately 2.9.

For the squat AAC wall, the consequences of the conservative value of the tensile strength of the unit become even more evident (see Figure 6-16). The reliabilities rise to values over $\beta = 8.0$. The reliability within the practical range is even greater than for nearly concentric compression.

Figure 6-17 shows the reliability of AAC walls for different values of the shear slenderness λ_v. It can be seen that even slender walls with $\lambda_v = 2.0$ hit the target region and above for axial load over $n_{Gk} = 0.06$. The reliability of AAC walls designed according to DIN 1053-1 is observed to be significantly larger than the reliability of CB and CS walls. A comparison versus the eccentricity emphasizes this fact (see Figure 6-18).

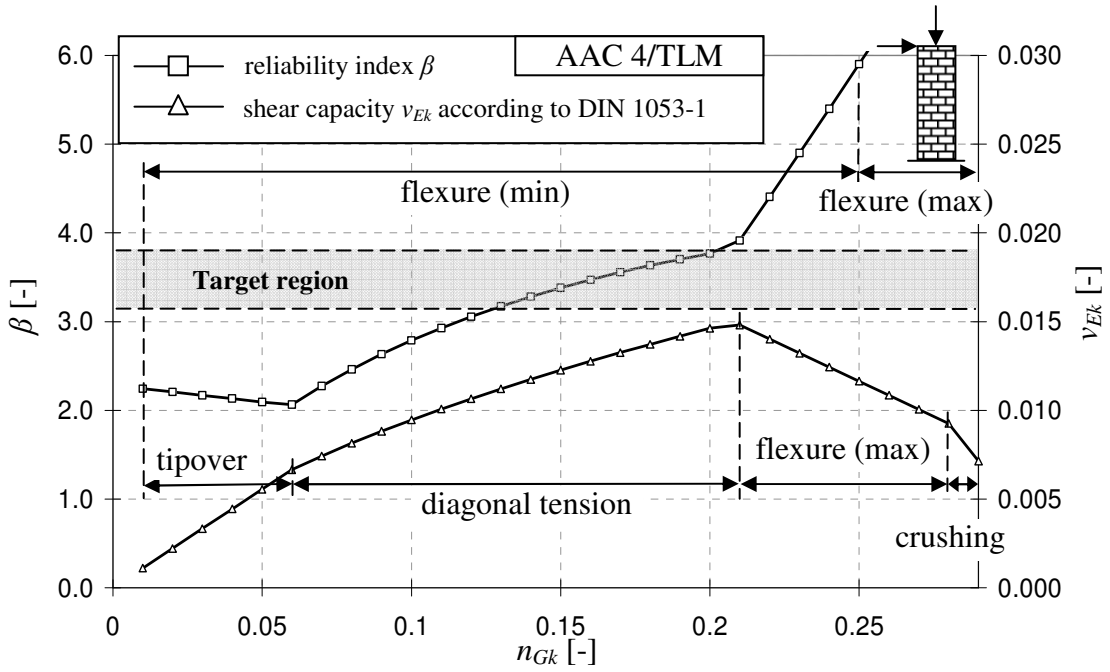

Figure 6-15 *Reliability index β and shear resistance v_{Ek} vs. axial dead load n_{Gk} for an AAC wall with $\lambda_v = 3.0$ (designed according to DIN 1053-1)*

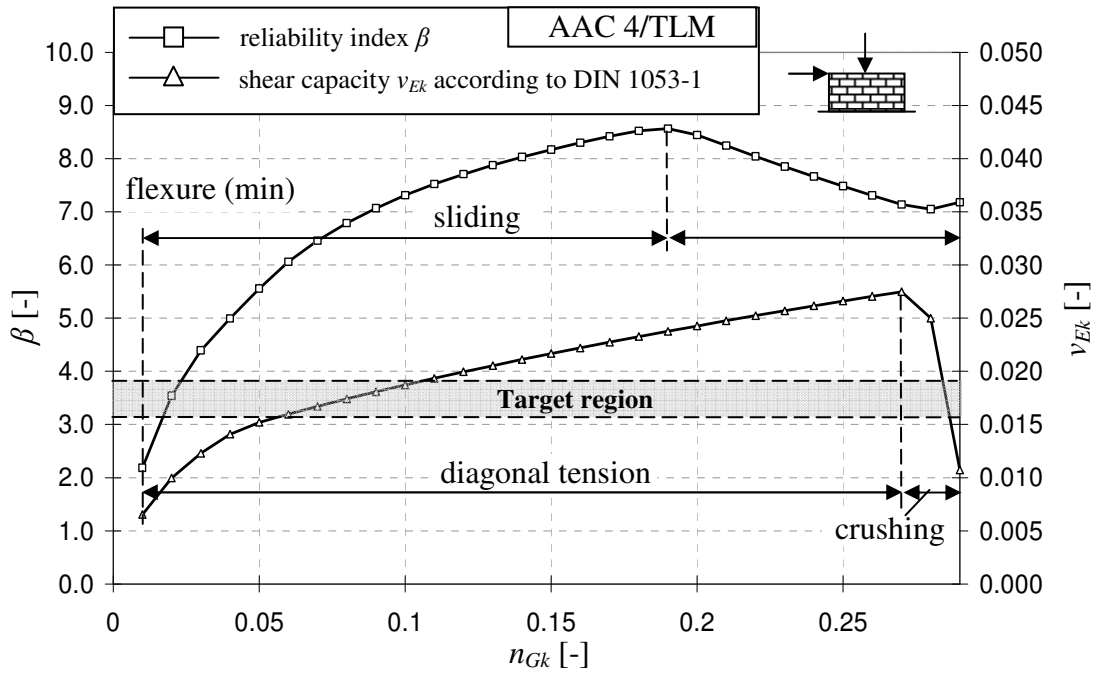

Figure 6-16 *Reliability index β and shear resistance v_{Ek} vs. axial dead load n_{Gk} for an AAC wall with λ_v = 0.5 (designed according to DIN 1053-1)*

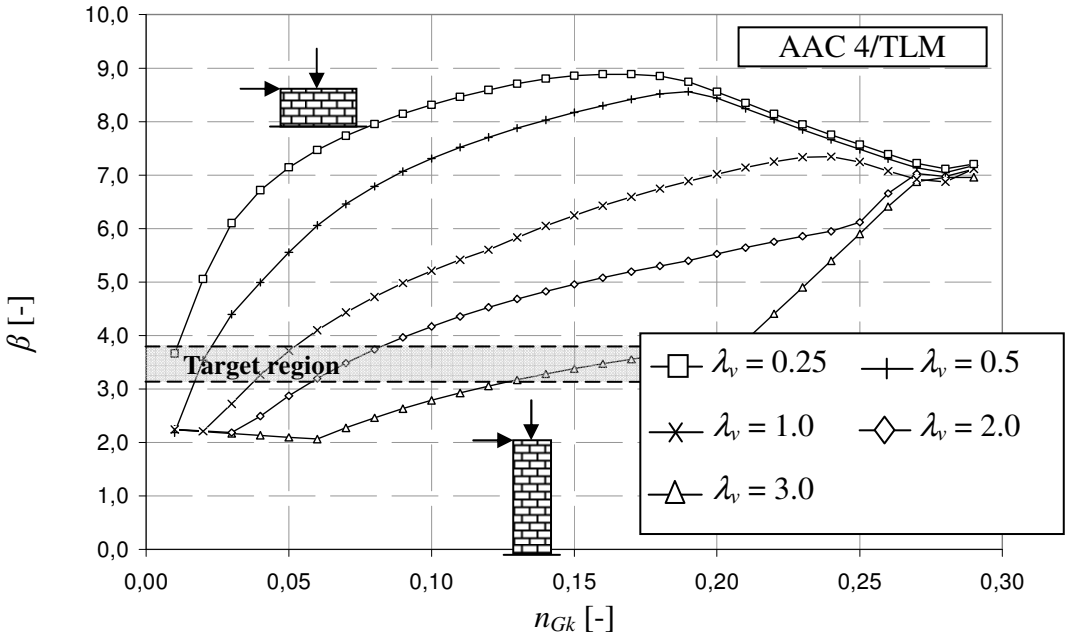

Figure 6-17 *Reliability index β vs. dead load n_{Gk} for different values of the shear slenderness λ_v for AAC walls (designed according to DIN 1053-1)*

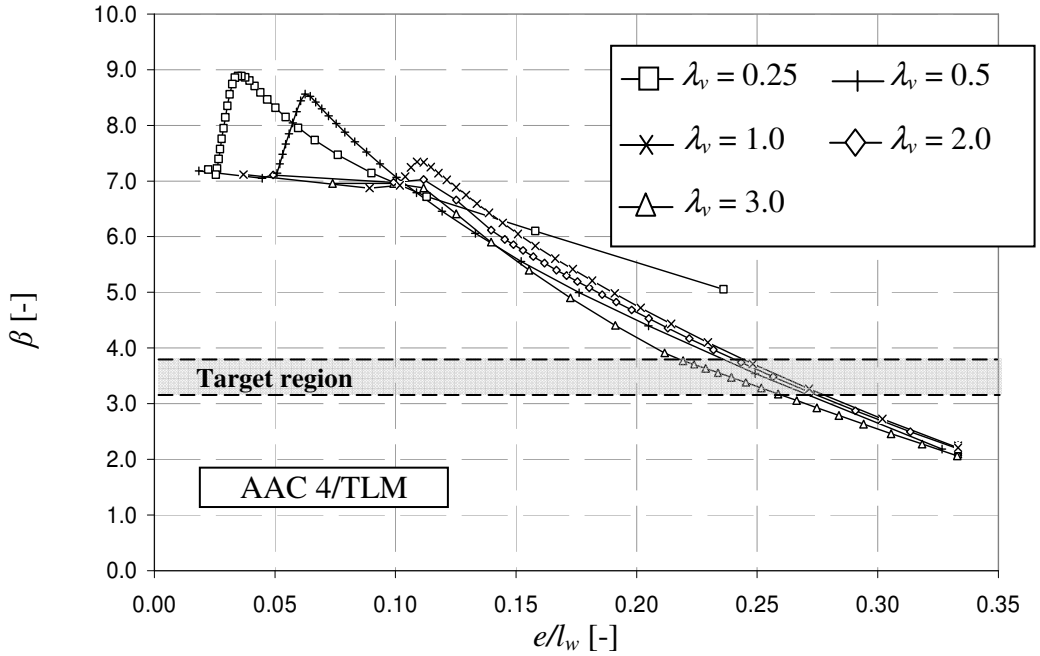

Figure 6-18 *Reliability index β vs. eccentricity ratio e/l_w for different values of the shear slenderness λ_v for AAC walls (designed according to DIN 1053-1)*

6.7.3 DIN 1053-100

With DIN 1053-100, the partial safety format was introduced into masonry design in Germany. This made it possible to apply the safety factors not only on the strength but also on the load and so the aforementioned shortcoming of DIN 1053-1 with regard to the length under compression was overcome. Thus, the reliability of walls designed according to DIN1053-100 is expected to be significantly larger than for walls designed according to DIN 1053-1.

In Figure 6-19, the reliability index β and the shear capacity v_{Ek} for a slender CS wall ($\lambda_v = 3.0$) are plotted versus the axial dead load n_{Gk} and the predicted failure modes are indicated, similarly to the figures presented in the previous section. It can be seen that failure due to flexure limits the reliability for small levels of axial load. In contrast to DIN 1053-1, failure by tip over of the entire wall cannot govern because of the corresponding common load combination stipulated by the code (see section 5.3.2). Note that small values of nGk represent large values of the eccentricity and large values correspeond to members subjected more concentric compression. Consequently, the eccentricity is not limited for small levels of axial load as was the case for DIN 1053-1 (see Figure 6-4). For even larger values of the shear slenderness λ_v, only flexural failure is predicted in the probabilistic analysis and according to the code. Thus, only the eccentricity influences the reliability and for equal values of eccentricity, equal reliabilities are obtained. In the case of CS, flexural failure governs for every value of axial load when the shear slen-

derness is above $\lambda_v \approx 4.0$ with an average minimum reliability within the practical range of about $\beta = 2.7$.

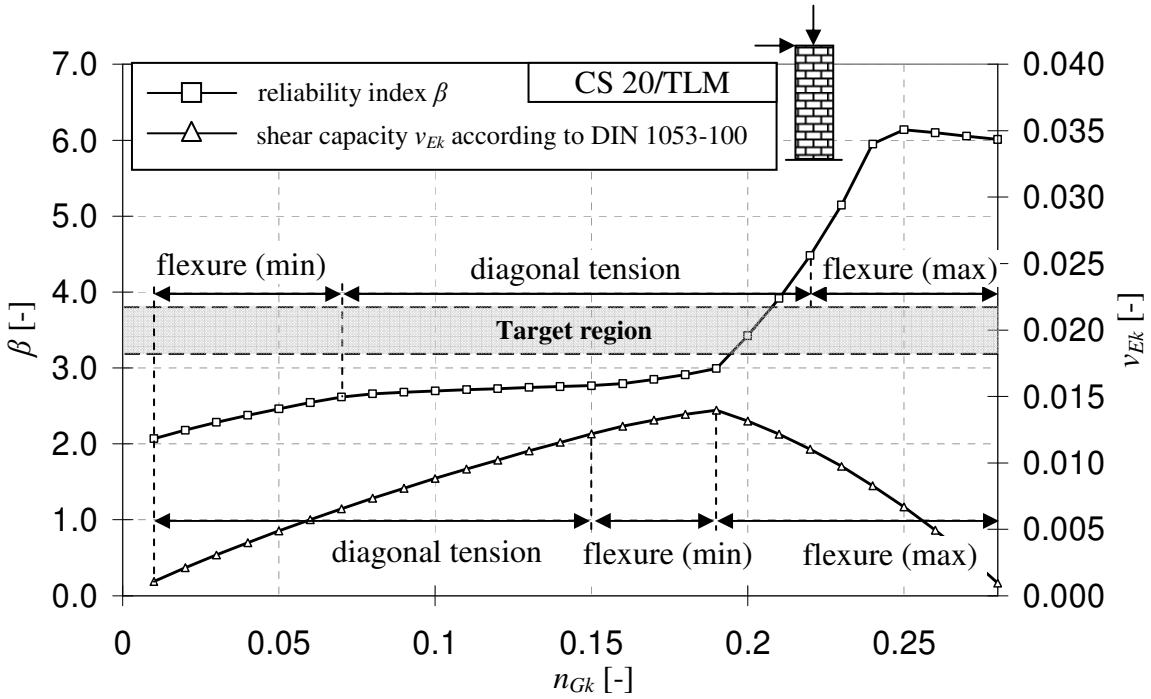

Figure 6-19 *Reliability index β and shear resistance v_{Ek} vs. axial dead load n_{Gk} for a CS wall with $\lambda_v = 3.0$ (designed according to DIN 1053-100)*

The reliability index β and the eccentricity e/l_w are compared in Figure 6-20. The findings of the previous section (large eccentricity means small reliability) are verified. The sharp increase in reliability occurs at the same point as the sharp drop in eccentricity.

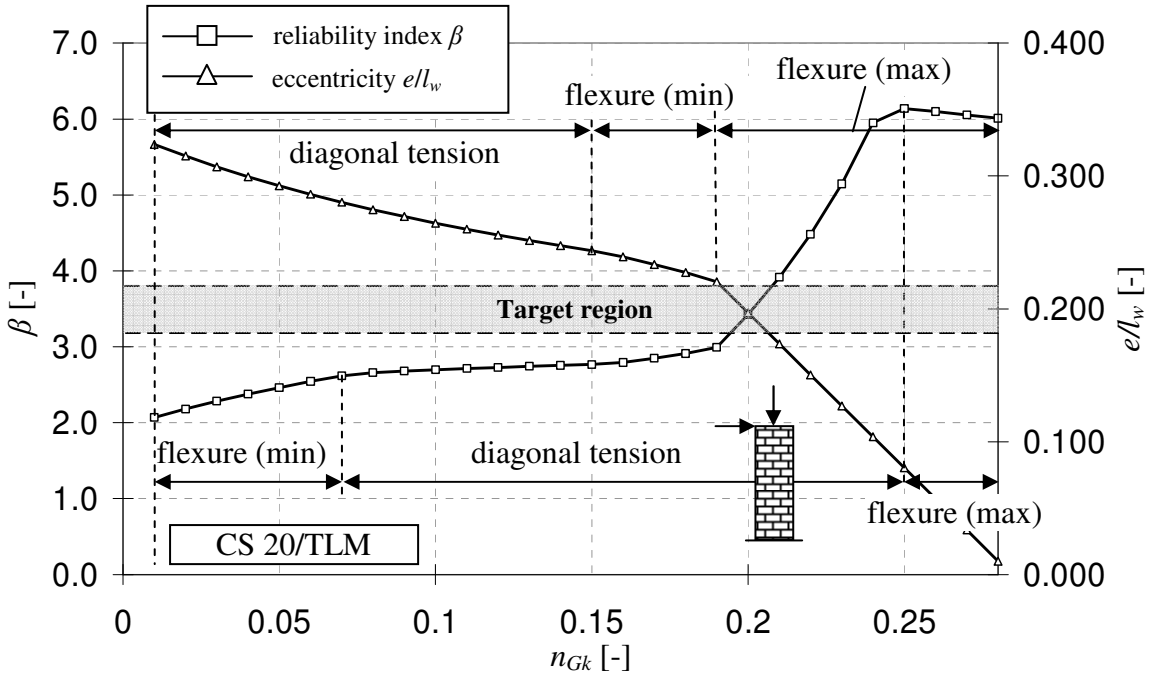

Figure 6-20 *Reliability index β and eccentricity e/l_w vs. axial dead load n_{Gk} for a CS wall with $\lambda_v = 3.0$ (designed according to DIN 1053-100)*

Note that the reliability analysis was carried out for fully utilized masonry walls. In practice, walls may not be utilized to the full capacity. However, in case of slender shear walls, higher degrees of utilization are likely. It should also be noted that the flexural tensile strength has been neglected. For large eccentricities and flexural failure, *Glowienka (2007)* observed a sudden rise in the reliability due to flexural tensile strength. He investigated walls subjected to out-of-plane flexure, i.e. walls that are only subjected to wind load from one direction. Masonry shear walls are subjected to wind load from two directions which may result in a complete loss of flexural tensile strength over the wall length. The DIN codes stipulate a limitation on the strain in the bottom course to prevent this, however, the strain limit is a fixed value that cannot be verified. For this reason, flexural tensile strength is neglected here.

Table 6.7-2 shows a selection of sensitivity values for the slender CS wall. It can be seen that the model uncertainties are the relevant basic variables for minimum axial load ($n_{Gk} = 0.01$). For higher axial load, the model uncertainty has less influence; the corresponding failure modes are governed by the compressive strength of the masonry. The wind load v_E has some influence but only for minimum axial load. As explained previously, the reason for the lack of influence is the eccentricity; in case of maximum load the cross-section remains under compression and thus the result is not sensitive to the horizontal load. In this case, the axial load is the most important load and thus the live load becomes more influential due to the large scatter.

Table 6.7-2 Select sensitivity values for a CS wall with $\lambda_v = 3.0$

n_{Gk}	e/l_w	FM[a]	β	$\alpha_{\Theta s}$	$\alpha_{\Theta dt}$	$\alpha_{\Theta c}$	$\alpha_{\Theta f}$	$\alpha_{\Theta E}$	α_{nG}	α_{nQ}	α_{vE}	α_{fm}	α_{ft}	α_{fv0}	α_{μ}
0.01	0.32	F	1.94	-	-	-	0.84	-0.00	0.33	-	-0.44	0.01	-	-	-
0.10	0.26	DT	2.51	-	0.88	-	-	-0.03	0.23	-	-0.37	-	0.16	-	-
0.18	0.23	DT	2.83	-	0.87	-	-	-0.04	0.21	-	-0.37	-	0.23	-	-
0.19	0.22	DT	2.93	-	0.87	-	-	-0.05	0.21	-	-0.37	-	0.23	-	-
0.20	0.20	DT	3.39	-	0.87	-	-	-0.05	0.21	-	-0.38	-	0.24	-	-
0.28	0.01	F	5.90	-	-	-	0.01	-0.20	-0.13	-0.54	-0.01	0.81	-	-	-

[a]FM=Failure Mode (S = sliding; DT = diagonal tension; C = crushing; F = flexure)

In case of squat walls, the distribution of the reliability basically stays the same. Figure 6-21 shows the reliability index β and the shear capacity v_{Ek} for a squat CS wall with $\lambda_v = 0.5$. Note the different failure modes than in the case of the slender wall. In the practical range of axial load, the reliability index does not fall below $\beta = 3.0$, and even reaches values of up to $\beta = 4.0$, thus hitting the target values recommended by *JCSS (2001)* and *DIN EN 1990*. At the point where maximum axial load governs the design, the reliability increases suddenly to a large value of about $\beta \approx 6.0$. This is almost the same value as in the case of the slender wall. The reason for this is that the capacity is independent of the slenderness when the cross-section is completely subjected to compression, i.e. the sensitivity to the eccentricity is small.

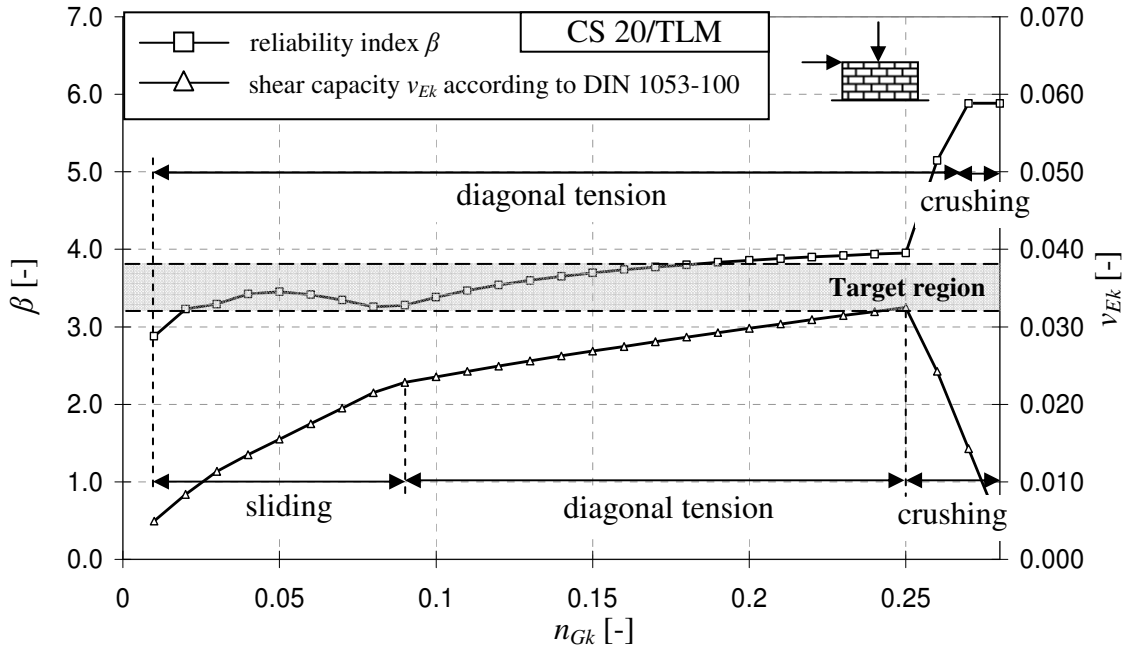

Figure 6-21 Reliability index β and shear resistance v_{Ek} vs. axial dead load n_{Gk} for a CS wall with $\lambda_v = 0.5$ (designed according to DIN 1053-100)

The sensitivity values in Table 6.7-3 show similar influences as for the slender wall. As long as the axial load is acting favourably, the model uncertainties are the largest influences. In case of crushing, the sensitivity to the model uncertainty decreases significantly as was the case for the flexural failure in the slender wall. In that case, the major influ-

ences are the axial live load and the compressive strength. Figure 6-22 presents the reliability index β versus the axial dead load n_{Gk} for different values of the shear slenderness λ_v.

Table 6.7-3 Select sensitivity values for a CS wall with $\lambda_v = 0.5$

n_{Gk}	e/l_w	FM[a]	β	$\alpha_{\Theta s}$	$\alpha_{\Theta dt}$	$\alpha_{\Theta c}$	$\alpha_{\Theta f}$	$\alpha_{\Theta l}$	α_{nG}	α_{nQ}	α_{vE}	α_{fm}	α_{ft}	α_{fv0}	α_{μ}
0.01	0.25	S	2.88	0.88	-	-	-	-0.02	0.25	-	-0.38	-	-	0.11	0.01
0.05	0.16	S	3.45	0.86	-	-	-	-0.03	0-23	-	-0.39			0.21	0.09
0.10	0.12	DT	3.38	-	0.80	-	-	-0.09	0.13	-	-0.34	-	0.47	-	-
0.24	0.07	DT	3.94	-	0.78	-	-	-0.09	0.12	-	-0.35	-	0.49	-	-
0.28	0.01	C	5.88	-	-	0.01	-	-0.20	-0.13	-0.54	-0.01	0.81	-	-	-
[a]FM=Failure Mode (S = sliding; DT = diagonal tension; C = crushing)															

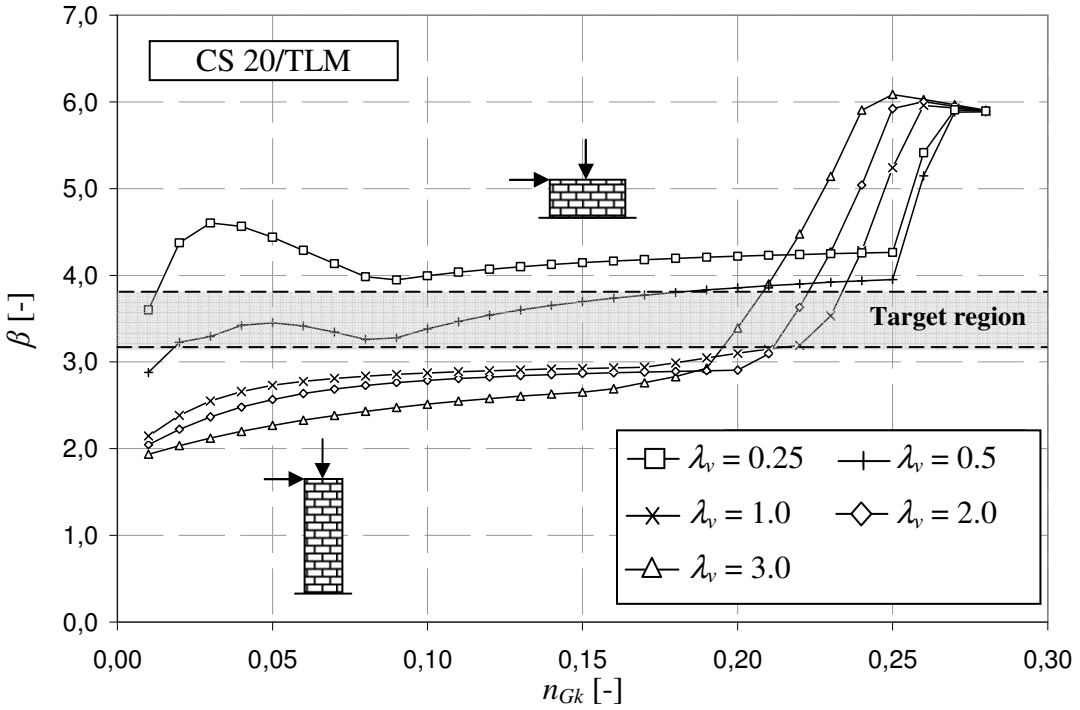

Figure 6-22 Reliability index β vs. dead load n_{Gk} for different values of the shear slenderness λ_v for CS walls (designed according to DIN 1053-100)

Generally, it can be stated that the reliability strongly depends on the shear slenderness. While squat walls easily reach the recommended reliability values of DIN EN 1990, the reliability of slender walls is likely to fall short. In the practical range, the reliability comes close to $\beta = 3.0$ for common walls ($\lambda_v \leq 2.0$). However, reliability can be increased significantly by choosing the right dimensions, i.e. increasing the length l_w of the wall.

Figure 6-23 shows the reliability index β of CS walls for different shear slenderness λ_v versus the eccentricity e/l_w. It can be seen that the eccentricity for slender walls reaches higher values than the eccentricity of squat walls. This is logical; slender walls likely fail in flexure, which occurs when the maximum eccentricity is reached due to the standardized design and the full utilization of the cross section. Squat walls fail in shear, where

large eccentricities do not occur. However, small eccentricities lead to larger reliability which agrees with the previous findings.

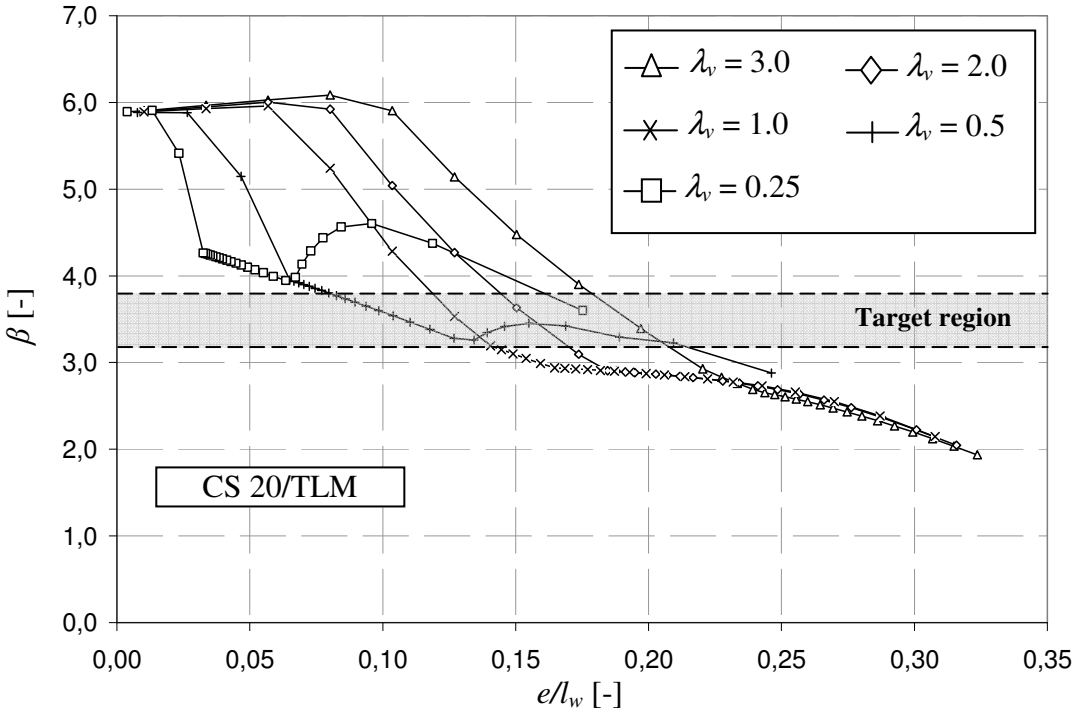

Figure 6-23 *Reliability index β vs. eccentricity ratio e/l_w for different values of the shear slenderness λ_v for CS walls (designed according to DIN 1053-100)*

In case of the other unit materials, the results are the same. Similarly to Figure 6-19, Figure 6-24 shows the reliability index β and the shear capacity v_{Ek} according to DIN 1053-100 for a slender CB wall. It can be see that the distribution is very similar to the CS wall. The average level of reliability is slightly higher and ranges from $\beta \approx 2.3$ to 3.5. The average value within the practical range is $\beta = 3.0$.

In Figure 6-25, different values of the shear slenderness are compared. It is observed that CB walls almost reach the target values of the reliability in every case. Only very slender walls fall short. The reason for this is the relatively large tensile strength of the unit assumed in the probabilistic analysis. This leads to greater capacities for diagonal tension compared to CS walls. Due to the favourable model uncertainty Θ_f in case of CB, the reliabilities obtained for CB walls are higher than for CS.

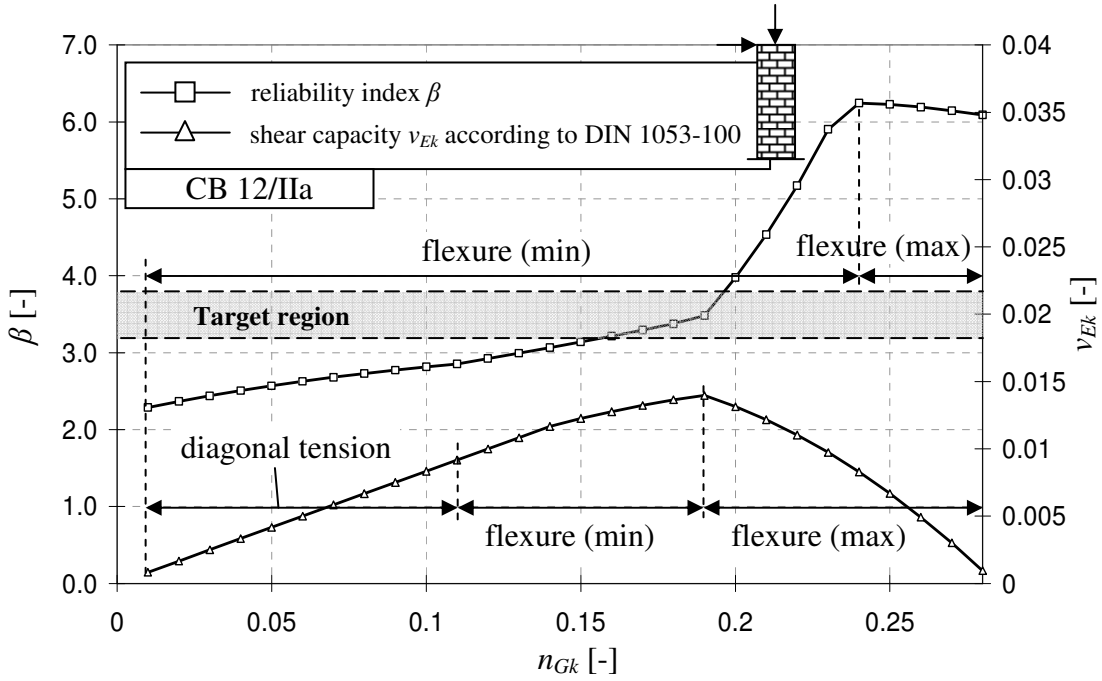

Figure 6-24 *Reliability index β and shear resistance v_{Ek} vs. axial dead load n_{Gk} for a CB wall with λ_v = 3.0 (designed according to DIN 1053-100)*

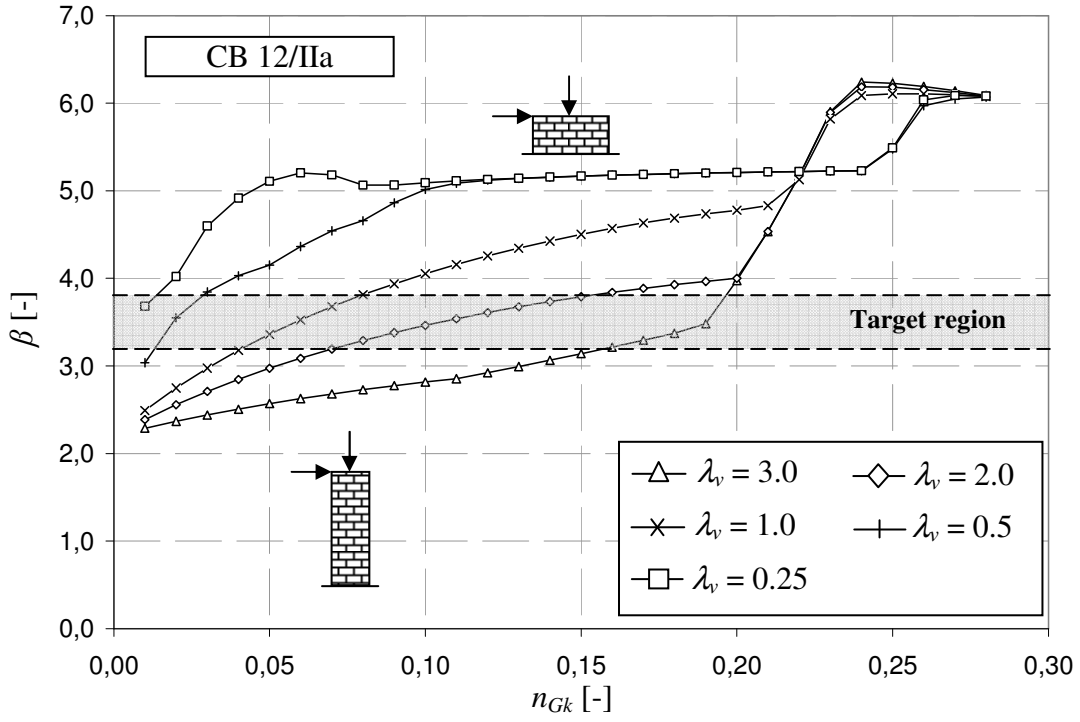

Figure 6-25 *Reliability index β vs. dead load n_{Gk} for different values of the shear slenderness λ_v for CB walls (designed according to DIN 1053-100)*

By plotting the reliability versus the eccentricity, the relevant range of the eccentricity again becomes obvious because of the concentration of values, as can be seen in Figure 6-26 (note the locations where the markers are close together).

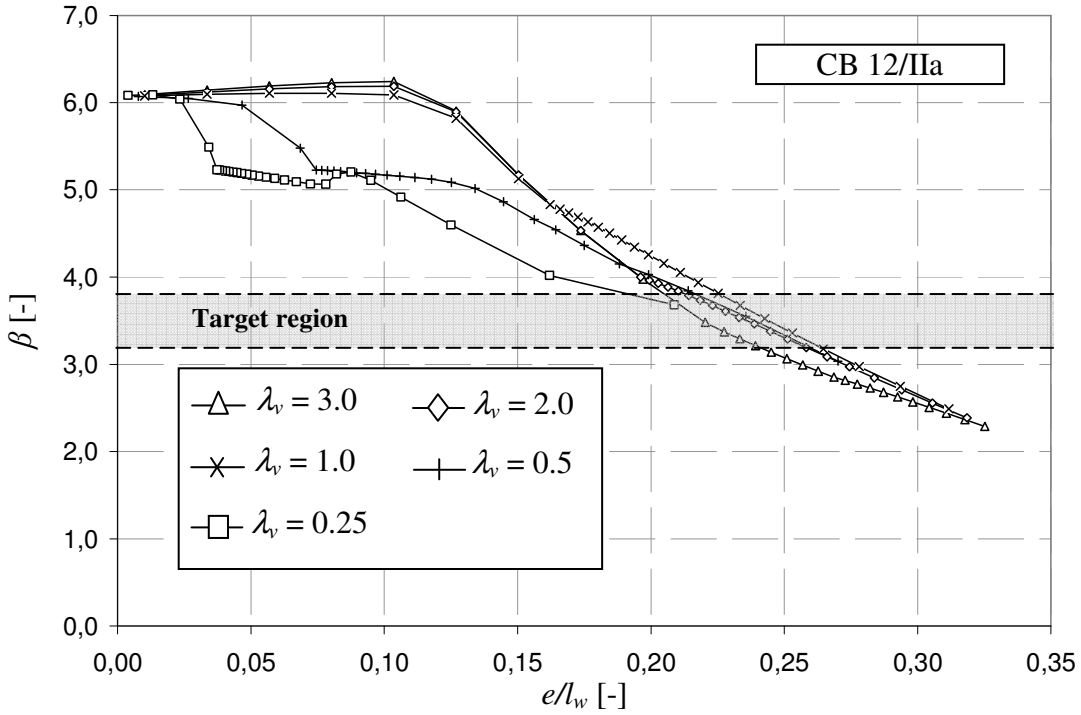

Figure 6-26 *Reliability index β vs. eccentricity ratio e/l_w for different values of the shear slenderness λ_v for CB walls (designed according to DIN 1053-100)*

In the case of AAC walls, the reliability of slender walls is almost equal to the other materials (see Figure 6-27). The sudden rise in reliability is observed again. The maximum value of reliability of $\beta = 7.5$ is higher than for CS and CB because of the smaller scatter and larger mean of the masonry compressive strength. As in the case of the other materials, the reliability is generally higher than that according to DIN 1053-1. The average reliability is $\beta = 3.7$.

With decreasing shear slenderness λ_v, diagonal tension governs the design according to the code, as shown in Figure 6-28. This leads to strongly increasing reliability due to the underestimated tensile strength in DIN 1053-100 (see section 4.5.5). The underestimation leads to very small capacities v_{Ek} according to the code when diagonal tension failure is expected. In the probabilistic analysis, sliding shear governs and results in large reliabilities because the small values of v_{Ek}, derived according to the code for diagonal tension, do not lead to high utilization of the wall. Figure 6-29 shows the reliability of differently slender walls over the eccentricity e/l_w.

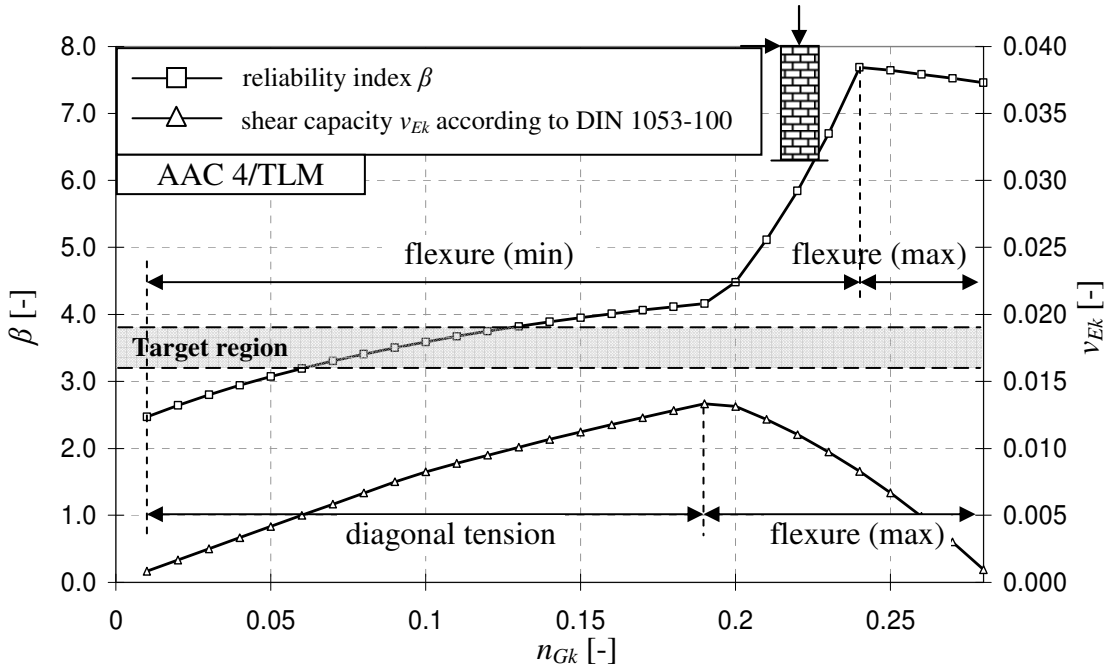

Figure 6-27 *Reliability index β and shear resistance v_R vs. axial dead load n_{Gk} for a AAC wall with λ_v = 3.0 (designed according to DIN 1053-100)*

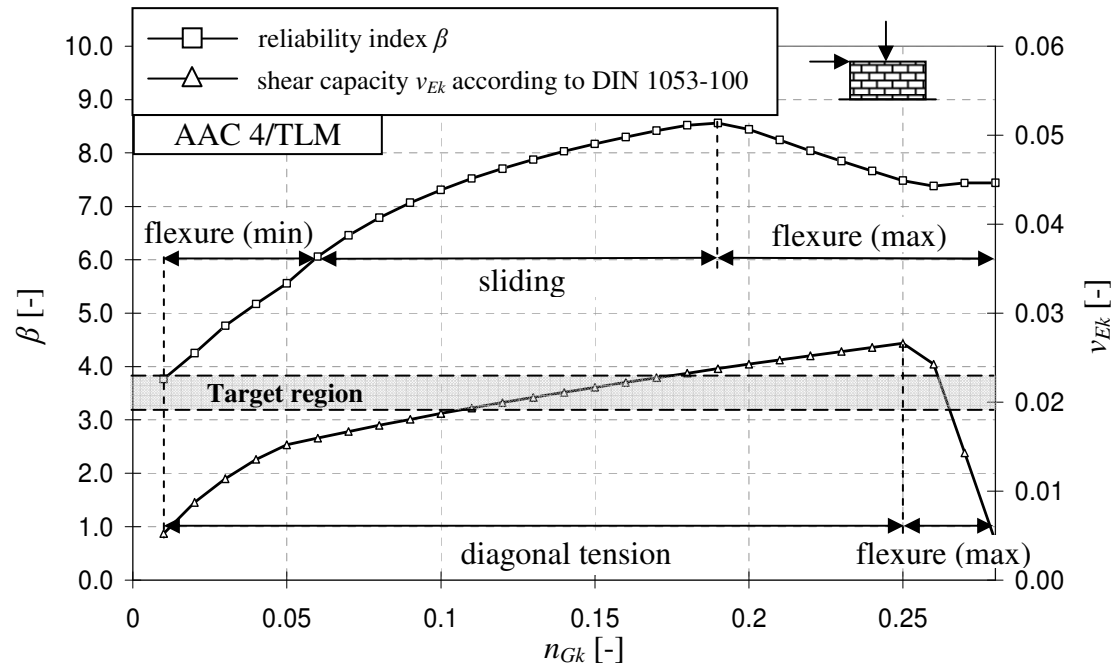

Figure 6-28 *Reliability index β and shear resistance v_R vs. axial dead load n_{Gk} for a AAC wall with λ_v = 0.5 (designed according to DIN 1053-100)*

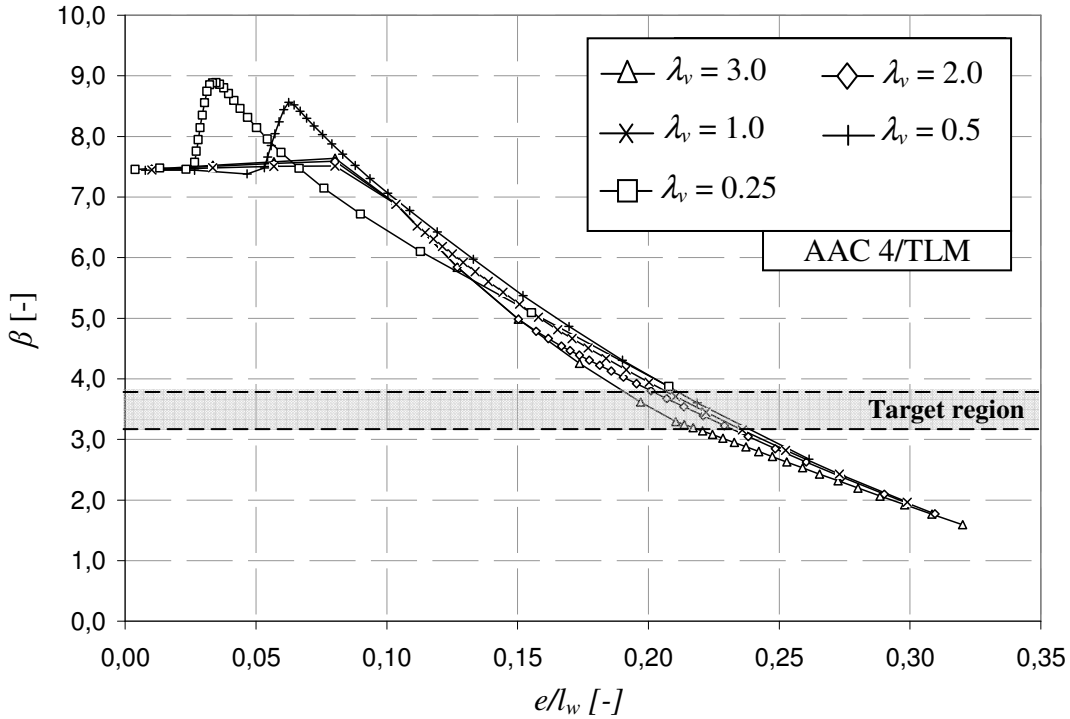

Figure 6-29 *Reliability index β vs. eccentricity ratio e/l_w for different values of the shear slenderness λ_v for AAC walls (designed according to DIN 1053-100)*

6.7.4 DIN EN 1996-1-1 and National Annex

DIN EN 1996-1-1/NA is also based on the partial safety factor concept. The main differences in comparison to DIN 1053-100 with regard to the the shear capacity are the larger values for the cohesion, the different design equation for diagonal tension failure and the consideration of the overlap u/h_b in the design equation for crushing (see section 5.5.3). All these differences affect the shear failure of squat walls.

The reliability of a slender CS wall is presented in Figure 6-30. Although the check against flexural failure is identical to DIN 1053-100, the distribution of reliability is not identical to DIN 1053-100 (see Figure 6-19). The reason for this is the difference in the code design equations for diagonal tension failure: DIN 1053-100 predicts diagonal tension failure while DIN EN 1996-1-1/NA predicts flexural failure with slightly larger capacities. This leads to slightly lower reliabilities in the case of low axial load. It can be seen that the reliability does not reach the target region. The average reliability over the practical range is $\beta \approx 2.5$.

In case of squat walls (Figure 6-31), the difference in the design equations of DIN 1053-100 and DIN EN 1996-1-1/NA has an even more pronounced effect. The capacities are smaller for CS as shown in section 5.5.4 (see Figure 5-16). Consequently, the reliabilities obtained are higher than the reliabilities according to DIN 1053-100 and the reliability is significantly higher than the target value of DIN EN 1990/NA within the entire practical range.

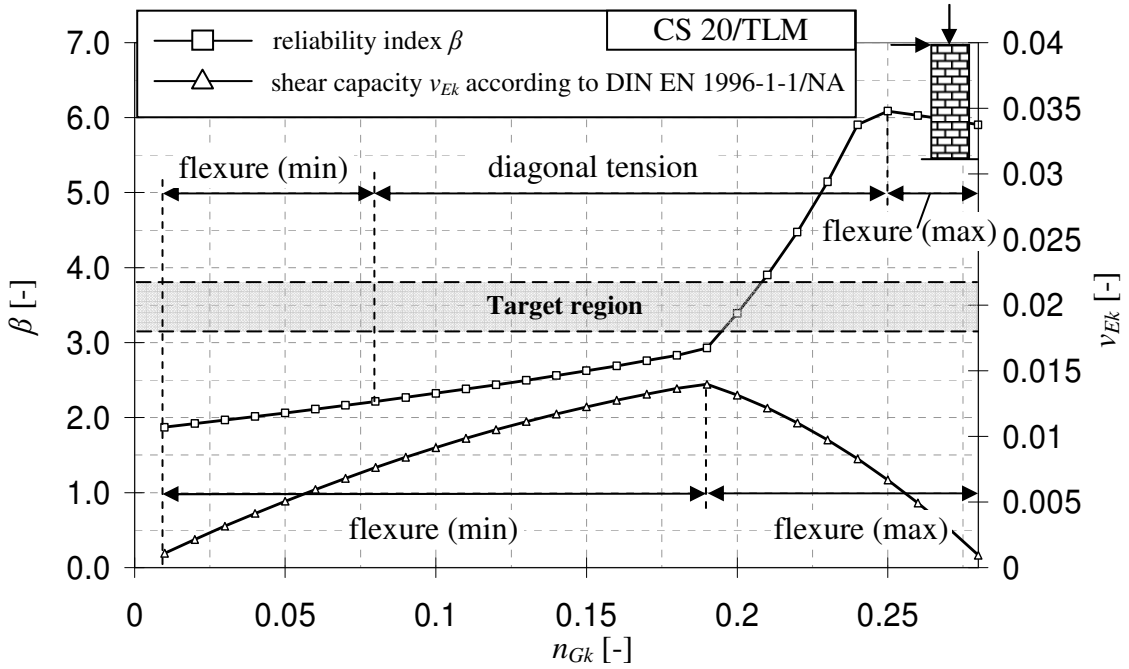

Figure 6-30 *Reliability index β and shear resistance v_{Ek} vs. axial dead load n_{Gk} for a CS wall with λ_v = 3.0 (designed according to DIN EN 1996-1-1/NA)*

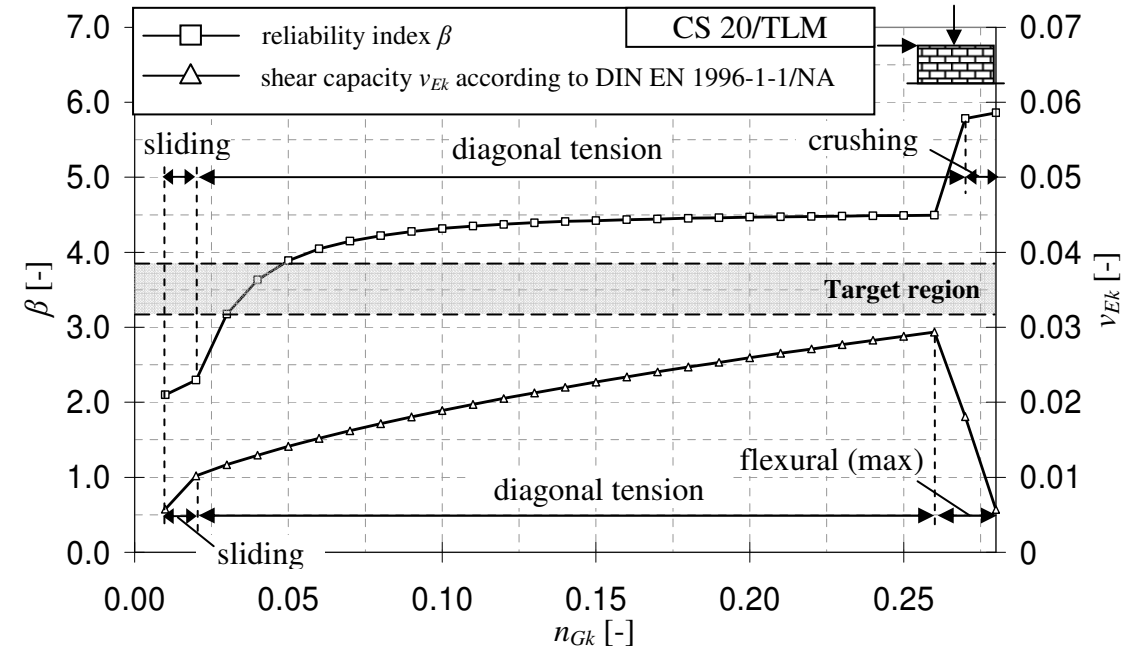

Figure 6-31 *Reliability index β and shear resistance v_R vs. axial dead load n_{Gk} for a CS wall with λ_v = 0.5 (designed according to DIN EN 1996-1-1/NA)*

Figure 6-32 shows the distribution of reliability for different values of λ_v for CS walls. It can be seen that the target reliability is reached for λ_v = 1.0 but the reliability stays below the target for low axial load and larger values of λ_v.

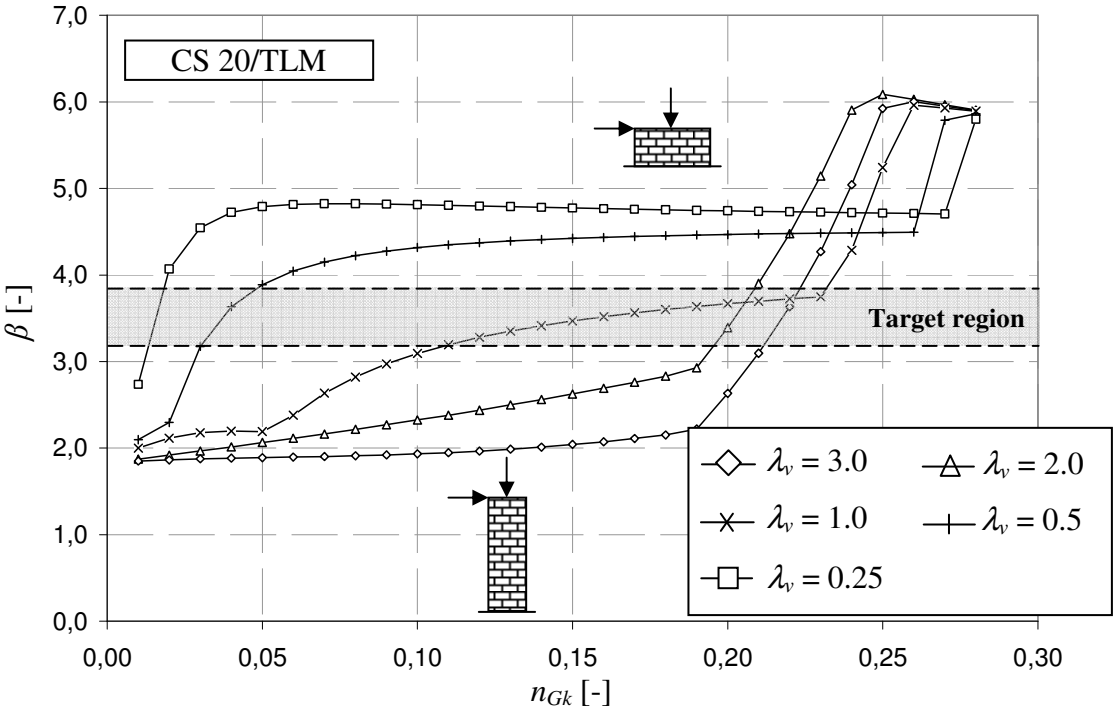

Figure 6-32 *Reliability index β vs. dead load n_{Gk} for different values of the shear slenderness λ_v for CS walls (designed according to DIN EN 1996-1-1/NA)*

The distribution of the reliability for CB walls is similar. The walls, however, provide slightly higher reliability. For slender walls, the average reliability within the practical range is $\beta \approx 2.8$ (see Figure 6-33). Squat CB walls have much higher reliability because of the respectively small capacity due to diagonal tension in the code design (see Figure 6-34).

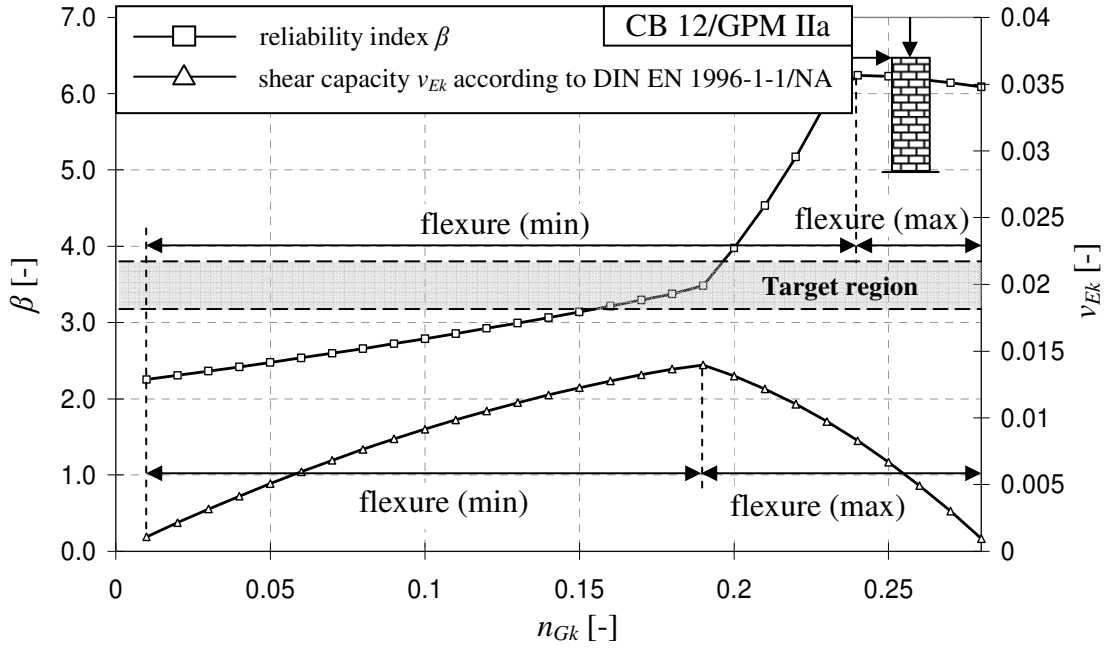

Figure 6-33 *Reliability index β and shear resistance v_{Ek} vs. axial dead load n_{Gk} for a CB wall with λ_v = 3.0 (designed according to DIN EN 1996-1-1/NA)*

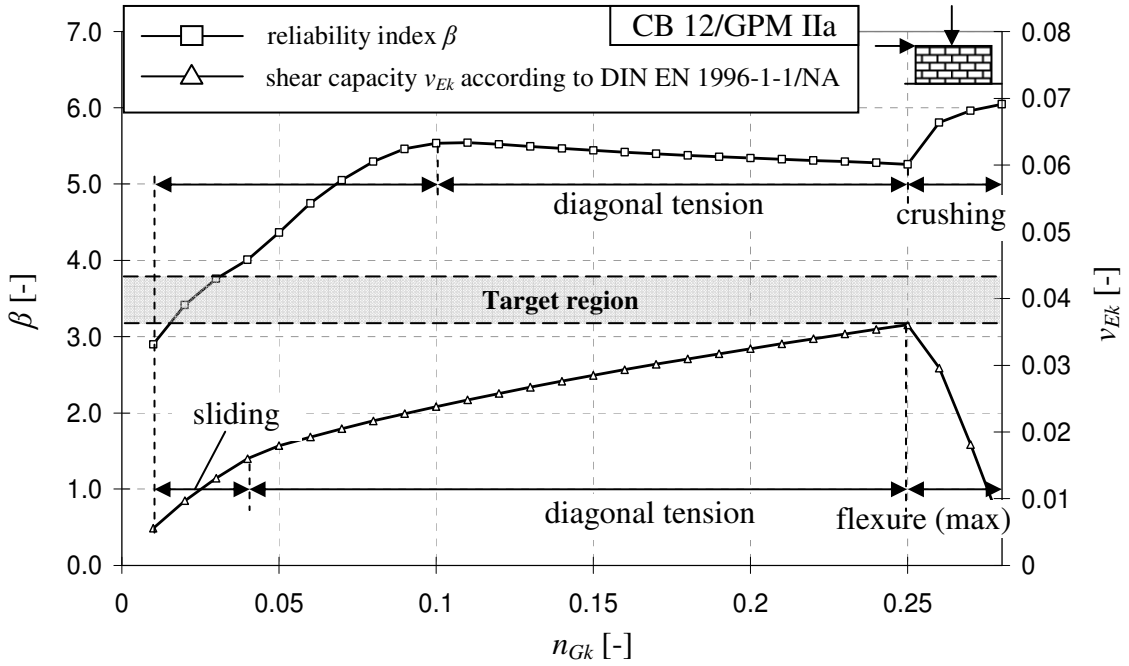

Figure 6-34 *Reliability index β and shear resistance v_{Ek} vs. axial dead load n_{Gk} for a CB wall with $\lambda_v = 0.5$ (designed according to DIN EN 1996-1-1/NA)*

The reliability of slender AAC (see Figure 6-35) walls is slightly higher than the reliability of slender CB walls. The difference is only significant for large axial load because of the different scatter of the compressive strength. The average reliability index over the practical range is $\beta \approx 3.3$. For average squat AAC walls (see Figure 6-36), the reliability falls short for low axial load but increases significantly with increasing n_{Gk}. The reliabilities for low axial load are even smaller than in the case of CB and CS due to the larger sliding shear capacity. In case of CB and AAC, the plots of reliability versus eccentricity only confirm earlier findings.

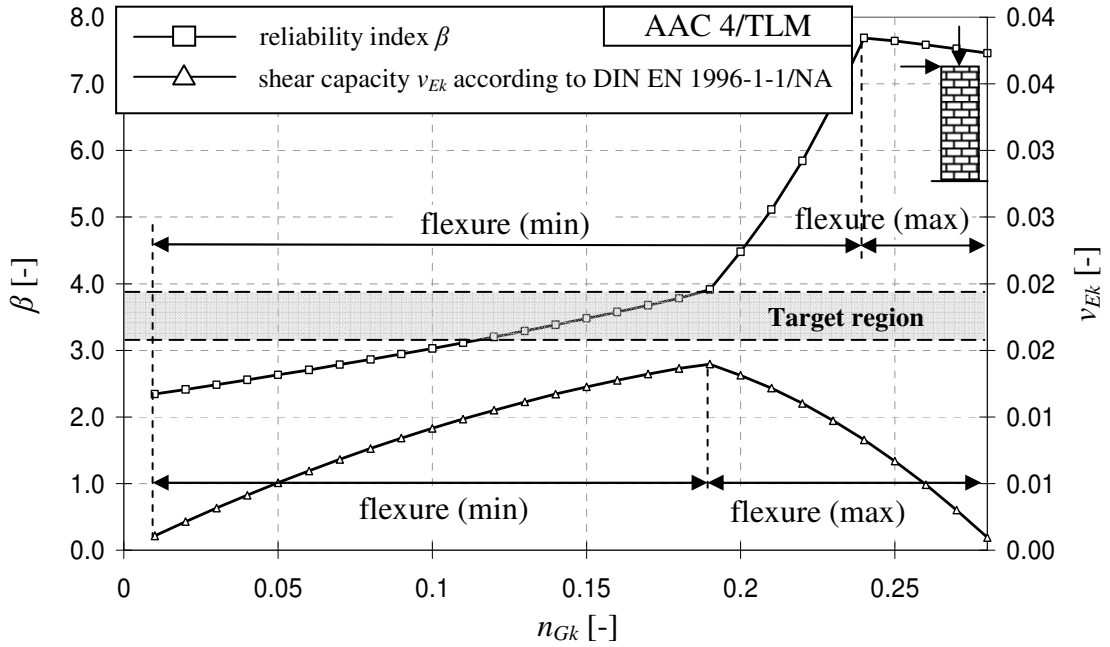

Figure 6-35 *Reliability index β and shear resistance v_{Ek} vs. axial dead load n_{Gk} for an AAC wall with λ_v = 3.0 (designed according to DIN EN 1996-1-1/NA)*

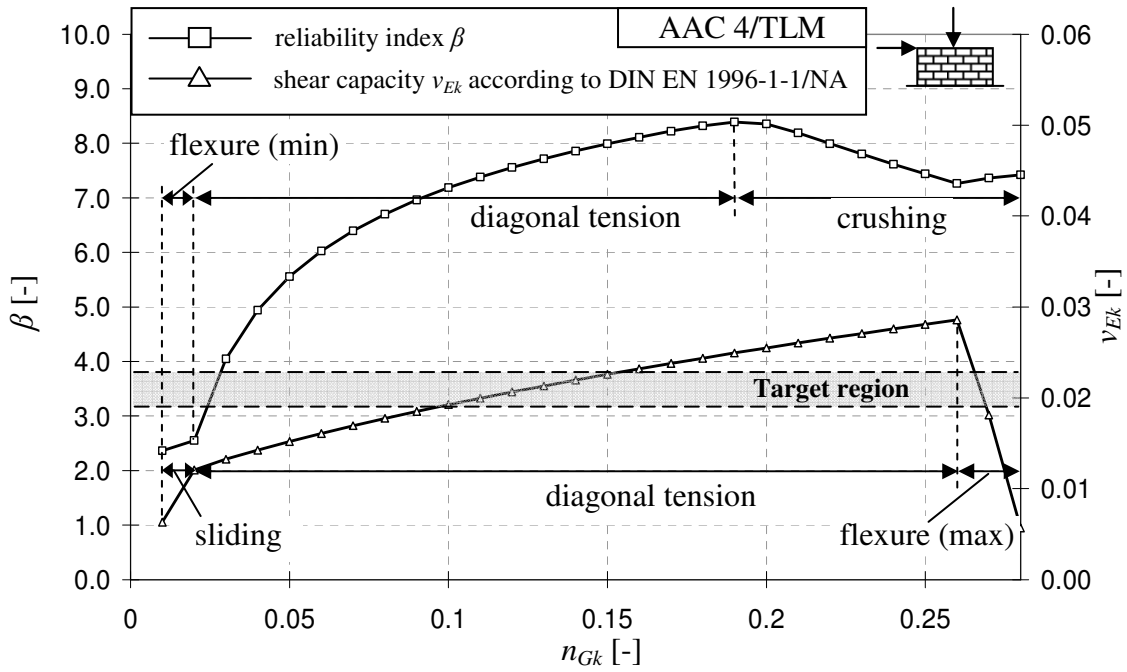

Figure 6-36 *Reliability index β and shear resistance v_{Ek} vs. axial dead load n_{Gk} for an AAC wall with λ_v = 0.5 (designed according to DIN EN 1996-1-1/NA)*

6.8 Assessment

6.8.1 General

A safety concept has to fulfil several requirements. The most important ones are:

- Provide sufficient safety
- Provide a constant level of reliability
- Provide efficiency
- Practical use in engineering practice

These requirements are thought to be fulfilled when a code has proven effective over a long period of time, i.e. the number of failures is small and the design is accepted in society and as well as amongst designers. In the following, the reliabilities obtained in the previous sections will be summarized and assessed. The "theoretical" level of reliability, which refers to the reliability related to full utilization of the cross-section, will be differentiated from the "actual" level of reliability, which will be determined taking into account the realistic level of utilization.

6.8.2 Theoretical Level of Reliability

In the probabilistic analyses of section 6.7, two basic findings became obvious:

- The reliability of slender walls is more critical than the reliability of squat walls.
- Large eccentricity results in smaller reliability.

These findings were verified for all three unit materials and all three codes. It was also found that a certain limit of shear slenderness exists above which the distribution of reliability remains constant because of the governing failure mode (only flexure) and the corresponding distribution of eccentricity e/l_w. This limit is approximately $\lambda_v \geq 3.5$. In the following, the focus will be set on slender walls because they are more critical.

Some differences were observed between the unit materials. The main reasons for the differences are the different stochastic properties of the model uncertainties, the tensile strength of the unit and compressive strength of the masonry. Additionally, in the case of AAC, the design according to the different codes led to significant differences since the tensile strength of the unit was greatly underestimated in DIN 1053-1 resulting in very large reliability of squat AAC walls designed according to DIN 1053-1. Figure 6-37 shows the reliability for slender walls ($\lambda_v = 3.0$) designed according to DIN 1053-1 for the different unit materials.

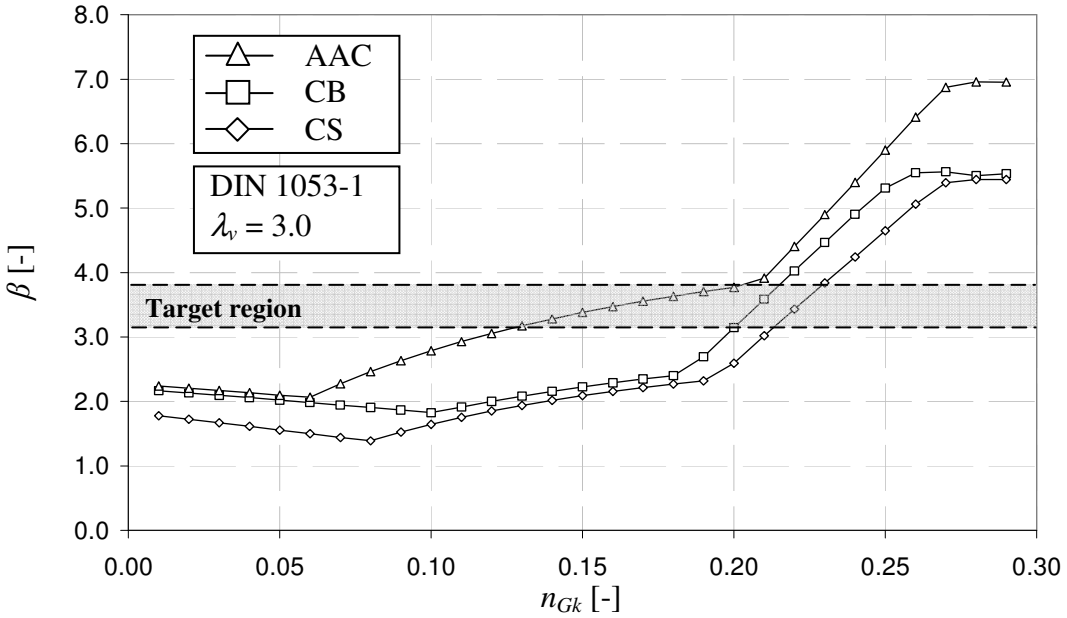

Figure 6-37 *Reliability index β vs. axial dead load n_{Gk} for slender walls designed according to DIN 1053-1*

As can be seen, CS has the lowest reliability while AAC has the largest. Note that different failure modes are governing in Figure 6-37. For example the large difference in reliability between AAC and the other materials in the range from $n_{Gk} = 0.05–0.20$ is due to the fact that diagonal tension governs in the case of AAC because of the underestimation of the unit tensile strength as explained above. The small reliability at low levels of axial load is caused by the model uncertainty; other than in case of AAC and CB, the model is not biased. In the case of AAC and CB, the model incorporates a "model safety".

Figure 6-38 shows the reliability of slender walls designed according to DIN 1053-100. Here, the aforementioned underestimation of the unit tensile strength for AAC has a smaller impact due to the effect of the semi-probabilistic safety concept. Once again, CS has the lowest level of reliability. However, reliability is generally higher than for the DIN 1053-1 because of the appropriate application of the safety factors. The reliabilities stay above 2.0 and even reach values above 3.0 for AAC and CB.

Figure 6-39 shows the same comparison for walls designed according to DIN EN 1996-1-1/NA. The distributions are similar to DIN 1053-100 (Figure 6-38). However, small differences are visible because the underestimation of the unit tensile strength for AAC has been eliminated and the equations for diagonal tension are different. When flexural failure governs, DIN 1053-100 and DIN EN 1996-1-1/NA provide identical levels of reliability.

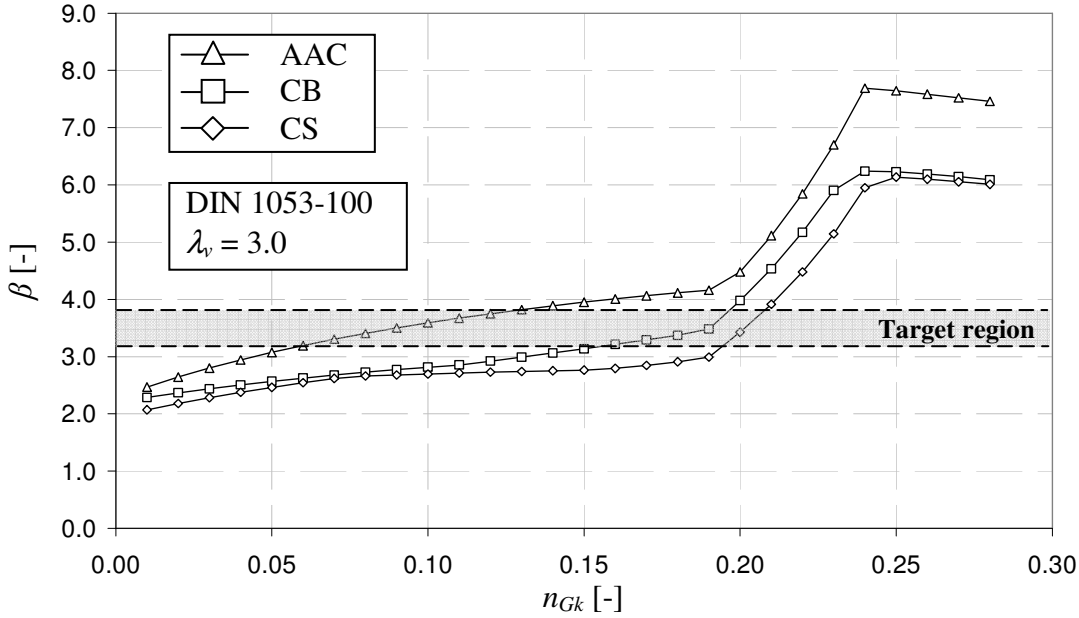

Figure 6-38 *Reliability index β vs. axial dead load n_{Gk} for slender walls (λ_v = 3.0) designed according to DIN 1053-100*

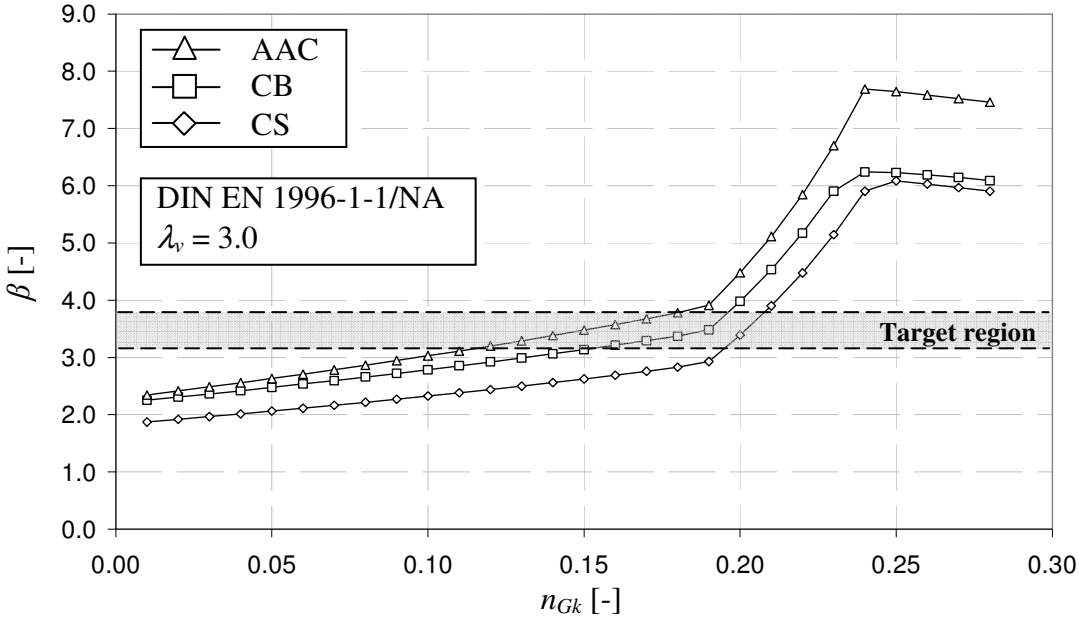

Figure 6-39 *Reliability index β vs. axial dead load n_{Gk} for slender walls (λ_v = 3.0) designed according to DIN EN 1996-1-1/NA*

The general tendency of reliability according to the different codes was also determined. Figure 6-40 shows a typical reliability distribution for a slender AAC wall and compares the different codes. It can be seen that DIN 1053-1 provides the lowest level of reliability while DIN 1053-100 provides the largest and DIN EN 1996-1-1/NA is in between. The reliabilities of DIN 1053-100 and DIN EN 1996-1-1/NA should actually be closer together; the difference at low axial load comes from the underestimation of the unit tensile strength in DIN 1053-100.

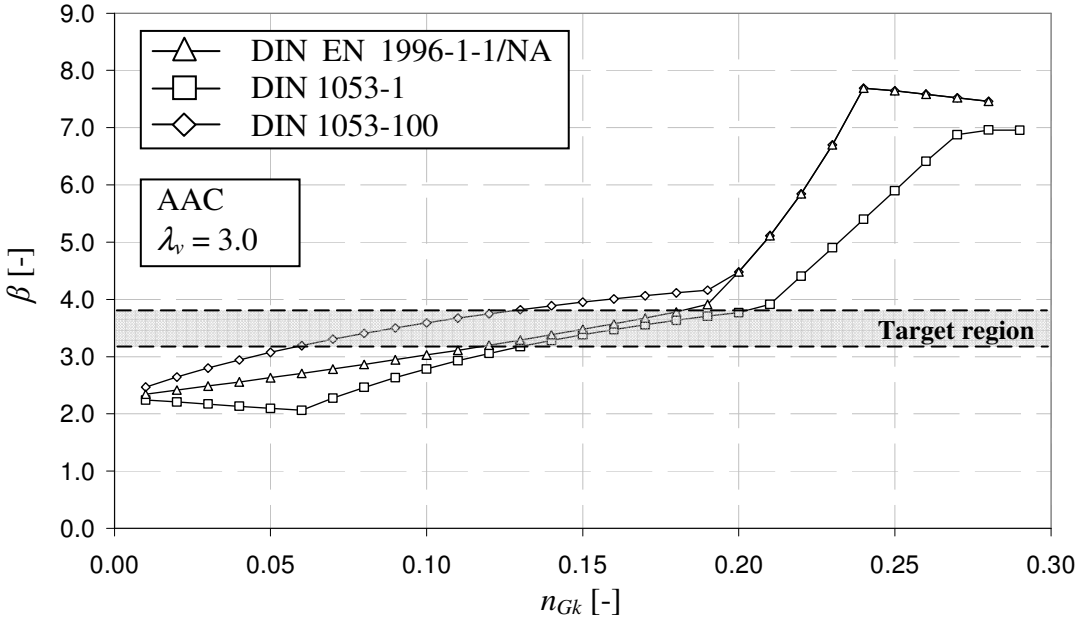

Figure 6-40 *Reliability index β vs. axial dead load n_{Gk} for a slender AAC wall (λ_v = 3.0) designed according to various codes*

Figure 6-41 shows the same comparison for a slender CB wall. Since the unit tensile strength is not underestimated in DIN 1053-100, the reliabilities according to DIN 1053-100 and DIN EN 1996-1-1/NA are almost identical. The marginally higher reliability according to DIN 1053-100 is caused by the slightly more conservative design model for diagonal tension.

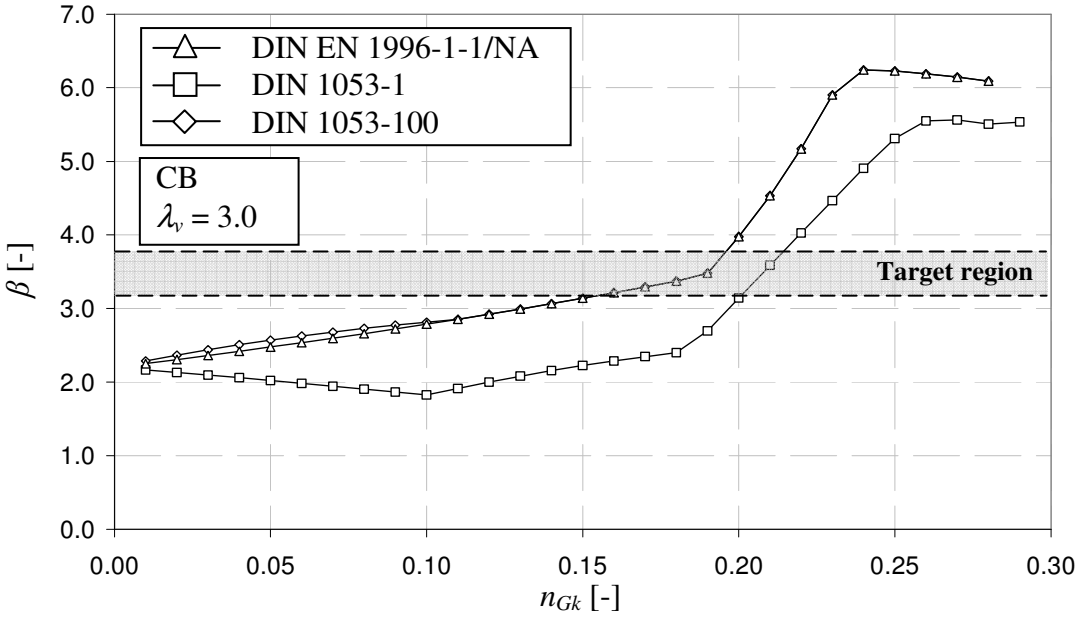

Figure 6-41 *Reliability index β vs. axial dead load n_{Gk} for a slender CB wall (λ_v = 3.0) designed according to various codes*

A similar comparison was made for squat walls, Figure 6-42 compares the reliabilities for the three codes in case of a CS wall with $\lambda_v = 0.5$. It can be seen that for the most part,

DIN EN 1996-1-1/NA leads to the highest reliability while DIN 1053-1 even provides greater reliability than DIN 1053-100. The reason for this is the shear modification factor α_s in DIN 1053-100, which can lead to larger shear capacity than in DIN 1053-1 and is lacking in DIN EN 1996-1-1/NA for small eccentricities.

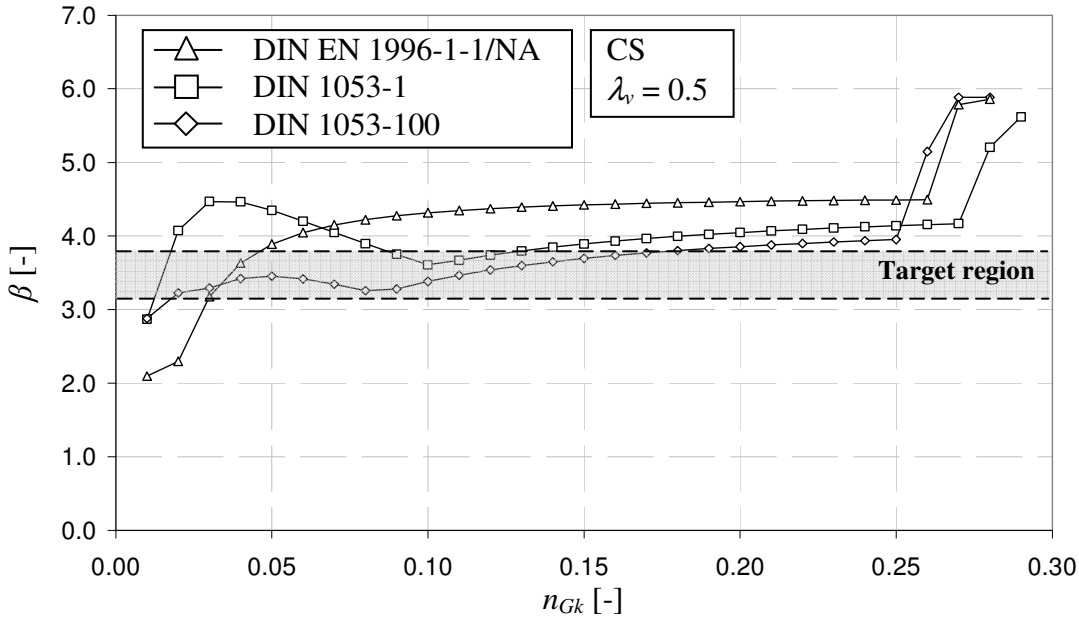

Figure 6-42 *Reliability index β vs. axial dead load n_{Gk} for a squat CS wall ($\lambda_v = 0.5$) designed according to various codes*

In general, it can be stated that the reliabilities of masonry walls designed according to DIN 1053-1 are significantly lower than the reliabilities according to the more recent codes which lead to almost identical reliability for the critical slender walls. The reason for this is mainly the application of the global safety factor. The method of partial safety factors leads to an increase in reliability due to the consistent application of the safety factors and to the smaller capacities that are predicted. A very important fact is also that for squat walls, the theoretical reliability reaches and exceeds the target values of *JCSS (2001)* and DIN EN 1990, while slender walls significantly fall short of the targets over most of the practical range.

6.8.3 Actual Level of Reliability

The theoretical reliabilities derived in the previous section for slender walls are significantly lower than the recommendations of *JCSS (2001)* ($\beta = 3.2$) and DIN EN 1990 ($\beta = 3.8$). This was especially true for the DIN 1053-1 despite the fact that this code satisfies the requirements desired in a code (see section 6.8.1). This code has been used in practice since 1982 and has proven effective over the years; masonry structures designed with it are accepted within society and structural failures due to high wind loads are not reported. This underlines the operational function of the reliabilities obtained.

Nevertheless, DIN EN 1990 suggests calibration of new codes on experiences. If no experiences are available, target values for the reliability of the individual member are provided that have to be met. These targets have been adopted from ISO 2394 where they were derived based on engineering assumptions. However, it is not logical to provide a single target value independent of the failure consequences that are related to a certain structure.

A very important fact in the assessment of the reliabilities obtained is the actual load level. In the study in section 6.7, a member with 100% utilization was assumed. This is correct for ultimate limit state. The level of utilization, α_u, is defined according to Eq. 6-17.

$$\alpha_u = \frac{v_E}{v_{Ek,100\%}} \qquad \text{Eq. 6-17}$$

where v_E is the actual existent wind load.

The absolute values of the sustainable shear force v_{Ek}, however, are different for every unit material since the compressive strength was used as the basis for normalization. Thus, the wind loads that can be recalculated for the high strength materials CS and CB are much larger than for AAC. In reality, the wind load is independent from the unit material. Thus, for actual structural members, a utilization of 100% is unlikely to occur for the high-strength materials and consequently, reliabilities will be higher on average. To assess this effect, the distribution of reliability of a CS wall and a CB wall for different levels of utilization are presented in Figure 6-43 and Figure 6-44.

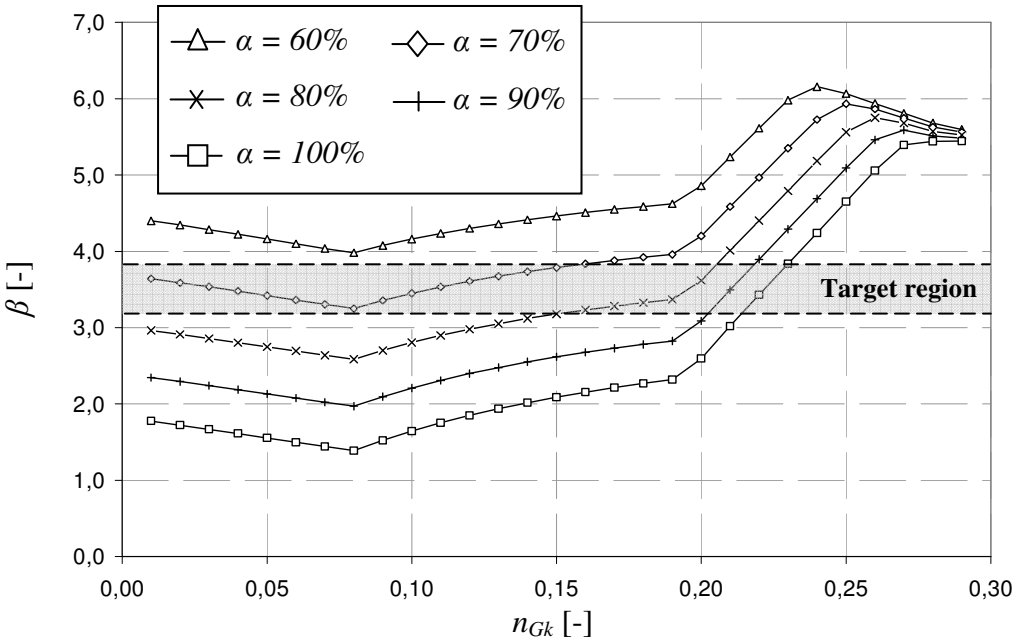

Figure 6-43 *Reliability of slender CS wall for different levels of utilization (λ_v = 3.0; design according to DIN 1053-1)*

As expected, the reliability increases significantly within the practical range. For very large axial force, the values do not differ much since the influence of the shear force is small in that case. An interesting observation is the linear relationship between α and the reliability, evident from the equal change in reliability from one level of α to the other. This allows the application of a constant factor to modify the capacity to reach the required level of reliability.

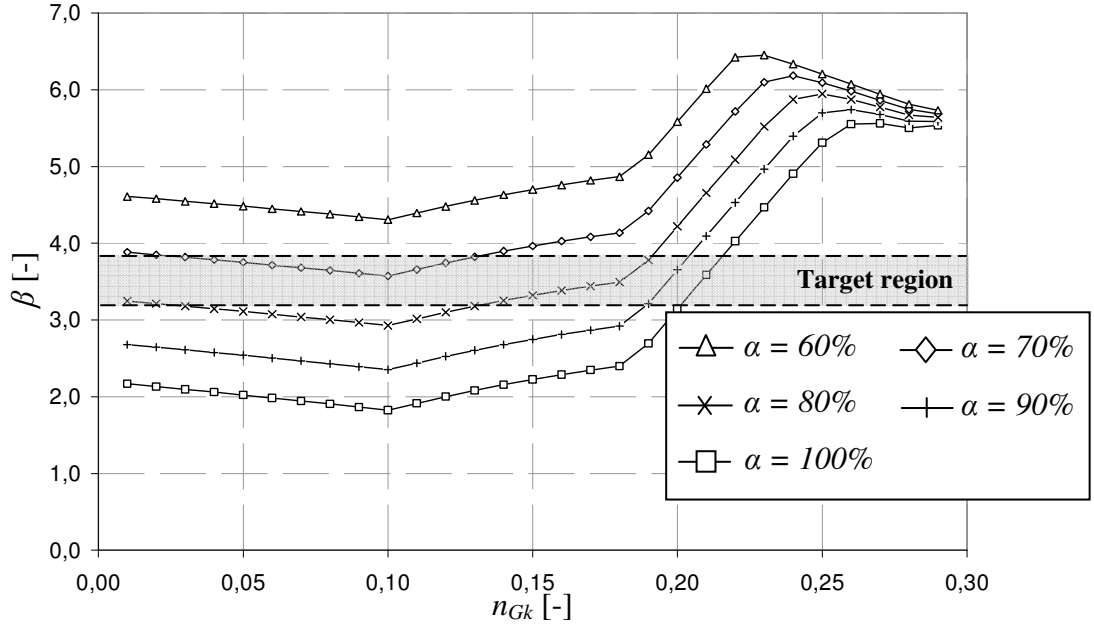

Figure 6-44 *Reliability of slender CB wall for different levels of utilization (λ_v = 3.0; design according to DIN 1053-1)*

To assess typical levels of utilization, consider a typical town house as presented in Figure 6-2. The height of the building is h = 9.0 m (3 storeys, flat roof). Typically, the distribution of the wind loads will be determined from linear FEM analysis. The determination of the wind load is carried out according to DIN 1055-4. The slabs were designed to have the shortest span and provide axial load to the shorter shear walls. Framing action of the walls and slabs is not examined since this is commonly neglected in design of the bracing walls.

With these values, the levels of utilization can be determined for the different unit types. The axial load will be determined under the assumption of one-way single span slabs with three stories. The thickness of the slabs is 20 cm, so that the axial dead load, including floor coverings, is 6.0 kN/m² per floor. Live load is not taken into account since it will likely act favourable.

Table 6.8-1 Axial dead load n_{Gk} for the example building

Wall	h_w/l_w	CS	CB	AAC
		n_{Gk}		
W1	2.26	0.027	0.048	0.063
W3	2.74	0.047	0.090	0.129
W5	1.39	0.084	0.168	0.250
W6	0.97	0.059	0.115	0.168
W7	2.18	0.071	0.139	0.206
W8	1.83	0.029	0.053	0.071
W9	3.31	0.028	0.050	0.067
W10	2.74	0.047	0.090	0.129

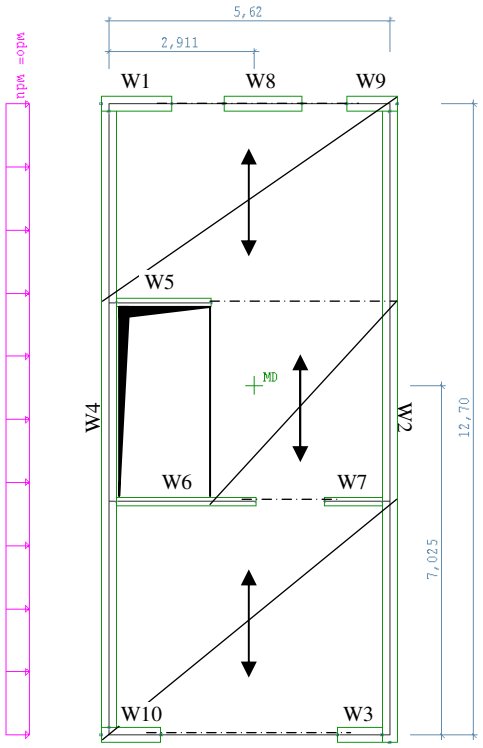

Wall	Horizontal force in kN[a]		
	CB	CS	AAC
W1	1.20	1.23	1.23
W3	0.30	0.33	0.31
W5	1.70	1.85	1.76
W6	5.41	5.87	5.59
W7	0.38	0.41	0.39
W8	1.62	1.76	1.67
W9	0.44	0.48	0.45
W10	0.31	0.33	0.31
[a]per storey			

Figure 6-45 *Example of a town house and corresponding horizontal forces*

For matters of simplicity, and since it is intended only to show a general tendency of the levels of utilization and to assess the realistic level of reliability of masonry structures I Germany, the capacities were determined according to DIN 1053-1. To assess the consequences of the different structural systems, two values of the parameter ψ (see Figure 5-2) are investigated.

In case of $\psi = 1.0$ a full reconcentration of the axial force due to the overturning moment of the slabs is considered so that the shear slenderness becomes $\lambda_v = h_w/l_w$. The second case with $\psi = 3.0$ (= number of storeys) is equal to modelling the shear wall as a building-high cantilever. In reality, ψ will likely be in between these two values. In Figure 6-46, the levels of utilization for the different walls of the example building are presented.

As expected, the utilization of the AAC walls is significantly larger than the utilization of the CS and CB walls (see Figure 6-46). Please note that non-linear effects are not considered herein, thus the actual utilization may still be lower. However, there is a clear tendency that CS and CB walls are utilized to a lesser extent than AAC walls. Wall W1 even reaches a utilization of 99% in case of AAC while the corresponding CB wall is only utilized up to 80%. In case of a CS wall, the utilization is 70%. As previously shown in Figure 6-43, this yields a reliability index of $\beta \approx 3.1$ for the CB and $\beta \approx 3.3$ for the CS wall which is significantly higher than the reliability index for full utilization of the cross-section. The higher reliability for AAC leads to the supposition that the experts involved in the standardization process "instinctively" accounted for the higher level of utilization of AAC walls. It can also be seen that the utilization of the walls drops significantly when the overturning moments of the slabs are considered. While a clear quantification of these moments can make a significant reduction of the wall length possible, admittedly, this is difficult. In reality, an approach with $\psi = 1.0$ will likely be used for convenience and efficiency. If the overturning moments are not large enough to center the axial load, this will probably lead to very small levels of utilization in the design of the shear walls and consequently to insufficient reliability due to wall length reduction.

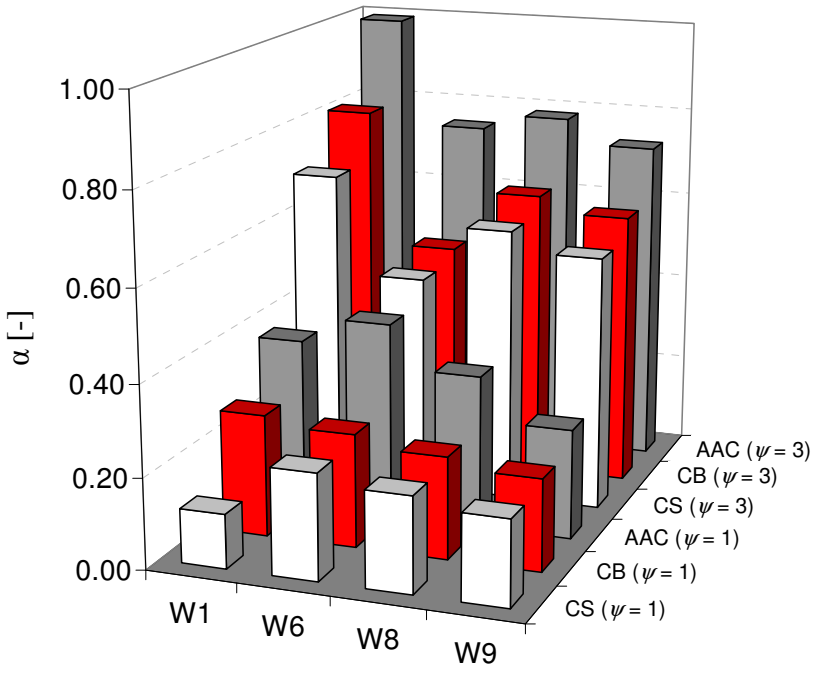

Figure 6-46 Levels of utilization α for the example building

Another important aspect in the reliability of masonry shear walls is the load redistribution in the system. *Jäger et al. (2008)* showed the potential for load redistribution in a masonry structure by non-linear FE analysis. While, the system reliability of the entire structure cannot be quantified yet; all the reliabilities obtained are only valid for the single member; the failure probability of the system will be significantly smaller. Other favourable effects, such as the contribution of supposedly non-load bearing walls or frame action

between walls and slabs can not be taken into account. The quantification of the system reliability should be the subject of future research.

Considering these facts, the capacities predicted by DIN 1053-1 seem justified. The highly utilized AAC walls reach the economic optimum derived in this chapter. The CB and CS walls are normally less utilized and thus also come close to the economic optimum of $\beta = 3.0$. This underlines the belief in proper empirical assessment of the masonry shear walls in the past; the provided reliability appears to be similar to the economic optimum. In conclusion, it must be stated that DIN 1053-1 represents the economic optimum.

6.9 Summary

In this chapter, the reliabilities provided by three design codes for common shear walls are assessed. Starting with an outline of the procedure, the required steps are explained. The limit state functions are provided in non-dimensional form.

The theoretical reliability of a selection of URM walls is then determined using SORM. All studies were conducted for an observation period of 50 years using distributions of extremes to take into account the time-dependence.

In general, it can be stated that very slender shear walls made of CS, CB and AAC units neither fulfil the requirements of the codes, nor meet the recommendations of *JCSS (2001)* and DIN EN 1990 in the case of small axial force and large eccentricity. For all materials it is found that reliability increases significantly for squat walls. Slender walls are critical and likely to fail in flexure.

The differences between the characteristic values of the material properties according to the codes and the derived stochastic models described in chapter 3 are illustrated. In particular, the unit tensile strength for AAC units is significantly underestimated in DIN 1053-1 and DIN 1053-100. This leads to extraordinarily large values of the reliability for squat AAC walls. This shortcoming was addressed in DIN EN 1996-1-1/NA. Thus, the reliability is smaller but still high when diagonal tension governs.

It is also shown that the model uncertainties are the dominant basic variables as long as minimum load governs. When maximum axial load governs (shear crushing and flexural failure under maximum load), model uncertainties lose their influence and only the masonry compressive strength and the axial load influence the results.

For CS walls the average reliability index for a slender wall with $\lambda_v = 3.0$ is $\beta \approx 2.6$ when the wall is designed according to DIN 1053-100 or DIN EN 1996-1-1/NA. These codes are new; the latter has not even been published yet. Due to the long history of use in practice, the reliability for walls designed according to DIN 1053-1 can be seen as a minimum average value in common masonry construction. The corresponding values are $\beta \approx 2.0$ for CS walls, $\beta \approx 2.1$ for CB walls and $\beta \approx 2.9$ for AAC walls. All values are valid for an ob-

servation period of 50 years. If the walls are designed according to DIN 1053-100 or DIN EN 1996-1-1, higher reliability is obtained due to more appropriate application of the safety factors in the design. The minimum values for the slender walls are equal for these two codes since the check against flexural failure is identical. Squat walls exhibit significantly higher reliability and provide reliabilities above the target region.

The values obtained in the reliability analysis represent theoretical values; the actual reliability provided by masonry shear walls will be higher due to the lower level of utilization of the walls in reality. The reliability analysis was conducted assuming full (100%) utilization of the walls. To assess the actual level of reliability, a typical house is analysed and the levels of utilization for the bracing walls are determined. Subsequently, the provided level of reliability for the "realistic" level of utilization is determined. The reliabilities obtained are similar for all three unit materials and higher than then the theoretical level of reliability.

The average reliabilities obtained are summarized in Table 6.9-1. These actual reliabilities are believed to represent the societally accepted minimum since concerns about the use of masonry buildings is not existent among the public.

Table 6.9-1 *Minimum average reliability index in common masonry construction (full utilization of the cross-section)*

Material	Average reliability index provided in common masonry construction[a]			
	theoretical[b]			actual[c]
	DIN 1053-1	DIN 1053-100	DIN EN 1996-1-1/NA	
CS (20/TLM)	2.0	2.7	2.6	3.2[d]
CB (12/GPM IIa)	2.1	3.0	3.0	3.1[e]
AAC (4/TLM)	3.0	3.7	3.3	3.0[f]

[a] corresponding to $\lambda_v = 3.0$ and $n_{Gk} = 0.05–0.2$
[b] full (100%) utilization of the wall
[c] determined on the basis of DIN 1053-1
[d] corresponding to a utilization of 70%
[e] corresponding to a utilization of 80%
[f] corresponding to a utilization of 100%

7 OPTIMIZATION OF THE TARGET RELIABILITY

7.1 Introduction

In the previous chapter, the reliability of masonry walls designed according to three German design codes was determined. Because of the wide acceptance of masonry buildings and the lack of safety concerns in the public, the results obtained can be interpreted as societally accepted values even though slender walls do not meet the target reliability of DIN EN 1990. Therefore, the question arises as to how a construction material like masonry which has proven "reliable" over a long period cannot fulfil code requirements under the chosen assumptions. Consequently, the code requirements should be examined. Therefore, a target has to be determined and compared to the existent level of reliability. In addition, whether or not a probabilistically optimized level of reliability verifies the results obtained from chapter 6 should be checked.

In the following sections, the target reliability for typical masonry structures will be determined by means of probabilistic cost-benefit optimization. The target reliability depends strongly on the point of view of the assessor. Just consider the different points of view in the simple example of selling a house: The seller's benefit is a sum of money while the buyer sees other benefits (more space, better environment, better life in general) and so the results of the individual analysis (Buy the house? Accept a certain price?) will be different. However, this study has to focus on one perspective. The target reliability will be determined from the socio-economic point of view, i.e. the target reliability determined here is intended to represent the value that is best for society representing the optimum compromise of efficiency and reliability.

This will be achieved by application of the techniques and methods described in section 2.6 and extending them to the special requirements of masonry construction. The goal is to derive a better recommendation for the target reliability for common masonry structures based on societal acceptance. For this, a number of periphery conditions have to be defined and missing data has to be estimated. However, by limiting the scope to masonry buildings, many conditions can be estimated with reasonable accuracy.

In the first step, the targeting function and the parameters of the optimization will be defined. The failure consequences will be assessed and verified for typical masonry buildings to estimate benchmarks for the subsequent optimization.

In this optimization, the service life of the masonry building plays an important role due to interest rates and derived benefit. The service life is normally estimated within the values provided by EN 1990. These recommendations are presented in the following table. Residential masonry buildings as well as office buildings should be part of class 4 and thus the design life should be 50 years.

Table 7.1-1 Design service life of structures according to EN 1990

Class	Design service life in yrs	Examples
1	10	Short-term structures with limited life[a]
2	10–25	Exchangeable parts of a structure, e.g. bridge supports
3	15–30	Agricultural and similar structures
4	50	Buildings and other common structures
5	100	Monumental structures, Bridges etc.
[a]NOTE: Structures and parts of structures that are intended to be reused, should not be regarded as short-term structures with limited life		

7.2 Modelling

7.2.1 General

In the first step, an appropriate targeting function will be derived. The formulation, as proposed by *Rosenblueth & Mendoza (1971)* (see section 2.6), is chosen:

$$Z(p) = B(p) - C(p) - D(p) \qquad \text{Eq. 7-1}$$

From there, the optimization parameter and the variables to suit the situation of a typical masonry structure have to be defined. The optimization parameter needs to be linked to the probability of failure. Additionally, the more the variables are independent from the optimization parameter, the less complex the optimization becomes and is thus more efficient. The partial safety factor on the wind load γ_w is chosen as the optimization parameter for simplicity and clarity since it is tangible and has a fixed range unlike other possible parameters such as the failure probability (actually the partial safety factor just represents the failure probability).

It is assumed here that failed structures would be systematically reconstructed. This would especially hold true for structures in urban regions, however, even in less prosperous regions, property will unlikely remain unused.

Next, the variables have to be defined. The benefit *B(p)* represents the rental income and the cost *C(p)* is the structural cost. A probabilistic optimization of a structure aiming at economic efficiency can only be useful if the optimization parameter influences either the benefit or the structural cost. If both are independent of the optimization parameter, the optimum result will always be maximum safety. Changes in γ_w affect the length of the shear walls which can potentially affect both the benefit and the cost. With regard to the benefit, while on the one hand differences in the length of the shear wall will not reduce rentable area significantly, longer shear walls do cause some architectural disadvantages such as less flexibility in the floor plan, limiting the use of the space, as well as the size of the openings. This could lead to lower market value of the building and thus lower rental income due to lower satisfaction of the renter. Therefore, the benefit is a function of the

optimization parameter. With regard to cost, the optimization parameter γ_w has only a minor effect on the structural cost. If longer shear walls are required, confining techniques will be applied in most cases and the increase in structural cost due to these techniques is negligible compared to the structural cost of the whole building. Therefore, the structural cost will be kept constant, $C(p) = c$. The failure consequences $D(p)$ depend on the optimization parameter via the failure probability P_f which is taken into account by the intensity of the assumed Poisson process for the failure.

Eq. 7-2 is the target function (see Eq. 7-1) after modification where φ is the interest rate, required to account for the time dependence due to the long service life, λ is the intensity of the Poisson process and H is the cost related to failure consequences (mainly fatalities). The interest rate φ represents the real interest rate. Various recommendations from 2% to 5% can be found in the literature (see *Rackwitz (2008)*). In this special case, the influence of the interest rate on the optimization result will be small since it has the same effect on both the benefit and the failure consequences. The annual interest rate is set as $\varphi = 0.03$.

$$Z(\gamma_w) = \frac{B(\gamma_w)}{\varphi} - c - (c + H) \cdot \frac{\lambda\left(P_f(\gamma_w)\right)}{\varphi} \qquad \text{Eq. 7-2}$$

Therefore, the distribution of the failure probability versus the optimization parameter γ_w is required. It can be determined in the same manner as explained in chapter 6; the walls are designed according to DIN 1053-100 but different values of γ_w are applied and then the failure probability and reliability index are determined. In the optimization, all parameters will be related to one m² of rentable area. Before the optimisation is executed, the parameters will be assessed and estimates for typical masonry structures will be derived. From there, a simulation will be conducted to classify the failure consequences of common masonry structures according to the classification method presented in section 2.6.4.

7.2.2 Modelling of the Benefit

The common benefit derived from typical masonry structures is rental income. New masonry structures normally do not represent cultural heritage and do not contribute to a societal benefit other than rental income and providing residential and commercial space.

Rent per m² is a typical indicator for the societal status of a region or city, high rent normally occurs in prospering and wealthy municipalities. Since it serves as a main indicator in real estate, values for the monthly rent per m² can be obtained relatively easy; many surveys on the rent are conducted every year, such as *IVD (2009),* in which average values for representative cities across Germany are determined. Figure 7-1 gives values for various German cities. The national average monthly rent per m² for a typical flat is 6.14 €/m². In prospering cities displayed in Figure 7-1 values above 9 €/m² are easily reached. From this data, a stochastic model for the benefit derived from a structure is de-

termined. If the benefit is independent from the optimization parameter, benefit just represents a parameter that shifts the target function along the *y*-axis.

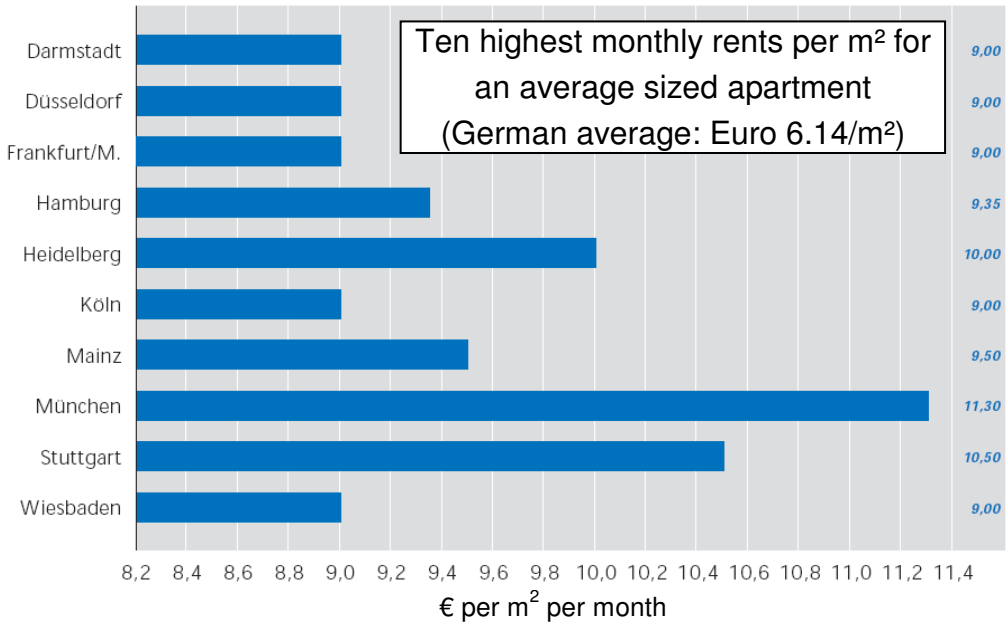

Figure 7-1 Average monthly rent per m² for various German cities according to IVD (2009)

Here, a linear relationship is assumed, as shown in Figure 7-2. A possible formulation is given by Eq. 7-3. In this equation the parameter A is the ratio of maximum benefit to the standard benefit and represents the impact of reliability enhancement measures. This parameter is difficult to determine because of its subjective nature. Thus, this parameter will be subject to sensitivity analysis in the optimization.

$$b(\gamma_w) = \frac{(A-1)\cdot b_0}{\gamma_{w,0} - \gamma_{w,\min}} \cdot \gamma_w + A \cdot b_0 \qquad \text{Eq. 7-3}$$

$$A = \frac{b_{\max}}{b_0} \qquad \text{Eq. 7-4}$$

where b_0 is the benefit in case of design according to the current code. Here, this is the benefit corresponding to $\gamma_{w,0} = 1.5$ and equals the values given in Figure 7-1 for an observation period of 1 year. The parameter b_{max} is the maximum obtainable rent. A formulation of this relationship directly using the failure probability would also have been possible but appears less demonstrative.

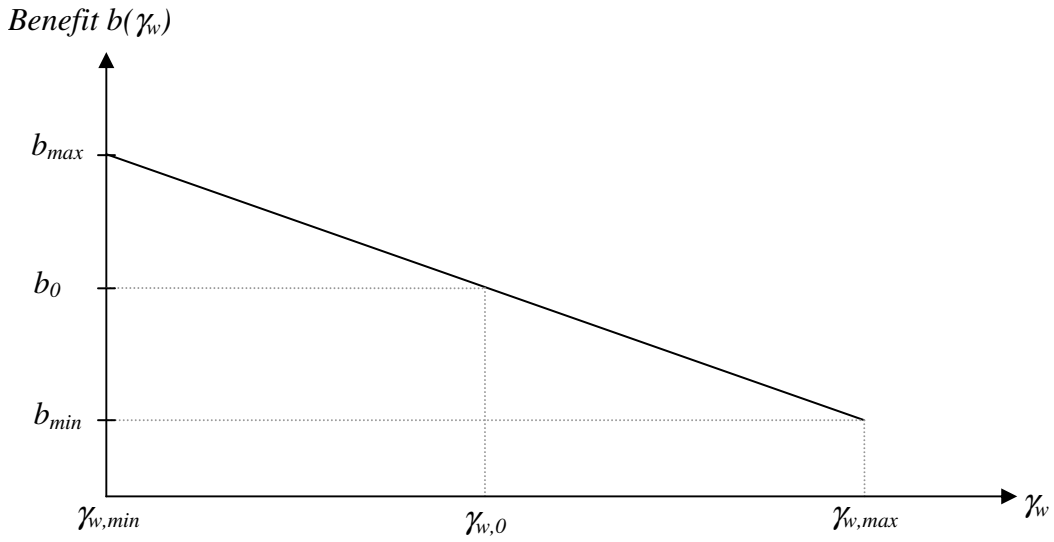

Figure 7-2 Linear approach for the benefit $b(\gamma_w)$

7.2.3 Modelling of the Structural Cost

The term structural cost c refers to the amount of money that the owner has to invest to build the structure. The cost of the land is not included since it is independent from structural failure (in case of residential and office buildings). After failure, it is assumed that the same structural cost (taking into account the interest and inflation in the time between completion and collapse of the structure) applies to rebuild the structure.

The structural cost depends on the geographic region. Naturally, building in prosperous regions is more expensive than in other regions. However, the location of a building mainly affects the prices for property and the effect on the material and labour costs etc. is smaller.

To estimate the structural cost reference value, benchmarks are required. In Germany, typical cost for the construction of a good quality masonry house is about 180,000 € according to *BKI (2010)*. Estimating the area of a corresponding masonry house to be 150 m², the cost per m² is 1200 €/m². This benchmark is used to model the structural cost for a first assessment. Considering the range of structural costs across Germany, the structural cost will be assumed to have a coefficient of variation of 15%.

Table 7.2-1 Stochastic model for the structural cost c

Distribution	*m* [€/m²]	*CoV*
LN	1200.00	15%

These assumptions lead to a range in structural cost for a 150 m² house from 130,000 € to 240,000 € in more than 95% of all cases which is believed to represent the typical German conditions.

7.2.4 Classification of Failure Consequences

Fatalities represent the severest failure consequence. A monetary assessment of a fatality can never cover the personal loss and of course, this is not attempted herein. However, for the derivation of socio-economic optimal target reliability, a clear monetary standard for fatalities has to be applied. The most common approach is based on the Life Quality Index as explained in section 2.6.3.

In the following, the cost related to failure for typical masonry buildings will be assessed for three scenarios representing different levels of risk. For these scenarios, the risk indicator *f(p)* according to *JCSS (2001)* (see section 2.6.4) will be determined by MCS so that the provided benchmarks of this indicator, see Table 2.6-3, can be verified for typical masonry structures. Eq. 2-88 then becomes Eq. 7-5.

$$f(p) = \frac{C_0 + H}{C_0} = \frac{C_0 + n \cdot k \cdot SLSC}{C_0} \qquad \text{Eq. 7-5}$$

Masonry shear walls are only present in smaller buildings. Usually, when buildings are equipped with elevators, the elevator shafts are constructed of RC and are used for bracing. Confinement of masonry walls with concrete elements is also becoming more and more popular so that true masonry shear walls can normally only be found in smaller residential and office buildings. To assess these conditions, the following three scenarios are defined and evaluated:

- Scenario 1: Single family residential building (4 people; 150 m²)
- Scenario 2: Multi-family residential building (up to 20 people; 600 m²)
- Scenario 3: Office building for a company with a staff of 40 (800 m²)

The first case represents the typical detached house for a single family. The second case represents a multi-storey residential building with about 8 units. Case 3 represents a typical office building for an average size company. The number of people *n* inside the building at the time of failure will be modelled using different kinds of distributions for the scenarios. In Scenario 1, a discrete distribution is chosen. The estimated probabilities are based on engineering judgement and experience. It is assumed that most likely all 4 people are at home since this normally holds for evenings, mornings and nighttime. Considering sudden structural failure, it is unlikely that no fatalities occur.

In Scenario 2, similar assumptions as for Scenario 1 hold. In both scenarios, it has to be considered that people are in the building around the clock. During the day, people will go to work or school, resulting in less people in the building, but most of the time, people will be at home. To account for the larger number of people, a normal distribution with a mean of 15 people per 600 m² and a coefficient of variation of 20% is assumed.

Table 7.2-2 Distribution of number of people inside the building in Scenario 1

Number of people n	p	Number of people per m²
0	0.05	0
1	0.15	0.004
2	0.15	0.008
3	0.15	0.012
4	0.50	0.016

Table 7.2-3 Normal distribution of number of people n inside the building in Scenario 2

Distribution type	m [pers. / m²]	CoV
N	0.025	20%

In Scenario 3, the assumptions are similar. The coefficient of variation is assumed to be only 10% to account for the small fluctuation of the attendance of the employees. To account for the nights, this contribution will be multiplied with the factor 8/24 (work hours per day) = 1/3 in the assessment of the risk in the following section.

Table 7.2-4 Normal distribution of number of people n inside the building in Scenario 3 (office)

Distribution type	m [pers. / m²]	CoV
N	0.044	10%

These distributions are supposed to represent the number of people in the building at the time of failure. To assess the failure consequences, these numbers need to be converted into possible fatalities. For this purpose, *Rackwitz (2004)* suggests the factor k, provided in Table 2.6-2. For sudden structural failure in places of public entertainment, an estimate of $k = 0.1–0.5$ is recommended. Several reasons justify a low estimate of this value:

- In case of typical town houses, failure of a shear wall will not necessarily lead to failure of the entire structure since the adjacent houses brace the respective house.
- Plastic resources of the bracing system and framing action enable load redistribution and thus failure is not automatically brittle.
- It has often been observed that people survive even gas explosions of buildings due to favourable location in the house (in the door way, in the basement).
- The buildings in the three scenarios are well-known to the people (escape) in the building and are not crowded.

Due to the reasons above, k will be estimated with a mean of 0.1. To account for possible scatter, it will be modelled in the following classification of the failure consequences according to section 2.6.4 with the stochastic model provided in Table 7.2-5.

Table 7.2-5 Normal distribution of the parameter k

Distribution type	m	CoV
N	0.1	10%

To classify the failure consequences and to evaluate the values of *f(p)* provided by *JCSS (2001)* for masonry buildings, a Monte Carlo-Simulation of the parameter *f(p)* according to Eq. 2-90 is conducted using the derived stochastic models.

The simulation (number of simulations: 10,000), gives the distribution of *f(p)* for typical masonry structures in the three mentioned scenarios. In Figure 7-3, the distribution of *f(p)* in Scenario 1 is presented. It is can be seen that the minimum is $f(p) \approx 1.0$ when no fatalities occur and the maximum value reached is $f(p) \approx 5.0$. This corresponds to the range of values for average failure scenarios according to *JCSS (2001)*. 21.8% of all simulations led to values of $f(p) < 2.0$; 77.8% were within the range of $2.0 \leq f(p) \leq 5.0$. The mean is $f(p) = 2.81$ and represents the average risk for a simple residential building.

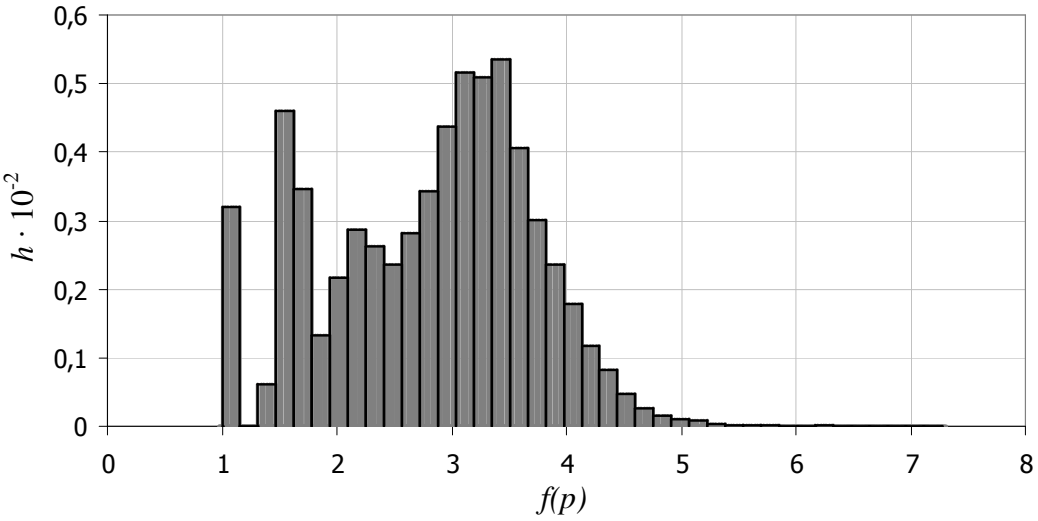

Figure 7-3 Distribution of f(p) in Scenario 1

In Scenario 2 (Figure 7-4), similar results as in Scenario 1 are obtained. The values of *f(p)* are larger than in Scenario 1 due to the larger number of possible fatalities and the corresponding higher value of the failure cost *H*. However, the range is still in the region of medium risk with a mean of $f(p) = 3.35$ with 97.8% of the simulations located within the range of $2.0 \leq f(p) \leq 5.0$.

In Scenario 3 (Figure 7-5), the risk is smaller than in the other scenarios due to the occupation of the building only during office hours. The mean of *f(p)* is 2.38 while 88.7% of the obtained values of *f(p)* are within the range of average risk.

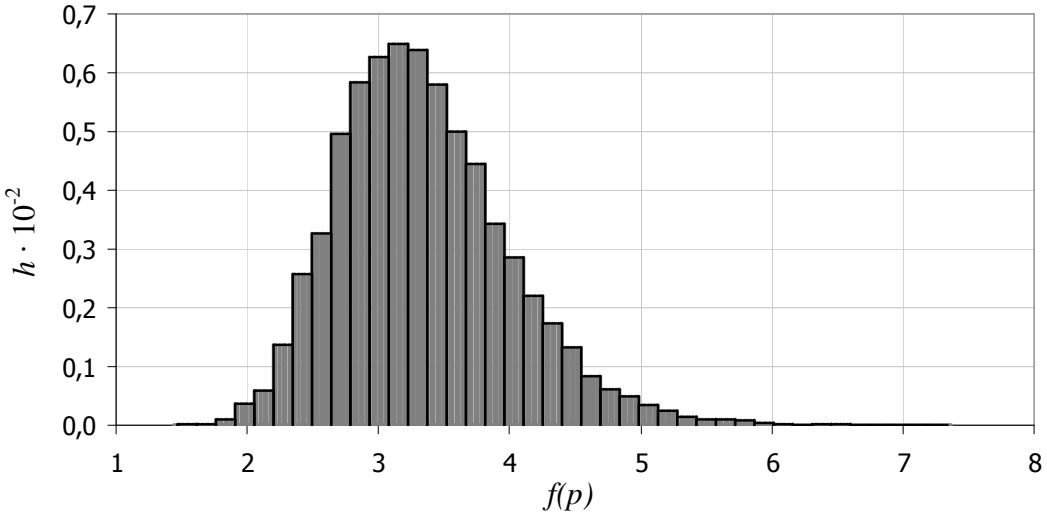

Figure 7-4 Distribution of f(p) in Scenario 2

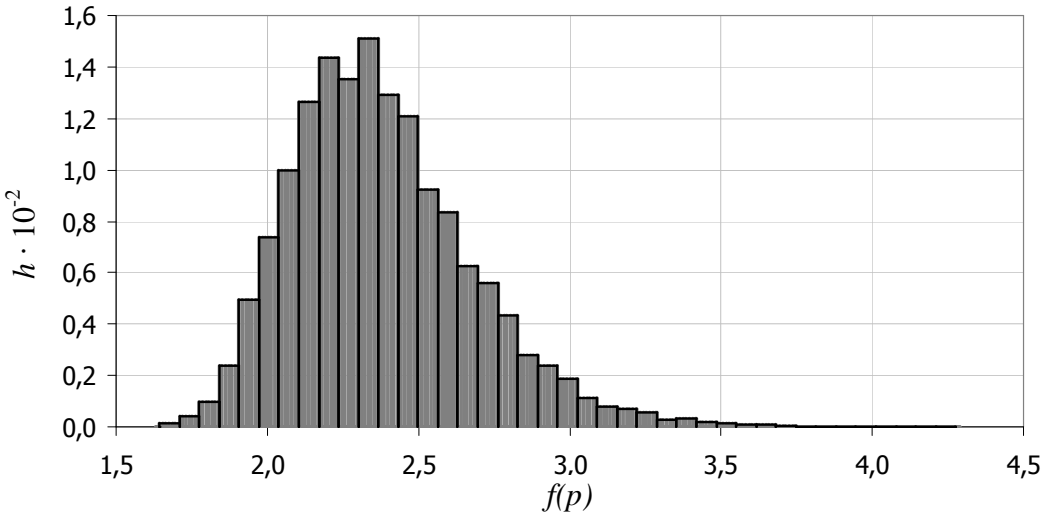

Figure 7-5 Distribution of f(p) in Scenario 3

To assess the sensitivity of the parameters, a sensitivity study was conducted. Figure 7-6 shows a typical tornado diagram representing the influence of the parameters on the result obtained for $f(p)$ in Scenario 2. As can be seen, the number of people in the building has the strongest influence while the parameter k has the lowest. However, for the chosen modelling, mean values of $f(p)$ stay within the range of $2 \leq f(p) \leq 5$.

In summary, it can be stated that masonry buildings definitely belong in the average risk class according to *JCSS (2001)*. Masonry buildings with high risk (apartment buildings) will most likely exhibit a value of $f(p) \approx 3.5$ while typical small residential and office buildings can be represented with $f(p) \approx 2.5$.

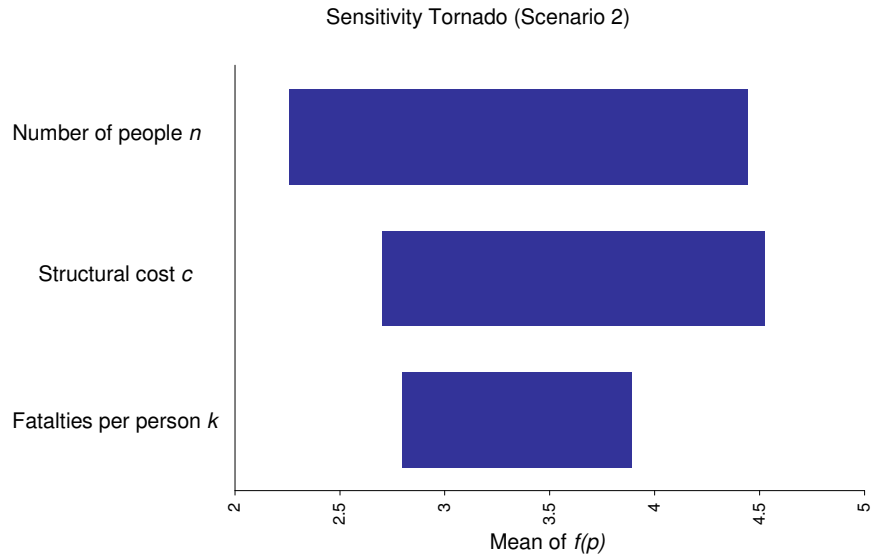

Figure 7-6 Tornado diagram for Scenario 2

7.2.5 Targeting Function and Procedure

The general form of the targeting function (Eq. 7-1) can be modified for better assessment following the findings of the previous sections. The first modification is the insertion of the benefit according to Eq. 7-3 and introducing γ_w as the optimization parameter. The fact that the structural cost $C(p) = C_0$ is constant also has to be considered. This gives:

$$Z(\gamma_w) = \frac{1}{\varphi} \cdot \left(\frac{(A-1) \cdot b_0}{\gamma_{w,0} - \gamma_{w,\min}} \cdot \gamma_w + A \cdot b_0 \right) \cdot A_w - C_0 - (C_0 + H) \cdot \frac{\lambda\left(P_f(\gamma_w)\right)}{\varphi} \cdot A_w \qquad \text{Eq. 7-6}$$

The factor A_w (see Eq. 2-84) accounts for times of reconstruction. Dividing this equation by C_0 yields

$$\frac{Z(\gamma_w)}{C_0} = \frac{1}{\varphi \cdot C_0} \cdot \left(\frac{(A-1) \cdot b_0}{\gamma_{w,0} - \gamma_{w,\min}} \cdot \gamma_w + A \cdot b_0 \right) \cdot A_w - 1 - f(p) \cdot \frac{\lambda\left(P_f(\gamma_w)\right)}{\varphi} \cdot A_w \qquad \text{Eq. 7-7}$$

The factor $f(p)$ can be assessed by application of the values obtained in section 7.2.4. The intensity of the Poisson process $\lambda(P_f(\gamma_w))$ can be calculated directly from the probability of failure (see Eq. 7-8).

$$\lambda\left(P_f(\gamma_w)\right) = -\ln\left(1 - P_f(\gamma_w)\right) \qquad \text{Eq. 7-8}$$

The targeting function is therefore defined and allows optimization with a minimum number of variables. The optimization follows the scheme presented in Figure 7-7.

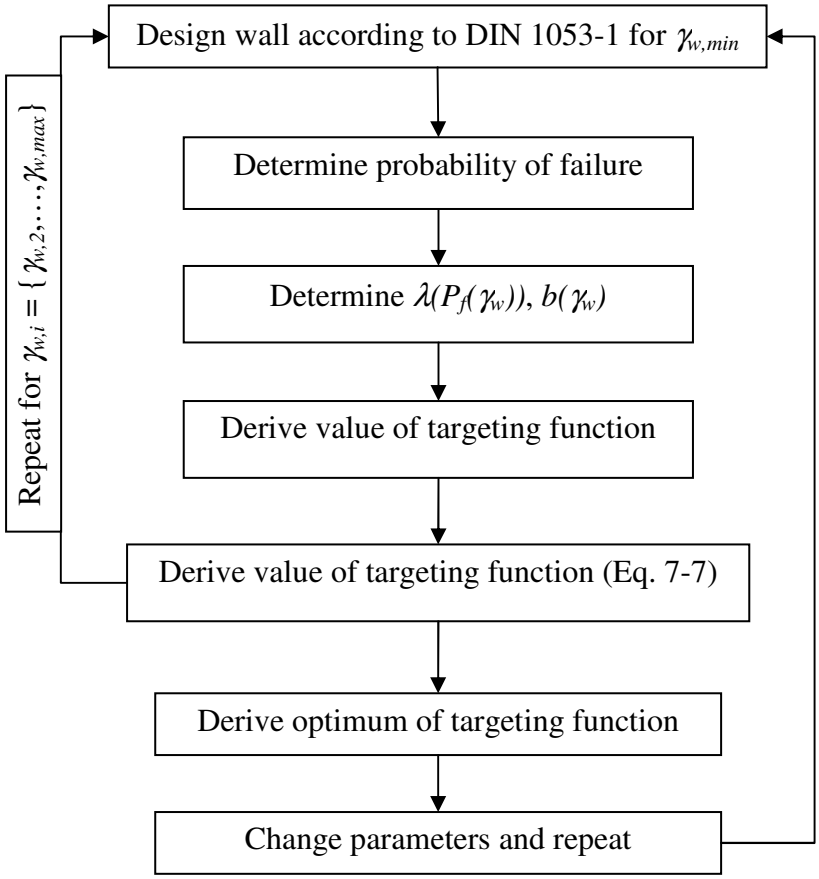

Figure 7-7 Flow chart of the optimization procedure

7.3 Results of the Optimization

The targeting function (Eq. 7-7) depends on a number of parameters. Most of the parameters were quantified in the previous section. However, the parameter A that influences the benefit $b(\gamma_w)$ must be estimated. In the following, the optimization will be conducted and the influence of the parameters will be analysed in order to determine the optimal reliability for common masonry structures.

The result of the optimization is an optimal value for the partial safety factor on the wind load γ_w which actually represents an optimal value of the failure probability, thus the results are not influenced by shear slenderness or level of axial load. However, the approximate relationship between failure probability and γ_w must be known since the distribution of the benefit versus γ_w has to correspond to the distribution of the failure probability P_f. To obtain probabilities of failure on the safe side and since slender walls were shown to be more critical, the optimization is executed for walls with a shear slenderness of $\lambda_v = 3.0$. Another positive effect of this choice is that the distribution of the relationship of P_f and γ_w is similar for all three investigated materials in case of slender walls. Thus, the

obtained results are also similar. A differentiation between the three materials and codes is unnecessary.

As was shown previously, the boundaries of the parameter $f(p)$ (see Table 2.6-3) suggested by the *JCSS (2001)* for medium failure consequences represent common masonry buildings. These values will be used here ($f(p) = \{2.5; 3.5\}$).

Generally, three parameters have an effect on the optimization results. The first one, the benefit-cost ratio, mirrors the payoff of the investment. Larger ratios will lead to smaller values of the optimized reliability because in case of large benefit, larger risk can be accepted and vice versa.

The second influence is the impact of the consequences of enhanced reliability on the benefit, denoted as A, in terms of satisfied users and possible higher rents. Larger values of A lead to smaller values of the optimized reliability since benefit increases more significantly with larger probability of failure. However, this parameter is highly subjective and depends on the perception of the buyer. Large values of A correspond to greater perceived benefit in case of purchase/construction but also mean large disappointment in the other case.

The third influence is the failure consequences accounted for by the factor $f(p)$. Of course, high potential of large failure consequences will also lead to a large value of the target reliability.

Table 7.3-1 Influences on the optimization results

Influence	Referred to as
benefit-cost ratio	b_0/C_0
factor representing the impact of higher reliability on the benefit	A
failure consequences	$f(p)$

The benefit-cost ratio depends on the location of the structure since the rent and the quality of furnishings and finishings are strongly influenced by the economic prosperity of a municipality. Three typical scenarios for Germany are defined in the following and used for assessment. These scenarios are supposed to represent an average rural, urban and high-class location of the structure.

Table 7.3-2 Standard scenarios

Scenario	b_0	C_0	b_0/C_0
rural	74 €/(m²·a)	1000 €/m²	0.074
urban	108 €/(m²·a)	1200 €/m²	0.090
high-class	142 €/(m²·a)	1400 €/m²	0.101

In the following, the optimization results for rural, urban and high-class locations will be presented. The assessment is carried out for different values of A. In Figure 7-8 to Figure 7-10, the targeting function is presented for $f(p) = 2.5$. It can be seen that larger values of A lead to smaller values of the optimal reliability. This is logical; greater benefit makes

greater risk acceptable. However, since large values of A not only represent a stronger gain in benefit for small values of γ_w but also a stronger reduction in benefit for large values of γ_w, the targeting function stays positive within a smaller range for larger values of A than for smaller values. Only positive values of the targeting function are useful.

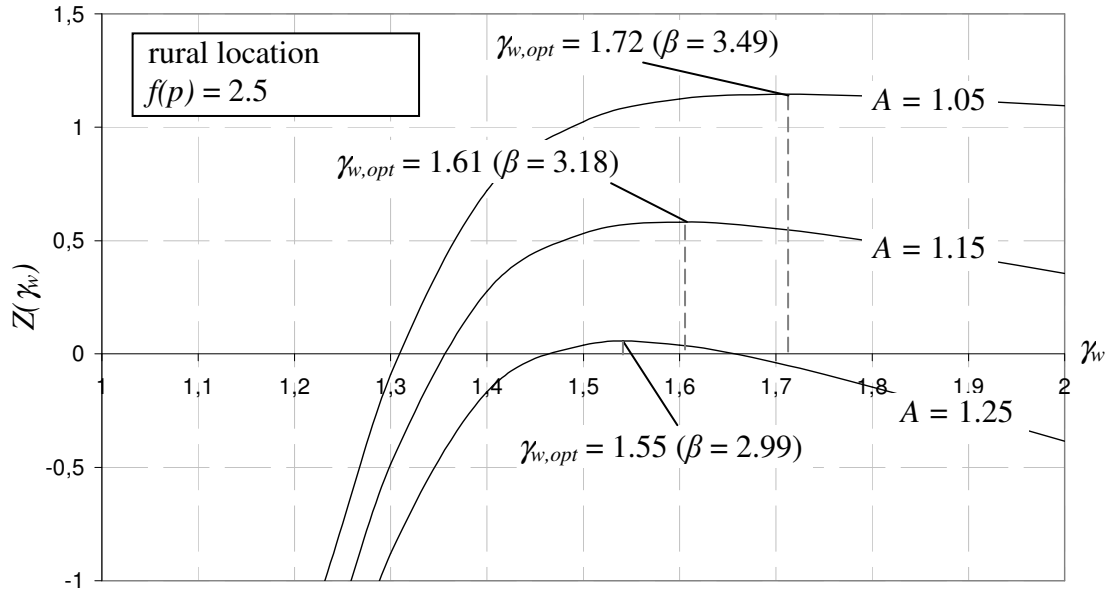

Figure 7-8 Influence of the parameter A for rural location (f(p) = 2.5)

As expected, the optimal reliability is slightly smaller for urban (Figure 7-9) and high-class (Figure 7-10) locations than for rural regions (Figure 7-8). Larger values of b_0/C_0 give smaller values of the optimal reliability since the benefit is governing compared to the structural cost.

The influence of the location of the structure is existent but not critical. The optimal reliability index changes by less than 0.2 depending on the location. This can be accepted since it is in the region of the acceptable scatter of β. The influence of the parameter A is stronger; changes up to 0.5 are detected for a change in A of 25%.

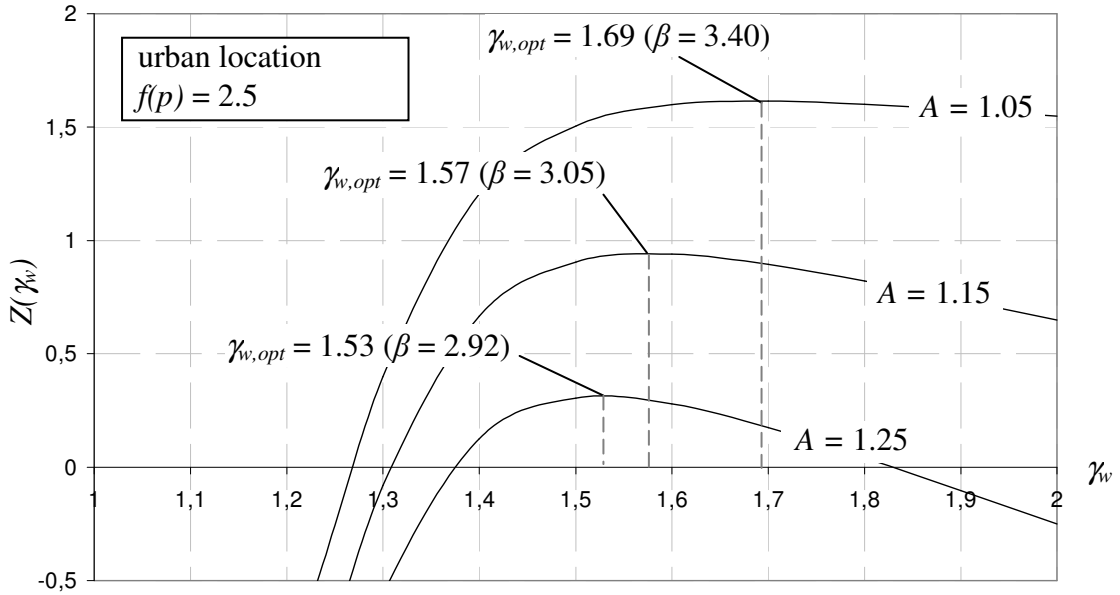

Figure 7-9 Influence of the parameter A for urban location (f(p) = 2.5)

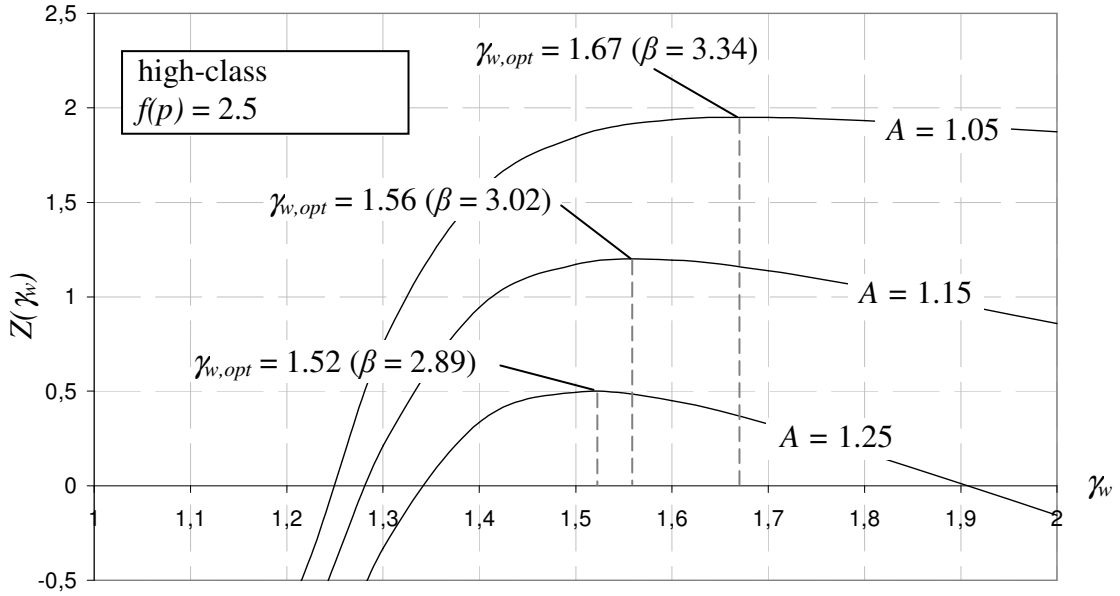

Figure 7-10 Influence of the parameter A for high-class location (f(p) = 2.5)

The influence of the failure consequences can be evaluated by varying *f(p)*. As determined in the previous section, the scenario of a masonry building with large failure consequences can be represented by $f(p) \approx 3.5$. The corresponding optimization results are presented in Table 7.3-3. The results show only minor impact of the factor *f(p)* when the average failure scenario ($f(p) = 2.5$) changes to a scenario of higher risk ($f(p) = 3.5$), (see Figure 7-11). Overall, the values derived for the target reliability lie within a range of $\beta = 2.9 - 3.5$ where the large values are only reached for very small values of *A*. With increasing *A*, the target reliabilities decrease and quickly reach values of 3.2 and below. However, the realistic value of *A* remains unknown.

Table 7.3-3 Summary of the obtained optimization results

$f(p)$	Rural			Urban			High-class			$\beta_{opt,ave}$
	A			A			A			
	1.05	1.15	1.25	1.05	1.15	1.25	1.05	1.15	1.25	
2.5	3.49	3.18	2.99	3.40	3.05	2.92	3.34	3.02	2.89	3.14
3.5	3.51	3.26	3.05	3.49	3.18	2.96	3.46	3.17	2.96	3.23

An important aspect that has to be included in the estimation of A is that in today's construction the length of shear walls is often limited because of the width of the property. So the question arises as to whether a house can or cannot be built. Thus, change in benefit can be significant. In addition, the requirement of longer shear walls would lead to a smaller number of (larger) town houses and thus to higher prices and more expensive living. Therefore, the benefit to the renter is smaller, since longer shear walls will increase the rent in the long-term. Shorter shear walls can therefore additionally contribute to the benefit of the renter by reducing rent in the long run. Note, that this argumentation is only appropriate assuming acceptable reliability is still provided; the question is not whether an unsafe house is better than no house.

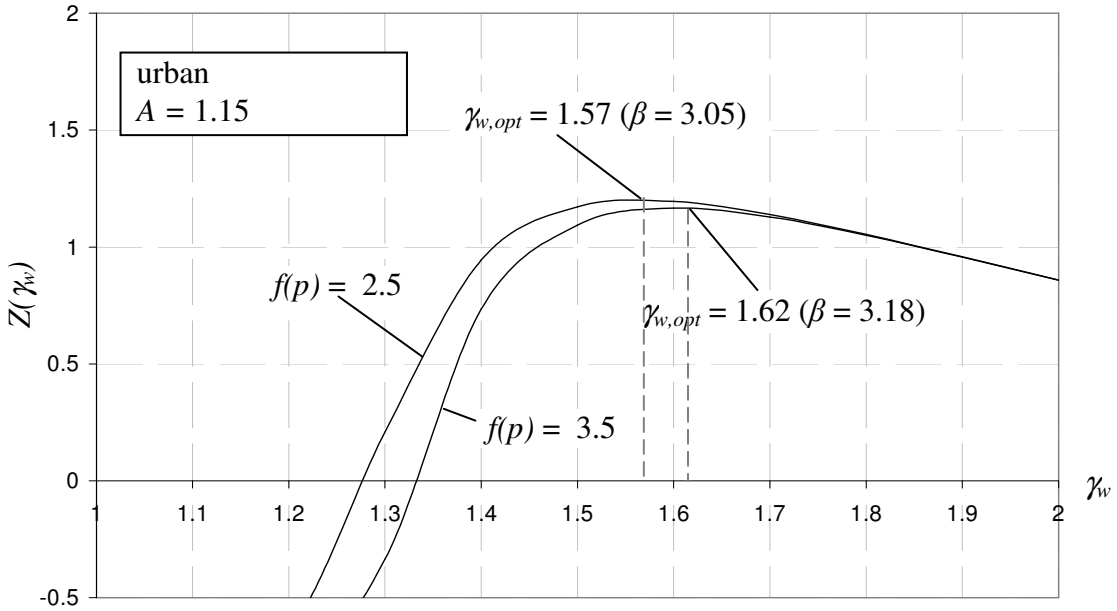

Figure 7-11 Comparison of the target functions for urban location and different values of f(p)

7.4 Conclusion

In the previous section, the economically optimal target reliability for typical masonry structures was determined. It was shown that the individual risk of a structure has a significant influence on the reliability but the scope for common masonry structures is limited. The optimisation results for different risks and scenarios are in the range of $\beta = 2.9 - 3.5$ and the average values for $f(p) = 2.5$ and $f(p) = 3.5$ are very close. Looking at the range of the results, the optimal target reliability of common masonry houses is

$\beta_{opt,target}$ = 3.2 with a deviation of $\Delta\beta = \pm 0.3$. This, again, is nearly equal to the results obtained for existing structures ("actual" level of reliability, see section 6.8.3 and Table 6.9-1). One must conclude here that the current design codes in Germany lead to acceptably reliable structures for the assumptions herein. Design according to DIN 1053-1 comes closer to the economic optimal value while DIN 1053-100 and DIN EN 1996-1-1/NA lead to more conservative design. The current partial safety factors do not require modification. The target reliability of DIN EN 1990 (β = 3.8) proves to be overly conservative; the recommendation of *JCSS (2001)* represents the economic optimum.

7.5 Summary

In this chapter, a probabilistic optimization for typical masonry structures was executed. For this purpose, a targeting function including benefit derived from the structure, the structural cost and the failure consequences was determined. The targeting function was rearranged and modified so that only a small number of parameters were identified to be influencing the results. These parameters are the location of the structure (represented by the ratio of benefit-to-structural cost), the severity of the failure consequences and the parameter A that represents the impact of changes to enhance structural reliability on the benefit. The material, the level of axial load and the shear slenderness of the walls do not influence the results.

By using collected data and engineering judgement, the contributions to the targeting function were quantified. Stochastic models were derived for the benefit and structural cost. The failure consequences, mostly governed by the costs to society to save lives (SLSC), were evaluated by assessment of three scenarios representing typical masonry buildings. The recommendations of *JCSS (2001)* for average failure consequences were verified by Monte Carlo simulation.

The optimization yielded economically optimal reliabilities for typical masonry structures. The parameter A has a significant influence on the results, although it is difficult to estimate. A value of A = 1.15 seems reasonable and is recommended by the author. The recommended economic optimal target reliability is β_t = 3.2 with an acceptable deviation of $\Delta\beta = \pm 0.3$.

It was found that the optimal reliabilities come very close to the actual provided reliability. Therefore, it can be concluded that the design of common masonry structures in German according to the design codes DIN 1053-1, DIN 1053-100 and DIN EN 1996-1-1/NA provide sufficiently reliable structures with DIN 1053-1 almost equalling the economic optimum.

8 SUMMARY AND OUTLOOK

The goal of this thesis was the assessment of the reliability of URM shear walls, the verification of the target reliability provided by DIN EN 1990 and the scientific derivation of a justified target reliability. The study was prompted by the large variety of safety factors all over the world which were assumed to be based on different values for the target reliability. In addition, reliability of masonry structures was mainly historically based on empirical optimization; a scientific assessment of the reliability was necessary especially considering the recent developments in standardization. The safety concept was changed from the concept of global safety factors in DIN 1053-1 to the semi-probabilistic safety concept in DIN 1053-100 which led to a reduction in the shear capacities predicted by the codes. No structural failure initiated by failure of a shear wall where wind load is the governing horizontal load has been reported in Germany. Thus, the question arose as to whether the old or new codes provide the more appropriate level of reliability and efficiency.

After the introduction and the outline of the study were presented in chapter 1, chapter 2 provided the reader with the required basics of reliability analysis. The concept of probabilistic analysis was explained and the methods of estimating stochastic moments were presented. The concept of reliability analysis and the corresponding methods for calculation of the failure probability were summarized. Additionally, the concept of probabilistic optimization based on the targeting function of *Rosenblueth & Mendoza (1971)* was explained and some recommendations for the target reliability were discussed. The concept of the Life Quality Index for the quantification of failure consequences due to loss of human life was briefly introduced.

In chapter 3, the typical loads that act on masonry shear walls were analysed. These are dead load due to the self-weight of the structure, live load due to occupancy of the building and wind load. The general concept of distributions of extremes was explained. Dead load is essential to the shear capacity of masonry members. As axial load in general, it can act favourably and unfavourably to the load-carrying capacity of the wall. It also represents the largest contribution to the axial load; the typical ratio of dead-to-live load in masonry buildings is 70:30. The stochastic model for the dead load was derived from the contributions of walls and slabs. Modelling the live load is significantly more complex than modelling the dead load due to the variability over time and location. Stochastic fields and processes must be applied. From there, the different contributions to the live load, the permanent and short-term load, were determined. For design purposes the point-in-time live load is converted to the distribution of extremes for an observation period of 50 years by using a *Gumbel* distribution to account for the time-dependence and to avoid time-variant probabilistic analyses using stochastic processes. In the next step, the wind load which is the relevant horizontal load for typical masonry shear walls was discussed.

The wind load strongly depends on the structure. Effects of resonance have to be taken into account, as well as the shape of the structure. Of course, the wind load also depends on the wind speed which is a function of many parameters, e.g. altitude or geographical location. The model presented by *König & Hosser (1982)* includes these aspects and makes it possible to derive a wind load acting on the structure. For the stochastic modelling of the wind load a *Weibull* distribution was chosen due to its upper limit. This makes sense; wind load is limited by a physical maximum. To derive the 50 year distribution of extremes, the stochastic shape parameter was determined from a database of wind measurements for an observation period of 1 year. Then, a Monte Carlo simulation was conducted and the distribution of the wind load was obtained. It was shown that the characteristic values of the wind load according to DIN 1055-4 are within an acceptable range. In the last step, the model uncertainties for axial and shear load were defined according to *JCSS (2003)*.

In chapter 4, the basic knowledge about the load-carrying behaviour of URM walls was provided. First, the general load-carrying behaviour of URM walls subjected to axial load and in-plane shear was explained and the relevant material properties were mentioned. Unreinforced masonry walls exhibit complex load-carrying behaviour; various failure modes are possible depending on the geometry of the wall, the absolute value of stress and the masonry properties, among other influences. The corresponding material properties were explained and assessed. Typical test procedures were discussed and the values from design codes were analysed for each material property. The stochastic models were derived from test data and values available in the literature. To minimize the uncertainty due to the limited sample size, some properties were updated with prior information by use of Bayesian techniques. In such a way, appropriate stochastic models were derived for all required material properties.

Chapter 5 introduces the reader to the methods of shear capacity prediction of masonry walls subjected to in-plane shear. The most common linear approaches were presented. The failure modes that are related to shear failure and the corresponding modelling were explained. Models based on plastic limit state analysis were also mentioned and briefly discussed but were not considered useful for the subject of this thesis. The models presented range from scientific models such as *Mann & Müller (1973)* and *Jäger & Schöps (2004)* to design models from various codes. The models were introduced and non-dimensional design equations were provided. A large variety of prediction models for the shear capacity were provided and discussed. The selection consists of various models; German and international design models were part of the assessment as well as scientific models. The models were checked with test data in order to identify the most realistic model. The model of *Mann & Müller* and the model of DIN EN 1996-1-1/NA were found to match the test data most accurately in case of sliding shear and diagonal tension depending on the unit material. For flexural failure, prediction on the basis of a fully-plastic

stress-strain relationship showed good agreement with the test data. Since the assessment of the tests was very uncertain due to the limited number of samples and other sources of uncertainty, a Bayesian update was again carried out applying prior information in terms of expert opinions. By performing the update, the stochastic properties of the prediction models were derived. However, the stochastic model for shear crushing had to be estimated since test data is not available. For each unit material, the most appropriate model for failure prediction was chosen as the basis for the subsequent probabilistic reliability analysis.

In chapter 6, the reliabilities provided by three design codes for common shear walls were assessed. Starting with an outline of the procedure, the required steps were explained. The limit state functions were provided in non-dimensional form for every failure mode.

In general, it was found that the theoretical reliability of URM shear walls depended on the shear slenderness with slender walls being significantly more critical than squat walls. This is also characterized by the relation of eccentricity and reliability: large eccentricity means small reliability. In case of slender walls, the target values of *JCSS (2001)* and DIN EN 1990 were not reached within the practical range of axial stress. These findings are valid for the unit materials examined (CS, CB, AAC); lightweight concrete was not investigated due to insufficient test data. It was also found that a jump in reliability occurs when maximum axial load governs the design. The reason for this jump is the difference in the predicted failure modes according to the stochastic model in the reliability analysis and in the design model.

Since the tensile strength of AAC units is significantly underestimated in DIN 1053-1 and DIN 1053-100, the design shear capacities in case of diagonal tension failure are very small. Thus, the values of the reliability of squat AAC walls are extraordinarily high for DIN 1053-1 and DIN 1053-100. This shortcoming was addressed in DIN EN 1996-1-1/NA, for which the reliability is smaller when diagonal tension is relevant but still high.

It was also shown that the model uncertainties were the dominating basic variables as long as minimum load governs. When maximum axial load governs (shear crushing and flexural failure under maximum load), model uncertainties lose their influence and only the masonry compressive strength and the axial load influence the results. Wind load was also found to be a relevant parameter but the influence was smaller than expected because of the small scatter in the *Weibull* distribution used.

Due to the long history of application, the reliability of walls designed according to DIN 1053-1 can be seen as a minimum average value in common masonry construction. The theoretical values assuming full utilization of the cross-section for slender walls were determined to be $\beta \approx 2.0$ for CS walls, $\beta \approx 2.1$ for CB walls and $\beta = 2.9$ for AAC walls. All values are valid for an observation period of 50 years. If the walls are designed according to DIN 1053-100 or DIN EN 1996-1-1, greater reliability is provided due to more

appropriate application of the safety factors in the design. The minimum values for the slender walls were very similar for these two codes since the check against flexural failure is identical. Slender walls were most likely to fail in flexure. For CS walls the average reliability index for a slender wall with $\lambda_v = 3.0$ is $\beta \approx 2.6$, for CB $\beta = 2.9$ and for AAC $\beta = 3.2$ when the wall is designed according to DIN 1053-100 or DIN EN 1996-1-1/NA. Again, these values are only valid for full utilization of the cross-section which is unlikely to occur for CS and CB walls due to the higher strength of the materials.

Since masonry has historically exhibited sufficient reliability, the "actual" level of reliability was determined by use of an example masonry house. The actual reliability was expected to be significantly greater than the previously obtained theoretical reliability due to taking into account the realistic utilisation which is believed to be smaller than 100%. Since the actual wind loads acting on a structure are equal and independent from the wall material, it is obvious that the high-strength materials CS and CB must be utilized to a lesser degree than AAC. The utilization of the bracing walls was determined and the reliability was calculated for the smaller levels of utilization. For the walls with the highest level of utilization reliabilities of $\beta \approx 3.2$ (CS), $\beta \approx 3.1$ (CB) and $\beta \approx 3.0$ (AAC) were determined.

To define a scientifically verified value for the target reliability especially for common masonry structures, a fully-probabilistic optimization was performed in chapter 7 for typical masonry building scenarios. For this purpose, a targeting function including benefit derived from the structure, the structural cost and the failure consequences was determined. The targeting function was rearranged and modified so that only a small number of parameters were identified to be influencing the results. These parameters were the location of the structure (represented by the ratio of benefit-to-structural cost), the severity of the failure consequences and the parameter A that represents the impact of changes to enhance structural reliability on the benefit. Since the optimization parameter is independent from the material, it was unnecessary to differ between the unit materials.

The contributions to the targeting function were quantified using data from the literature and engineering judgement. To classify the failure consequences, stochastic models were derived for benefit and structural cost and a Monte Carlo-simulation was conducted. It was found that the recommendations of *JCSS (2001)* for average failure consequences represent typical masonry structures very well. The failure consequences were classified as "medium" for typical masonry structures.

In the optimisation, optimal reliabilities between $\beta = 2.9$ and $\beta = 3.5$ were obtained for the scenarios and parameter combinations assessed. From here, a recommendation for the target reliability was derived which is $\beta_t = 3.2$ with an acceptable deviation of $\Delta\beta = \pm 0.3$. This value agrees with the "actual" reliabilities determined and leads to the conclusion

that masonry structures designed according to the investigated codes are sufficiently safe. Design according to DIN 1053-1 comes very close to the economically optimal value.

Future research should focus on the stress redistribution in masonry structures and the realistic determination of the load effects and realistic calculation of the utilization of the wall. There is great potential for further enhancement of the efficiency of masonry structures., The assessment of the realistic structural system is especially important in order to assess realistic levels of utilization. In addition, the test database should be expanded to improve the derived stochastic and deterministic design models for masonry properties and model uncertainties. The test procedures should include aspects of stochastic assessment in the execution of the tests, e.g. a repeated determination of the cohesion before the shear tests are conducted. Lightweight concrete and concrete blocks should be the subject of a future study. A more detailed assessment of the failure consequences linked to structural failure of residential and office structures should be conducted to obtain benchmarks for the cost related to failure to derive a detailed database for fully-probabilistic assessment and design.

9 REFERENCES

Books and Technical Papers:

Arteaga, A. (2004): Classification of actions – Development of skills facilitating implementation of Eurocodes: Basis of structural design, Garston, Watford, UK, in English

Bayes, T. (1763): An Essay towards solving a Problem in the Doctrine of Chances. By the late Rev. Mr. Bayes, communicated by Mr. Price, in a letter to John Canton, M.A. and F.R.S., Philosophical Transactions of the Royal Society of London, Vol. 53, in English

Benjamin, J.R. & Cornell, C.A. (1970): Probability, Statistics and Decision for Civil Engineers, McGraw-Hill Book Company, New York, in English

Benjamin, J.R. & Williams, H.A. (1958): The behaviour of one-story-brick shear walls, Proceedings of the American Society of Civil Engineers, papers 4, in English

BKI (2010): BKI Baukosten 2010: Statistische Kostenkennwerte für Bauelemente, Editor: Baukosteninformationszentrum Deutscher Architektenkammern, Müller, Cologne, in German

Bojsiljkov, V & Tomazevic, M. (2005): Optimization of shape of masonry units and technology of construction for earthquake resistant masonry buildings, research report, University of Ljubljana, in English

Bojsiljkov, V; Tomazevic, M; Lutman, M (2004): Optimization of shape of masonry units and technology of construction for earthquake resistant masonry buildings, research report, University of Ljubljana, in English

Brameshuber, W. & Schmidt, U. (2006): Untersuchungen zur Bestimmung von Stoffgesetzen von Kalksandsteinen und des Verbundes – Experimentelle Untersuchungen, research report F 7044/1, RWTH Aachen, in German

CEB (1976): First Order Reliability Concepts for Design Codes, CEB Bulletin d'Information, No. 112

Chalk, P. L. & Corotis, R. B. (1980): Probability Model for Design Live Loads, Journal of the Structural Division, Vol. 106, No. St10, ASCE, in English

CIB W81 (1989a): Actions on Structures, Self-weight loads, Report No. 115, Rotterdam, in English

CIB W81 (1989b): Actions on Structures, Live Load in Buildings, Report No. 116, Rotterdam, in English

Cornell, C.A. (1969): A Probability Based Structural Code, ACI Journal, Vol. 66, No. 12, in English

Costa, A. (2007): Experimental testing of lateral capacity of masonry piers, doctoral thesis, University of Pavia, in English

Coulomb (1776), C.A. de: Essai sur une application des regles de maximis et minimis a quelques problemes de statique relatifs a l'architecture, Memoires Acad. Science 1776

DGfM (2008): Annual report 2007/2008, Deutsche Gesellschaft für Mauerwerksbau e.V., Berlin

ESECMaSE (2004): Enhanced Safety and Efficient Construction of Masonry Structures in Europe (ESECMaSE), Deliverable 2.3, TU München

Fehling, E. & Stürz, J. (2006.a): Test results on the behaviour of masonry under static (monotonic and cyclic) in plane lateral loads, Technical Report D7.1a of the collective research project ESECMaSE, 2006, in English

Fehling, E. & Stürz, J. (2006.b): Experimentelle Untersuchungen zum Schubtragverhalten von Porenbetonwandscheiben, Research Report, Universität Kassel, 2006, in German

Ferry Borges, J. & Castanheta, M. (1971): Structural Safety, Laboratorio Nacional de Engenharia Civil, Lisbon, in English

Freundenthal, A.M. (1947): Safety of Structures, Trans. ASCE, Vol. 112, in English

Freundenthal, A.M. (1956): Safety and Probability of Structural Failure, Trans. ASCE, Vol. 121, in English

Galambos, T.V.; Ellingwood, B.; MacGregor, J.G.; Cornell, C.A. (1982): Probability Based Load Criteria, Assessment of Current Design Practice, Journal of the Structural Division, Vol. 108, St5, in English

Ganz, H.R. (1985): Mauerwerksscheiben unter Normalkraft und Schub, doctoral thesis, Swiss Federal Institute of Technology Zurich, in German

Gayton, N.; Mohamed, A.; Sørensen, J. D.; Pendola, M.; Lemaire, M. (2004): Calibration methods for reliability-based design codes, Structural Safety, Volume 26, Issue 1, in English

Glock, C. (2004): Traglast unbewehrter Beton- und Mauerwerkswände, doctoral thesis, Technische Universität Darmstadt, in German

Glowienka, S. (2007): Zuverlässigkeit von Mauerwerkswänden aus großformatigen Steinen, doctoral thesis, Institut für Massivbau, Technische Universität Darmstadt, Darmstadt, in German

Graubner, C.-A. & Glowienka, S. (2005a): Contrasting different safety concepts, meeting of the FIB-Comission 2, Vienna, in English

Graubner, C.-A. & Glowienka, S. (2005b): Zuverlässigkeitsanalysen von Stahlbetondruckgliedern unter besonderer Berücksichtigung des Teilsicherheitsbeiwertes γ_G auf der Einwirkungsseite, research report of DAfStb project V 425, Berlin, in German

Graubner, C.-A. & Glowienka, S. (2007): Probabilistisch fundierte Analyse von Tragreserven bei Mauerwerksgebäuden zur kostengünstigeren Bemessung von Druckgliedern und Biegebauteilen unter Eigenlast, research report, Institut für Massivbau, TU Darmstadt, in German

Graubner, C.-A. & Simon, E. (2001): Zur Schubtragfähigkeit von Mauerwerk aus großformatigen Steinen, Mauerwerk-Kalender 2001, Ernst & Sohn, Berlin, in German

Graubner, C.-A. & Brehm, E. (2009): Analyse der maßgebenden Einwirkungskombinationen zur rationellen Bemessung von unbewehrtem Bauteilen im üblichen Hochbau, research report F07-6-2009 of the Institut für Massivbau, Technische Universität Darmstadt, in German

Grünberg, J. (2004): Grundlagen der Tragwerksplanung - Sicherheitskonzept und Bemessungsregeln für den konstruktiven Ingenieurbau - Erläuterungen zur DIN 1055-100, Deutsches Institut für Normung e.V., Berlin, in German

GruSiBau (1981): Grundlagen zur Festlegung von Sicherheitsanforderungen für bauliche Anlagen (GruSiBau), NA Bau, Beuth Verlag, Berlin, in German

Gumbel, E. J. (1958): Statistics of Extremes, Columbia University Press, New York

Gunkler, E.; Budelmann, H.; Sperbeck, S. (2009): Schubtragfähigkeit von Kalksandsteinwänden aus KS XL-PE mit geringem Überbindemaß, research report No. 25/09,

Hasofer, A.M. & Lind, N.C. (1974): An Exact and Invariant First order Reliability Format, Journal of the Eng. Mech. Div., ASCE, Vol. 100, EM1, in English

Hausmann, G. (2007): Verformungsvorhersage vorgespannter Flachdecken unter Berücksichtigung der stochastischen Eigenschaften, doctoral thesis, Technische Universität Darmstadt, in German

Hendry, A.W. & Sinha, B.P. (1969): Racking Tests on Storey-Height Shear Wall Structures with Openings Subjected to Pre-compression; Designing, Engineering and Constructing with Masonry Products

Hendry, A.W. & Sinha, B.P. (1971): Shear Tests on Full Scale Single Storey Brickwork Structures Subjected to Pre-Compression, Civ. Engng. Publ. Wks. Rev. 66

Holicky, M. & Markova, J. (2002): Calibration or Reliability Elements for a Column, JCSS workshop on reliability based code calibration, Zurich

Höveling, H.; Steinborn, T.; Schöps, P. (2009): Schubtragfähigkeit von Mauerwerk aus Porenbeton-Plansteinen und Porenbeton-Planelementen“, research report AiF-Nr. 14642BG, Leibniz Universität Hannover

IVD (2009): IVD-Wohn-Preisspiegel 2008/2009, IVD Immobilienverband Deutschland, Berlin, in German

Jäger, W. & Schöps, P. (2004): Kosteneinsparung durch Ansatz realitätsnaher Bemessungskonzepte für die Schubbeanspruchung von Mauerwerksbauten, research report F 2461 of the Federal Ministry of Transport, Building and Urban Development, Berlin, in German

Jäger, W. & Schöps, P. (2005): Sichtung und Vorauswertung von Schubversuchen, research report, Technische Universität Dresden, in German

Jäger, W.; Fehling, E.; Schermer, D.; Stürz, J.; Schöps, P. (2008): Chancen und Möglichkeiten von ESECMaSE – Konsequenzen für die Modellierung von Mauerwerksgebäuden, Mauerwerk, Volume 12, Issue 4, August 2008, in German

Jäger, W.; Ortlepp, S.; Schöps, P.; Richter, C. (2011): Vergleich der normativen Ansätze zum Nachweis von Aussteifungsscheiben im Gebäude nach DIN 1053-1/-100, EN 1996-1-1 und dem Forschungsvorhaben ESECMaSE hinsichtlich des Sicherheitsniveaus, research report ZP 52-515.86-1309/09, Deutsches Institut für Bautechnik (DIBt), Berlin, in German

JCSS (2001): Probabilistic Assessment of Existing Structures, RILEM Publications. S.A.R.L., in English

JCSS (2003): Probabilistic Model Code, Joint Committee on Structural Safety, www.jcss.ethz.ch, in English

Kasperski, M. (2000): Festlegung und Normung von Entwurfswindlasten, Habilitation, Ruhr-Universität Bochum, in German

Kelch, T. & Norman, W. (1931): Methods used in testing masonry specimens for bonding tension and shear, Journal American Ceramic Society, Vol. 2, in English

Kickler, J. (2003): Bruchmechanische Berechnungsmethoden im Mauerwerksbau, Ernst & Sohn, Bautechnik 80, Vol. 8, Berlin, in German

Kirtschig, K. & Kasten, D. (1980): Zur Festlegung von Mauerwerksklassen bei Ingenieurmauerwerk – In Mauerwerk-Kalender 1980, Ernst & Sohn, Berlin

König, G. & Hosser, D. (1982): Baupraktische Beispiele und Hinweise zur Festlegung von Sicherheitsanforderungen für bauliche Anlagen nach Empfehlung des NABau, Bauingenieur 57, Springer, Berlin, in German

König, G.; Mann, W.; Ötes, A. (1988): Untersuchungen zum Verhalten von Mauerwerksbauten unter Erdbebeneinwirkung, IRB-Verlag, Frankfurt am Main, in German

Kranzler, T. (2008): Tragfähigkeit überwiegend horizontal beanspruchter Aussteifungsscheiben aus unbewehrtem Mauerwerk, doctoral thesis, Institut für Massivbau, Technische Universität Darmstadt, Darmstadt, in German

Kühlmeyer, M. (2001): Statistische Auswertungsmethoden für Ingenieure, Springer Velag, Berlin, in German

Löring, S. (2005): Zum Tragverhalten von Mauerwerksbauten unter Erdbebeneinwirkung, doctoral thesis, Universität Dortmund, in German

Madsen, H.O., Krenk, S., Lind, N.C. (1986): Methods of Structural Safety, Prentice-Hall Inc., Englewood Cliffs, New Jersey, in English

Magenes, G. (2007): Report on static-cyclic tests at University of Pavia, Presentation at ESECMaSE Dissemination Meeting, Cologne, 2007

Mann, W. & Müller, H. (1973): Bruchkriterien für querkraftbeanspruchtes Mauerwerk und ihre Anwendung auf gemauerte Windscheiben, Die Bautechnik, Heft 12, Ernst & Sohn, Berlin, in German

Mann, W. & Müller, H. (1978): Schubtragfähigkeit von Mauerwerk, in: Mauerwerk-Kalender 3, Ernst & Sohn, Berlin, in German

Mann, W. (1983): Druckfestigkeit von Mauerwerk – Eine statistische Auswertung von Versuchsergebnissen in geschlossener Darstellung mithilfe von Potenzfunktionen, Mauerwerk-Kalender 1983, Ernst & Sohn, Berlin, in German

Marten, K. (1975): Zur Festlegung wirklichkeitsnaher Nutzlasten und Lastabminderungsfaktoren, doctoral thesis, TU Darmstadt, in German

Mayer, M. (1926): Die Sicherheit der Bauwerke, Springer, Berlin, in German

Melchers, R.E. (1999): Structural reliability and prediction, John Wiley & Sons Ltd., Chichester, in English

Meyer, U. (2005): Weißdruck der Erdbeben-Norm DIN 4149 – Ausgabe April 2005, AMz-Bericht 7/2005, Arbeitsgemeinschaft Mauerziegel im Bundesverband der Deutschen Ziegelindustrie e.V., Bonn, in German

Mojsilovic, N. & Marti, P. (1997): Strength of Masonry Subjected to Combined Actions, ACI Structural Journal, No. 6, 1997, English

Mojsilovic, N. & Schwartz, U. (2006): Swiss Masonry Code Design Charts for Shear Walls, Proceedings of the 7th International Masonry Conference, International Masonry Society, London, in English

Mojsilovic, N. (1995): Zum Tragverhalten von kombiniert beanspruchtem Mauerwerk, doctoral thesis, Swiss Federal Institute of Technology, Zurich, in German

Nathwani, J. S.; Lind, N. C.; Pandey, M. D. (1997): Affordable Safety by Choice: The Life Quality Method, Institue for Risk research, University of Waterloo, Waterloo, Canada, in English

Niemann, H. (2009): Prognose extremer Sturmstärken mit Hilfe von PROGumbel, Niemann & Partner, Workshop on PROGumbel, November 19-20, Bochum, in German

Ötes, A. & Löring, S. (2003): Tastversuche zur Identifizierung des Verhaltensfaktors von Mauerwerksbauten für den Erdbebennachweis, research report for the DGfM, December, Dortmund, in German

Page, A.W. (1978): Finite Element Model for Masonry, Journal of the Structural Division, ASCE, Vol. 104, 1978, in English

Page, A.W. (1980): A Biaxial Failure Criterion for Brick Masonry in the Tension-Tension Range, The International Journal of Masonry Construction, Vol. 1, in English

Page, A.W. (1981): The Biaxial Compressive Strength of Brick Masonry, Proceedings of the Institution of Civil Engineers, Vol. 71, in English

Page, A.W. (1982): An Experimental Investigation of the Biaxial Strength of Brick Masonry, proceedings of the 6th International Brick Masonry Conference, Rome, in English

Pandey, M. D.; Yuan, X.-X.; Noortwijk, J. M. (2005): Gamma process model for reliability analysis and replacement of aging structural components, The 9th International Conference of Structural Safety and Reliability (ICOSSAR-9), Rome, Italy, 19 - 23 June 2005, in English

Pandey, M.D.; Nathwani, J.S.; Lind, N.C. (2006): The derivation and calibration of the life-quality index (LQI) from economic principles, Structural Safety, 28, in English

Papula, L. (2001): Mathematik für Ingenieure und Naturwissenschaftler – Band 3, 4th Edition, Friedrich Vieweg & Sohn, Braunschweig/Wiesbaden, in German

Parker, C.K.; Tanner, J.E.; Varela, J.L. (2007): Evaluation of ASTM Methods to Determine Splitting Tensile Strength in Concrete, Masonry, and Autoclaved Aerated Concrete, Journal of ASTM International, Vol. 4, No. 2, in English

Popal, R. & Lissel, S.L. (2010): Numerical Evaluation of Existing Mortar Joint shear Tests and a New Test Method, Proceedings of the 8th International Masonry Conference in Dresden, International Masonry Society, London, in English

Pottharst, R. (1977): Zur Wahl eines einheitlichen Sicherheitskonzeptes für den konstruktiven Ingenieurbau, Mitteilungen des Institutes für Massivbau der Technischen Universität Darmstadt, Ernst & Sohn, Berlin, in German

Probst, P. (1981): Ein Beitrag zum Bruchmechanismus von zentrisch gedrücktem Mauerwerk, doctoral thesis, Technische Universität München

Rackwitz, R. & Fießler, B. (1978): Structural Reliability under Combined Random Load Sequences, Computers and Structures, Vol. 9, in English

Rackwitz, R. & Streicher, H. (2002): Optimization of Target Reliabilities, JCSS Workshopn on Reliability Based Code Calibration, Swiss Federal Institute of Technology, Zurich, Switzerland, March 21-22, 2002, in English

Rackwitz, R. (1982): Predictive Distribution of Strength under Control, Berichte zur Zuverlässigkeitstheorie der Bauwerke, Sonderforschungsbereich 1982, Heft 66/1982, TU München, in English

Rackwitz, R. (1996): Einwirkungen auf Bauwerke, in: Der Ingenieurbau: Tragwerkszuverlässigkeit, Einwirkungen. Ernst & Sohn, Berlin, in German

Rackwitz, R. (2004): Zuverlässigkeit und Lasten im konstruktiven Ingenieurbau, TU München, in German

Rackwitz, R. (2008): The Philosophy Behind the Life Quality Index and Empirical Verification, Basic Documents on Risk Assessment in Engineering, Joint Committee on Structural Safety, Document 4, in English

Raiffa, H. & Schlaifer, R. (1961): Applied Statistical Decision Theory. Harvard University Press, Cambridge University Press, Cambridge, Massachusetts, in English

RCP (2004): STRUREL, A structural reliability analysis program system, RCP GmbH, Munich, in English

Rosenblueth, E. & Mendoza, E. (1971): reliability Optimization in Isostatic Structures, Jounral of the Eng. Mech. Div., ASCE, 97, EM6, in English

Rüger, B. (1999): Test- und Schätzmethoden, Band I: Grundlagen, Oldenbourg, Munich, in German

Schermer, D. (2007): Report on static-cyclic test at University of Munich, Presentation at ESECMaSE Dissemination Meeting, Cologne, 2007

Schermer, D. (2004): Verhalten von unbewehrtem Mauerwerk unter Erdbebenbeanspruchung, doctoral thesis, Technische Universität München, in German

Schmidt, H. (2003): Versagenswahrscheinlichkeit unbewehrter Wand-Decken-Verbindungen bei Gasexplosionen im Fertigteilbau, doctoral thesis, Technische Universität Darmstadt, in German

Schobbe, W. (1982): Konzept zur Definiton und Kobination von Lasten im Rahmen der deutschen Sicherheitsrichtlinie, Mitteilungen aus dem Institut für Massivbau der Technischen Universität Darmstadt, Verlag Ernst & Sohn, Berlin, in German

Schubert, P. & Caballero Gonzalez, A. (1995): Vergleichende Untersuchungen zur Haftscherfestigkeitsprüfung nach DIN 18 555 Teil 5 und EN, Institut für Bauforschung, Research report F 449 in: Kurzberichte aus der Bauforschung, Volume 6, issue 12, in German

Schubert, P. (2003): Eigenschaftswerte von Mauerwerk, Mauersteinen, Mauermörtel und Putzen, in: Irmschler, H.-J., Schubert, P. (eds.).: Mauerwerk-Kalender 2003, Ernst & Sohn, Berlin, in German

Schubert, P. (2010): Eigenschaftswerte von Mauerwerk, Mauersteinen, Mauermörtel und Putzen, in: Jäger, W. (ed.): Mauerwerk-Kalender 2010, Ernst & Sohn, Berlin, in German

Schubert, P.; Schmidt, U.; Hannawald, J. (2003): Neubewertung der rechnerischen Schubtragfähigkeit von Ziegelmauerwerk, research report F 808, RWTH Aachen, in German

Schuëller, G. (1981): Einführung in die Sicherheit und Zuverlässigkeit von Tragwerken, Ernst & Sohn, Berlin, in German

Schueremans, L. (2001): Probabilistic evaluation of the structural reliability of unreinforced masonry, doctoral thesis, Katholieke Universiteit Leuven, in English

Simon, E. (2002): Schubtragverhalten von Mauerwerk aus großformatigen Steinen, doctoral thesis, Technische Universität Darmstadt, in German

Six, M. (2001): Sicherheitskonzept für nichtlineare Traglastverfahren im Betonbau, doctoral thesis, Technische Universität Darmstadt, in German

Skjong, R. and Ronold, K.O. (1998): Societal Indicators and Risk Acceptance", Offshore Mechanics and Arctic Engineering Conference, OMAE 1998, in English

Sørensen, J. D. (2002): Calibration of Partial Safety Factors in Danish Structural Codes, JCSS workshop on reliability based code calibration, Zurich, JCSS, in English

Spaethe, G. (1992): Die Sicherheit tragender Baukonstruktionen, Springer, Vienna, in German

Stafford-Smith, B. & Carter, C. (1971): Hypothesis for Shear Failure of Brickwork, ASCE Journal of the Structural Division, Vol. 97, in English

Tengs, T.O.; Adams, M.E.; Pliskin, J.S.; Safran, D.G.; Siegel, J.E.; Weinstein, M.C.; Graham, J.D. (1995): Five-Hundred Life-Saving Interventions and Their Cost Effectiveness, Risk Analysis, Volume 15, Issue 3, June 1995, in English

Tomazevic, M. (1982): Lateral load distribution in masonry buildings, Proceedings of the Sixth International Brick Masonry Conference, Rome, in English

Tschötschel, M. (1989): Zuverlässigkeitstheoretisches Konzept für Mauerwerkskonstruktionen, doctoral thesis, Technische Universität Leipzig, in German

Vogt, H. (1961): Modellversuche mit bewehrten und unbewehrten Ziegelkonstruktionen, Die Ziegelindustrie, Heft 4, 1961

Zelger, C. (1964): Festigkeitsprobleme beim Mauerwerksbau mit vorgefertigten Elementen, Die Ziegelindustrie, Heft 24, 1964, in German

Zilch, K. & Krauns, N. (2004): Material parameters of masonry units – Input for WP 3, Deliverable D5.1, Enhanced Safety and Effcient construction of Masonry Structures in Europe (ESECMaSE), TU Munich, in English

Codes and Technical Guidelines:

CSA S304.1 (2004): Code of practice for the use of masonry – part 1: Structural use of unreinforced masonry, Canadian Standards Association, Mississauga, in English

DIN 1053-1 (1996): Mauerwerk – Teil 1: Berechung und Ausführung, Beuth Verlag, Berlin, in German

DIN 1053-100 (2007): Mauerwerk – Teil 100: Berechnung auf Grundlage des semiprobabilistischen Sicherheitskonzeptes, Beuth Verlag, Berlin, in German

DIN 1055-100 (2004): Grundlagen der Tragwerksplanung – Sicherheitskonzept und Bemessungsregeln für den konstruktiven Ingenieurbau, Beuth Verlag, Berlin, in German

DIN 1055-4 (2005): Einwirkungen auf Tragwerke – Teil 4: Windlasten, Beuth Verlag, Berlin, in German

DIN 18555-5 (1986): Prüfung von Mörteln mit mineralischen Bindemitteln – Teil 5: Festmörtel; Bestimmung der Haftscherfestigkeit von Mauermörteln, Beuth Verlag, Berlin

DIN EN 1052-1 (1998): Prüfverfahren für Mauerwerk – Teil 1: Bestimmung der Druckfestigkeit, German version of EN 1052-1, Beuth Verlag, Berlin, in German

DIN EN 1052-3 (2002): Prüfverfahren für Mauerwerk - Teil 3: Bestimmung der Anfangsscherfestigkeit (Haftscherfestigkeit); German version of EN 1052-3, Beuth Verlag, Berlin

DIN EN 1990 (2010): Eurocode 0: Grundlagen der Tragwerksplanung, Beuth Verlag, Berlin, in German

DIN EN 1990/NA (2010): Nationaler Anhang – National festgelegte Parameter - Eurocode 0: Grundlagen der Tragwerksplanung, Beuth Verlag, Berlin, in German

DIN EN 1996-1-1 (2005) and Correction (2010): Eurocode 6: Bemessung und Konstruktion von Mauerwerksbauten - Teil 1-1: Allgemeine Regeln für bewehrtes und unbewehrtes Mauerwerk, Beuth Verlag, Berlin, in German (available in English)

DIN EN 1996-1-1/NA (2011): National Anhang – National festgelegte Parameter - Eurocode 6: Bemessung und Konstruktion von Mauerwerksbauten - Teil 1-1/NA: Allgemeine Regeln für bewehrtes und unbewehrtes Mauerwerk, Beuth Verlag, Berlin, in German

DIN EN 771-1 (2005): Festlegungen für Mauersteine – Teil 1: Mauerziegel, Beuth Verlag, Berlin, in German

DIN EN 771-4 (2005): Festlegungen für Mauersteine – Teil 4: Porenbetonsteine, Beuth Verlag, Berlin, in German

DIN EN 772-1 (2000): Prüfverfahren für Mauersteine – Teil 1: Bestimmung der Druckfestigkeit, Beuth Verlag, Berlin, in German

DIN EN 772-2 (2005): Prüfverfahren für Mauersteine – Teil 2: Bestimmung des prozentualen Lochanteils in Mauersteinen (mittels Papierdruck), Beuth Verlag, Berlin, in German

DIN EN 998-2 (2003): Festlegung für Mörtel im Mauerwerksbau – Teil 2: Mauermörtel, German version of EN 1052-1 (1998), Beuth Verlag, Berlin, in German

DIN V 4165-100 (2005): Porenbetonsteine – Teil 100: Plansteine und Planelemente mit besonderen Eigenschaften, Beuth Verlag, Berlin, in German

DIN 1055-3 (2006): Einwirkungen auf Tragwerke – Teil 3: Eigen- und Nutzlasten im Hochbau, Beuth Verlag, Berlin, in German

ISO 2394 (1998): General principles on reliability of structures, ISO International Organization for Standardization, Geneva, Switzerland, in English

SIA 266 (2003): Mauerwerk, Schweizer Ingenieur – und Architektenverein, Zurich, in German

Appendix

General

The following tables present the test data used in the assessment of the models in section 5.6. Parameters that had to be estimated are marked by shaded cells. The failure modes in these tables have been identified from pictures and figures of the specimens after failure. For easier data management, the unit types are referred to as in the original source.

Table A- 1 References and sources of test data

Reference in the table	Source
D.J.&S.	Jäger & Schöps (2004)
Div.J&S.	Jäger & Schöps (2005)
DO.Lö.	Löring (2005)
Gun_FHL	Gunkler et al. (2009)
Höv.	Höveling et al. (2005)
KS.D7.1a	Fehling & Stürz (2006a)
KS.EAACA.	Fehling & Stürz (2006b)
MU.D7x.	Schermer (2007)
PV.Co.	Costa (2007)
PV.D7x.	Magenes (2007)
ZAG1.	Bojsiljkov et al. (2004)
ZAG3.	Bojsiljkov & Tomazevic (2005)

Table A- 2 Abbreviations

Abbreviation	Refers to
FM	**Failure Mode**
DT	Diagonal Tension
F	Flexure
S	Sliding Shear
HJ	**Head Joint**
U	Unfilled
F	Filled

Reference	Unit					Mortar	Specimen								Test results					Material properties					
	Type, Dimensions																						f_{bt}		
	Type	l_b	t	h_b	f_b		l_w	h_w	λ_v	HJ	u	u/h_b	u/l_b	h_b/l_b	N_{obs}	n_{obs}	V_{obs}	v_{obs}	FM	μ	f_{xl}	f_{v0}	hor	sp	f_m
		mm	mm	mm	N/mm²		m	m	[-]		mm	[-]	[-]	[-]	kN	[-]	kN	[-]		[-]	N/mm²				
KS.D7.1a.16	KS-R	250	175	250	34.5	TLM	1.25	2.5	1	U	125	0.5	0.5	1	220	0.043	91	0.018	S	0.55	0.35	0.28	1.67		23.6
KS.D7.1a.17	KS-opti	250	175	250	21.5		1.25	2.5	1	U	125	0.5	0.5	1	220	0.067	86	0.026	S	0.55	0.35	0.28	1.49		15
MU.D7x.x	KS-opti	250	175	250	21.5		2.5	2.5	0.5	U	125	0.5	0.5	1	280	0.043	154	0.023	S	0.55	0.35	0.28	1.49		15
PV.D7x.2	KS-opti	250	175	250	21.5		1.25	2.5	1	U	125	0.5	0.5	1	220	0.067	86	0.026	F	0.55	0.35	0.28	1.49		15
PV.D7x.3	KS-opti	250	175	250	21.5		1.25	2.5	1	U	125	0.5	0.5	1	110	0.034	49	0.015	S	0.55	0.35	0.28	1.49		15
PV.D7x.4	KS-opti	250	175	250	21.5		1.25	2.5	1	U	125	0.5	0.5	1	440	0.134	140	0.043	DT	0.55	0.35	0.28	1.49		15
PV.D7x.5	KS-opti	250	175	250	21.5		1.25	2.5	1	F	125	0.5	0.5	1	220	0.067	99	0.030	F	0.55	0.35	0.28	1.49		15
PV.D7x.6	KS-opti	250	175	250	21.5		1.25	2.5	2	U	125	0.5	0.5	1	220	0.067	45	0.014	F	0.55	0.35	0.28	1.49		15
PV.D7x.7	KS-opti	250	175	250	21.5		2.5	2.5	0.5	U	125	0.5	0.5	1	440	0.067	223	0.034	S	0.55	0.35	0.28	1.49		15
PV.D7x.8	KS-opti	250	175	250	21.5		2.5	2.5	1	U	125	0.5	0.5	1	440	0.067	168	0.026	DT	0.55	0.35	0.28	1.49		15
DO.Lö.V1	KS XL-RE	500	175	250	33.4		2.5	2.5	1	U	250	1.0	0.5	0.5	219	0.033	103	0.016	F	0.6	0.3	0.90	1.20		15
DO.Lö.V4	KS XL-RE	500	175	250	33.4		1.25	2.5	1	U	250	1.0	0.5	0.5	147	0.045	70	0.021	F	0.6	0.3	0.90	1.20		15
DO.Lö.V7	KS XL-RE	500	175	250	33.4		2.5	2.5	0.59	U	250	1.0	0.5	0.5	223	0.034	151	0.023	S	0.6	0.3	0.90	1.20		15
D.J&S.S1	KSLR (P)	250	240	250	12.2		2	2.5	0.63	U	125	0.5	0.5	1	845	0.241	220	0.063	DT	0.35	0.29	0.67	1.12		7.3
Gun_FHL_01	Element	998	175	498	32.1		2.5	2.5	0.5	U	99.6	0.2	0.1	0.5	219	0.024	140.1	0.016	DT	0.6		0.72	1.78		20.6
Gun_FHL_02	Element	998	175	498	32.1		2.5	2.5	0.5	U	199	0.4	0.2	0.5	219	0.024	111.2	0.012	DT	0.6		0.72	1.78		20.6
Gun_FHL_04	Element	998	175	498	32.1		2.5	2.5	1	U	249	0.5	0.25	0.5	219	0.024	89.4	0.010	F	0.6		0.72	1.78		20.6
Gun_FHL_05	Element	998	175	498	32.1		1.25	2.5	0.5	U	99.6	0.2	0.1	0.5	109	0.024	44.2	0.010	DT	0.6		0.72	1.78		20.6
Gun_FHL_07	Element	998	175	498	32.1		1.25	2.5	0.5	U	249	0.5	0.25	0.5	219	0.049	80.5	0.018	DT	0.6		0.72	1.78		20.6
Gun_FHL_08	Element	998	175	498	32.1		1.25	2.5	1	U	99.6	0.2	0.1	0.5	109	0.024	24	0.005	F	0.6		0.72	1.78		20.6
Gun_FHL_08b	Element	998	175	498	32.1		1.25	2.5	1	U	99.6	0.2	0.1	0.5	313	0.069	56.7	0.013	F	0.6		0.72	1.78		20.6

Reference	Unit					Mortar	Specimen								Test results					Material properties					
	Type, Dimensions																						f_{bt}		
	Type	l_b	t	h_b	f_b		l_w	h_w	λ_v	HJ	u	u/h_b	u/l_b	h_b/l_b	N_{obs}	n_{obs}	V_{obs}	v_{obs}	FM	μ	f_{xl}	f_{v0}	hor	sp	f_m
		mm	mm	mm	N/mm²		m	m	[-]		mm	[-]	[-]	[-]	kN	[-]	kN	[-]		[-]	N/mm²				
KS.D7.1a.1	HLz-conv.	365	175	250	19.3	M5	2.2	2.5	0.57	U	183	0.73	0.5	0.68	380	0.147	160	0.062	DT	0.6	0.24	0.24	0.21	1	6.7
KS.D7.1a.2	HLz-conv.	365	175	250	19.3	TLM	2.2	2.5	0.57	U	183	0.73	0.5	0.68	380	0.147	140	0.054	DT	0.68	0.24	0.24	0.21	1	6.7
KS.D7.1a.3	HLz-conv.	365	175	250	19.3	M5	2.2	2.5	0.57	U	183	0.73	0.5	0.68	380	0.147	118	0.046	DT	0.6	0.24	0.24	0.21	1	6.7
KS.D7.1a.4	HLz-conv.	365	175	250	19.3	TLM	2.2	2.5	0.57	U	183	0.73	0.5	0.68	380	0.147	147	0.057	DT	0.68	0.24	0.24	0.21	1	6.7
KS.D7.1a.5	HLz-opti	365	175	250	14.1	TLM	2.2	2.5	0.57	U	183	0.73	0.5	0.68	380	0.147	120	0.047	DT	0.68	0.24	0.24	0.28	0	6.7
KS.D7.1a.6	HLz-opti	365	175	250	14.1	M5	2.2	2.5	0.57	U	183	0.73	0.5	0.68	380	0.147	149	0.058	DT	0.6	0.24	0.24	0.28	0	6.7
KS.D7.1a.7	HLz-opti	365	175	250	14.1	TLM	1.1	2.5	1.14	U	183	0.73	0.5	0.68	190	0.147	60	0.047	F	0.68	0.24	0.24	0.28	0	6.7
KS.D7.1a.8	HLz-opti	365	175	250	14.1	M5	1.1	2.5	1.14	U	183	0.73	0.5	0.68	190	0.147	56	0.043	DT	0.6	0.24	0.24	0.28	0	6.7
KS.D7.1a.9	HLz-opti	365	175	250	14.1	TLM	2.2	2.5	0.57	U	183	0.73	0.5	0.68	95	0.037	72	0.028	S	0.68	0.24	0.24	0.28	0	6.7
KS.D7.1a.10	HLz-opti2	365	175	250	16.9	TLM	2.2	2.5	0.57	U	183	0.73	0.5	0.68	380	0.147	150	0.058	DT	0.68	0.24	0.24	0.17	1	6.7
KS.D7.1a.11	HLz-opti2	365	175	250	16.9	M5	2.2	2.5	0.57	U	183	0.73	0.5	0.68	380	0.147	162	0.063	DT	0.6	0.24	0.24	0.17	1	6.7
KS.D7.1a.12	HLz-opti2	365	175	250	16.9	TLM	1.1	2.5	1.17	U	183	0.73	0.5	0.68	190	0.147	70	0.054	F	0.68	0.24	0.24	0.17	1	6.7
KS.D7.1a.13	HLz-opti2	365	175	250	16.9	TLM	1.1	2.5	1.17	U	183	0.73	0.5	0.68	95	0.074	43	0.033	F	0.68	0.24	0.24	0.17	1	6.7
KS.D7.1a.14	HLz-opti2	365	175	250	16.9	TLM	1.1	2.5	1.17	U	183	0.73	0.5	0.68	48	0.037	25	0.019	F	0.68	0.24	0.24	0.17	1	6.7
KS.D7.1a.15	HLz-opti2	365	175	250	16.9	TLM	2.2	2.5	0.57	U	183	0.73	0.5	0.68	95	0.037	75	0.029	S	0.68	0.24	0.24	0.17	1	6.7
DO.Lö.V6	HLz	500	175	250	17.3	MG IIa	1.25	2.5	1.02	U	250	1	0.5	0.5	121	0.099	55	0.045	F	0.6	0.48	0.2	0.4	1	5.6
DO.Lö.V8	HLz	500	175	250	17.3	MG IIa	2.5	2.5	0.62	U	250	1	0.5	0.5	222	0.091	133	0.054	DT	0.6	0.48	0.2	0.4	1	5.6
DO.Lö.V11	HLz	500	175	250	17.3	MG IIa	2.5	2.5	1	U	250	1	0.5	0.5	223	0.091	100	0.041	F	0.6	0.48	0.2	0.4	1	5.6
ZAG3.BNW1	HLz	250	300	250	11.5	M5	2.5	1.9	0.76	F	125	0.5	0.5	1	442	0.144	285	0.093	DT	0.6	0.24	0.4	0.75	1	4.1
ZAG3.BNW2	HLz	250	300	250	11.5	M6	2.5	1.9	0.76	F	125	0.5	0.5	1	893	0.29	467	0.152	F	0.6	0.24	0.4	0.75	1	4.1
ZAG3.BNW3	HLz	250	300	250	11.5	M7	2.5	1.9	0.76	F	125	0.5	0.5	1	667	0.217	385	0.125	F	0.6	0.24	0.4	0.75	1	4.1
ZAG3.BSW	HLz	300	175	200	27.3	M15	2.7	2	0.72	F	150	0.75	0.5	0.67	950	0.214	417	0.094		0.6	0.24	0.4	1	1	9.4
ZAG3.BZW1	HLz	250	300	250	12.3	M5	2.5	1.9	0.76	U	125	0.5	0.5	1	713	0.221	352	0.109	F	0.6	0.24	0.4	0.75	1	4.3
ZAG3.BZW2	HLz	250	300	250	12.3	LM5	2.5	1.9	0.76	U	125	0.5	0.5	1	398	0.221	243	0.135	S	0.68	0.24	0.3	0.75	1	2.4
ZAG3.BTW	HLz	400	250	200	14.2	LM5	2.4	1.8	0.73	F	200	1	0.5	0.5	510	0.218	359	0.153	F	0.6	0.24	0.3	1	1	3.9

Reference	Unit					Mortar	Specimen								Test results					Material properties					
	Type, Dimensions				f_b		l_w	h_w	λ_v	HJ	u	u/h_b	u/l_b	h_b/l_b	N_{obs}	n_{obs}	V_{obs}	v_{obs}	FM	μ	f_{xl}	f_{v0}	f_{bt}		f_m
	Type	l_b	t	h_b																			hor	sp	
		mm	mm	mm	N/mm²		m	m	[-]		mm	[-]	[-]	[-]	kN	[-]	kN	[-]		[-]	N/mm²				
ZAG1.BNL.1	HLz	245	300	250	10	M5	1.03	1.5	1.46	F	123	0.49	0.5	1.02	184	0.145	55	0.043	F	0.6	0.48	0.5	0.3	1	4.1
ZAG1.BNL.2	HLz	245	300	250	10	M5	1.03	1.5	1.46	F	123	0.49	0.5	1.02	368	0.29	99	0.078	DT	0.6	0.48	0.5	0.3	1	4.1
ZAG1.BNL.3	HLz	245	300	250	10	M5	1.03	1.5	1.45	F	123	0.49	0.5	1.02	184	0.145	56	0.044	F	0.6	0.48	0.5	0.3	1	4.1
ZAG1.BNL.4	HLz	245	300	250	10	M5	1.03	1.5	1.46	F	123	0.49	0.5	1.02	368	0.29	112	0.088	DT	0.6	0.48	0.5	0.3	1	4.1
ZAG1.BNL.5	HLz	245	300	250	10	M5	1.03	1.5	1.46	F	123	0.49	0.5	1.02	368	0.29	109	0.086	DT	0.6	0.48	0.5	0.3	1	4.1
ZAG1.BNL.6	HLz	245	300	250	10	M5	1.03	1.5	1.46	F	123	0.49	0.5	1.02	184	0.145	66	0.052	DT	0.6	0.48	0.5	0.3	1	4.1
ZAG1.BGL.1	HLz	245	300	250	10	M5	0.99	1.5	1.52	U	123	0.49	0.5	1.02	353	0.276	102	0.08	DT	0.6	0.48	0.5	0.3	1	4.3
ZAG1.BGL.2	HLz	245	300	250	10	M5	0.99	1.5	1.52	U	123	0.49	0.5	1.02	353	0.276	103	0.081	DT	0.6	0.48	0.5	0.3	1	4.3
ZAG1.BGL.3	HLz	245	300	250	10	M5	0.99	1.5	1.52	U	123	0.49	0.5	1.02	353	0.276	94	0.074	DT	0.6	0.48	0.5	0.3	1	4.3
ZAG1.BPL.1	HLz	245	300	250	11.9	M5	0.99	1.5	1.52	F	123	0.49	0.5	1.02	353	0.189	106	0.057	DT	0.6	0.48	0.5	0.36	1	6.3
ZAG1.BPL.2	HLz	245	300	250	11.9	M5	0.99	1.5	1.52	F	123	0.49	0.5	1.02	353	0.189	110	0.059	DT	0.6	0.48	0.5	0.36	1	6.3
ZAG1.BPL.3	HLz	245	300	250	11.9	M5	0.99	1.5	1.52	F	123	0.49	0.5	1.02	353	0.189	111	0.059	DT	0.6	0.48	0.5	0.36	1	6.3
ZAG1.BZL.1	HLz	243	300	250	15.1	M5	0.99	1.5	1.52	U	122	0.49	0.5	1.03	353	0.192	100	0.054	F	0.6	0.48	0.5	0.45	1	6.2
ZAG1.BZL.2	HLz	243	300	250	15.1	M5	0.99	1.5	1.52	U	122	0.49	0.5	1.03	353	0.192	104	0.056	F	0.6	0.48	0.5	0.45	1	6.2
ZAG1.BZL.3	HLz	243	300	250	15.1	M5	0.99	1.5	1.52	U	122	0.49	0.5	1.03	353	0.192	102	0.055	F	0.6	0.48	0.5	0.45	1	6.2
ZAG1.BML.1	HLz	245	300	250	8.6	TLM	0.99	1.5	1.51	U	123	0.49	0.5	1.02	353	0.154	114	0.05	F	0.6	0.19	0.63	0.26	1	7.7
ZAG1.BML.2	HLz	245	300	250	8.6	TLM	0.99	1.5	1.52	U	123	0.49	0.5	1.02	536	0.234	155	0.068	F	0.6	0.19	0.63	0.26	1	7.7
ZAG1.BML.3	HLz	245	300	250	8.6	TLM	0.99	1.5	1.52	U	123	0.49	0.5	1.02	536	0.234	173	0.076	F	0.6	0.19	0.63	0.26	1	7.7

Table A- 6

Reference	Unit					Mortar	Specimen								Test results					Material properties					
	Type, Dimensions																						f_{bt}		
	Type	l_b	t	h_b	f_b		l_w	h_w	λ_v	HJ	u	u/h_b	u/l_b	h_b/l_b	N_{obs}	n_{obs}	V_{obs}	v_{obs}	FM	μ	f_{xl}	f_{v0}	hor	sp	f_m
		mm	mm	mm	N/mm²		m	m	[-]		mm	[-]	[-]	[-]	kN	[-]	kN	[-]			N/mm²				
KS.EAACA.1	PP	500	175	250	4.2	TLM	2.5	2.5	0.5	U	250	1	0.5	0.5	240	0.211	90	0.079	DT	0.6	0.3	0.28	0.5		2.6
KS.EAACA.2	PP	500	175	250	4.2		2.5	2.5	0.5	U	250	1	0.5	0.5	480	0.422	103	0.091	DT	0.6	0.3	0.28	0.5		2.6
KS.EAACA.3	PP	500	175	250	4.2		2.5	2.5	0.5	U	250	1	0.5	0.5	96	0.084	58	0.051	DT	0.6	0.3	0.28	0.5		2.6
KS.EAACA.4	PP	500	175	250	4.2		2.5	2.5	0.5	U	100	0.4	0.2	0.5	240	0.211	113	0.099	DT	0.6	0.3	0.28	0.5		2.6
KS.EAACA.5	PP	500	175	250	4.2		2.5	2.5	0.5	U	100	0.4	0.2	0.5	96	0.084	67	0.059	DT	0.6	0.3	0.28	0.5		2.6
KS.EAACA.6	PP	500	175	250	4.2		1.5	2.5	0.83	U	250	1	0.5	0.5	144	0.211	47	0.069	DT	0.6	0.3	0.28	0.5		2.6
KS.EAACA.8	PP	500	175	250	4.2		2.5	2.5	0.5	U	250	1	0.5	0.5	240	0.211	98	0.086	DT	0.6	0.3	0.28	0.5		2.6
KS.EAACA.9	PP	500	175	250	4.2		2.5	2.5	0.5	F	250	1	0.5	0.5	240	0.211	120	0.105	DT	0.6	0.3	0.28	0.5		2.6
DO.Lö.V3	PP	500	300	250	3		1.25	2.5	1	U	250	1	0.5	0.5	120	0.139	47	0.054	F	0.6	0.28	0.28	0.13		2.3
DO.Lö.V10	PP	500	300	250	3		2.5	2.5	0.57	U	250	1	0.5	0.5	223	0.129	111	0.064	S	0.6	0.28	0.28	0.13		2.3
PV.Co.1	PP	625	300	250	3.3		1.48	2.8	1.86	U	220	0.88	0.35	0.4	300	0.282	68	0.064	F	0.66	0.3	0.23	0.85		2.4
PV.Co.2	PP	625	300	250	3.3		3.13	2.8	0.88	U	313	1.25	0.5	0.4	300	0.133	138	0.061	F	0.66	0.3	0.23	0.85		2.4
PV.Co.3	PP	625	300	250	3.3		4.38	2.8	0.63	U	313	1.25	0.5	0.4	300	0.095	200	0.063	S	0.66	0.3	0.23	0.85		2.4
PV.Co.4	PP	625	300	250	3.3		1.48	2.8	1.86	U	220	0.88	0.35	0.4	200	0.188	48	0.045	F	0.66	0.3	0.23	0.85		2.4
Div.J&S.33.3	PPW	500	240	250	2.5		2.5	2.5	0.5	U	250	1	0.5	0.5	125	0.063	83	0.042	DT	0.6	0.28	1	0.51		3.3
Div.J&S.33.5	PPW	500	240	250	2.6		2.5	2.5	0.5	U	100	0.4	0.2	0.5	131	0.066	84	0.042	DT	0.6	0.28	1	0.52		3.3
Div.J&S.33.2	PPW	500	240	250	2.5		2.5	2.5	0.5	U	250	1	0.5	0.5	243	0.123	103	0.052	DT	0.6	0.28	1	0.51		3.3
Div.J&S.33.4	PPW	500	240	250	2.8		2.5	2.5	0.5	U	250	1	0.5	0.5	441	0.223	139	0.07	DT	0.6	0.28	1	0.57		3.3
Div.J&S.33.6	PPW	500	240	250	2.6		2.5	2.5	0.5	U	100	0.4	0.2	0.5	240	0.121	164	0.083	DT	0.6	0.28	1	0.52		3.3
Div.J&S.34.3	PPW	500	240	250	5.1		2.5	2.5	0.5	U	250	1	0.5	0.5	135	0.068	105	0.053	DT	0.6	0.28	1	0.66		3.3
Div.J&S.34.5	PPW	500	240	250	4.6		2.5	2.5	0.5	U	100	0.4	0.2	0.5	240	0.121	148	0.075	DT	0.6	0.28	1	0.6		3.3
Div.J&S.34.4	PPW	500	240	250	5.1		2.5	2.5	0.5	U	250	1	0.5	0.5	450	0.227	184	0.093	DT	0.6	0.28	1	0.66		3.3
Div.J&S.34.1	PPW	500	240	250	5.2		2.5	2.5	0.5	U	250	1	0.5	0.5	735	0.371	202	0.102	DT	0.6	0.28	1	0.68		3.3
Div.J&S.34.6	PPW	500	240	250	4.6		2.5	2.5	0.5	U	100	0.4	0.2	0.5	735	0.371	184	0.093	DT	0.6	0.28	1	0.6		3.3

Reference	Unit					Mortar	Specimen								Test results					Material properties					
	Type, Dimensions																						f_{bt}		
	Type	l_b	t	h_b	f_b		l_w	h_w	λ_v	HJ	u	u/h_b	u/l_b	h_b/l_b	N_{obs}	n_{obs}	V_{obs}	v_{obs}	FM	μ	f_{xl}	f_{v0}	hor	sp	f_m
		mm	mm	mm	N/mm²		m	m	[-]		mm	[-]	[-]	[-]	kN	[-]	kN	[-]			N/mm²				
Div.J&S.34.8	PPW	500	240	250	5.1		2.5	2.5	0.5	F	100	0.4	0.2	0.5	793	0.401	273	0.138	DT	0.6	0.28	1	0.66		3.3
Div.J&S.40.1	PPW	625	240	250	5		2.5	2.5	0.5	U	311	1.25	0.5	0.4	330	0.167	155	0.078	DT	0.6	0.28	1	0.65		3.3
Div.J&S.50.1	PPW	600	250	250	4.7		3.4	2.3	0.66	F	300	1.2	0.5	0.42	200	0.071	145	0.052	F	0.6	0.75	0.55	0.67		3.3
Div.J&S.50.2	PPW	600	250	250	4.7		3.4	2.3	0.66	F	300	1.2	0.5	0.42	200	0.071	115	0.041	DT	0.6	0.75	0.52	0.56		3.3
Div.J&S.50.3	PPW	600	250	250	5.1		3.4	2.3	0.66	F	300	1.2	0.5	0.42	200	0.071	128	0.046	S	0.6	0.75	0.53	0.65		3.3
Div.J&S.70.1	PP	625	240	250	5		1.25	2.5	1	F	313	1.25	0.5	0.4	330	0.355	113	0.122	F	0.6	0.28	1	0.65		3.1
Div.J&S.70.2	PP	625	240	250	5		1.25	2.5	1	F	313	1.25	0.5	0.4	330	0.355	112	0.12	F	0.6	0.28	1	0.65		3.1
Höv_6	PP2	500	240	249	3.1		2.5	2.5	0.5	F	100	0.4	0.2	0.5	270	0.147	131.1	0.071	DT	0.6	0.22	0.58	0.37		3.1
Höv_7	PP2	500	240	249	3.1		2.5	2.5	0.5	U	100	0.4	0.2	0.5	270	0.147	102.5	0.056	DT	0.6	0.22	1.35	0.37		3.1
Höv_8	PP4	499	240	249	5.2		2.5	2.5	0.5	U	100	0.4	0.2	0.5	495	0.17	180.2	0.062	DT	0.6	0.54	1.35	0.62		4.9
Höv_9	PP4	499	240	249	5.2		2.5	2.5	0.5	F	100	0.4	0.2	0.5	495	0.17	220.1	0.075	DT	0.6	0.54	1.35	0.62		4.9
Höv_10	PP4	499	240	249	5.2		2.5	2.5	0.5	U	100	0.4	0.2	0.5	660	0.226	203	0.07	DT	0.6	0.54	1.35	0.62		4.9
Höv_11	PP4	499	240	249	5.2	TLM	2.5	2.5	0.5	F	100	0.4	0.2	0.5	660	0.226	220.9	0.076	DT	0.6	0.54	1.35	0.62		4.9
Höv_12	PP2	500	240	249	3.1		2.5	2.5	0.5	U	100	0.4	0.2	0.5	360	0.196	126.6	0.069	DT	0.6	0.22	0.58	0.37		3.1
Höv_13	PP2	500	240	249	3.1		2.5	2.5	0.5	F	100	0.4	0.2	0.5	360	0.196	159.8	0.087	DT	0.6	0.22	0.58	0.37		3.1
Höv_15	PP4	499	240	249	5.2		2.5	2.5	0.5	U	100	0.4	0.2	0.5	330	0.113	185.8	0.064	DT	0.6	0.54	1.35	0.62		4.9
Höv_16	PPE4	624	236	624	4.4		2.5	2.5	0.5	F	125	0.2	0.2	1	495	0.192	189.2	0.073	DT	0.6	0.53	1.35	0.62		4.4
Höv_17	PPE4	624	236	624	4.4		2.5	2.5	0.5	U	125	0.2	0.2	1	330	0.128	169.3	0.066	DT	0.6	0.53	1.35	0.62		4.4
Höv_19	PP2	500	240	249	3.1		2.5	2.5	0.5	U	50	0.2	0.1	0.5	126	0.068	76.1	0.041	DT	0.6	0.22	0.58	0.37		3.1
Höv_20	PP4	499	240	249	5.2		2.5	2.5	0.5	F	50	0.2	0.1	0.5	660	0.226	242.1	0.083	DT	0.6	0.54	1.35	0.62		4.9
Höv_21	PPE4	624	236	624	4.4		2.5	2.5	0.5	F	125	0.2	0.2	1	660	0.256	210.1	0.082	DT	0.6	0.53	1.35	0.62		4.4
Höv_22	PPE4	624	236	624	4.4		2.5	2.5	0.5	U	125	0.2	0.2	1	660	0.256	178	0.069	DT	0.6	0.53	1.35	0.62		4.4
Höv_24	PPE4	624	236	624	4.4		2.5	2.5	0.5	U	125	0.2	0.2	1	231	0.09	116.5	0.045	DT	0.6	0.53	1.35	0.62		4.4
Höv_25	PP4	499	240	249	5.2		2.5	2.5	0.5	U	50	0.2	0.1	0.5	825	0.283	210.4	0.072	DT	0.6	0.54	1.35	0.62		4.9
Höv_26	PP4	499	240	249	5.2		2.5	2.5	0.5	F	50	0.2	0.1	0.5	623	0.213	260.4	0.089	DT	0.6	0.54	1.35	0.62		4.9

Dissertationsreihe

Prof. Dr.-Ing. Carl-Alexander Graubner
Institut für Massivbau
Technische Universität Darmstadt

Heft 1: **Stefan Kempf (2001)**
Technische und wirtschaftliche Bewertung der Mindestbewehrungsregeln für Stahlbetonbauteile

Heft 2: **Katja Reiche (2001)**
Nachhaltigkeitsanalyse demontagegerechter Baukonstruktionen - Entwicklung eines Analysemodells für den Entwurf von Gebäuden

Heft 3: **Michael Six (2001)**
Sicherheitskonzept für nichtlineare Traglastverfahren im Betonbau

Heft 4: **Eric Simon (2002)**
Schubtragverhalten von Mauerwerk aus großformatigen Steinen

Heft 5: **Holger Schmidt (2003)**
Versagenswahrscheinlichkeit unbewehrter Wand-Decken-Verbindungen bei Gasexplosionen im Fertigteilbau

Heft 6: **Andreas Bachmann (2003)**
Ein wirklichkeitsnaher Ansatz der böenerregten Windlasten auf Hochhäuser in Frankfurt/Main

Heft 7: **Duy Tien Nguyen (2004)**
Rotationskapazität von biegebeanspruchten Stahlbetonbauteilen mit Schubrissbildung

Heft 8: **Gert Wolfgang Riegel (2004)**
Ein softwaregestütztes Berechnungsverfahren zur Prognose und Beurteilung der Nutzungskosten von Bürogebäuden

Heft 9: **Christian Glock (2004)**
Traglast unbewehrter Beton- und Mauerwerkswände - Nichtlineares Berechnungsmodell und konsistentes Bemessungskonzept für schlanke Wände unter Druckbeanspruchung

Heft 10: **Kati Herzog (2005)**
Lebenszykluskosten von Baukonstruktionen - Entwicklung eines Modells und einer Softwarekomponente zur ökonomischen Analyse und Nachhaltigkeitsbeurteilung von Gebäuden

Heft 11: **Andreas Garg (2006)**
Spannungszustände in Fahrbahnplatten weit gespannter Stahlverbundbrücken - Empfehlungen für die Herstellung der Ortbeton-Fahrbahnplatte von Talbrücken mit der Schalwagenmethode

Heft 12: **Tilo Proske (2007)**
Frischbetondruck bei Verwendung von Selbstverdichtendem Beton - Ein wirklichkeitsnahes Modell zur Bestimmung der Einwirkungen auf Schalung und Rüstung

Heft 13: **Simon Glowienka (2007)**
Zuverlässigkeit von großformatigem Mauerwerk - Probabilistische Analyse von großformatigem Mauerwerk aus Kalksandstein und Porenbeton mit Dünnbettvermörtelung

Heft 14: **Alexander Renner (2007)**
Energie- und Ökoeffizienz von Wohngebäuden - Entwicklung eines Verfahrens zur lebenszyklusorientierten Bewertung der Umweltwirkungen unter besonderer Berücksichtigung der Nutzungsphase

Heft 15: **Guido Hausmann (2007)**
Verformungsvorhersage vorgespannter Flachdecken unter Berücksichtigung der stochastischen Eigenschaften

Heft 16: **Stefan Daus (2007)**
Zuverlässigkeit des Klebeverbundes von nachträglich verstärkten Betonbauteilen – Sicherheitskonzept für den Verbundnachweis von oberflächig geklebter Bewehrung

Heft 17: **Thomas Kranzler (2008)**
Tragfähigkeit überwiegend horizontal beanspruchter Aussteifungsscheiben aus unbewehrtem Mauerwerk

Heft 18: **Lars Richter (2009)**
Tragfähigkeit nichttragender Wände aus Mauerwerk – Ein nichtlineares Berechnungsmodell und Bemessungsverfahren für biegebeanspruchte Innen- und Außenwände

Heft 19: **Markus Spengler (2010)**
Dynamik von Eisenbahnbrücken unter Hochgeschwindigkeitsverkehr Entwicklung eines Antwortspektrums zur Erfassung der dynamischen Tragwerksreaktion

Heft 20: **Linh Ngoc Tran (2011)**
Berechnungsmodell zur vereinfachten Abschätzung des Ermüdungsverhaltens von Federplatten bei Fertigträgerbrücken

Heft 21: **Carmen Schneider (2011)**
Steuerung der Nachhaltigkeit im Planungs- und Realisierungsprozess von Büro- und Verwaltungsgebäuden. Entwicklung eines Instrumentes zur Vorbewertung und Optimierung der Nachhaltigkeitsqualität.

Heft 22: **Frank Ritter (2011)**
Lebensdauer von Bauteilen und Bauelementen. Modellierung und praxisnahe Prognose.

Heft 23: **Benjamin von Wolf-Zdekauer (2011)**
Energieeffizienz von Anlagensystemen zur Gebäudekühlung. Ein nutzenbezogener Bewertungsansatz.

Heft 24: **Eric Brehm (2011)**
Reliability of Unreinforced Masonry Bracing Walls – Probabilistic Approach and Optimized Target Values

TECHNISCHE UNIVERSITÄT DARMSTADT
INSTITUT FÜR MASSIVBAU
PROF. DR.-ING. CARL-ALEXANDER GRAUBNER

Eric Brehm

Reliability of Unreinforced Masonry Bracing Walls

Bracing walls are essential members in typical masonry structures. However, design checks are only performed rarely in Germany. The reason for this is a paragraph in the German design code DIN 1053-1 that allows for the neglection of this design check. This paragraph is based on different construction methods than they are the current state of the art. Additionally, the capacities according to current design codes have been calibrated on basis of previous design codes and experience. Consequently, the provided level of reliability remains unknown.

In this paper, a systematic analysis of the provided level of reliability is conducted. Analytical models for the prediction of the shear capacity of the walls are analyzed and assessed with test data to identify the most realistic model. A complete stochastic model is set up and the reliability of typical bracing walls is determined. It is differed between the theoretical level of reliability and the “actual” level of reliability taking into account the realistic utilization of the walls.

Finally, an optimal target value for the reliability is derived by full-probabilistic optimization to be able to assess the previously determined provided reliabilities. An efficient use of masonry in the design according to DIN 1053-1 can be verified.

ISBN 978-3-942886-02-4